Water management
from basin to biofilm

by

Krista Bonfantine

B.S., Colorado State University

M.S., University of New Mexico

Ph.D., Deakin University

Submitted in fulfilment of the requirements for the degree of

Doctor of Philosophy

Deakin University

June 2021

Candidate Declaration

I am the author of the thesis entitled

"Water management from basin to biofilm"

submitted for the degree of Doctor of Philosophy.

This thesis may be made available for consultation, loan and limited copying in accordance with the Copyright Act 1968.

'I certify that I am the student named below and that the information provided in the form is correct'

Full Name:

Krista Lynn Bonfantine

Signed: .....

Date: 10 June 2021

Statement of publications

Accepted manuscripts produced as part of this thesis:

Bonfantine, K.L., Trevathan-Tackett, S.M., Matthews, T.M., Neckovic, A., Gan, H.M. (in press). Dumpster diving for diatom plastid 16S rRNA genes. *PeerJ.* Accepted 13 May 2021.

Statement of authorship

I certify the following about this thesis:

a. I am the creator of all or part of the whole work(s) (including content and layout) and that where reference is made to the work of others, due acknowledgment is given.

b. The work(s) are not in any way a violation or infringement of any copyright, trademark, patent, or other rights whatsoever of any person.

c. That if the work(s) have been commissioned, sponsored or supported by any organisation, I have fulfilled all of the obligations required by such contract or agreement.

d. That any material in the thesis which has been accepted for a degree or diploma by any university or institution is identified in the text.

e. I have complied with all permitting and research integrity requirements.

Statement of communications

Bonfantine, K., 2020. *A molecular test of e-flow effectiveness using biofilms as bioindicators*. American Water Resources Association Virtual Water Resources Conference.

Bonfantine, K., 2020. eDNA – The Roots of a New Ecology. Deakin Centre for Integrative Ecology Wild Webinar Series. https://www.youtube.com/watch?v=nBlBXJOhCPs

Bonfantine, K., 2020. *How does stream biofilm respond to small environmental flow releases?* Barwon Water R&D Podcast Series.

Bonfantine, K., 2019. *Stream health and slime.* Deakin University Three Minute Thesis (3MT) Finalist

Bonfantine, K. 2019. *How does stream biofilm respond to small environmental flow releases?* Australian Freshwater Sciences Society Annual Conference. Deakin University. Waurn Ponds, VIC

Bonfantine, K., 2019. *Stream slime as a bioindicator.* Deakin Centre for Integrative Ecology Annual Conference. Melbourne, VIC

Bonfantine, K. 2018. *Do small flow releases alter the composition and nutritional quality of biofilms?* Virtual poster at the Australian Freshwater Sciences Society Annual Conference. Adelaide, SA.

Abbreviations

AAET	Morton's areal actual evapotranspiration
AET	Actual evapotranspiration
AFDM	Ash-free dry mass
AIC	Akaike's Information Criterion
ALA	α-linolenic acid
ANOVA	Analysis of variance
APET	Morton's wet-environment areal potential evapotranspiration
ARA	Arachidonic acid
ASV	Amplicon sequence variant
B	Barham River
BACI	Before-after-control-impact
BOM	Bureau of Meteorology
CC	Creative commons
CFA	County Fire Authority
Chl	Chlorophyll
CTF	Cease-to-flow
DELWP	Department of Environment, Land, Water and Planning
DEM	Digital elevation model
df	Degrees of freedom
DHA	Docosahexaenoic acid
Diss	Dissimilarity
DISTLM	Distance-based linear modelling
DNA	Deoxyribonucleic acid
DO	Dissolved oxygen
DOC	Dissolved organic carbon
EFA	Essential fatty acids
EPA	Eicosapentaenoic acid
ET	Evapotranspiration
FID	Flame ionisation detector
GC	Gas chromatography
GLA	Gamma-linolenic acid
ITS	Internal transcribed spacer region
LFF	Low flow fresh
LIN	Linolenic acid
MC	Monte Carlo
MDS	Multi-dimensional scaling

ML	Megalitres
MS	Mean squares
MUFA	Monounsaturated fatty acids
NCBI	National Center for Biotechnology Information
NH_4	Ammonia
nMDS	Non-metric multidimensional scaling
NO_2	Nitrite
NO_3	Nitrate
OTU	Operational taxonomic unit
PCO	Principal coordinates analysis
PCR	Polymerase chain reaction
PD	Painkalac Downstream
PERMANOVA	Permutational multivariate analysis of variance
PERMDISP	Permutational analysis of multivariate dispersions
PET	Potential evapotranspiration
PLFA	Phospholipid fatty acid
PPET	Morton's point potential evapotranspiration
PR	P, Reactive
PU	Painkalac Upstream
PUFA	Polyunsaturated fatty acids
Q	Discharge
RDP	Ribosomal database project
RNA	Ribonucleic acid
SD	Standard deviation
SFA	Saturated fatty acids
SIMPER	Similarity percentages
SPCond	Conductivity, as specific conductance
SRA	Sequence read archive
SS	Sum of squares
TCN	Total nitrogen as N
Temp	Temperature
TKN	Total Kjeldahl N
TON	Total oxidised N as N
TP	Total phosphorous
V	Velocity
VVG	Visualising Victoria's Groundwater
WMIS	Water Measurement Information System

Acknowledgements

First and foremost, I need to express my deepest thanks to Ryan and Emma for joining me on this PhD adventure to the other side of the world. Ryan's commitment to my morning coffee also deserves gratitude and acknowledgement. The love and support that my parents, extended family and dear friends conveyed across the vast distance made it possible for me to reach the doctoral finish line.

I would especially like to thank my amazing supervisors, Annalisa Durdle and Xavier Conlan, who took me in as an academic orphan and stuck by me to the end. I am forever grateful for their assistance, emotional support and never-ending good humour.

I am indebted to an entire village of Deakin University staff and students who facilitated the weeks of field and lab work required for this research. I extend a massive thank you to my undergraduate volunteers, Courtney Bourke and Meg Spiteri, who devoted weeks of their lives to slime and managed to keep smiling. David Dodemaide and Ty Matthews were also skilled field hands who generously shared their knowledge and made long days fun. David also provided a vital role as my cultural attaché, helping me to make sense of all things Australian for the last four years. Ashley McQueen and Galen Holt were intrepid partners in the field and in the wilderness that is R and I am eternally grateful for their assistance. Antoine Dujon was also a valuable and capable escort through the statistics swamp. I thank Lawrence Webb, Georgia Dwyer and Morgan Ellis for getting wet on my behalf.

I must also recognise the contributions of other Deakin staff who supported my research. I deeply grateful to Kate Towart for repeatedly dusting me off and propping me up throughout this entire process. Thanks, Kate for being my Apollo Creed. Richard Alexander not only drilled more than 300 holes in small wood blocks, he connected me to a wonderful network of friends and colleagues that improved my life and my research. I will always appreciate his generosity and friendship. Kim Quayle was another steady friend and champion through this journey. No one in our office was spared so Egan Doeven and Ryan Nai were constantly tapped for their helpful technical expertise and equipment. I am thankful for the microscope training and access provided by Aaron Schultz, without whom, I wouldn't have captured any snapshots of the slime. I can't list all of my fellow PhD students that have provided ideas, inspiration and laughs over the years but I am thankful for all of the support and encouragement I have received. I am thrilled to have a new, international network of nerds (you know who you are).

My understanding of the Painkalac catchment was shaped as much by the resident experts of the area as by my academic research. The local community provided invaluable context and character to this project. I would like to thank Gretel Lamott, Nan McNab and Margaret Lacey for graciously sharing their time and knowledge. I also appreciate the technical perspective that Rory Nathan provided. Gregory Day brought the region alive for me through his storytelling and I am enriched by his friendship. Graeme and Pat McKenzie not only welcomed me onto their property but also into their home and I am so glad to know them. My personal and professional experience as a guest on Wadawurrung country has been life-

changing and I want to recognise the Traditional Owners for their stewardship and faith in caring for this magical place.

Barwon Water provided the research funding that made this project possible and Jared Scott supported this project from day one with all the data and resources I could ask for. The little group of PhD students that his colleague, Michael Thomas, brought together provided much-needed social sustenance during the isolation of the COVID months. Michael, Christina Semasinghe and Đức Nguyễn, I appreciate all your kindness and support.

Additional funding for this project was provided by the Holsworth Wildlife Research Endowment – Equity Trustees Charitable Foundation & the Ecological Society of Australia. I am glad to have benefitted personally from this endowment and to have witnessed its impact across many other student research projects.

I would like to collectively recognize all the members of the Australian Freshwater Sciences Society that helped to guide and shape this research. I am grateful for their technical expertise and encouragement.

An amazing circle of Surf Coast women supplied essential support during this endeavor and my friend Kerry Borg was a persistent cheerleader of my opus. Thanks, ladies!

Finally, thank you to all the other kind souls who assisted me on this voyage.

Abstract

Water management from basin to biofilm

2021

Krista Bonfantine

Water falling from sky to land, gathers within a basin and aggregates as it makes its way downhill. The freshwater resources produced by this consolidation sustain habitats and people so a balance must be struck between ecosystem supply and human demand. Measurement of the efficacy of this compromise is constantly evolving with improved understanding of the consequences of degradation and the development of new tools to probe freshwater ecosystems.

My research applied a multidisciplinary approach (hydrological, biological, chemical) to assess the health of Painkalac Creek, a small coastal stream in Victoria, Australia. At the basin level, the assessment of well-being began with a water balance that quantified and compared the amount of water coming in and going out of the catchment. This accounting exercise, which is more simple in theory than practice, demonstrated the downward trajectory of surface and groundwater supplies within a pattern of large year-to-year variation. I estimated that 60% of the 160 ML/year that was previously diverted continues to be lost to evaporation from the reservoir each year. My analysis also highlighted the importance of the maritime influence on

local hydrology and revealed some uncertainty in the parameters used in water resource planning and management

The other components of my ecosystem health assessment focused on biotic indicators of stream health. Because stream biota integrate environmental conditions and impacts through time, aquatic insect communities have been used to assess stream health for over a century but emerging technology allows smaller, more responsive biological communities to be profiled. The biofilm that coats every hard surface in a stream is a ubiquitous and ecologically important community that can serve as a bell-weather of stream health but characterisation of the microscopic community has been challenging until recently. Now, with DNA-based tools, the stream biofilm community can be described as never before.

I conducted a field experiment that used wood blocks on floating frames to cultivate stream biofilm over a series of three-week periods. The experiment was designed to assess a specific water management activity but first I had to test the performance of stream biofilm as a bioindicator community and establish relationships between biofilm ecology and flow conditions. I investigated the bacterial, algal, and fungal components of the biofilm community using three DNA metabarcoding regions (16S, 23S and ITS), respectively. All three regions demonstrated utility in describing biofilm community structure and were significantly correlated with physicochemical variables and fatty acid composition. The fatty acid content was less strongly correlated to environmental conditions and biological community structure but provided some important insights into the nature of biofilm as a food resource for higher trophic levels. My research findings

highlighted the importance of the stream microbiome as an indicator of stream health and I developed a novel method to characterise the stream microbiome.

Painkalac Creek was dammed in the late 1970's to supply domestic water but the communities have since been connected to an alternate water source. The water that was previously diverted now remains in the reservoir and is released through the dam according to an environmental flow prescription designed to support stream health. My experiment was designed to assess whether the scheduled summer flow pulses were improving the condition of Painkalac Creek, downstream of the dam. To do this, I compared the biofilms below Painkalac Dam to biofilms from Painkalac Creek upstream of the reservoir and in the nearby Barham River. Distinct communities of bacteria, algae and fungi were associated with increased flow in the unregulated stream reaches but not in the regulated reach, below the dam. Across all biological, biochemical and physical data analysed, the only significant change produced by environmental flow pulses in Painkalac Creek was an altered thermal regime resulting from warm water released from the reservoir. My findings suggest that environmental flow releases from reservoirs may need to be designed to more closely mimic unregulated river systems to produce the desired changes in ecological condition. Improved knowledge of flow-ecology relationships will help water resource managers optimise ecological benefits from managed flows.

Table of Contents

List of Tables

List of Figures

Introduction

Painkalac Dam was constructed in the late 1970s to capture the water of Painkalac Creek and supply the coastal communities of Aireys Inlet and Fairhaven along the Surf Coast of Victoria, Australia. The water of Painkalac Creek was diverted, treated and delivered to households until 2016, when the local water supply was replaced by a regional pipeline. The stream now flows full again but remains fractured by the dam.

River vitality rests upon the rhythms of the natural flow regime so water management strategies generally aim to mimic natural flow patterns (Poff *et al.*, 1997; Bunn & Arthington, 2002). Flow descriptions, designed to 'stretch' supply and create the healthiest possible ecological condition with less water (Postel & Richter, 2003), can be implemented using dam releases to reproduce natural flow patterns (Richter & Thomas, 2007). In 2018, Barwon Water began operating Painkalac Dam in accordance with an environmental flow prescription designed to support stream health.

This research focuses primarily on assessing the ecological benefits of the environmental flows in Painkalac Creek, specifically the summer flow pulses. Because the pulses were scheduled ahead of time, a manipulative experiment could be designed to measure the efficacy of the prescription using stream biofilm communities as indicators of ecological health. The quantity and quality of the biofilm could be assessed in novel ways due to recent technological advancements in DNA sequencing (Baird & Hajibabaei, 2012) and fatty acid profiling (Ruess & Müller-Navarra, 2019). Improved knowledge of how flow magnitude, timing and duration influence the base of the stream food web can help optimise ecological benefits from managed flows.

1.1. Thesis overview

The small, coastal basin that collects rainfall and feeds Painkalac Creek was once a water supply catchment that sustained two local communities but the combination of high rainfall variability and small catchment volume was deemed too unreliable to be sustainable. When the communities were connected to a larger regional supply network in 2016, the full catchment volume was restored after 40 years of withdrawals, but the stream remains impounded by Painkalac Dam. The dam operation schedule is recognised as an important instrument in regulating downstream ecological conditions so releases are managed according to an environmental flow prescription developed during the Millennium Drought (1999-2009). Although the shortage-sharing strategy is no longer as urgent since the decade-long drought and the withdrawals have ended, the focus on optimising ecological health with dwindling water supplies remains relevant and vital.

The underlying assumption for environmental flow delivery is that active management is required to balance various competing demands for water but the managed flows in Painkalac Creek are currently driven by the presence of a dam rather than the absence of water. Beyond the environmental flows, the health of Painkalac Creek reflects the broader hydrologic regime and the condition of the catchment so thesis first considers the basin-level hydrology in Chapter 2 to provide context for the subsequent chapters that examine stream health.

For over a century, stream health has been assessed using aquatic macroinvertebrates as bioindicators because stream biota integrate the dynamic environmental conditions of flowing water (Bonada *et al.*, 2006). Freshwater biofilms have been suggested as better bioindicators (Burns & Ryder, 2001) but the microorganisms of the biofilm community have been challenging to characterise and

quantify (Pawlowski *et al.*, 2016; Hajibabaei *et al.*, 2016). The only members of the biofilm community that have an established track record as bioindicators are diatoms (Charles *et al.*, 2021; Sagova-Mareckova *et al.*, 2021) but characterisation of the full suite of autotrophic and heterotrophic organisms in the biofilm community (Weitere *et al.*, 2018) is now possible using DNA-based methods (Pawlowski *et al.*, 2018). The emerging technology is providing new opportunities to measure microbial community dynamics and evaluate stream health at the base of the food web (Pawlowski *et al.*, 2018; Sagova-Mareckova *et al.*, 2021).

I designed a manipulative field experiment to compare the responses of the stream biofilm community to managed and natural flows. Chapter 3 evaluates the use of biofilm as a bioindicator by considering biofilm abundance, diversity, and nutritional food quality using molecular techniques and phospholipid fatty acid concentrations. Chapter 4 applies these data to test the effectiveness of the environmental flow prescription. Chapter 5 details a novel method for retrieving eukaryotic diatom community data from a DNA assay typically used to examine populations of bacteria and other prokaryotes.

Water management occurs across multiple spatial scales with scientific approaches that range from global-scale remote-sensing technology to cellular-scale diatom bioassessment. Likewise, this research considers spatial scales across nine orders of magnitude from the basin measured in kilometres to the biota measured in micrometres.

1.2. Painkalac catchment

Painkalac Creek runs through the traditional lands of the Wadawurrung people and formed a border with Gadubanud lands (Niewójt, 2010). Painkalac Creek is one of several short, coastal streams that drain the southeast side of the Otway Ranges in Victoria, Australia (Figure 1.1). The Painkalac Catchment sits along the descending edge of the water-harvesting feature that is the Otway Ranges. Near the top of the Otway Range, at almost 500 metres in elevation, the Weeaproinah weather station records an average annual rainfall of 1937 mm (accessed 2/12/2020, http://www.bom.gov.au/climate/). The Otway Ranges serve as a water tower for the entire Surf Coast, Geelong, and Colac region, conveying water above-ground and storing it below-ground.

The top of the Painkalac catchment sits at an elevation of approximately 430 metres and the creek descends quickly to sea level over its 20 km length (Doeg, Vietz & Boon, 2007). The catchment is 6252 hectares (62.52 km^2) in size (Figure 1.2) with about 3400 hectares (34 km^2) (Doeg *et al.*, 2007; Parks Victoria, Victoria, & DSE, 2009) above Painkalac Reservoir. The Painkalac Creek catchment has been protected under a special designation since 1979 to protect water quality and in 2005, much of the basin became part of the Great Otway National Park. The catchment is managed as a 'Reference Area Zone' within the Park in order to maintain the undisturbed, reference land and vegetation conditions (Parks Victoria *et al.*, 2009). With the exception of a tree plantation along the upper edge of the catchment and a few dirt tracks, the catchment above the reservoir is forested.

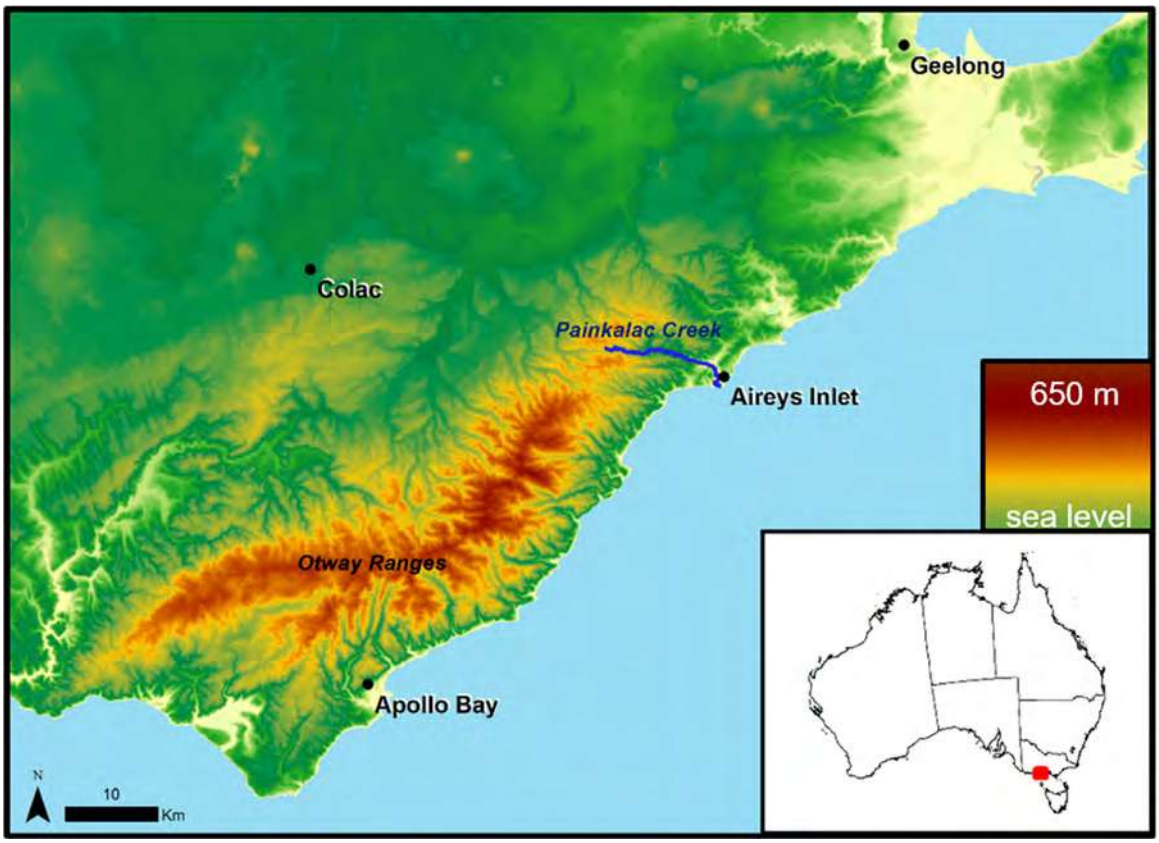

Figure 1.1. Digital elevation model (DEM) of the Surf Coast region in Victoria, Australia, including the location of Painkalac Creek. Surf Coast region is shown in red on the inset map of Australia. SRTM derived 1 Second DEM (Gallant *et al.*, 2011) Painkalac Creek from Regional Surface Hydrology Lines, Geoscience Australia (Crossman & Li, 2015).

The entire Painkalac Catchment burned during the Ash Wednesday fires (Figure 1.2). On the 16th of February 1983, a fire started at approximately 2:45 PM near Deans Marsh and raced through the grassland at a rate of 22 km/hr (Billing, 1983). With fine fuel moistures of 2.7% measured elsewhere in Victoria, relative humidity of 11% and temperatures exceeding 40°C, conditions were ideal for rapid fire spread. A running crown fire moved across the Otways, with spot fires leaping 10 km ahead of the flaming front, to reach Fairhaven by approximately 5:30 PM. The wind took on a new ferocity at 7:00 PM with gusts measuring over 100 km/hr. Just before the fire arrived, roofs were blown off houses in Aireys Inlet and mattresses were seen sailing through the air (Bill Bubb, personal communication, 7 August, 2018.). Large trees were ripped out of the

ground in places (Bill Bubb, personal communication, 7 August, 2018) including where a fire tornado cut an 800 m swath through Moggs Creek (Billing, 1983). The fires devastated the local communities and reshaped the vegetation of the entire catchment.

Figure 1.2. Painkalac catchment highlighted in blue within the red perimeter of the Ash Wednesday fires. White symbols denote water chemistry sampling locations. Watershed/catchment boundary developed from HydroSHEDS hydrologically conditioned digital elevation model (Lehner & Grill, 2013). (Painkalac Creek from Regional Surface Hydrology Lines. Geoscience Australia (Crossman & Li, 2015) and Ash Wednesday fire extent (DSE, 2008).

The Painkalac Creek catchment is mostly derived from Lower Cretaceous felspathic sandstone and mudstone parent material (Forsyth & Ransome, 1978). The upper catchment, above Painkalac Reservoir is part of the Early Cretaceous age Eumeralla Formation comprised of sandstone, mudstone, conglomerate, and siltstone (VVG, 2021). The reservoir sits at the head of an alluvial valley comprised of unconsolidated silt, sand and gravel. The water chemistry of Painkalac Creek is dominated by sodium and chloride ions with low levels of calcium, magnesium, and bicarbonate (Figure 1.3), based on water samples that were collected from the upper catchment and analysed by ALS Global (map: Figure 1.2)(Geelong, AU).

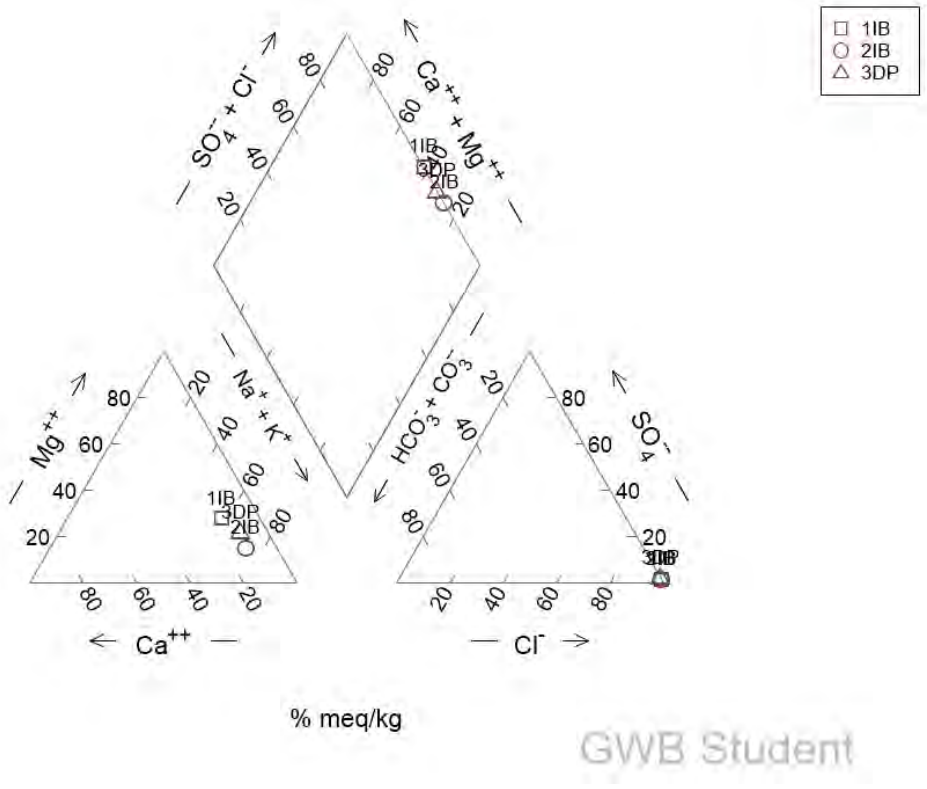

Figure 1.3 Piper diagram showing chemical composition of Painkalac Creek. Three water samples (1IB, 2IB, 3DP) were analysed. Upper diamond depicts groundwater facies with cations reported to the lower left and anions on the lower right. Produced using Geochemist's Workbench Student Edition.

Painkalac Creek is perhaps best known for its estuary which crosses the Great Ocean Road (Figure 1.4A). The intermittent estuary remains closed for much of the year but high flows and/or estuary opening actions create periodic connections between the coastal basin and the Great Southern Ocean (Figure 1.4B). The movements and breeding success of native diadromous fish such as short-finned eels (*Anguilla australis*) and galaxiids (*Galaxias maculatus, G. truttaceus*) are tied to these fleeting periods of linkage.

Figure 1.4 A) Great Ocean Road Bridge over Painkalac Estuary. B) Painkalac Creek flowing into the sea in September 2017.

1.3. Painkalac Dam

Prior to the 1970s, residents of the coastal communities of Aireys Inlet and Fairhaven relied on rainwater tanks for their water supply. In an effort to provide a consistent water supply to the growing communities, a dam was proposed in 1966 to capture the flow of Painkalac Creek (Forsyth & Ransome, 1978). Painkalac Dam was completed in 1978 (Figure 1.5Figure 1.6Figure 1.7A), but it took a few years to finance and install the plumbing to bring the new water supply into homes. The infrastructure was completed shortly before the Ash Wednesday fires swept across the region in 1983. The firestorm levelled Aireys Inlet, melted the new copper pipes and drained the service basin that transferred water between Painkalac Reservoir and the community (Figure 1.7B) (Bill Bubb, personal communication, 7 August, 2018). In place of the water, the fire left behind a black sludge that had to be scraped out to bring the water supply back on-line. The distribution plumbing was replaced as the houses were rebuilt, but many locals sold their charred blocks and moved on. Importantly, newcomers never knew Aireys Inlet without a central, reticulated water supply from Painkalac Reservoir.

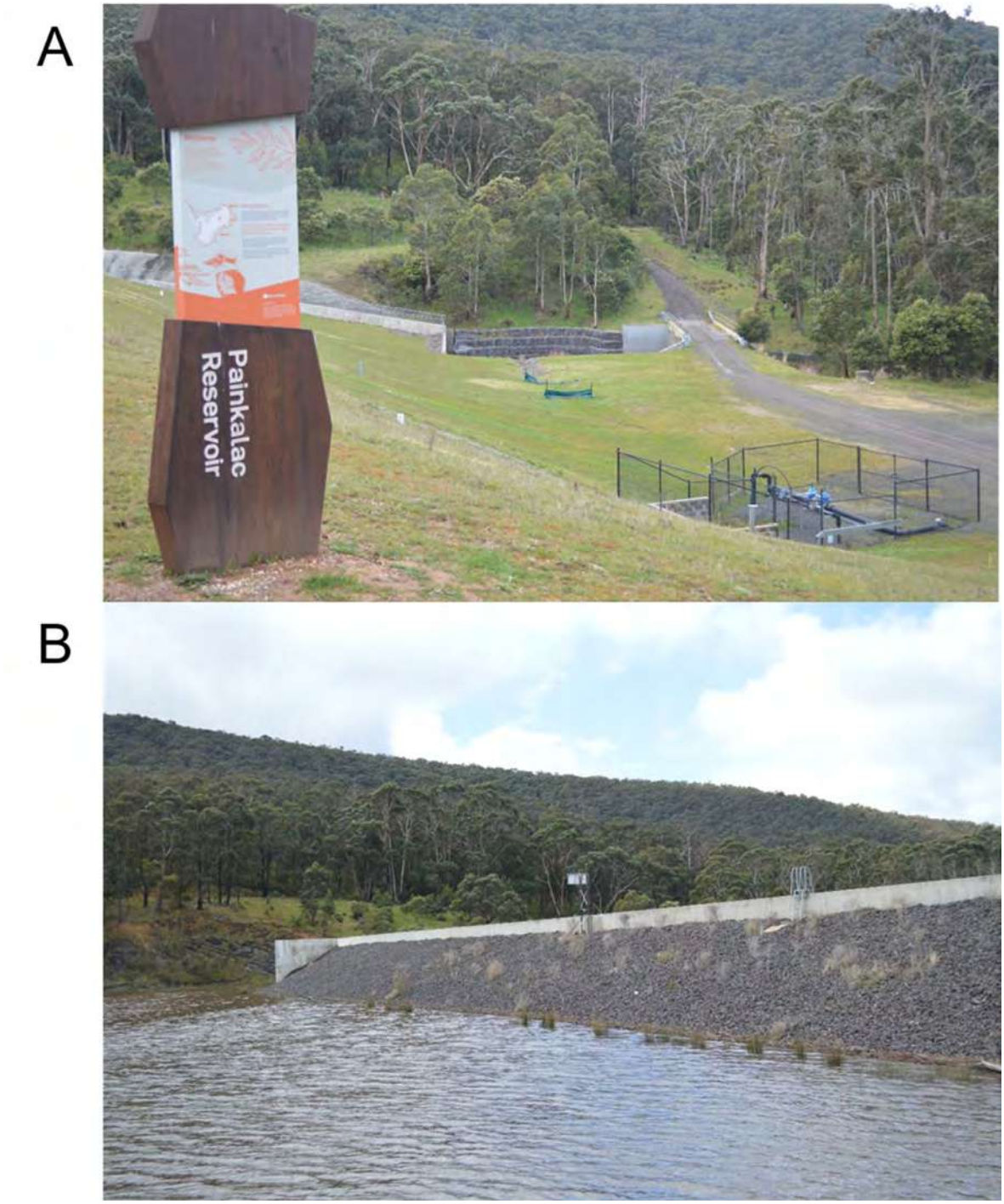

Figure 1.5 A) Downstream and B) upstream face of Painkalac Dam at full capacity (2017). Environmental flows are delivered by opening the valves within the fenced plumbing.

Figure 1.6. Painkalac Creek and Painkalac Reservoir, with Painkalac catchment highlighted. The Painkalac Reservoir polygon was developed from Maxar Vivid imagery (0.5m resolution, 01/10/2019)

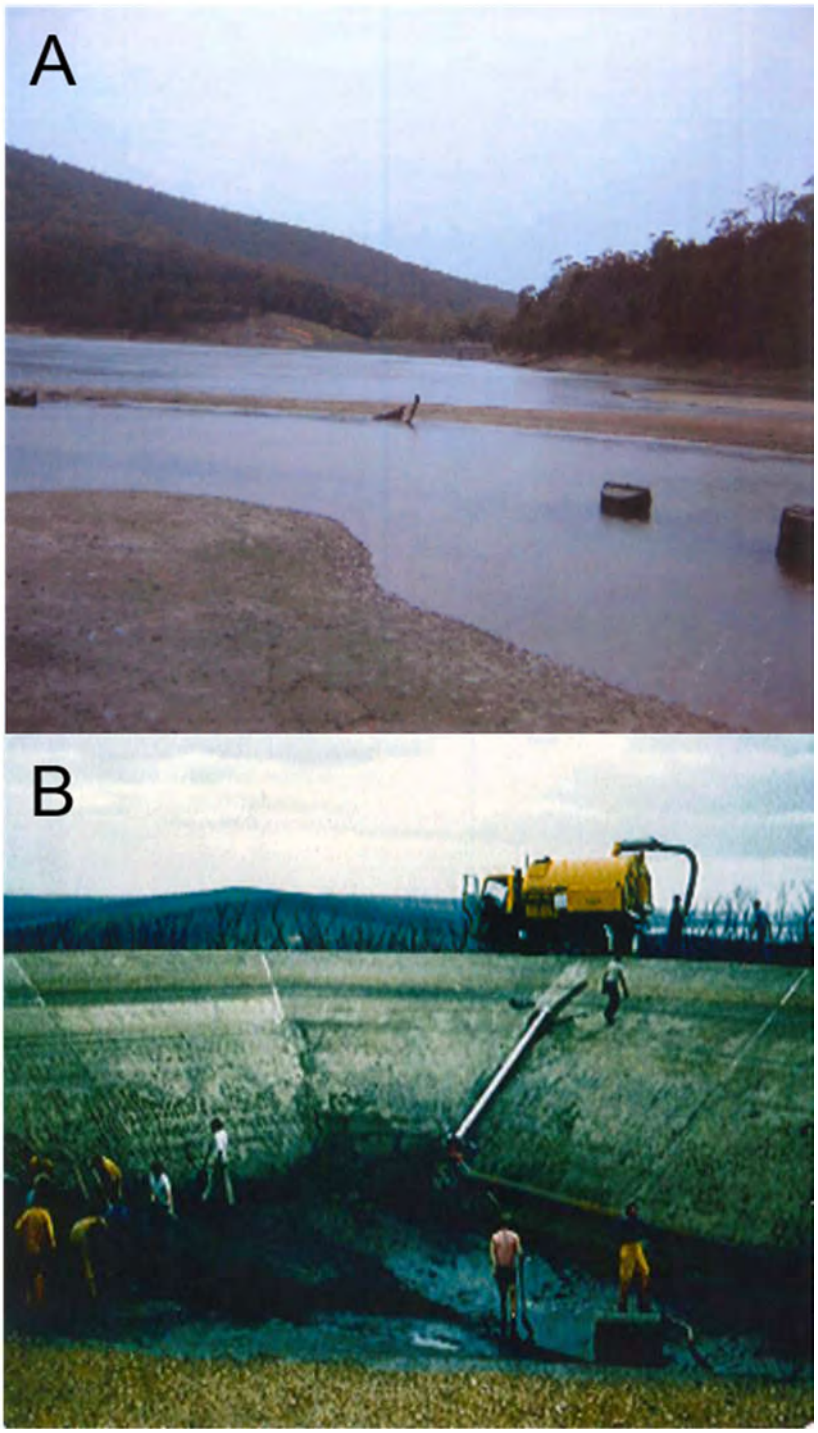

Figure 1.7. Painkalac Reservoir filling up and CFA fire brigade members removing ash from the service basin following the Ash Wednesday fires. CFA: Country Fire Authority. Photos courtesy of Bill Bubb.

Between 1999 and 2009, southeast Australia experienced a severe drought referred to as the Millennium Drought. During the extended drought period, officials from the water management authority, Barwon Water, became concerned about the reliability of the small reservoir. They began designing a connection to the regional pipeline but they faced strong opposition from the community.

The community sentiment that was shared with the researcher during this project was a strong sense of bioregionalism, the sense that the Painkalac catchment was fundamentally different from the surrounding catchments. Community members have been frustrated by the lack of recognition of the nuance around the catchment and the water managers have been frustrated by the community's lack of understanding around the reliability, or lack there-of, of the small system. Water managers, who are most often trained as engineers, see water as water and the emotional and spiritual attachments to place are not part of their training, experience, or planning process.

Painkalac Creek supplied Aireys Inlet and Fairhaven until 2016 when the communities were connected to an alternate supply network. The water treatment and delivery infrastructure were removed but Painkalac Reservoir is still maintained as a recreational site. The water (160 ML/yr) that once sustained the community is sustaining the creek once again, albeit through regulated flow delivery.

1.4. Environmental flows

Environmental flows are defined as 'the quantity, quality and timing of water flows required to sustain freshwater and estuarine ecosystems and the human livelihoods and well-being that depend on these ecosystems' (Brisbane Declaration, 2007). Environmental flow requirements quantify an acceptable degree of alteration to the flow regime of a river while maintaining valued features of the ecosystem (Tharme, 2003). Since its emergence in the 1970s, the science of environmental flow assessment has produced hundreds of approaches for defining environmental flow requirements for various ecosystems worldwide. This multiplicity of methodologies reflects the global diversity of ecosystems, management scales, data availability, analytical capacity, and the incorporation of social and ecological values in myriad ways.

As a field, environmental flow science has been criticised for focusing mainly on method development with little attention given to monitoring, evaluation, and revision of strategies (Souchon *et al.*, 2008; Davies *et al.*, 2014). Significant advances have been made in characterising stream hydrology and natural flow regimes but understanding of the flow-ecology relationships which underpin most environmental flow methodologies remains limited (Poff & Zimmerman, 2010; Davies *et al.*, 2014; Warfe *et al.*, 2014). As a result, the ecological benefits of environmental flow actions are often inferred or assessed only for target species. There is a collective call for improved ecological monitoring to understand environmental flow outcomes and improve decision-making (Poff & Zimmerman, 2010; Shafroth *et al.*, 2010; Gillespie *et al.*, 2015; King *et al.*, 2015). It has been suggested that environmental flow projects should function as restoration ecology experiments (Bunn & Arthington, 2002; Arthington & Pusey, 2003) to inform management and clarify cause-effect relationships between flow and ecological variables

such as biological community structure (vegetation, macroinvertebrate, or fish), instream habitat, or vegetation biomass (Poff & Zimmerman, 2010; Shafroth *et al.*, 2010). The environmental flows in Painkalac Creek provide a unique opportunity to test ecological responses to the environmental flow manipulations.

1.5. Research aim

The primary goal of this research was to assess the ecological impacts of the Painkalac Creek environmental flow prescription, particularly the summer low flow freshes (LFF) that are recognised as an important component of the natural flow regime. The LFF were pre-scheduled and could therefore support a manipulative experiment that used stream biofilm as a bioindicator community. The nutritional quality of the biofilm was evaluated by characterising the phospholipid fatty acid (PLFA) content and the structure of bacterial, algal, and fungal assemblages within the biofilm was examined using multiple DNA barcoding regions (16S, 23S, ITS). The lack of diatom abundance data from the selected DNA assays led to the development of a novel approach for gleaning diatom data from the 16S bacterial assay. By comparing the regulated stream reach that received the scheduled environmental flow releases to two unregulated reaches with natural streamflow pulses, I tested whether the environmental flows shifted the community structure or nutritional quality of biofilm communities. To the author's knowledge, this study is the first to use DNA metabarcoding or PLFA to measure ecological responses to environmental flows.

The Basin

2.1. Chapter overview

A river basin, catchment, or watershed is the contributing land area for a particular body of water. The characteristics of rivers are driven in large part by basin-level processes such as topography, geology, and land use practices. This chapter considers the hydrologic character and hydroclimate of the Painkalac catchment basin (Figure 2.1) within a water budget conceptual framework and examines key features of the hydrograph. Also known as a water balance, a water budget calculates various hydrologic compartments based on the balancing of system inputs and outputs. A water budget can help to establish management guidelines and support sustainable water management by considering system supply against demand. The effects of impoundment and withdrawals are also examined using some key features of the hydrograph including the frequency of cease-to-flow events (Bond & Kennard, 2017).

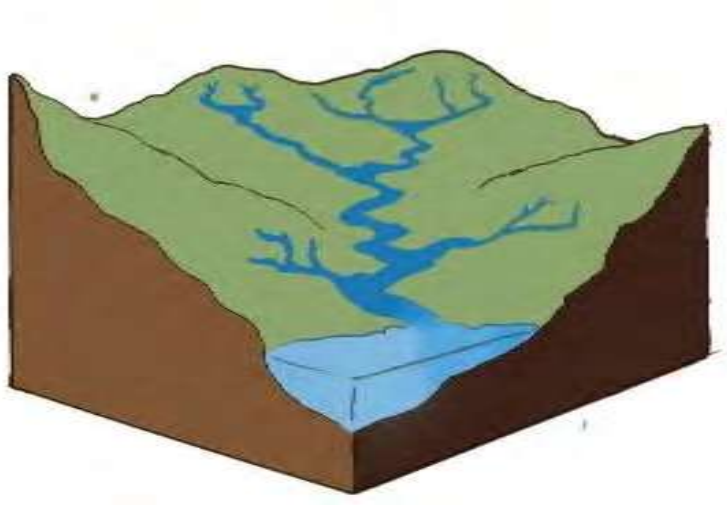

Figure 2.1. Schematic diagram of Painkalac catchment and reservoir (Credit: Emma Hess).

2.2. Introduction

Accurate knowledge of the water balance is the primary requirement for water resource management (Crosbie *et al.*, 2010) and provides a framework for characterising hydrological behaviour and assessing the impacts of changes on the partitioning of rainfall into hydrologic compartments (Zhang, Dawes & Walker, 2001). The amount of rain that falls and is lost to the stream, the groundwater, and the atmosphere is described by Equation 2.1:

$$P = ET + R + G \qquad 2.1$$

Where P is precipitation, ET is evapotranspiration, R is surface runoff measured as streamflow, and G is groundwater recharge. Precipitation, as the input to the system, varies spatially and temporally and it is important to note that mean annual precipitation is declining in many regions of the globe as the atmospheric demand for water increase with increasing temperature. Global climate models suggest a mean annual runoff reduction of 10 to 30 percent in Victoria by 2030, relative to 1990 (Post *et al.*, 2010) and a precipitation decline of 24% with runoff reduction of 69% predicted by the end of the century under one scenario in Western Australia (Charles *et al.*, 2007).

Runoff volume, as measured at a stream gauge, is divided by the area of the catchment to provide a mean runoff depth which can be compared to precipitation depth. The proportion of the precipitation that becomes streamflow, the 'runoff ratio,' is driven by topographic, climatic, vegetative, and edaphic properties (Hornberger *et al.*, 2014). The runoff ratio drives flow simulation, water supply forecasting, infrastructure design, reservoir management, and impact assessments (Coron *et al.*, 2012). Annual runoff is more variable in Australia and southern Africa than anywhere else in the world (Peel,

McMahon & Finlayson, 2004) and the runoff ratio is generally low, estimated at about 10% across southeast Australia (Chiew *et al.*, 2011).

Groundwater recharge is the drainage or percolation of water beyond the root zone of vegetation to the underlying aquifer and more generally, infiltration is the movement of water from the surface to the subsurface (Scanlon *et al.*, 2006). The infiltration rate is closely tied to runoff processes and is determined by vegetation and soil properties (Crosbie *et al.*, 2010) and as such, infiltration and recharge patterns are highly variable spatially (Ludwig *et al.*, 2005) and seasonally (Coron *et al.*, 2012). The groundwater recharge component of the water balance is sometimes omitted under the assumption that recharge rates are stable on an annual basis (e.g. Dooge, Bruen & Parmentier, 1999) but groundwater flow processes can be highly dynamic (Brunner, Simmons & Cook, 2009) and groundwater flow between surface catchments can strongly affect catchment water budgets (Coron *et al.*, 2012). In an Australian context, recharge is poorly understood with relatively few measurements of groundwater recharge across the continent due to the complexity, spatial heterogeneity and associated high cost of estimating recharge (Petheram *et al.*, 2014). Nevertheless, sustainable groundwater management to meet human and ecosystem needs requires accurate estimates of groundwater recharge (Scanlon *et al.*, 2006).

Evapotranspiration (ET) is the encompassing term for the proportion of the precipitation that leaves the system through the combined processes of evaporation from the soil surface, sublimation, and transpiration by plants (Thornthwaite, 1948; Ladson, 2011). The amount of ET is affected by both physical and biological processes including net radiation, rainfall interception, advection, turbulent transport, canopy resistance, leaf area, and plant water availability (Zhang *et al.*, 2001). The theoretical maximum, 'potential evapotranspiration' (PET), is the rate at which ET would occur without any

constraint in available moisture (Thornthwaite, 1948) and is distinguished from actual evapotranspiration (AET) which is the amount of water transferred from a surface to the atmosphere as water vapour (McMahon *et al.*, 2013). In arid regions, catchments are capable of losing more water than is gained through precipitation so PET frequently exceeds AET and AET functionally equals precipitation (Huxman *et al.*, 2005). In humid regions, AET is limited by energy rather than rainfall (Zhang *et al.*, 2001) and AET is only slightly lower than PET (Morton, 1983).

Because it cannot be measured directly, AET is generally estimated by relating PET to the available water (Brooks, Ffolliott & Magner, 2012) using estimates based on pan evaporation measurements or by applying evapotranspiration algorithms to climate data (Chiew *et al.*, 2002). In the past, calculations of ET were made using data from sparsely located weather stations but more recently, procedures have been developed that utilise gridded weather data (Allen *et al.*, 2021). In 2001, the Australian Bureau of Meteorology released a set of Evapotranspiration Maps for Australia (Chiew *et al.*, 2002) and several gridded evapotranspiration estimates are now available including various estimates produced by Morton models (Morton, 1983; Zajaczkowski & Jeffrey, 2020). Morton models have been widely applied in Australia because they do not require wind data which were not readily available until recently (McMahon *et al.*, 2013). Morton's point potential ET (PPET) is the ET that would occur from a small area with an unlimited water supply, which is approximately the same as the evaporation measured by a Class A pan device. Morton's wet-environment areal potential ET (APET) represents the ET that would occur from a large area under the condition of an unlimited water supply (McMahon *et al.*, 2013). The APET measure is the same as the classic PET, calculated from Priestley and Taylor (1972), with adjustments for large-scale advection effects during winter (Morton, 1986). The areal actual ET (AAET) is the ET that takes place from a large

area under the existing water supply conditions. Morton's complementary relationship estimates AAET using values for PPET and APET (Morton, 1983).

A fundamental assumption in the forecasting of hydrologic conditions is that future conditions can be predicted based on past conditions. In this assumption, known as 'stationarity', water supply, distribution, and treatment systems are designed based on probabilistic predictions bounded by historic conditions (Milly *et al.*, 2008). The boundaries provided by the 'historic range of variability' have been pushed by anthropogenic watershed alterations and by external climate factors that oscillate on time scales beyond the instrumental record, but uncharacteristic events are becoming less of an exception and more of a rule. More than decade ago, mounting violations to the assumption of stationarity caused a group of climate scientists to assert that, "stationarity is dead" (Milly *et al.*, 2008) because under a changing climate, every component of a hydrologic regime can exhibit non-stationarity (Horne *et al.*, 2019).

Evidence is accumulating that historical relationships between rainfall and runoff are breaking down. During Australia's Millennium drought (1997-2009), unprecedented reductions in observed runoff could not be fully explained by reductions in rainfall (Chiew *et al.*, 2014; Saft *et al.*, 2015) with changes in mean annual runoff approximately two to three times the percent changes in mean annual rainfall (Chiew *et al.*, 2009). In their analysis of 228 catchments in south-eastern Australia during the drought, Saft *et al.* (2015) found that about half (46%) of the catchments exhibited a significant change in the runoff ratio. In the American Southwest, reconstruction of historical climate based on tree-ring chronologies has shown that recent runoff ratio trends are unprecedented across a 445 year record (Lehner *et al.*, 2017). Dry antecedent conditions and disconnections between surface and groundwater have been proposed as explanations (Chiew *et al.*, 2011) but overall, there is a large degree of uncertainty when rainfall runoff

models are run under climatic conditions that are significantly different from the calibration conditions (Coron *et al.*, 2012). Projections for Australia's future climate are generally drier and the conditions experienced during the Millennium Drought are expected to occur more frequently (Chiew *et al.*, 2011).

2.3. Methods

2.3.1 Rainfall

There is no single, long-term precipitation record for the Painkalac Creek catchment so daily rainfall data were examined from several weather stations (BOM, 2020a)(Table 2.1). The first rainfall measurement for the immediate area was recorded at the Eastern View weather station (#090037) on 3rd June 1923 but that station closed in December 1980. The Aireys Inlet weather station (#090180) replaced the Eastern View station and the first rainfall recorded was 26 June 1994. In estimating the water budget, only the years 2010-2020 were considered to match the other datasets.

Table 2.1. Australian Bureau of Meteorology weather station details (BOM, 2020a)

Station	Number	Elevation (m)	Dates	Mean rainfall (mm)	Lat	Long	Percent complete
Aireys Inlet	090180	105	1994-2021	623.6	38.4583	144.0883	96
Eastern View	090037	unknown	1914-1980	735.5	38.4500	144.1000	86

Figure 2.2. Painkalac catchment highlighted in blue with symbols denoting locations of stream gauges (DELWP, 2016a), weather stations (BOM, 2020a), and monitoring bores (DELWP, 2016b).

2.3.2 Evapotranspiration

Class A pan evaporation and Morton's areal actual, point potential, and wet environment areal potential evapotranspiration records for the Aireys Inlet station (#90180) were obtained from the SILO Data Drill for a period of analysis from 01/01/2010 to 31/12/2020 (www.longpaddock.qld.gov.au/silo, (Jeffrey *et al.*, 2001)). Evaporation from the reservoir was also estimated using the Class A pan method (Brooks *et al.*, 2012). The average annual evaporated volume was calculated using:

$$E = C_e E_p A \qquad 2.2$$

where C_e = pan coefficient; E_p = pan evaporation (m/yr); and A = reservoir area (m^2). A conservative average pan coefficient of 0.70 was applied to the annual Class A pan evaporation value (Khan, 2008; Brooks *et al.*, 2012).

2.3.3 Temperature

Daily mean, maximum, and minimum temperatures were obtained from the Australian Bureau of Meteorology (BOM, 2020b). Air temperature has been recorded at the Cape Otway lighthouse since 1864 but local measurements from Aireys Inlet were not collected until 2010 (Table 2.2).

Table 2.2. Available temperature data (BOM, 2020b)

Station	Number	Elevation (m)	Dates	Lat	Long
Aireys Inlet	090180	105	2010-2020	38.4583	144.0883
Cape Otway Lighthouse	090015	82	1864-2020	38.8556	143.5128

The regional air temperature trend was visualised using the Show Your Stripes tool (Hawkins, 2019) that depicts the local Berkeley Earth land/ocean temperature

record as colours that are +/- 2.6 standard deviations of the average annual temperature in 1971-2000 (Rohde & Hausfather, 2020).

In order to consider the local temperature trend, and particularly the frequency of hot days, the number of days with a maximum temperature of more than 32°C for the thirty year record of the Aireys Inlet (station # 090180) was calculated following the design by O'Day (2016). This hot day tally was then visualised on a bar plot using the grouping and tallying functions within the Tidyverse package (Wickham *et al.*, 2019) and a linear regression line was added.

2.3.4. Hydrology

Catchment delineation

Catchment boundaries were delineated using the 'Create Watersheds' tool in ArcGIS Online. The stream gauge locations were treated as pour points and the contributing watershed area was determined from the HydroSHEDS hydrologically conditioned digital elevation model (Lehner & Grill, 2013).

Streamflow

Flow data were obtained through the Water Measurement Information System of Victoria (WMIS) (DELWP, 2016a). The gauges, co-managed by WMIS and Barwon Water, each have a concrete weir and the discharge rating curves are regularly evaluated (Table 2.3). Measurement of streamflow in Painkalac Creek began on 27 March, 1974 (#235232), just below the reservoir. Gauging of the upstream reach of Painkalac Creek, above the reservoir, began in 1999, near the approximate start of the Millennium Drought. Inflow to Painkalac Reservoir is approximated by the measured discharge at station 235257

because other inputs are small, ephemeral channels. The measured discharge above the reservoir was used as an estimate of surface runoff for the water balance model.

Prior to analyses, streamflow data were checked and cleaned. Extrapolated rating values were allowed but values where the rating table was exceeded or the data was suspect were removed. Periods of missing data ≤7 days in length were filled using linear interpolation.

Table 2.3 Stream gauge details (DELWP, 2016a). Catchment area calculated using HydroSHEDS (Lehner *et al.*, 2017).

Station name	Station ID	Installation date	Lat	Long	Catchment Area (km^2)
Painkalac Upstream	235257	25/03/1999	-38.436317	144.045981	33.26
Painkalac Downstream	235232	26/03/1974	-38.442204	144.070519	36.39

To investigate changes in the hydrologic regime associated with the operation of Painkalac Dam and the domestic water diversion, the streamflow before, during, and after the reservoir withdrawals were compared. Hydrologic statistics were compiled using R 3.5.0 (R Core Team, 2019), the Hydrostats package (Bond, 2015b), and the Hydrologic Time-Series Summary Tool (Bond, 2015a). The period of missing discharge data for station 235232 (07/04/1992-20/01/1999) was excluded from the analysis. The monthly mean stream discharge for the drought period (1999-2009) was compared to the period since (2010-2019) to visualise the drought hydrograph. Internal Barwon Water operational data and WMIS gauge data (stationID: 235232) (DELWP, 2016a) were used to visualise the relationship between released flows and flows measured at the gauge.

Groundwater

Aquifer and groundwater details were obtained from the Victorian Department of Environment, Land, Water and Planning Groundwater resource reports (DELWP, 2019)

and the statewide bore monitoring network data (DELWP, 2016b). The Painkalac catchment is encompassed by the Otway-Torquay Groundwater Catchment. The lower portion of the catchment is mapped as part of the Jan Juc groundwater management area but the upper portion of the catchment has not been ascribed to a particular groundwater management unit. There is one station that is part of the state observation bore network (#116460), located on the eastern edge of the Painkalac catchment (Figure 2.2).

Reservoir size

The surface area of Painkalac Reservoir was estimated manually using a recent ESRI high-resolution World Imagery Basemap featuring Maxar Vivid imagery (0.5m resolution, 01/10/2019) (Figure 2.3). Based on the steep topography and consistent reservoir storage volume throughout the year, a single reservoir area of approximately 13.5 hectares (0.135 km^2) was applied throughout the year. The total input volume to the reservoir was calculated by adding the stream discharge (#235257) to the volume of water produced from the annual precipitation (mm) applied to the reservoir area of 0.135 km^2.

Figure 2.3. Painkalac Reservoir polygon on Maxar Vivid aerial imagery (0.5m resolution, 01/10/2019).

2.4 Results & Discussion

Please note, in the subsequent data chapters, the results and discussion sections will be presented separately but the discussion is embedded within the results in this chapter to provide a concise summary of the catchment conditions.

2.4.1 Rainfall

The annual mean rainfall at the Aireys Inlet station (#090180) is 653 ± 72 mm, based on the period of record, since 1995 (BOM, 2020a). The highest daily rainfall recorded at Aireys Inlet was 100.8 mm on 22 March, 2017 and the wettest month on record was March, 1995 when 309 mm of rain was recorded. July and August are, on average, the wettest months but extreme rainfall events occur throughout the year (Figure 2.4). A mean annual precipitation of 624 mm (2010-2020) was used as the precipitation term for the water budget to match the evapotranspiration dataset.

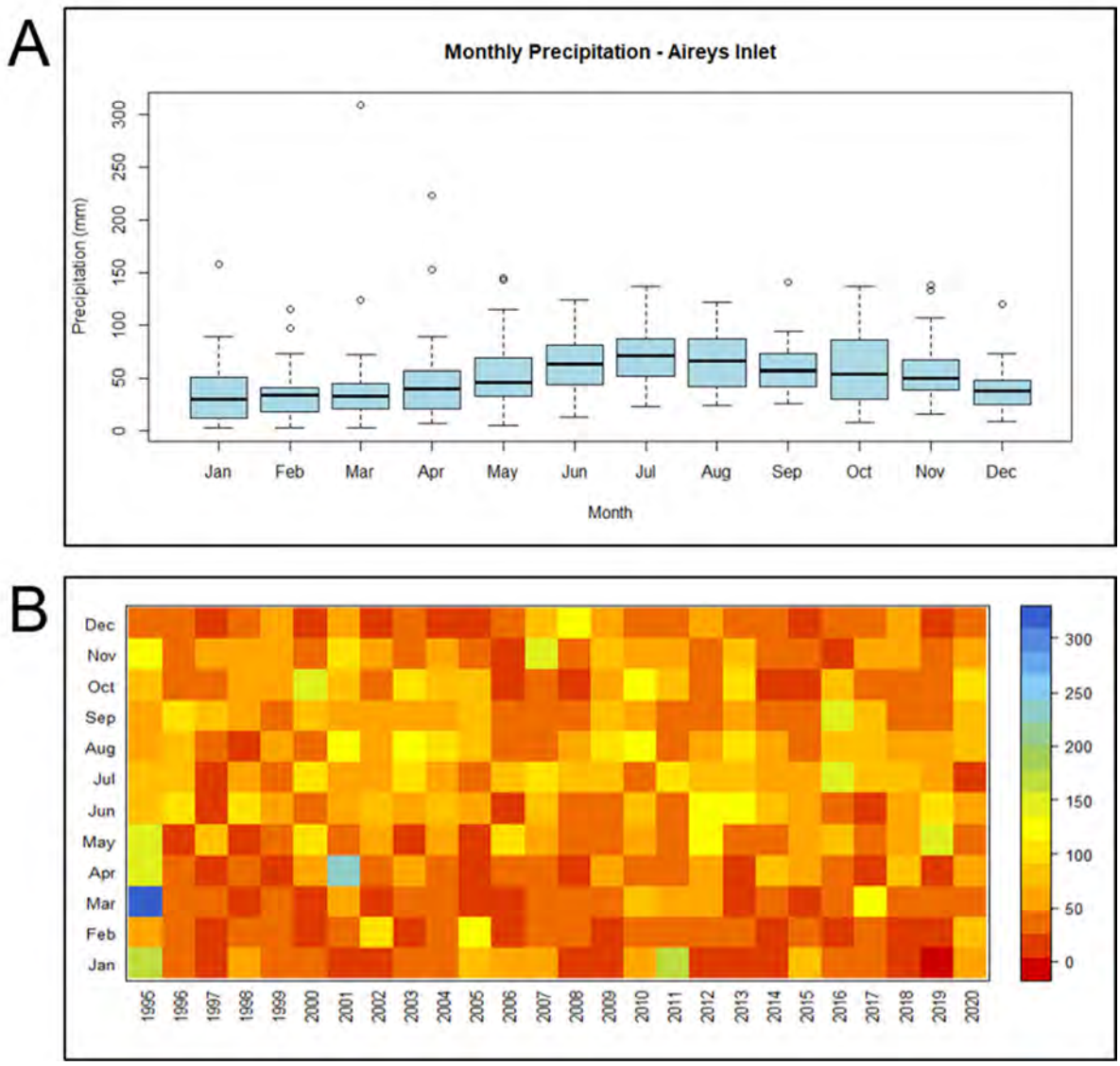

Figure 2.4 Monthly precipitation (mm) at Aireys Inlet (#090180) 1995-2020 as A) Boxplot and B) heatmap.

2.4.2 Evapotranspiration

Morton's PPET averages 1350 mm/year, which is similar to the evaporation measured by a Class A pan device (1322.7 mm/year) (Table 2.1.). Morton's APET averages 1013.7 mm/year and average AAET is 1350.2 mm/yr.

Table 2.4. Evapotranspiration values (mm) for Aireys Inlet from 1/1/2010 - 31/12/2020 (stationID:90180, www.longpaddock.qld.gov.au/silo, (Jeffrey *et al.*, 2001)). APET = Morton's areal potential evaporation, PPET = Morton's point potential evapotranspiration, AAET = Morton's areal actual evapotranspiration, and Pan evap. = measured Class A pan evaporation).

Year	APET	PPET	AAET	Pan Evap.
2010	1043.1	1284.1	802.7	1225.3
2011	1024.6	1306.6	743.3	1183
2012	1059.1	1398.8	718.2	1344.9
2013	1049.4	1396.1	704.6	1396.8
2014	1072.7	1383.6	760.9	1362.2
2015	1011.0	1352.5	667.8	1383
2016	956.4	1312.3	600.1	1324.8
2017	1007.8	1336.4	678.5	1325.7
2018	1008.3	1393.1	623.5	1374.9
2019	1012.4	1432.2	590.5	1424.2
2020	906.4	1256.6	555.3	1204.5
Average	**1013.7**	**1350.2**	**676.9**	**1322.7**

Based on the 13.5 ha estimated reservoir area, an average annual pan evaporation of 1322 mm/year, and a pan coefficient of 0.70, the average volume of water that evaporates each year from Painkalac Reservoir is estimated as 124.8 ML/year. To estimate the difference between the evaporation from the water surface and the ET of the vegetation it replaced, the difference of Morton's average PPET and AAET for 2010-2020 was calculated as 673.4 mm. When this value is applied to the reservoir area (0.135 km^2), it is estimated that an additional 90.7 ML/year evaporates from the water body. This means that almost 60% of the 160 ML/year that was previously diverted continues to be lost to evaporation each year as a result of the impoundment. An annual

evaporative loss of approximately 18% of reservoir yield is consistent with the 20% loss estimated for major reservoirs in Australia (McMahon *et al.*, 2013).

2.4.3 Runoff

Runoff in the Painkalac catchment is highly variable in terms of volume and ratio. The mean annual runoff volume, measured at the Painkalac Upstream gauge (stationID:235257), was 2022 ML and the mean runoff ratio was 9.3% (Table 2.5). The runoff ratio for the Painkalac catchment is consistent with an estimate of 10% across southeast Australia (Chiew *et al.*, 2011) and the data reflect Australia's extreme runoff variability (Peel *et al.*, 2004). Comparing the high and low years of 2013 and 2015, there was more than a 20-fold difference in runoff volume. Although 2015 was the lowest runoff volume, the runoff ratio was the highest measured (18.9%) versus in 2013, when the rainfall was highest, and the proportion that ran off was lowest (1.3%).

Table 2.5 Streamflow and runoff for upper Painkalac catchment from 2010 to 2020. (Rainfall (BOM, 2020a). Runoff is total annual upstream discharge (DELWP, 2016a, stationID: 235257). Runoff depth is runoff volume divided by catchment area of 33 km2. Runoff ratio is the ratio of runoff depth to rainfall.)

Year	Rainfall (mm)	Runoff volume (ML)	Runoff depth (mm)	Runoff ratio (%)
2010	768	2923	88.6	11.5
2011	708	1629	49.3	7.0
2012	726	2965	89.9	12.4
2013	703	4376	132.6	18.9
2014	498	1147	34.8	7.0
2015	489	204	6.2	1.3
2016	717	3589	108.7	15.2
2017	610	1985	60.1	9.9
2018	434	725	22.0	5.1
2019	525	1392	42.2	8.0
2020	686	1310	39.7	5.8
Average	**624**	**2022**	**61.3**	**9.3**

2.4.4 Water budget

On average, 61 mm of water is measured running off the upper Painkalac Catchment each year although the estimated annual losses from ET (677 mm) exceed the estimated precipitation inputs of 624 mm (Figure 2.5)

	Depth (mm)	Volume (ML)
Rain	624	+20,838
Evapotranspiration	677	-22,608
Runoff	61	-2,033

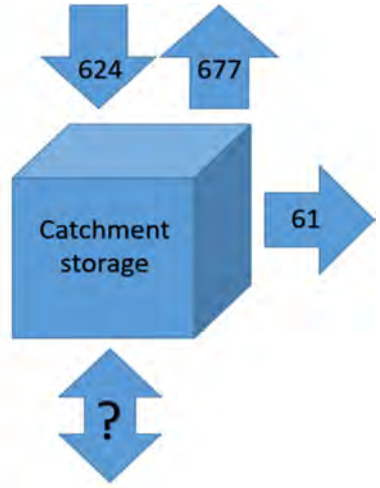

Figure 2.5. Water balance for upper Painkalac catchment (2010-2020).
Rain = Annual mean rainfall (BOM, 2020a). Evapotranspiration is Morton's AAET (stationID:90180, www.longpaddock.qld.gov.au/silo, (Jeffrey *et al.*, 2001)). Runoff volume is total annual upstream discharge (DWELP 2016a, stationID:235257) and runoff depth is volume/33 km^2 catchment area.

Two possible explanations for this observation are the low spatial resolution of the forcing meteorological data (Zhang *et al.*, 2016) and deficiency in the representation of the maritime influence on local hydrology (Noske, Lane & Sheridan, 2017). Because AAET cannot be measured directly, it is estimated from weather observations and estimates of solar radiation (Ladson, 2011) and the estimate of AAET is a broad-scale, derived value that may not provide adequate resolution at a local catchment scale (Chiew *et al.*, 2002). Morton's models have been widely applied in Australia because they do not require wind data (McMahon *et al.*, 2013) but AAET is considered an approximate estimate of AET that should only be used when more accurate data are unavailable (Zajaczkowski & Jeffrey, 2020).

If the groundwater flux is considered to be zero and only one term of the water budget is unknown, another estimate of AET can be calculated from precipitation minus streamflow (Brooks *et al.*, 2012). By this method, the estimated value of AET is 563 mm, which is less than the precipitation input value. However, groundwater flow between surface catchments can strongly affect catchment water budgets (Coron *et al.*, 2012) particularly with underlying geologic strata such as limestone (Brooks *et al.*, 2012). Due to the underlying limestone and the apparent groundwater influence on surface flow, the zero groundwater flux assumption is not appropriate here.

Hydrologic data from the small coastal catchments draining the southeast side of the Otway Ranges are not generally included in regional hydrology investigations because they do not meet the size threshold of 50 km^2 (e.g. Post *et al.*, 2010; Saft *et al.*, 2015), at least above the stream gauge. As a result, existing hydrologic models can perform poorly in these coastal ecosystems (Noske *et al.*, 2017). The limited predictive capacity and overestimation of water stress has been attributed to the maritime influence that reduces temperatures and elevates the relative humidity (Noske *et al.*, 2017). Interactions of fog, dew and precipitation with vegetation and topography would be expected to produce variability in local soil moisture dynamics. When a catchment straddles the energy-limited/water-limited divide, different algorithms are required for estimating AET across the catchment (McMahon *et al.*, 2013).

Morton's approach has been used extensively in hydrologic modelling (Cai & Jones, 2005) but the approach is losing favour as better meteorological data becomes available (Zajaczkowski & Jeffrey, 2020). Estimates of ET should be implemented in hydrologic forecasting with some caution but as data inputs and algorithms improve, ET estimates are also expected to improve (Frost, Ramchurn & Oke, 2017) and the

estimation of evapotranspiration is generally moving towards remote sensing-based approaches (Guerschman *et al.*, 2009; Nagler *et al.*, 2016; Jarchow *et al.*, 2017).

2.4.5 Reservoir storage

With a designed capacity of 516 ML, Painkalac Reservoir can hold about one third of the mean annual catchment volume or alternatively, it can store approximately four months' worth of rain. On average, 2,106 ML has flowed into Painkalac Reservoir annually and 2,033 ML has flowed out, between 2010 and 2020 (Table 2.6). In five of 11 years, the volume of water measured at the gauge below the reservoir exceeded the estimated volume of water coming into the reservoir. While small differences might be explained by gauging error, large differences suggest a groundwater contribution to streamflow in the downstream reach and the difference of 61.5 percent in 2015 deserves more attention.

The annual mean volume of water stored in Painkalac Reservoir is 441 ML, based on records provided by Barwon Water. The reservoir is maintained at a minimum of 50% capacity to protect the integrity of the dam so the maximum flood control capacity is only about 250 ML. In most years, Painkalac Reservoir fills to capacity in a single storm (Figure 2.6).

Table 2.6. Estimated inflow, outflow and storage volume for Painkalac Reservoir Input is total upstream discharge (ML)(DELWP, 2016a stationID: 235257) plus precipitation on reservoir area (ML) (BOM, 2020a). Output is downstream discharge (DELWP, 2016a stationID: 235232). The difference is described by Input-Output which, when divided by the input, represents the % difference.

Year	Input	Output	Storage Volume	Input-Output	% difference
2010	3027	2466	415	560	18.5
2011	1724	2193	500	-469	-27.2
2012	3063	3266	485	-203	-6.6
2013	4471	3587	443	884	19.8
2014	1214	1019	465	195	16.1
2015	270	103	389	166	61.5
2016	3685	4271	392	-586	-15.9
2017	2067	2185	518	-117	-5.7
2018	784	888	445	-104	-13.3
2019	1463	1325	409	137	9.4
2020	1402	1057	395	345	24.6
Average	**2106**	**2033**	**441**	**73.6**	**7.4**

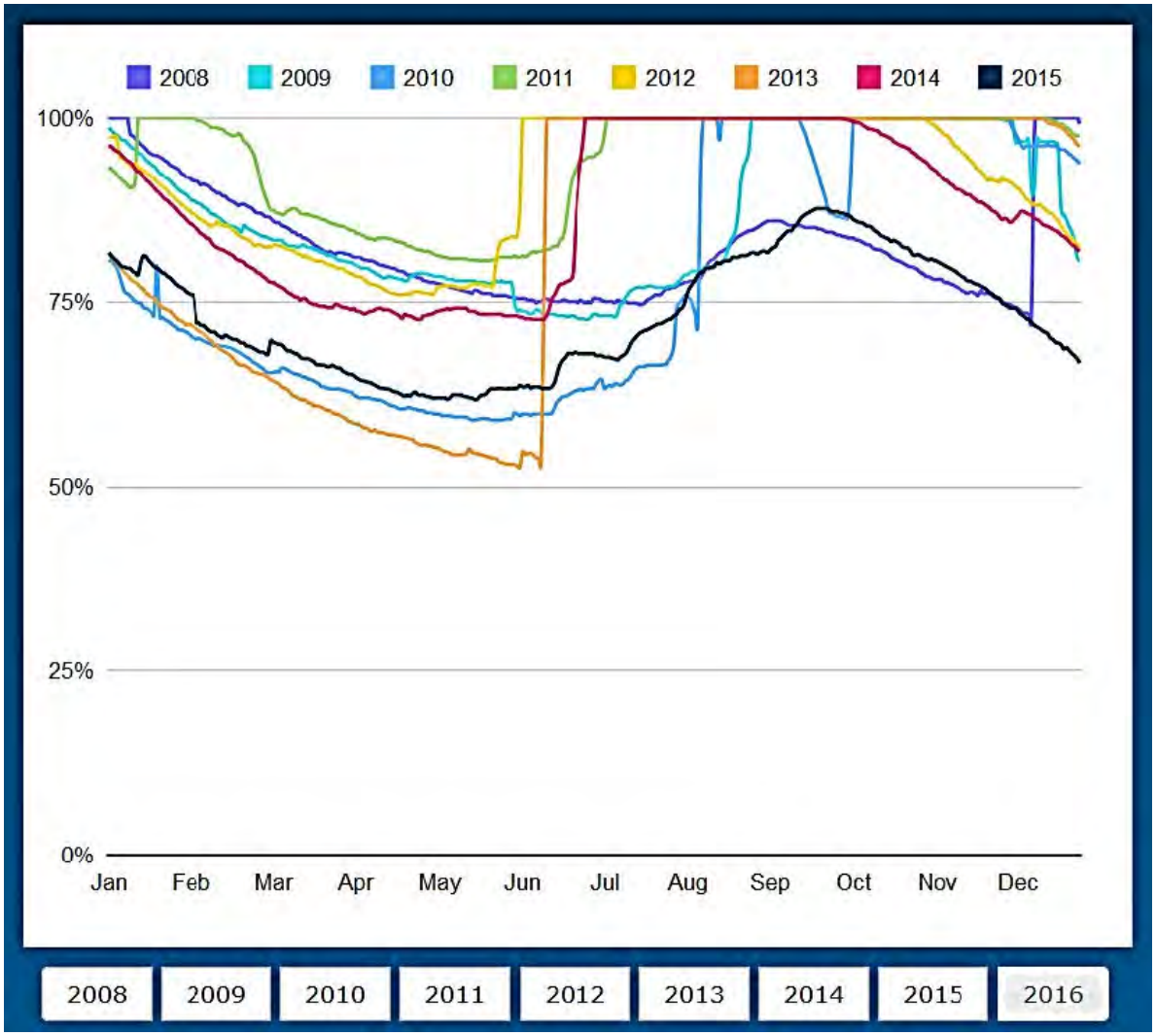

Figure 2.6. Painkalac Reservoir storage as percent capacity by month (2008-2015) (Barwon Water, 2016).

2.4.6 Groundwater

The Painkalac Downstream reach flows through an alluvial deposit of unconsolidated sediment and no naturally occurring rocks were observed at any site (Figure 2.7). Groundwater levels were not measured as part of the project but the behaviour of surface water in Painkalac Creek provides some insights into groundwater conditions.

Figure 2.7. Looking across Painkalac Creek at freshly exposed soft sediment face, just below the dam outlet.

When Painkalac Reservoir was supplying domestic water, water released from the dam often failed to reach the gauge during summer (Figure 2.8). As groundwater levels recede, surface water bodies can become disconnected from the underlying groundwater system, leaving a region of unsaturated flow between the two water compartments (Brunner *et al.*, 2009). In this disconnected hydrologic regime, the infiltration rate from the surface water bodies is effectively independent of changes in the groundwater table. The creek may have functioned as a losing stream that poured water into the aquifer below. Now that withdrawals have ceased, this effect appears to have stabilised and since 2018, dam releases reach the downstream gauge with the released discharge closely

matching the measured discharge at the gauge. Environmental flows released during 2018 were consistently recorded at the gauge and flow was maintained throughout the summer along the entire downstream reach. As a result, the stream now consistently remains connected to the estuary throughout the year.

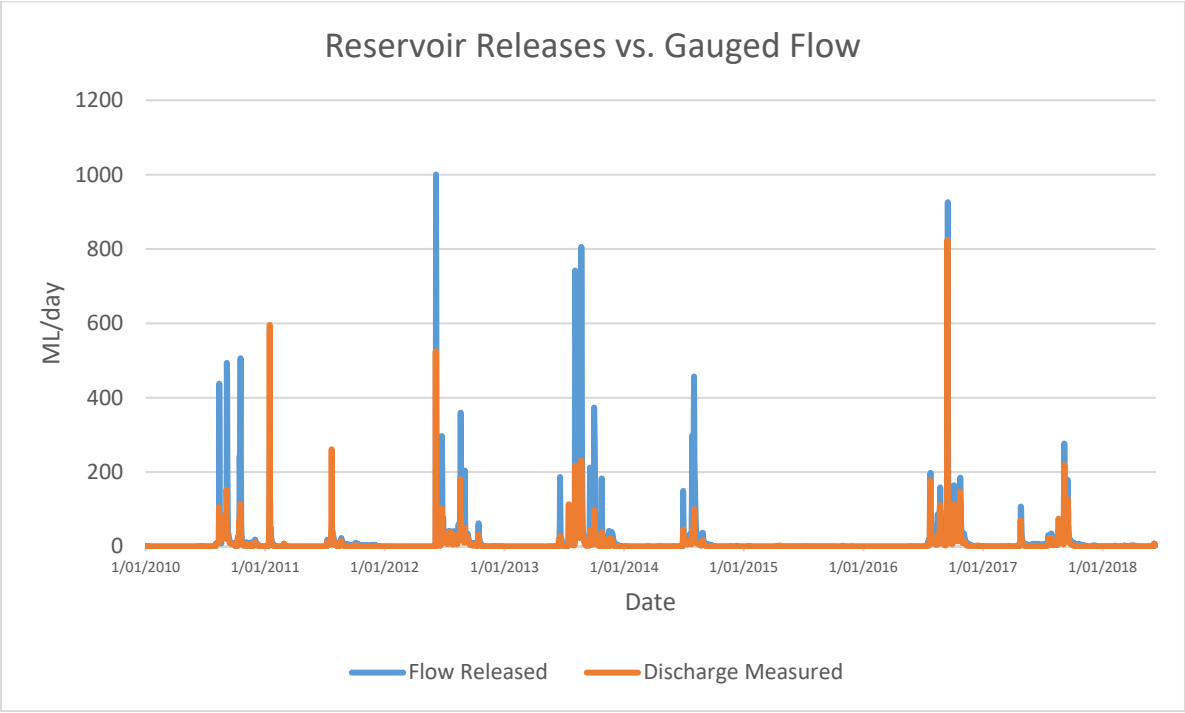

Figure 2.8. Painkalac Reservoir releases (Barwon Water data) versus gauged downstream discharge (2010-2018) (DELWP 2016a stationID:235232)

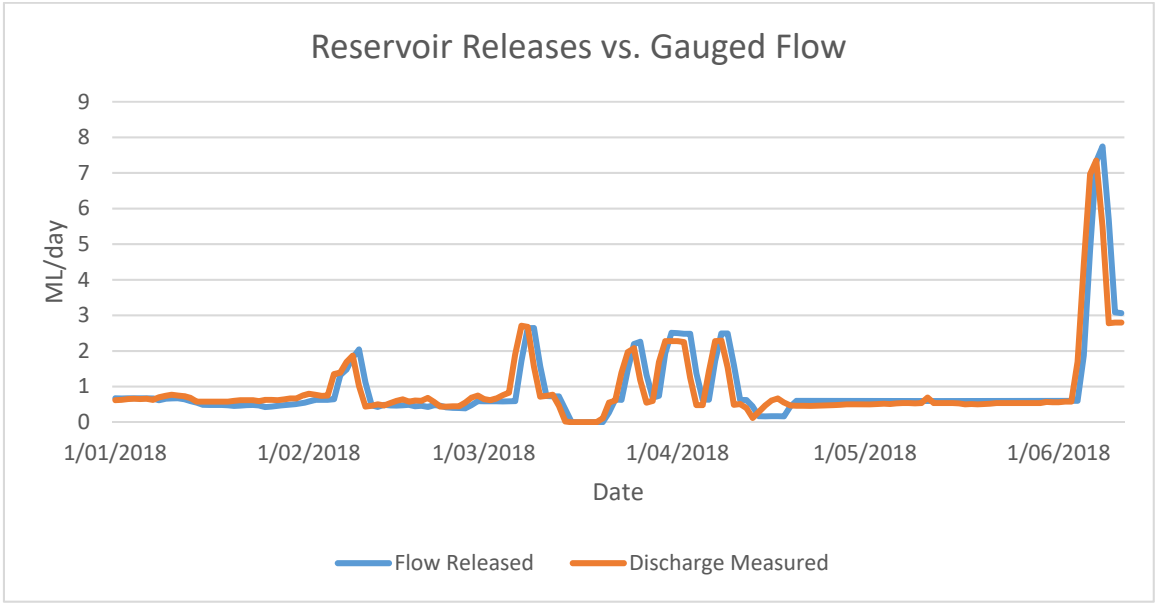

Figure 2.9. Painkalac Reservoir releases versus measured discharge for period: 01/01/2018 to 11/06/2018 (DELWP, 2016a stationID: 235232),

Drilling records for the monitoring bore at the edge of the surface catchment (#116460)(Figure 2.2) show several layers of clay overlying the water-bearing limestone formation which suggests a confined aquifer system (VVG, 2021). When the well was drilled in 1994, the potentiometric surface of the aquifer was 159 m below the ground surface but by 2020 it had descended to 169 m (Figure 2.10). The hydrostatic head pattern indicates that for the last 25 years, discharge from the aquifer has exceeded recharge. The depletion not only indicates a decline in total catchment storage volume, it also highlights a potential risk for seawater intrusion into the coastal aquifer (Werner, 2010).

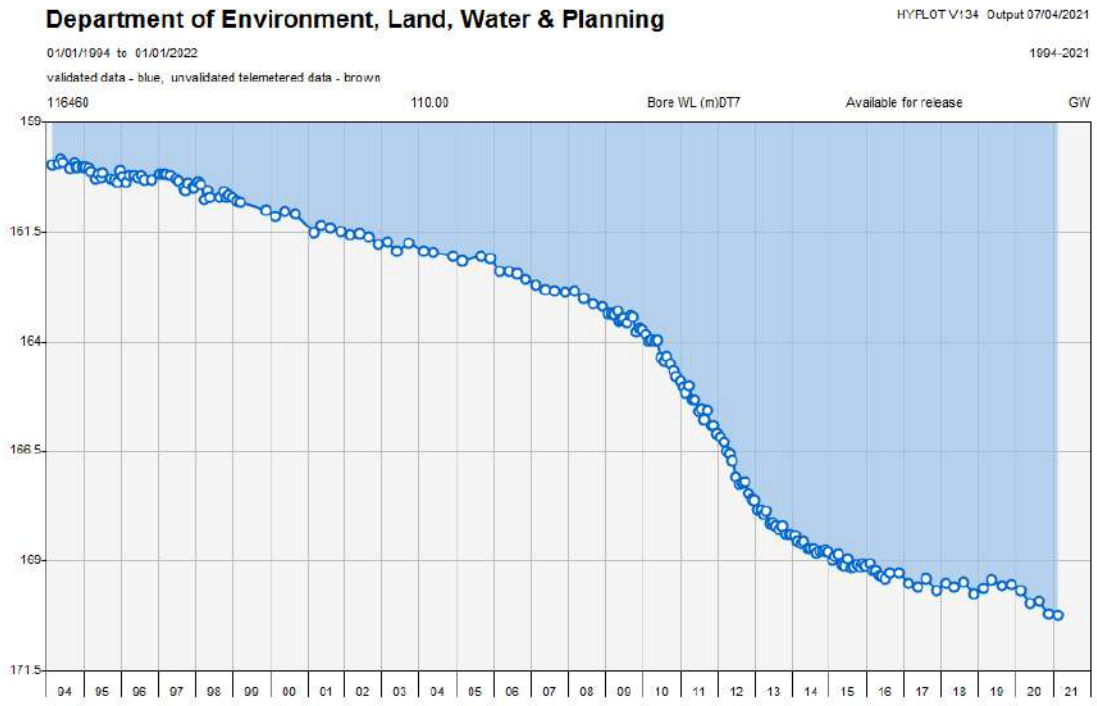

Figure 2.10. Groundwater levels at monitoring bore #116460 (DELWP, 2016b)

2.4.7 Stream hydrology

The Painkalac Upstream reach flows mainly over bedrock with a few deep pools (Figure 2.11). There is minimal floodplain and limited bank storage capacity in the steep, narrow valley so the system is generally flashy with rapid wetting and drying cycles. The annual coefficient of variation for the upstream reach is 86.4. Cease-to-flow (CTF) events occur 34% of the time with an average duration of 24 days since gauging began in 1999 (Bond, 2015a; DELWP, 2016b). The longest CTF in the upstream reach lasted 246 days.

Figure 2.11. Looking upstream at Duck Pond Track gauge site when Painkalac Creek had dried to disconnected pools. Streambed is a pocked and fractured mudstone. The buoy and experimental frame are visible towards the back of the pool. The steel pole to the right is the stream height gauge (DELWP, 2016a stationID: 235257).

Streamflow in the downstream reach has been diminishing over time, from a mean discharge of 21.60 ML/day based on the three pre-dam years to a mean of 5.70 ML/day from 2016-2020 (Table 2.7,Figure 2.12). Although the withdrawals have ceased, the mean annual flow remains low (Figure 2.13).

Table 2.7. Periods of analysis and summaries of Painkalac Creek discharge for three periods: prior to dam (Pre-dam), during the dam operation with withdrawals (Dam), and dam in operation without any withdrawals (DamNW) applied to Painkalac Creek discharge data just below the dam (DELWP, 2016a stationID: 235232) for the specified time periods.

Period	start	end	min	Q10	mean	median	Q90	max	Annual cv
Pre-dam	1974-03-27	1977-12-31	0.10	44.90	21.60	1.50	0.30	2682.90	68.27
Dam	1978-01-01	2016-05-02	0.00	17.90	9.50	0.50	0.00	2300.50	34.97
DamNW	2016-05-03	2020-12-31	0.00	10.20	5.70	0.80	0.40	824.40	53.96

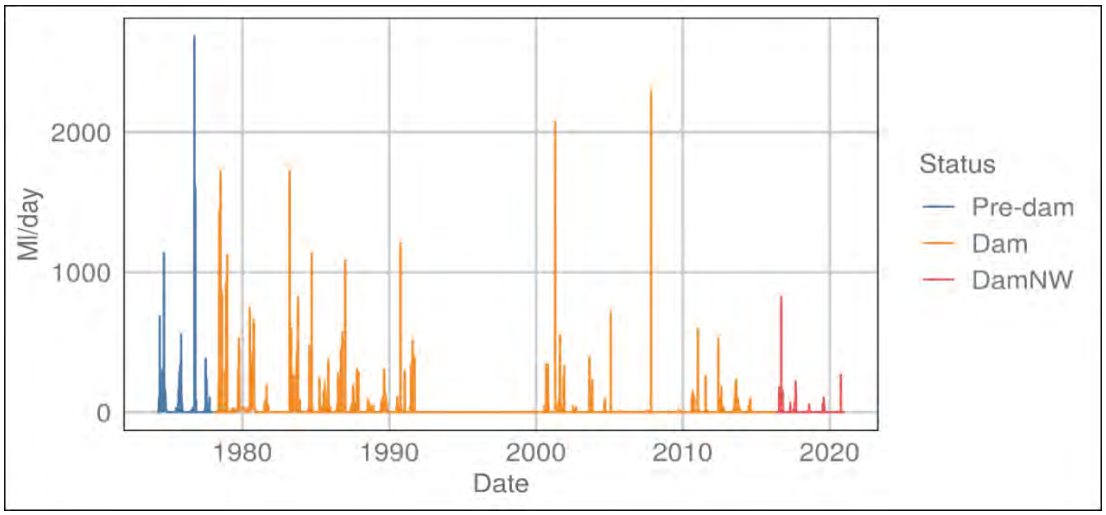

Figure 2.12. Painkalac Creek hydrograph 1974-2020 with three periods (Bond, 2015a; DELWP, 2016a stationID: 235232). Blue portion is prior to dam completion, orange series is the withdrawal period, and red series is the hydrograph since withdrawals ceased. No discharge measurements occurred from 07/04/1992 to 20/01/1999.

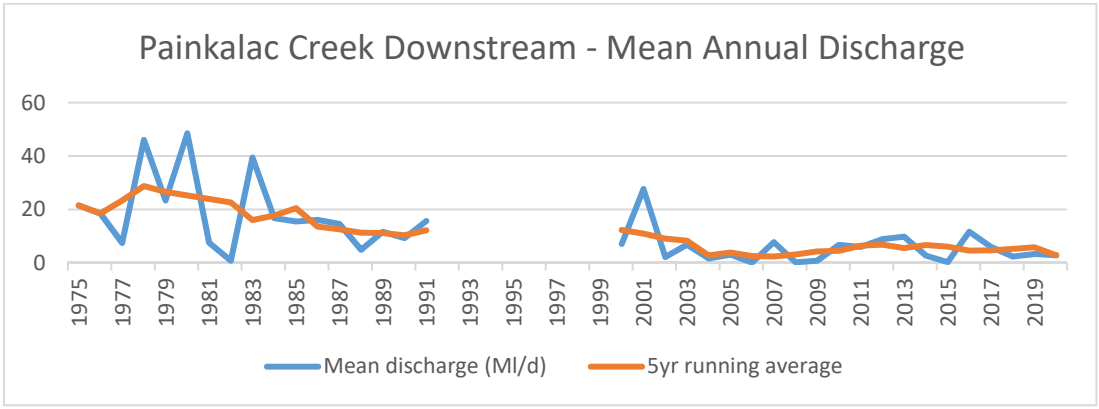

Figure 2.13. Painkalac Creek Downstream discharge (1975-2019) (DELWP, 2016a stationID: 235232). Mean annual discharge is shown in blue with the 5 year running average shown in orange. No discharge data is available from 07/04/1992-20/01/1999.

The pre-dam annual coefficient of variation in streamflow was 68.27 which dropped to 34.97 during the withdrawal period and has increased again since withdrawals have ceased. Before the dam was constructed and since the withdrawals ceased, CTF occurred only 1% of the time but while withdrawals were taking place, CTF events occurred 16% of the time in the downstream reach. When withdrawals were taking place, during the Millennium Drought, a 227-day CTF period extended from November 2006 until July 2007. Streamflow was generally lower during the drought but the most striking change was the absence of winter peak flows (Figure 2.14).

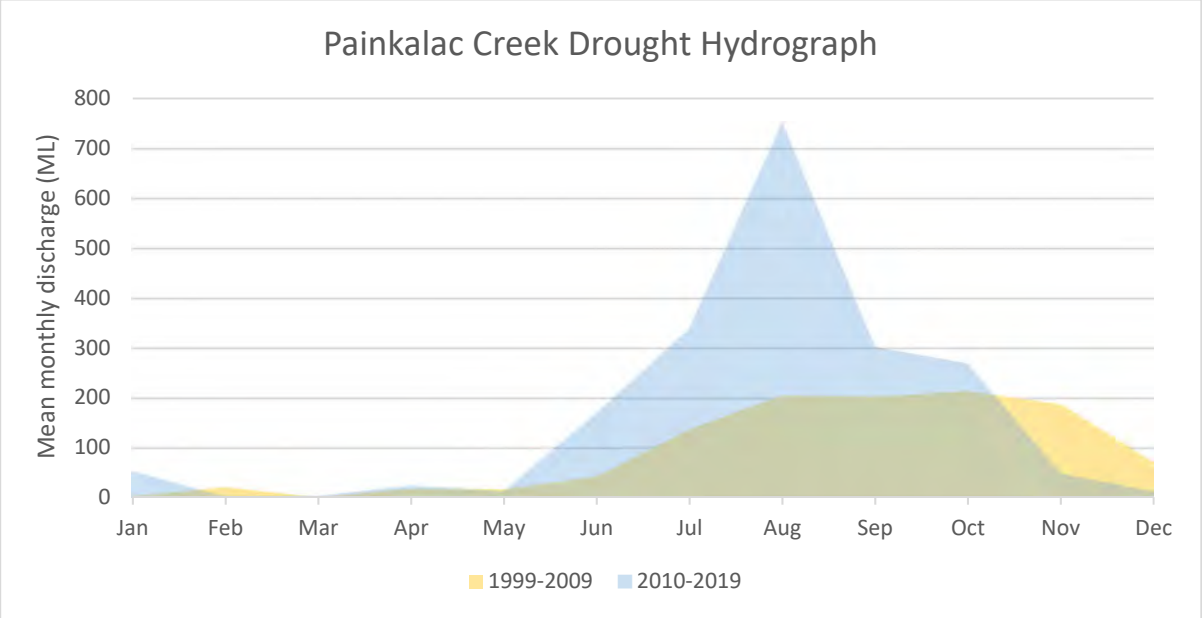

Figure 2.14. Painkalac Creek mean monthly discharge for Millenium Drought (1999-2009, yellow) and post-drought (2010-2019, blue) periods (DELWP, 2016b stationID: 235257)

2.4.8 Temperature

Regional temperatures are increasing and Victoria is consistently warmer than it was a century ago (Figure 2.15). Hot days are becoming more common in Aireys Inlet, with a maximum of 20 days exceeding 32°C in 2019 (Figure 2.16).

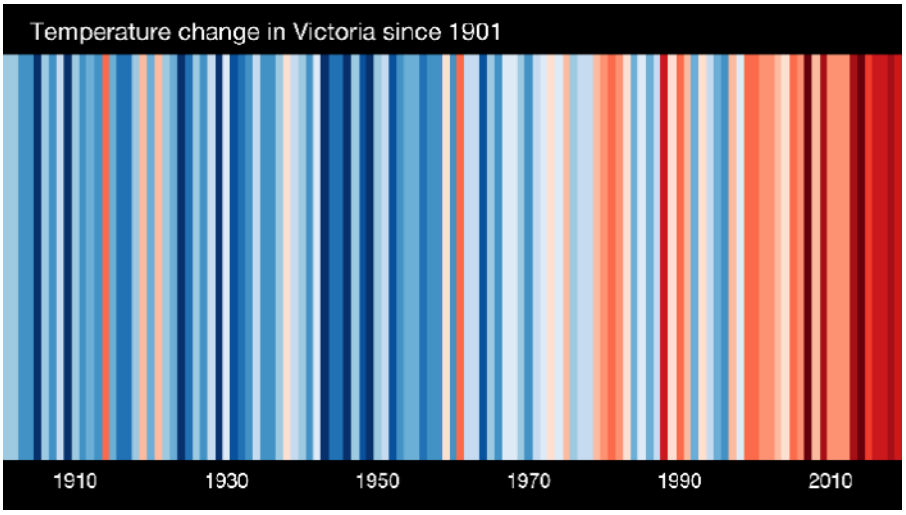

Figure 2.15. Warming stripes for Victoria since the start of the 20th century (Image Credit: Ed Hawkins, University of Reading, CC BY 4.0). Colours are +/- 2.6 standard deviations of the average annual temperature in 1971-2000 (Rohde & Hausfather, 2020).

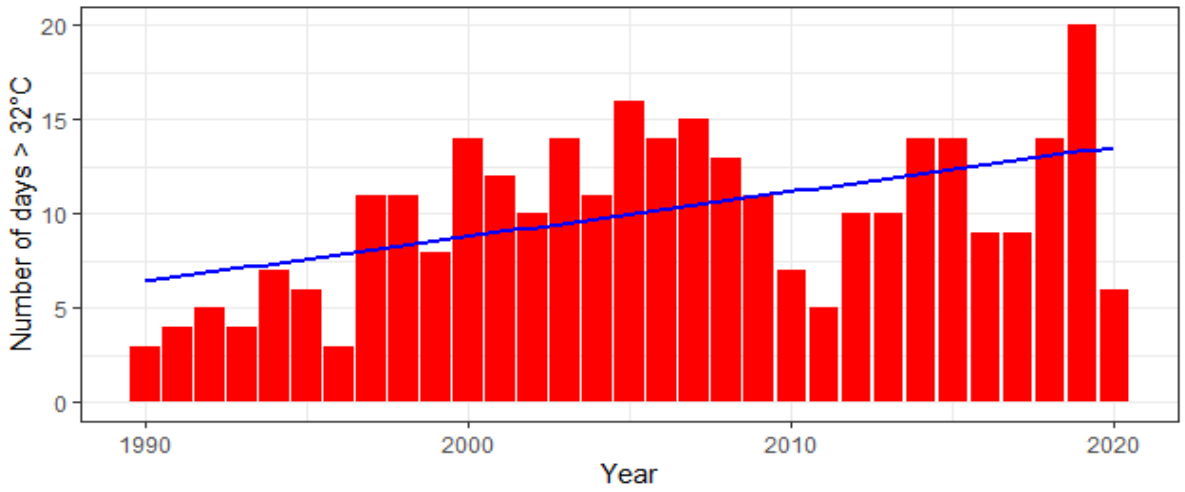

Figure 2.16. Number of hot days per year in Aireys Inlet (station: 090180 (BOM, 2020b)). Red bars represent number of days in each year with a maximum temperature greater than 32° C. Blue line is a fitted linear regression model.

2.5 Conclusion

The Painkalac Basin is characterised by high variability in runoff, declining trends in streamflow and groundwater levels, and increasing temperatures. Improved estimates of the components of the catchment water balance are required to better guide local water resource management in the future. Improved understanding of runoff-generation processes, evapotranspiration and groundwater dynamics are necessary to manage sustainable use and guide policymakers in coping with climatic extremes (Allen *et al.*, 2021). Locally, better hydrologic data are important in prioritising prescribed fire treatments to mitigate hydrologic risks to communities and water supplies (Noske *et al.*, 2017). Closer examination of local rainfall measurements, radar data and catchment-scale runoff generation processes (UM & DSE, 2012) together with the application of emerging remote-sensing approaches (Guerschman *et al.*, 2009; Jarchow *et al.*, 2017) will improve water resource accounting, planning, and management.

Without the withdrawals, the stream flows more consistently throughout the year and cease-to-flow periods are rare downstream of the dam. However, almost 60% of the 160 ML/year that was previously consumed continues to be lost to evaporation each year as a result of the impoundment. This loss from the system is particularly important in low rainfall years and there is a possibility that a sustained drought period of low precipitation coupled with these evaporative losses could drive the reservoir storage volume below 50%.

Painkalac Reservoir provides limited flood control capacity due to its small size relative to the catchment runoff volume. Because runoff in the Painkalac catchment is extremely variable with a 20-fold difference between years, and as extreme rainfall events can occur throughout the year, it is difficult to anticipate and manage the flood

storage capacity of the reservoir. The reservoir often fills to capacity in a single storm and remains full until late summer. During the periods when the reservoir is full, all inflow spills over, maintaining a natural flow regime downstream.

Biofilm as a Bioindicator

3.1. Chapter overview

This chapter uses a manipulative field experiment to evaluate stream biofilm as a bioindicator. This study investigated the phospholipid composition and community structure of biofilm samples and associated water quality in two streams in Victoria, Australia. Biological community profiles from DNA metabarcoding were compared against phospholipid profiles to consider whether phospholipid fatty acid (PLFA) composition accurately characterised community structure and assessed sensitivity to abiotic variables. I then applied these data to evaluate the performance of the environmental flow prescription by comparing the experimental outcomes of natural flow pulses and environmental flow pulses (Chapter 4).

3.2. Introduction

Freshwater biofilms have been suggested as ideal bioindicators of river health because they are responsive to environmental conditions, ubiquitous and ecologically significant (Burns & Ryder, 2001). However, their potential has not been fully realised due to challenges in accurately and efficiently characterising the diverse constituents of stream biofilm communities (Battin *et al.*, 2016). Recent advances in molecular sequencing, including high-throughput sequencing and metabarcoding, offer new opportunities to measure microbial community dynamics and evaluate stream health at the base of the food web (Sagova-Mareckova *et al.*, 2021).

Microscopic biofilm communities develop wherever water meets hard surfaces, including human teeth, medical implants and boat hulls (Costerton, 1999). Biofilm

communities are ubiquitous across a range of aquatic substrates, both living and dead, including submerged vegetation, logs, sand and rocks (Burns & Ryder, 2001; Sigee, 2005). In a stream, biofilm communities comprise algae, fungi, bacteria and other microorganisms within a gelatinous extracellular matrix (Wetzel, 1983; Lock *et al.*, 1984; Sigee, 2005). Colonisation of new substrate occurs within hours, and cells may divide more than twice daily (Lowe & Pan, 1996).

Stream biofilms are ecosystems-in-miniature with a complex network of trophic interactions including various autotrophic producers, consumers such as protozoans and metazoans, and a range of decomposers (Weitere *et al.*, 2018). Heterotrophic biofilm community members form part of the microbial loop responsible for stream decomposition and nutrient cycling (Sigee, 2005), while autotrophic members (also referred to as benthic algae or periphyton) are responsible for most of the photosynthesis in sunlit streams (Lowe & LaLiberte, 2017). Biofilm communities are shaped by disturbances, stressors, resource availability, hydraulic conditions and biotic interactions (Larned, 2010) but composition of the microscopic community has been challenging to characterise.

Morphological identification relies on the assessment of features under a microscope so the largest members of the biofilm community have the longest history of quantification. Diatoms have been routinely used as bioindicators in freshwater ecosystems for decades (Stevenson, Pan & Van Dam, 2010) but identification difficulties have limited the use of other microorganisms (Pawlowski *et al.*, 2016). Most fungi can only be morphologically distinguished by their spores, hence identification generally requires that reproduction be induced under laboratory conditions (Gulis & Suberkropp, 2003; Bärlocher, Stewart & Ryder, 2011). As a result, few studies have included fungal identification, and fungal biomass has often been estimated using ergosterol (a sterol in

fungal cell membranes) as a biochemical proxy (e.g. Gulis & Suberkropp, 2003; Bärlocher *et al.*, 2011).

Bacterial identification is similarly challenging. Early studies of bacteria used lab cultures to produce 'viable counts', but in some cases less than 0.5% of bacteria were cultivated (Scholz & Boon, 1993) because highly selective techniques excluded many organisms based on their nutritional and environmental needs (Sigee, 2005). Under the microscope, bacterial cells must be stained to stand out from other particulate matter (Boulton & Boon, 1991; Scholz & Boon, 1993; Sigee, 2005). Direct counting is labour-intensive, therefore bacterial cells tend to be counted in broad categories based on colour, shape and size (e.g. Hieber & Gessner, 2002).

By overcoming microbial identification challenges, the use of DNA-based identification tools provides a novel opportunity to investigate biofilm communities and a growing body of evidence demonstrates consistent performance between morphological and molecular techniques (Ji *et al.*, 2013). The assessment of particular taxonomic marker genes is referred to as 'amplicon sequencing' or 'metabarcoding' (Creer *et al.*, 2016). In metabarcoding, a primer pair tags a gene region so that the encompassed fragment (amplicon) will be amplified during a polymerase chain reaction (PCR) (Ji *et al.*, 2013). High-throughput sequencing allows thousands or even millions of amplicons to be read simultaneously, producing a long list of DNA sequences (Ji *et al.*, 2013). The resulting sequences (also known as 'reads') are cleaned and attributed to known taxa based on a series of steps collectively referred to as a 'bioinformatics pipeline' (Porter & Hajibabaei, 2018).

Different taxonomic marker genes, or barcodes, are used to distinguish different taxa and the selection and standardisation of appropriate marker genes is an active research area (Porter & Hajibabaei, 2018). Marker choice can significantly impact

community resolution through primer bias and differential performance across various sequence lengths and taxonomic groups (Porter & Hajibabaei, 2018). Assessment of biofilm communities requires the investigation of at least two gene regions, one for prokaryotes and another for eukaryotes (Bradley, Pinto & Guest, 2016; Pawlowski *et al.*, 2018).

The level of taxonomic resolution required for effective biomonitoring is a debated and complex topic (Rimet & Bouchez, 2012; Pawlowski *et al.*, 2018). There are several accepted methods for taxonomic assignment (Porter & Hajibabaei, 2018) and taxonomic reference databases vary in terms of completeness and reliability (Keck *et al.*, 2017). In this study, taxonomy was assigned using a similarity-based method (Porter & Hajibabaei, 2018) based on a score calculated from the statistical significance of matches. For many groups of organisms, including microbial metazoa and diatoms, there is a 'genome deficit' where reference sequences are sparse (Zimmermann *et al.*, 2014; Creer *et al.*, 2016). Reads can be assigned to high-level taxa based on phylogeny, but lower levels of taxonomic assignment require that the species be correctly identified in a database. Taxonomic identification is progressing slower than sequencing, so unnamed sequences are quickly accumulating. For example, only 115,000–140,000 fungal species are currently named, of the predicted 2.2–3.8 million species (Lücking & Hawksworth, 2018). The ability to extract meaningful information about individual taxa is therefore being outstripped by the rate of genomic data generation (Thompson *et al.*, 2017).

Since molecular techniques can characterise thousands of microorganisms per sample, the focus of biomonitoring is shifting from individual indicator taxa to the entire community, or microbiome. The term microbiome, originally coined by Whipps and colleagues (1988) and recently refined (Berg *et al.*, 2020), describes a characteristic microbial community occupying a reasonable, well-defined habitat with distinct physio-

chemical properties. The microbiome includes the microorganisms and the environmental 'theatre of activity' which defines their specific ecological niche. Because members of the microbiome include bacteria, archaea, fungi, algae, and small protists (Marchesi & Ravel, 2015), the term is suitable for describing the stream biofilm community. Just as different plant structures (leaves, roots, bark etc.) harbour different microbiota and each compartment of the human body contains its own microbiota (Berg *et al.*, 2020), the aquatic microbiome can be characterised by various ecological compartments including water (Ling *et al.*, 2018), sediment (Wolff, Clements & Hall, 2021) and biofilm (Fish & Boxall, 2018).

Another tool that has been used to describe microbial communities is phospholipid characterisation. Lipids and their fatty acids are components of all living organisms (Couturier *et al.*, 2020). Phospholipids produced only by photosynthetic organisms, but required for most animals, are termed essential fatty acids (EFA) (Arts, Ackman & Holub, 2001). In aquatic systems, eicosapentaenoic acid (EPA, 20:5n3), docosahexaenoic acid (DHA, 22:6n3) and arachidonic acid (ARA, 20:4n6) were traditionally recognised as EFAs (Galloway & Winder, 2015), but linolenic acid (LIN, 18:2n-6) and α-linolenic acid (ALA, 18:3n-3) are now also considered essential (Parrish, 2009).

Consumers largely rely on the production of EFAs by aquatic primary producers to provide basic nutrition (Ruess & Müller-Navarra, 2019), so algal-derived EFAs play an important role in secondary production in streams (Dalu *et al.*, 2016). In biofilm, phospholipid fatty acid (PLFA) content correlates with factors such as light and nutrient levels (Larned, 2010; Hill, Rinchard & Czesny, 2011) and varies through space (Guo *et al.*, 2015) and time (Schnurr *et al.*, 2020). Since algae may respond to limiting abiotic factors

by increasing their lipid production, PLFA content may also vary among individuals and across populations (Sharma, Schuhmann & Schenk, 2012; Schnurr *et al.*, 2020).

In aquatic ecosystems, PLFAs have been used as taxonomic biomarkers (e.g. Whorley & Wehr, 2016), trophic biomarkers (e.g. Dalsgaard *et al.*, 2003; Galloway & Winder, 2015) and as a measure of food quality (e.g. Hill *et al.*, 2011; Larson *et al.*, 2013). The use of PLFA to characterise microbial community structure is especially common in soil studies (Orwin *et al.*, 2018), but PLFA biomarkers have also been used as a proxy of aquatic community structure (e.g. Scholz & Boon, 1993; Webb-Robertson, Bunn & Bailey, 2011). Phospholipids are considered strong biomarkers because they are essential components of cell membranes, deteriorate quickly after cell death, are absent from storage lipids and anthropogenic contaminants and exhibit high turnover rates (Mrozik, Nowak & Piotrowska-Seget, 2014). The main disadvantages of PLFA biomarkers are that they have low taxonomic resolution and individual PLFAs may be associated with multiple organisms across a diverse set of taxa (Willers, Rensburg & Claassens, 2015). For example, the marker 16:1n7 has been attributed to both diatoms (Hill *et al.*, 2011) and fungi (Akinwole *et al.*, 2014). In a study of 2,000 algal strains, Lang *et al.* (2011) found clear relationships between fatty acid markers at the taxonomic levels of division and class, but patterns were variable at lower taxonomic levels. Consequently, overlapping associations may blur the classifications of phylogenetic or functional groups based on PLFA profiles (Webb-Robertson *et al.*, 2011).

The trophic conservation of fatty acids was first suggested by Lovern (1934) and encouraging results came out of laboratory experiments in the 1960s, suggesting clear patterns of transfer from one trophic level to the next (Dalsgaard *et al.*, 2003). However, when PLFA metrics were applied to field research, the distinct patterns observed in pure cultures were not observed in complex environmental samples (Willers *et al.*, 2015).

While some classes of benthic primary producers possess a distinct pattern of PLFA, there is too much overlap between groups to accurately determine their contributions to higher trophic levels (Kelly & Scheibling, 2012).

The nutritional quality of the biofilm for higher trophic levels is also described by PLFA composition. Characterising lipid quality is important in aquaculture but rarely conducted in stream ecology (Parrish, 2009). In general, aquatic studies report levels of EFAs (EPA, DHA and ARA) to quantify food resource quality in freshwater ecosystems. These studies do not suffer from the same obstacles as biomarker studies because PLFAs can be quantified collectively as a food resource regardless of microbial source (e.g. Napolitano *et al.*, 1994; Schnurr *et al.*, 2020).

Just as PLFA have been used to describe biota, biota have been used as indicators of environmental conditions and relationships between environmental pollutants and aquatic biota have been recognised since the mid-1800s (Bellinger & Sigee, 2015). Bioindicators are organisms that readily reflect some measure of the habitat where they are found (McGeoch & Chown, 1998), and they indicate ecosystem condition by assimilating the collective and cumulative impacts of stressors and contaminants (Burger, 2006). Correspondence between biological assemblage data and environmental data supports has supported the development of various biotic indices of ecological condition (Hill *et al.*, 2000).

Freshwater ecosystems have most commonly been assessed using aquatic macroinvertebrates as bioindicators (Bonada *et al.*, 2006), but stream biofilm has been suggested as a more responsive and representative bioindicator community (Burns & Ryder, 2001). In addition to being ubiquitous and abundant, biofilm assemblages are characterised by high species richness, short life cycles and efficient dispersal, which translate to rapid and detectable responses to environmental changes (Lowe & Pan,

1996; Burns & Ryder, 2001). This responsiveness to stressors at local to global scales (Sagova-Mareckova *et al.*, 2021) also qualifies biofilm as a biomonitoring tool that can be uniformly applied across large spatial scales (Bonada *et al.*, 2006). Anthropogenic impacts on streams include changes in stream form (geomorphology) and function (hydrology) as well as water contamination by human sewage, heavy metals, persistent organic pollutants and nutrients (Stoeck *et al.*, 2018). An ideal biomonitoring tool should discriminate between these different impact types to effectively guide management interventions (Bonada *et al.*, 2006; Bunn *et al.*, 2010).

Diatoms are the only microbiota within the biofilm community currently incorporated into routine freshwater biomonitoring programs (Sagova-Mareckova *et al.*, 2021). DNA metabarcoding affords new opportunities to use microbial communities as effective bioindicators, but in order to do so, biota-environment relationships must be established. The sensitivity or tolerance of particular organisms to stressors establishes their performance as indicators of stream health (Bonada *et al.*, 2006). Numerous studies have demonstrated the sensitivity of different protist taxonomic groups to environmental stressors (Pawlowski *et al.*, 2016; Stoeck *et al.*, 2018), but a compendium of microbial taxa and functional groups associated with different stressors is lacking (Sagova-Mareckova *et al.*, 2021).

This study tested the performance of biofilms as bioindicators by characterising three interrelated metrics of stream health: biological communities, environmental conditions and phospholipid composition (Figure 3.1). I conducted a field experiment in two coastal streams in Victoria, Australia. Artificial substrates were provided for biofilm colonisation on floating frames installed across three river reaches. Twelve sets of biofilm were characterised by their PLFA content and biofilm community structure was investigated on a subset of nine sets using DNA multi-metabarcoding. Three amplicons

were sequenced to examine bacterial, algal and fungal communities within stream biofilm. I examined the bacterial component of the biofilm using the standard 16S gene region (Lane *et al.*, 1985). For algae, I selected the 23S plastid rRNA region based on its performance across multiple algal lineages (Sherwood & Presting, 2007) and ability to distinguish autotrophs (Sherwood, Chan & Presting, 2008). For fungi, I selected a standard fungal barcode, the internal transcribed spacer region (ITS) (Op De Beeck *et al.*, 2014).

My primary aim was to determine whether the community structure derived from DNA metabarcoding could discriminate between stream reaches and whether the three different assemblages (bacteria, algae and fungi) achieved a similar level of discrimination. Secondly, I explored the relationships between each biological community, environmental conditions and phospholipid patterns. This experiment establishes new quantitative relationships between abiotic conditions, PLFA composition and biofilm communities in freshwater ecosystems. To my knowledge, this study is the first to apply DNA metabarcoding and phospholipid profiling concurrently in a freshwater ecosystem.

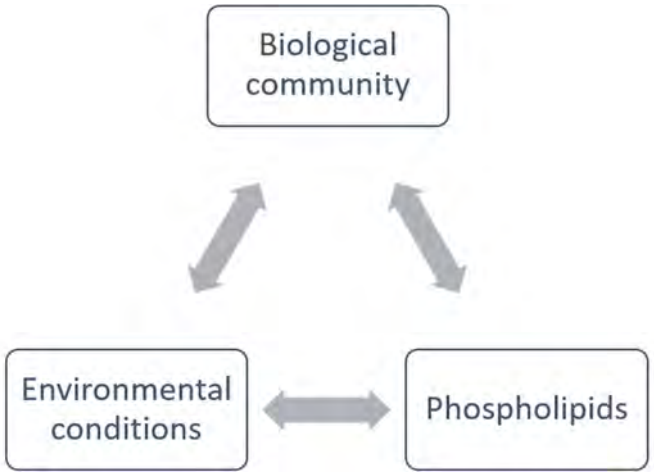

Figure 3.1. Relationships between biological community, PLFA content and abiotic conditions. PLFA: phospholipid fatty acid.

3.3. Methods

3.3.1. Study area

A field experiment was conducted in Victoria, Australia, from October 2018 to March 2019 to evaluate biofilm responses to changes in flow (Figure 3.2). The experiment was designed to measure the ecological effects of environmental flow releases using a before-after-control-impact design (BACI) (Underwood, 1992). I compared the impacted (regulated) Painkalac Downstream (PD) reach to two control reaches, the Painkalac Upstream (PU) reach and the Barham River (B) (located 50 km southwest of Painkalac Reservoir; Figure 3.2). The Barham River was selected as a control reach because it was the closest unregulated river with perennial flow. Table 3.1 compares catchment characteristics for Painkalac Creek and the Barham River.

Twelve monitoring sites were placed in Painkalac Creek in 2017, a subset of which were selected for the biofilm experiment based on similar water depth and canopy closure. Three sites were established below the reservoir and two control sites were established above. Three additional sites were also established in the Barham River. Each monitoring site consisted of a 20 m stream reach that was photographed and sampled during each site visit. Experimental datasets were first used to evaluate the performance of biofilm as a bioindicator prior to assessing the impacts of environmental flows.

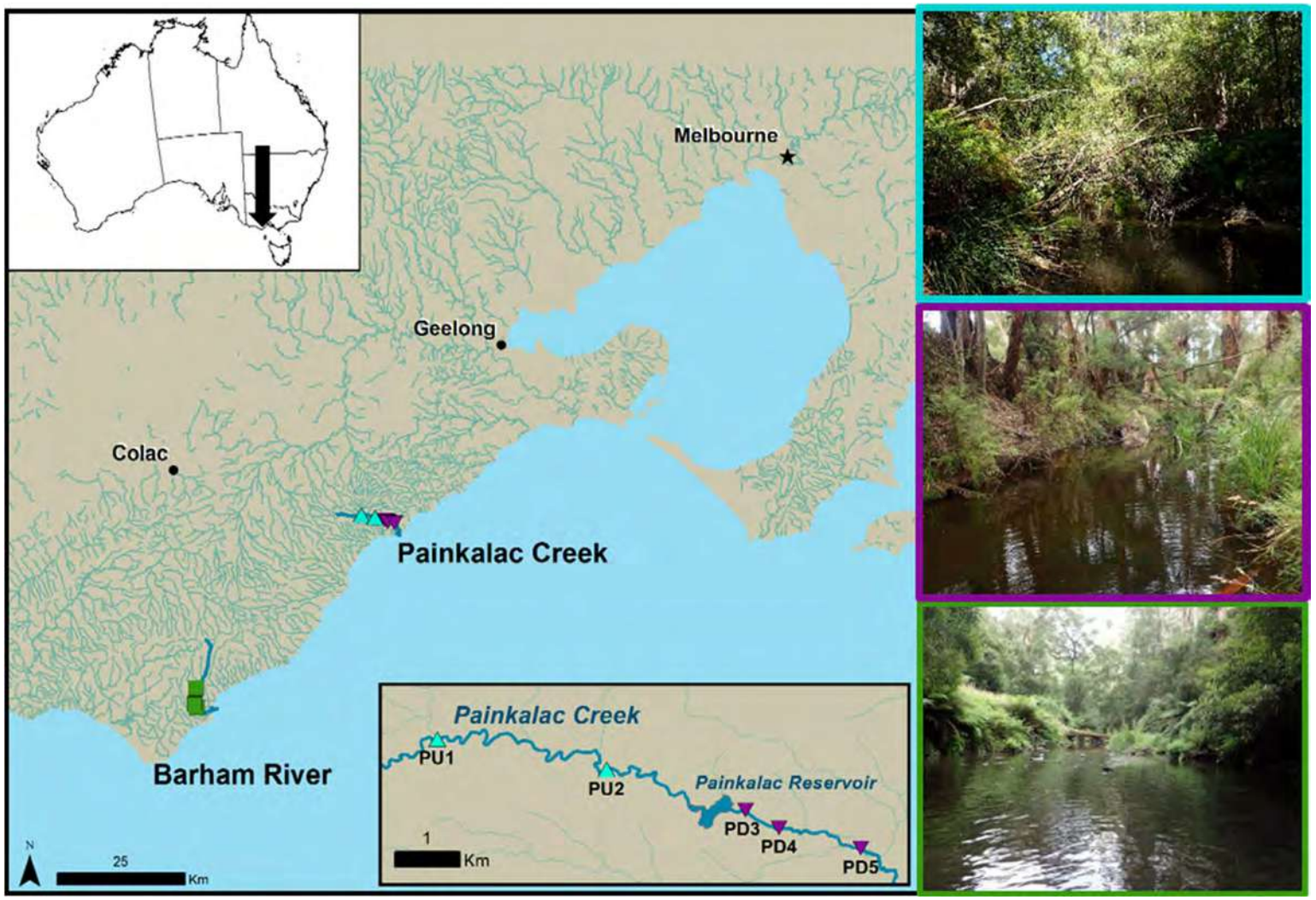

Figure 3.2. Research site locations in Painkalac Creek and the Barham River, Victoria, Australia.

Table 3.1. General catchment characteristics for Painkalac Creek and the Barham River (Mondon, Sherwood & Chandler, 2003).

River	Painkalac Creek	Barham River
Catchment size	61 km^2	79.5 km^2
Annual precipitation	865 mm	1,377 mm
Annual discharge	6,380 ML	32,910 ML

3.3.2. Physicochemical conditions

Flow data for each river was obtained through the Water Measurement Information System of Victoria (WMIS) (DELWP, 2016a). During each site visit, three random locations were selected within each 20 m monitoring site (using a random number table) for water quality measurement and sample collection.

A YSI Professional Plus handheld multiparameter meter was used to measure temperature, dissolved oxygen concentration, pH and specific conductance (Table 3.2). Turbidity (NTU) was measured using a Hach turbidimeter, model 2100Q. One composite water sample from the three random locations was collected for nutrient analysis (250 mL in a new plastic collection bottle) and a second composite water sample was collected for dissolved organic carbon (DOC) analysis (100 mL in an amber glass bottle). Water samples were stored in the field in a portable electric freezer set to −8°C. Upon return to the lab each day, nutrient samples were frozen (−20°C) and DOC samples were refrigerated (4°C) according to analysis protocols. These samples were then delivered to ALS Global in Geelong, Victoria, for laboratory analysis of total nitrogen, total Kjeldahl nitrogen, ammonia, nitrate, nitrite, total oxidised nitrogen, total phosphorous, reactive phosphorous and DOC.

Table 3.2. Environmental, nutrient and biomass variables with measurement locations and methods. PCHEMs are environmental variables used to evaluate relationships between abiotic, biotic and phospholipid fatty acid metrics. A list of all environmental variables and analysis factors is provided in **Error! Reference source not found.**.

Variable	Shortname	Measured in	Method	PCHEM
Temperature (°C)	Temp	Field	YSI multimeter	✓
Dissolved oxygen (% saturation and mg/L)	DO	Field	YSI multimeter	✓
Conductivity, as specific conductance (µS/cm at 25°C)	SPCond	Field	YSI multimeter	✓
pH	pH	Field	YSI multimeter	✓
Turbidity (nephelometric turbidity units, NTU)	turbidity	Field	Hach turbidity meter	✓
Mean velocity (m/s)	V	Field	Valdeport meter	✓
Canopy closure (%)	Canopy	Field	Convex densiometer	
Ammonia (mg/L)	NH_4	Lab	ALS	✓
Dissolved organic carbon	DOC	Lab	ALS	
Nitrate (mg/L)	NO_3	Lab	ALS	✓
Nitrite (mg/L)	NO_2	Lab	ALS	✓
P, Reactive (mg/L)	PR	Lab	ALS	
Total nitrogen as N (calculated)	TCN	Lab	ALS	✓
Total oxidised N as N (mg/L)	TON	Lab	ALS	
Total Kjeldahl N (mg/L)	TKN	Lab	ALS	✓
Total phosphorous (mg/L)	TP	Lab	ALS	✓
Biofilm chlorophyll concentration (mg/m^2)	Chl	Lab	ALS (µg/L)	
Ash free dry mass (sample weight minus ash weight)	AFDM	Lab	NuSea lab	
Mean discharge	Q	(DELWP, 2016a)	Rating curve	✓

3.3.3. Biofilm field experiment

Some authors have used the term 'stream periphyton' synonymously with stream biofilm but others have restricted the definition of periphyton to the photoautotrophic component of the biofilm community. To avoid confusion in this study, I use the term 'biofilm' to include the full suite of microeukaryotes and prokaryotes comprising the benthic biofilm community in flowing waters. Due to the wood substrate used in the experiment, the sampling was limited to epixylic biofilm (occurring on wood surfaces) but for simplicity, I use the general term 'biofilm' throughout.

In early summer 2018, a set of three wood blocks was deployed at each of the eight sites. The blocks were composed of kiln-dried mountain ash (*Eucalyptus regnans*), 2.4-cm thick with a 7.5-cm × 8.0-cm surface (area = 60 cm^2). The blocks were secured to a plastic-coated wire frame suspended from floats to maintain the blocks at a consistent depth of ~5 cm from the water surface, regardless of fluctuations in flow. Each frame held two sets of blocks in a staggered position. A maximum of six blocks were installed at a time. The floating frame was attached to an anchor line (rock substrate) or post (soft bottom) to maintain the frame's position within the stream channel (Figure 3.3).

The initial water depth at each frame location ranged from 0.45 m to 1.06 m. The water velocity at the frame location was measured using a Valdeport Model 801 electromagnetic velocity meter during each site visit. The sensor was placed at the height of the blocks and velocity and total water depth were measured at two corners and the midpoint along one side of the frame.

Figure 3.3. Floating experimental frame. A) Floating experimental frame attached to an anchor post with one set of blocks. B) Close-up showing two sets of wood blocks at different stages of biofilm development.

Each set of blocks was deployed for three weeks. Site visits with water quality monitoring occurred at each block deployment and collection. After each three-week deployment period, three blocks from each site were removed from the frame. Prior to removing the blocks, photos were taken of the entire frame and each of the blocks (Figure 3.4A). The shallow position of the blocks and glare on the water surface prevented photos from being taken directly above each block.

Prior to collecting the biofilm sample, the side and bottom surfaces of each block were scraped off into the stream, downstream of the experimental frame. On two site visits, the biofilm from these extraneous surfaces was collected at each site and microscopic images were taken for documentation. The biofilm on the top surface of each block was scraped off with a flat blade into a stainless steel funnel inserted into a 50-mL Falcon© tube (Figure 3.4B). A minimal amount of Millipore water was then used to rinse any stray biofilm off the inside of the funnel and into the Falcon© tube. The funnel was removed and additional water was added to reach the nearest 2.5 mL graduation on the

tube. This sample volume was recorded and the sample was shaken to homogenise the mixture.

A disposable pipette was inserted at consistent depth into the sample and a 0.5-mL subsample was removed. This subsample was "painted' onto a 47-mm Whatman GF/F glass-fibre filter. The filter paper was folded into aluminium foil, stored in a portable electric freezer set to −8°C and placed in a −4°C freezer upon return to the lab. The samples were later analysed by ALS Global for chlorophyll a concentration. Chlorophyll a concentrations were converted from a volumetric basis to mass per unit area based on the combined surface area of the three blocks of 60 cm^2.

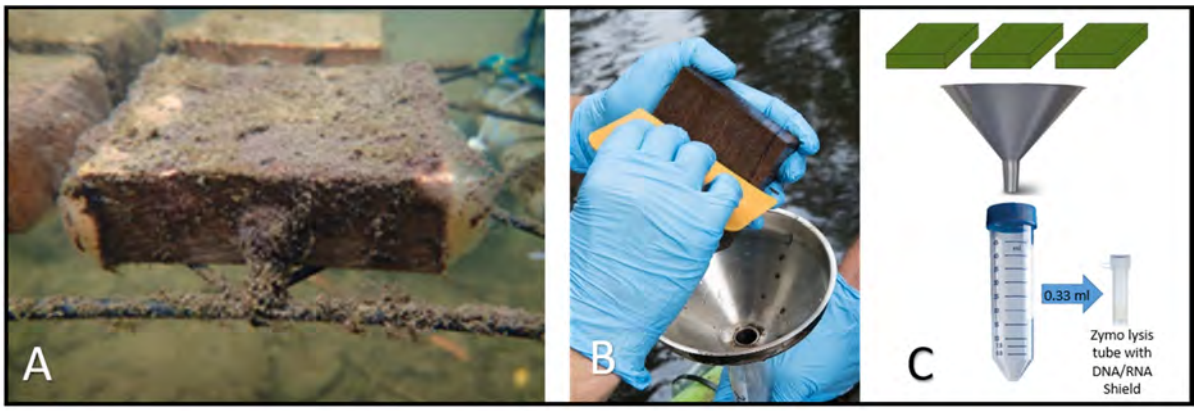

Figure 3.4. Biofilm methods. A) Wood block with three weeks of biofilm growth. B) Scraping the biofilm into a funnel and Falcon© tube. C) Three blocks were pooled into each sample and subsamples were removed and preserved.

For block sets 1 and 2, a 0.25-mL subsample was collected from the Falcon© tube and added to a preloaded vial with 0.5 mL DNA/RNA Shield (Zymo Analytics) for DNA analysis (Figure 3.4C). Based on the relatively low DNA concentration extracted from six of the samples from the first set of blocks, the method was adjusted to maximise the volume of biofilm collected and provide a second DNA sample as a backup. From block set #3 forward, two 0.33-mL subsamples were removed from each Falcon© tube for DNA analysis.

A disposable pipette was used to transfer one 0.33-mL subsample into each of the prepared containers, which had been preloaded with 0.66 mL of DNA/RNA Shield preservative in the laboratory. The primary sample container was a Zymo Analytics tube containing lysis beads (0.1 and 0.5 mm) and the secondary (backup) container was a 1.5-mL microcentrifuge tube. The capped samples were briefly shaken to ensure contact between the biofilm sample and the preservative. The DNA samples were placed in a portable electric freezer set to −8°C in the field. Upon return to the laboratory, the filled Falcon© tubes were placed in a −4°C freezer lying at an angle to maximise exposed surface area. Samples were later transported in a cooler to the Deakin Queenscliff facility and frozen at −80°C in preparation for freeze-drying and subsequent analysis of biomass and fatty acid concentration.

3.3.4. Laboratory methods

DNA extraction

DNA from preserved samples was extracted using a bead beating-based Zymobiomics Miniprep Kit (ZymoResearch). The initial extraction process, conducted on four samples from block set #1, followed the Zymo protocol (through step #11; https://files.zymoresearch.com/protocols/_d4300t_d4300_d4304_zymobiomics_dna_miniprep_kit.pdf). After the process produced low DNA yield, two steps were extended, the lysing from 5 to 20 min and elution from 3 to 5 min. The final extraction protocol (block sets #2–12) followed the Zymo protocol with the extended lysing and elution steps. The sample containers were lysed using a Vortex Genie2 at a maximum vortex speed of 3,200 rpm for 20 minutes. To improve DNA recovery, elution of DNA from the spin column used pre-heated Tris-EDTA buffer (56°C) with an incubation time of 5 minutes. DNA

concentration was quantified with a Qubit 4 Fluorometer (Thermo Fisher Scientific). Extracted DNA was stored cold (4°C) in microcentrifuge tubes.

DNA metabarcoding

Of the 12 sets of cultured biofilm, only sets #4–12 were sequenced. The elevated flow conditions in the Painkalac Downstream reach during November were not part of the experimental design and DNA concentrations from the early samples were generally low, so the decision was made to skip DNA sequencing on sets #1–3, as replication was established within the reach rather than individual sites.

The purified DNA from the nine selected biofilm sets was sent to MR DNA (Shallowater, Texas, USA) for amplicon sequencing on the Illumina platform. Three assays were performed on each sample to quantify prokaryotes (16S), fungi (ITS1-2) and algae (23S) reads (Table 3.3. Primer set details.Table 3.3). The V4 variable region of the 16S rRNA gene was amplified using the 515 (Parada, Needham & Fuhrman, 2016)/806RB (Apprill *et al.*, 2015) primer set with a barcode on the forward primer. The ITS1-2 region was amplified using the ITS1F-Bt1 (Gardes & Bruns, 1993) and ITS2R (White *et al.*, 1990) primer pair. The plastid 23S rRNA genes were amplified using the primer set developed by Sherwood and Presting (2007).

Table 3.3. Primer set details.

16S	illCUs515F	GTGYCAGCMGCCGCGGTAA
	new806RB	GGACTACNVGGGTWTCTAAT
ITS1-2	ITS1F-Bt1	CTTGGTCATTTAGAGGAAGTAA
	ITS2R	GCTGCGTTCTTCATCGATGC
23S	algEa1F	GGACAGAAAGACCCTATGAA
	algE1R	TCAGCCTGTTATCCCTAGAG

A single-step PCR was performed using the HotStarTaq Plus Master Mix Kit (Qiagen, Valencia, CA) under the following conditions: 94°C for 3 minutes, followed by 30–35 cycles of 94°C for 30 seconds, 53°C for 40 seconds and 72°C for 1 minute, after which a final elongation step at 72°C for 5 minutes was performed. Successful amplification and the relative intensity of bands were verified in 2% agarose gel. Multiple barcoded samples were pooled together in equal proportions (based on molecular weight and DNA concentrations) and purified using calibrated Ampure XP beads (Beckman Coulter).

The pooled and purified PCR product were sequenced on the Illumina MiSeq System (Illumina, San Diego, CA) using the run configuration of 2 × 300 bp. Raw paired-end reads were processed using the MR DNA analysis pipeline. Briefly, paired-end reads were merged and depleted of barcodes followed by the removal of sequences shorter than 150bp or with ambiguous bases. Mothur was used for denoising, operational taxonomic unit (OTU) clustering at 97% similarity and chimera removal (Schloss *et al.*, 2009). OTUs were classified using BLASTn against a curated database derived from RDPII (http://rdp.cme.msu.edu) and NCBI (https://www.ncbi.nlm.nih.gov/). The sequence data from this study were deposited under BioProject PRJNA588337 in the Sequence Read Archive (SRA) of the National Center for Biotechnology Information (NCBI).

Light microscopy

On two occasions, the sides of the each set of substrate blocks were scraped into sample containers and stored overnight at 4°C. Subsamples were transferred to glass slides and the living samples were examined under a compound light microscope with a maximum magnification of 1,000×. An attached digital camera was used to capture representative

photos at multiple scales (200×, 400× and 1,000×). General identification and notes on abundance were collected, but organisms were not counted.

Total lipid and ash

Biofilm samples were freeze-dried and extracted for total lipid content according to the method described by Conlan *et al.* (2014) as follows. Dry samples were soaked overnight in 3 mL of a dichloromethane:methanol (CH_2Cl_2:CH_3OH) solution. The following morning, the supernatant was removed and filtered. The remaining solid was re-suspended in 2–3 mL of CH_2Cl_2:CH_3OH and soaked for 10 minutes and filtered. This process of drawing off the liquid, resoaking the solid material and filtering was repeated three times. The resulting combined filtrate (~9 mL) was combined with a wash solution consisting of 4.5-mL potassium chloride (KCl) (0.44%) and methanol H_2O/CH_3OH (3:1). The mixture was shaken vigorously and left overnight. The following morning, the lower layer of extracted lipid was recovered (~2.5 mL) and the remaining solvent was evaporated under nitrogen. The lipid content was quantified gravimetrically on a four-figure balance (AB 204, Mettler). Ash-free dry mass (AFDM) was measured as the mass loss between the freeze-dried samples and the samples incinerated in a muffle furnace (450°C, 12 hours) (Model WIT, C & L Fetlow). AFDM is reported as gm^{-2} based on an artificial substrate (wood block) area of 60 cm^2 per sample.

Phospholipid composition

Following extraction and saponification, fatty acids were esterified into methyl esters using the acid catalysed methylation method (Christie, 2003). An internal standard (100 µL of 23:0, 0.75 mg mL^{-1}) (Sigma-Aldrich, Inc.) was added along with 2 mL of freshly prepared acetyl chloride:methanol reagent (1:10). Sample vials were then sealed, shaken

and placed in an oven at 100°C for 1 hour. Once cooled to room temperature, 2 mL of potassium carbonate (K_2CO_3 (1 M)) was added, followed by 1.7 mL of hexane to dissolve the fatty acid methyl esters. The sample was centrifuged and the hexane supernatant recovered and placed in a gas chromatography (GC) vial for GC injection.

Fatty acid methyl esters (FAMEs) were isolated and identified using an Agilent Technologies 7890A GC System (Agilent Technologies) equipped with a BPX70 capillary column (120-m × 0.25-mm internal diameter, 0.25-µm film thickness, SGE Analytical Science), a flame ionisation detector (FID), an Agilent Technologies 7693 auto sampler and a split injection system (split ratio 20:1). The injection volume was 1 µL and the injector and detector temperatures were 300°C and 270°C, respectively.

The temperature program at 60°C was held for 2 minutes, then from 60°C to 150°C at 20°C/min, and held at 150°C for 2 minutes, from 150°C to 205°C at 1.5°C/min, from 205°C to 240°C at 5°C/min, and at 240°C for 24 minutes. The carrier gas was helium at 1.5 mL/min at constant flow. Each of the fatty acids was identified relative to known external standards (a series of mixed and individual standards from Sigma-Aldrich, Inc., and from NuChek Prep Inc.), using the software GC ChemStation (Rev B.04.03, Agilent Technologies). The resulting peaks were corrected by the theoretical relative FID response factors (Ackman, 2002) and quantified relative to the internal standard. The concentration of each PLFA was reported as mg/g lipid.

3.3.5. Statistical analysis

Most statistical analyses were performed using the multivariate statistical package Primer v7 with PERMANOVA+ (Clarke & Gorley, 2015). Data distribution was initially examined using a draftsman plot consisting of a set of pairwise scatter plots for all combinations of selected variables. Appropriate transformation was applied to variables

exhibiting skewed distributions. For all datasets, a RELATE seriation test (which compares the data matrix to a linear sequence) was used to detect seasonal patterns.

Biodiversity

The level of taxonomic assignment was variable across the three amplicons (Figure 3.5). The taxonomic resolution for the 23S assay was low with most (69.7%) 23S sequences returning percent homologies of 80–85%. Only 3.2% of 23S sequences and almost half (48.8%) of ITS sequences returned ≥95% homology. The 16S sequences were more evenly represented and 64.8% of 16S sequences had ≥90% similarity. Because low-level taxonomy was missing for many OTUs, I analysed biological community structure mainly at the OTU level with additional detail provided by phylum and class-level analyses.

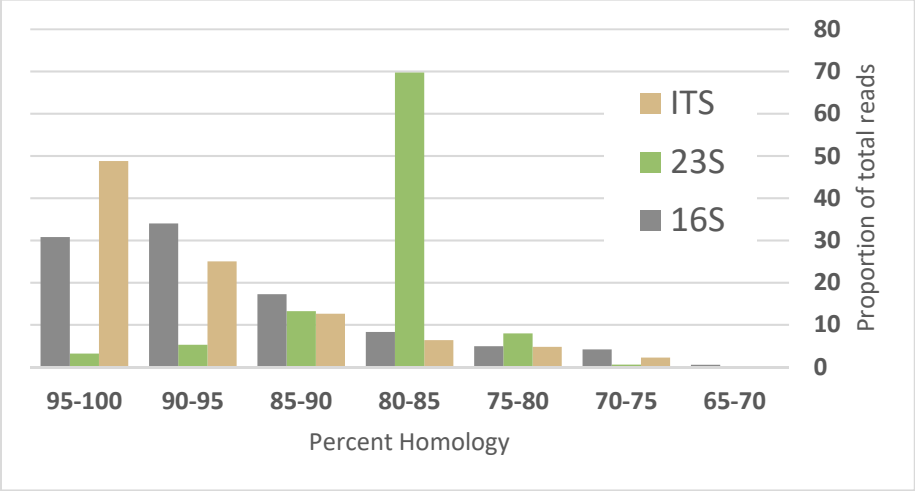

Figure 3.5. Percent homology returned for sequenced reads for each amplicon (16S = grey, 23S = green and ITS = brown).

Only OTUs from the target taxon were used to construct the OTU table for each amplicon. To ensure the 16S OTU-level analysis only considered bacteria, I removed all OTUs identified as chloroplast reads in the targeted bioinformatics process (described in 0). For the 23S assay, I selected the OTUs assigned to the Viridiplantae (including green

algae) and Eukaryota (including red algae) clades. For the ITS assay, only OTUs assigned as Fungi were selected. For the 23S and ITS assays, phylum- and class-level tables were constructed by aggregating target taxa reads. The 16S phylum table was constructed across all phyla (not just bacteria) to consider relative proportions of Cyanobacteria and diatoms (Bacillariophyta) in addition to bacterial phyla.

To conservatively construct each OTU table, sequences with <80% homology were ignored and extremely rare OTUs were filtered to include only those with ≥0.1% abundance in a sample. The read counts were normalised to proportions (McKnight *et al.*, 2019) by applying a 'standardise by total' approach (Clarke & Gorley, 2006) and a Bray-Curtis (B-C) similarity matrix (Bray & Curtis, 1957) was constructed for each amplicon. Relative abundance was visualised using a shade plot (Clarke, Tweedley & Valesini, 2014) and homogeneity of dispersion between groups was tested using PERMDISP (Anderson, Gorley & Clarke, 2008). Violations to assumptions of homogeneity guided appropriate transformation for each dataset. Bacteria were log-transformed, algae were square-root transformed and fungi were fourth-root transformed, which reduced the impact of dominant taxa in the B-C similarity analysis.

Beta-diversity among the three river reaches was examined using two-factor permutational multivariate analysis of variance (PERMANOVA) (Anderson, 2001) with 9,999 unique permutations. The random 'site' factor was nested within the fixed 'reach' factor. The PERMANOVA routine was applied to the B-C abundance matrix for each assay to evaluate temporal and spatial patterns of biological community structure and a non-metric multidimensional scaling (nMDS) plot was constructed to visualise differences between communities (Kruskal, 1964).

A snapshot of community structure was developed by analysing the class-level abundance data of the target taxa for fungi and algae. I was interested in the relationships

between diatom abundance, PLFA composition and environmental variables, so I performed the taxonomic summary for 16S on the phylum-level data. The chloroplast sequences I identified (detailed in 0) were relabelled based on PhytoREF taxonomic assignments (Decelle *et al.*, 2015) before the read counts were normalised to proportions by phylum (McKnight *et al.*, 2019). A Bray-Curtis (B-C) similarity matrix (Bray & Curtis, 1957) was constructed for the phylum-level 16S dataset.

Environmental variables

Environmental conditions were summarised across the three reaches and data distribution was evaluated. Following transformation (when necessary), abiotic variables were normalised and resemblance was examined using Euclidean distance. The same two-factor PERMANOVA routine described for the biodiversity analyses was applied to the resemblance matrix of normalised Euclidean distance for environmental variables (Temp, DOsat, SPCond, pH, turbidity, NH_4, NO_3, NO_2, TCN, TKN, TP, V and Q; see Table 3.2). Mean TON was not considered as it was strongly correlated (0.99) with nitrate levels. Nutrient dynamics and limitation across the three stream reaches were considered by calculating the proportion of nitrogen to phosphorous in stream water. Deviation from the Redfield ratio of 106C:16N:1P (Redfield, 1958) provides an indication of potential nutrient limitation (Stelzer & Lamberti, 2001). Average values of TCN/TP were plotted by site and reach using R v.3.6.0 (R Core Team, 2019).

Environmental variables and biota

Relationships between biological resemblance matrices and patterns within a given matrix were examined using the RELATE routine in Primer. RELATE performs an element-by-element comparison of the resemblance matrices using a Spearman rank

correlation. The biofilm community data were related to the physicochemical data using the BIOENV and DISTLM routines in Primer. The BIOENV routine calculates weighted Spearman rank correlations between each B-C biotic matrix and the Euclidean distance matrix of the abiotic variables. The weighted Spearman rank correlation coefficient ranges between 1 and −1, where 0 represents the absence of any match, 1 represents complete agreement and −1 represents complete opposition between matrices (Clarke & Warwick, 2001).

Distance-based linear modelling (DistLM) is a PRIMER routine for analysing and modelling the relationship between a multivariate data cloud (as described by a resemblance matrix) and a set of predictor variables (Anderson *et al.*, 2008). DistLM implements a distance-based redundancy analysis (McArdle & Anderson, 2001) consisting of a multivariate multiple regression of the principle coordinate axes on predictor variables. In this study, DistLM was performed over 9,999 permutations using either the 'forward' or 'best' selection procedure and either R^2 or Akaike's Information Criterion (AIC). Where useful, an ordination plot of the fitted values from the model, created using a distance-based redundancy analysis (dbRDA), was included to visualise the relationship between predictor and response variables.

Phospholipid analysis

Phospholipid fatty acid composition (51 individual PLFAs) was evaluated by applying the PERMANOVA routine to the Euclidean distance matrix of square root-transformed individual PLFA content. Lipid quality was assessed by considering the concentrations of individual EFAs and lipid classes.

3.4. Results

3.4.1. Environmental conditions

Environmental conditions differed across the three stream reaches (Figure 3.6.), with the Barham River characterised by high dissolved oxygen, high pH, low conductivity, low turbidity and low DOC. The Painkalac Downstream reach was significantly warmer (18.9°C ± 1.3) than the Painkalac Upstream reach (16.5°C ± 1.4) and conductivity was significantly lower downstream ($P<0.001$).

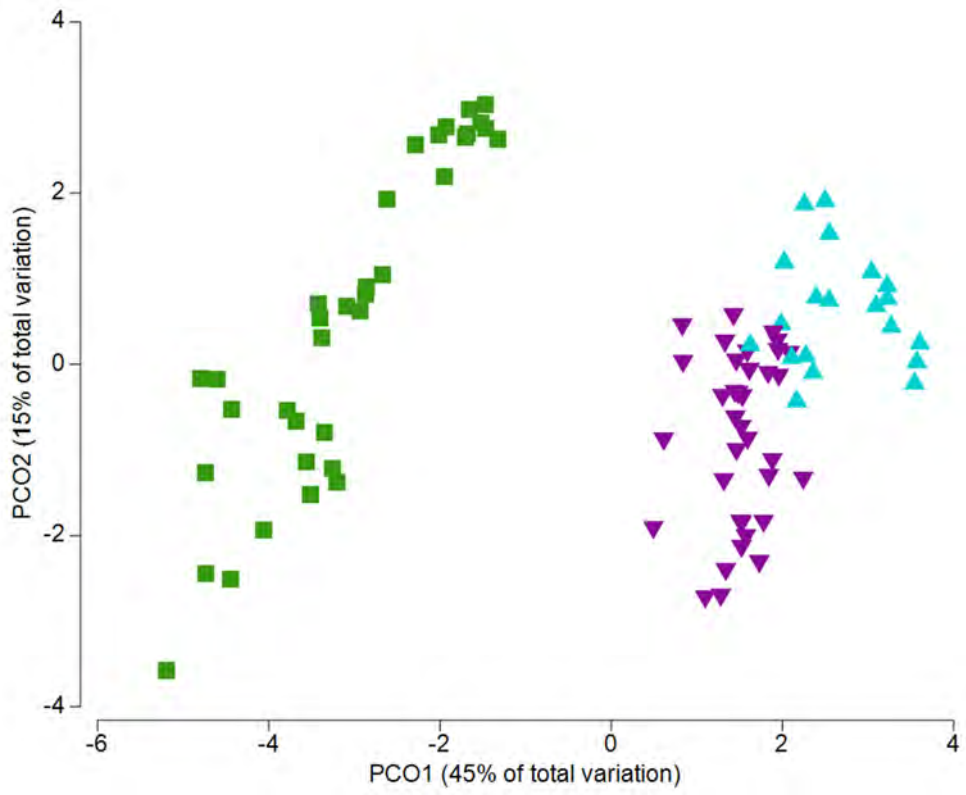

Figure 3.6. Principal component ordination of physicochemical variables. Colours and symbols indicate reach (Barham: green, Painkalac Downstream: purple, and Painkalac Upstream: turquoise).

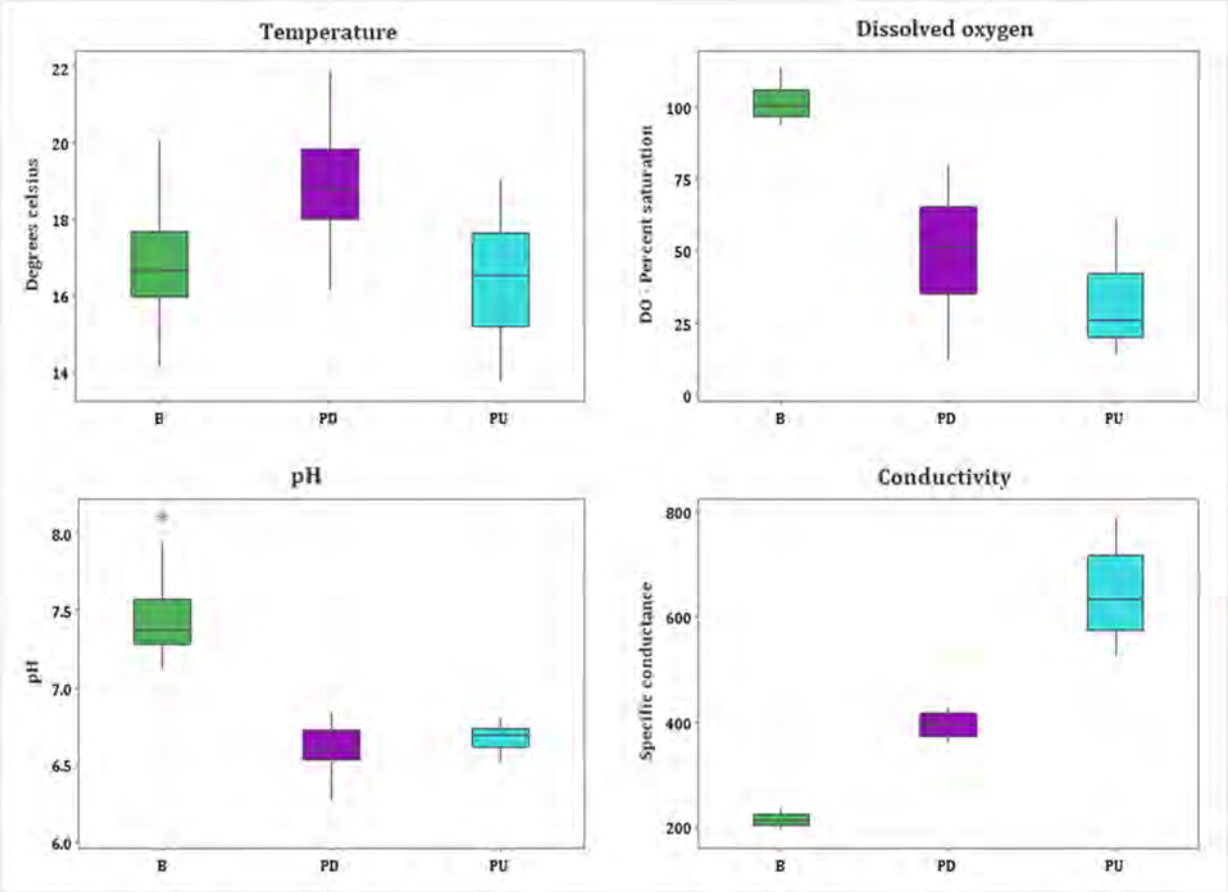

Figure 3.7. Boxplots summarising measurements of temperature, dissolved oxygen, pH and conductivity by reach. Colours indicate reach (Barham: green, Painkalac Downstream: purple, and Painkalac Upstream: turquoise).

Table 3.4. Mean physicochemical values and mean velocity for each site. Variables are defined in Table 3.2.

Site	Temp (°C)	DO (% sat)	SPCond (µS/cm)	pH	Turbidity (NTU)	NH_4 (mg/L)	DOC (mg/L)	NO_2 (mg/L)	TP (mg/L)	TCN (mg/L)	NO_3 (mg/L)	TKN (mg/L)	TON (mg/L)	Velocity (m/s)
PU1	16.81	23.07	694.99	6.69	8.22	0.04	9.52	0.01	0.03	0.74	0.01	0.74	0.01	0.01
PU2	16.20	36.47	590.57	6.66	13.24	0.04	13.33	0.01	0.04	0.80	0.01	0.80	0.01	0.01
PD3	19.84	49.32	393.73	6.65	4.24	0.04	13.67	0.01	0.02	0.81	0.04	0.76	0.04	0.02
PD4	18.63	32.67	393.65	6.46	4.95	0.03	14.05	0.01	0.02	0.82	0.03	0.79	0.03	0.02
PD5	18.21	65.96	396.79	6.69	14.29	0.04	14.43	0.01	0.03	0.79	0.02	0.77	0.02	0.02
B1	16.69	102.96	208.47	7.43	1.97	0.03	1.69	0.01	0.04	0.71	0.43	0.27	0.43	0.14
B2	16.65	101.18	219.70	7.42	2.64	0.03	1.97	0.01	0.05	0.51	0.25	0.27	0.25	0.08
B3	16.99	101.50	217.79	7.48	3.31	0.03	2.02	0.01	0.04	0.53	0.24	0.29	0.24	0.05

The nutrient dynamics of the two Painkalac Creek reaches were similar, with the highest nitrogen to phosphorous ratio (TCN/TP) occurring in November 2018 (Figure 3.8). The highest values in the Barham River were associated with a flow pulse in December 2018 (Figure 3.8). In the Barham River, the nitrogen to phosphorous ratio was strongly correlated with discharge (R^2 = 0.81, P<0.001), but there was no significant correlation in the other two reaches.

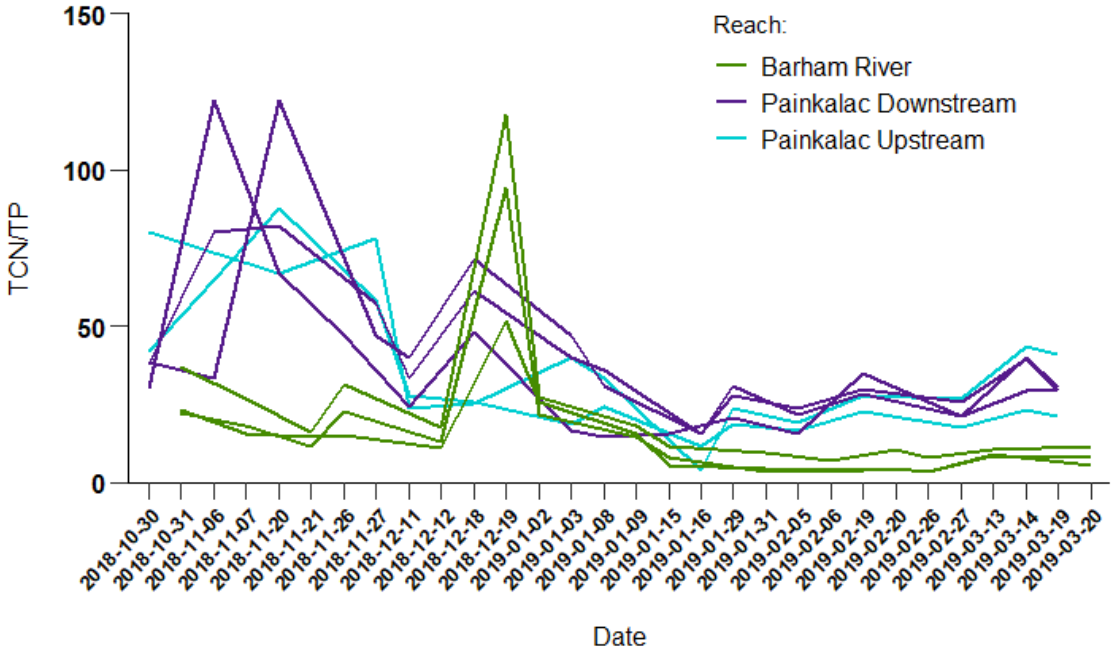

Figure 3.8. Time series of total nitrogen to total phosphorous ratios (TCN/TP). Colours denote reach, with each site plotted as a line.

3.4.2. Phospholipid composition

The most abundant PLFA across all 94 samples were palmitic acid (16:0, 22.1–200.7 mg/g lipid) and palmitoleic acid (16:1n-7, 5.5–220.1 mg/g lipid) (Table 3.5). The concentration of EPA (20:5n-3) was strongly correlated (0.96) with that of gamma-linolenic acid (GLA, 18:3n-6).

Table 3.5. PLFA concentration (mg/g lipid) across 94 samples.

PLFA	Min	Max	Mean
6:0	0.0	36.8	3.7
8:0	0.0	14.9	2.3
10:0	0.0	7.7	1.5
11:0	0.0	8.1	1.6
12:0	0.0	14.6	2.3
13:0	0.0	9.4	3.0
14:0	3.4	40.8	14.9
15:0	0.0	20.9	2.3
16:0	22.1	200.7	78.4
17:0	0.5	38.3	6.7
18:0	2.7	61.7	13.2
20:0	0.0	13.1	3.5
21:0	0.0	2.9	0.8
22:0	0.0	17.9	3.6
24:0	1.3	15.1	4.5
14:1n-5	0.0	10.2	1.5
15:1n-5	0.0	4.8	1.0
16:1n-11	0.0	1.4	0.3
16:1n-7	5.5	220.1	57.7
16:1n-9	0.0	7.5	1.2
17:1n-7	0.0	26.3	4.3
18:1n-7	0.0	37.1	10.7
18:1n-9	3.7	95.8	23.9
18:1n-9 t	0.0	4.7	1.1
20:1(isomers)	0.0	3.8	0.9
22:1(isomers)	0.0	5.4	0.2
16:4n-1	0.0	14.5	1.8
18:3n-3	4.0	82.6	28.5
18:4n-3	0.0	16.4	4.4
20:3n-3	0.0	4.4	0.3
20:4n-3	0.0	1.5	0.3
20:5n-3	1.2	106.0	19.9
21:5n-3	0.0	12.6	3.2
22:5n-3	0.0	1.8	0.3
22:6n-3	0.0	8.6	1.7
24:5n-3	0.0	6.5	2.6
24:6n-3	0.0	31.0	2.4
16:2n-4	0.0	29.3	7.3
16:3n-4	0.0	28.6	5.4
18:2n-4	0.0	2.5	0.7
18:3n-4	0.0	1.3	0.2
18:2n-6 t	0.0	1.8	0.3
18:2n-6	3.5	69.0	20.4
18:3n-6	1.0	29.9	7.6
20:2n-6	0.0	2.3	0.2
20:3n-6	0.0	3.3	0.9
20:4n-6	0.0	13.0	4.1
22:2n-6	0.0	5.0	0.3
22:4n-6	0.0	3.3	0.5
22:5n-6	0.0	2.6	0.7
Unknown 1	0.0	8.3	2.0

In terms of individual EFA, biofilm samples from the Barham River had significantly lower levels of LIN than the samples from either Painkalac reach (P<0.05; Figure 3.9). The EPA levels in the biofilm from the Barham River were significantly higher than the biofilm from the Painkalac Upstream reach (P=0.016) but not significantly different from the Painkalac Downstream samples (P=0.058). Biofilm samples from the Painkalac Upstream had significantly less ARA than the samples from the other two reaches (P<0.05). If the sum of these five EFA is treated as a measure of quality, there were no significant differences in biofilm nutritional quality among the three reaches (P>0.05).

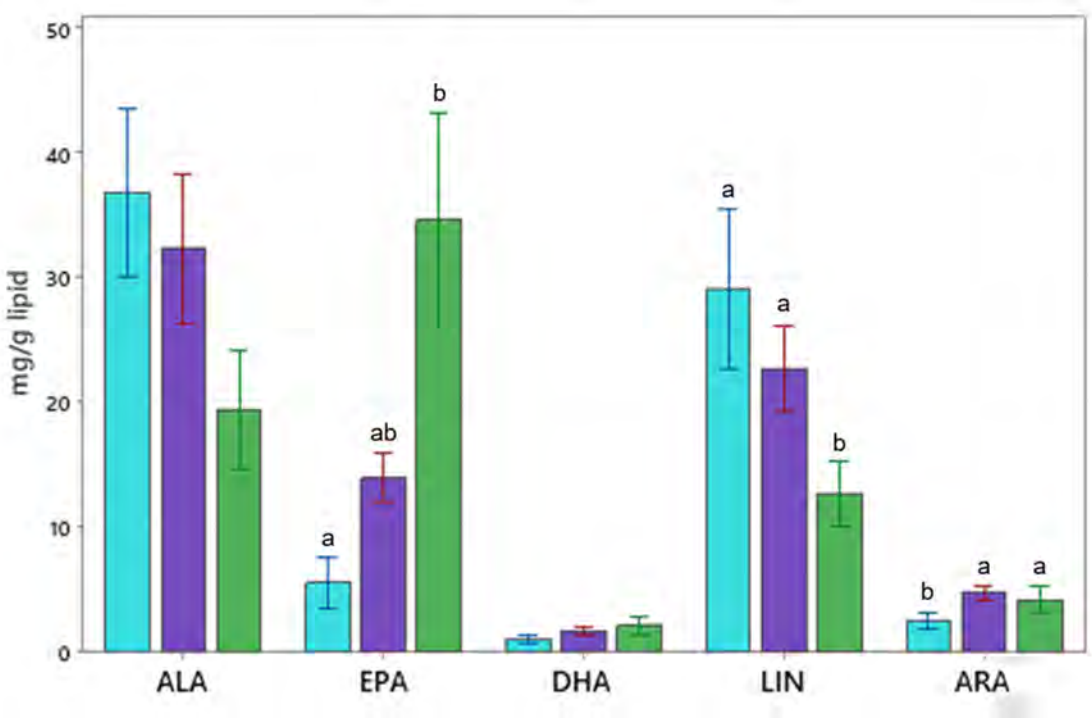

Figure 3.9. Interval plot of essential fatty acids (EFA) by reach. Colours indicate reach (Painkalac Upstream: turquoise, Painkalac Downstream: purple, and Barham: green). ALA: α-linolenic acid, EPA: eicosapentaenoic acid, DHA: docosahexaenoic acid, LIN: linolenic acid and ARA: arachidonic acid. Values are presented as means ±1 standard deviation. Letters indicate significant differences as determined with Tukey post-hoc tests (P <0.05). Means that do not share a letter are significantly different.

When major fatty acid classes were considered, there were significant differences among reaches (Figure 3.10). Biofilm samples from the Painkalac Upstream reach had significantly higher levels of saturated fatty acids (SFA) than the samples from the Barham River (P=0.036). The biofilm from the Barham and Painkalac Upstream reaches also contained significantly different levels of EPA+DHA (P=0.019). The level of EPA+DHA was strongly correlated with the relative abundance of diatoms based on 16S phylum-level data ($\rho = 0.45$, $P<0.0001$).

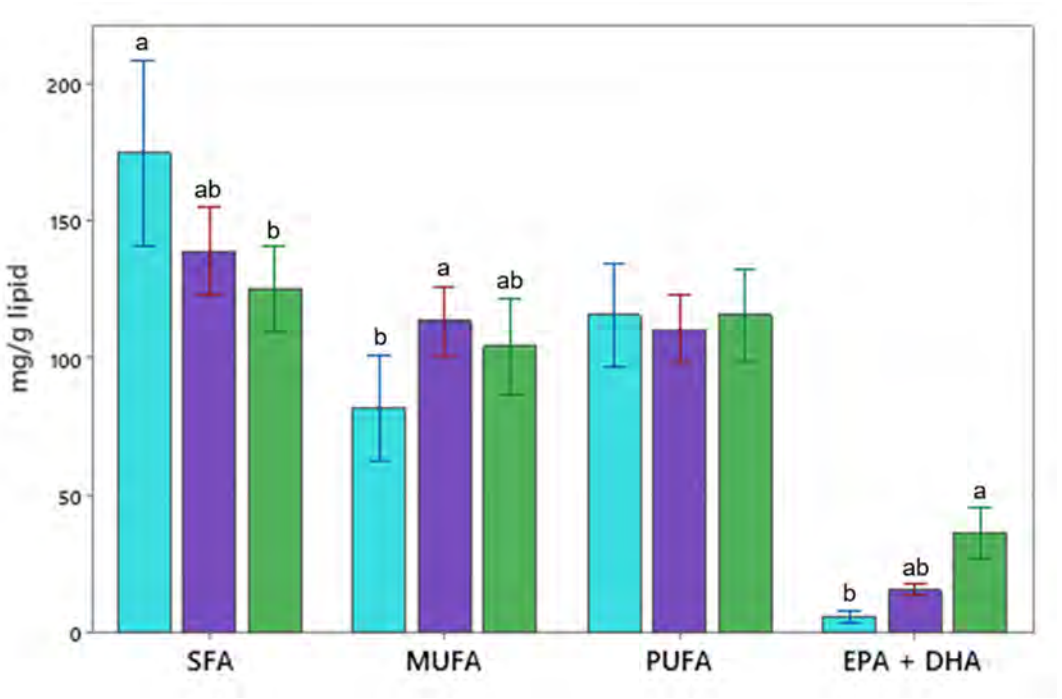

Figure 3.10. Interval plot of major acid class composition by reach. Colours indicate reach (Painkalac Upstream: turquoise, Painkalac Downstream: purple, and Barham: green). SFA: saturated fatty acids, MUFA: monounsaturated fatty acids, PUFA: polyunsaturated fatty acids, EPA + DHA: eicosapentaenoic acid and docosahexaenoic acid. Values are presented as means ±1 standard deviation. Letters indicate significant differences as determined with Tukey post-hoc tests ($P < 0.05$). Means that do not share a letter are significantly different.

Across all 51 PLFA characterised, I found significant differences in the phospholipid composition within (pseudo-$F_{5,71}$ = 2.24, P<0.001) and among river reaches (pseudo-$F_{2,71}$ = 5.50, P<0.01) based on the PERMANOVA results. There were no significant differences in the homogeneity of dispersion among sites (PERMDISP P = 0.12) or reaches (PERMDISP P = 0.22). There was evidence of a seasonal trend in PLFA composition (ρ = 0.28, P = 0.0001) based on the RELATE test.

3.4.3. Biodiversity

Across the 72 stream biofilm samples, the average number of reads per sample were similar for the three amplicons (Table 3.6). After filtering for target taxa, 80% homology and 0.1% abundance, there were 1,258 bacteria OTUs, 1,287 algal OTUs and 896 fungal OTUs for analysis.

Table 3.6. Summary of average numbers of reads, operational taxonomic units (OTUs), target taxa and numbers of target OTUs for each assay.

Amplicon	Average reads	OTUs	Target taxa	Target OTUs
16S	68,273	22,684	Bacteria	1,258
23S	57,193	43,630	Algae	1,287
ITS	59,853	7,931	Fungi	896

Bacteria

There were significant differences in bacterial assemblage structure among the three river reaches, indicated by the distinct clusters on the nMDS plot (Figure 3.11). PERMANOVA results showed that the composition of the bacterial assemblage varied within (pseudo-$F_{5,7}$ = 4.02, P<0.01) and among river reaches (pseudo-$F_{2,71}$ = 9.03, P<0.001). There were no significant differences in the homogeneity of dispersion among sites (PERMDISP P = 0.1759) or reaches (PERMDISP P = 0.0958). Based on the RELATE test, there was evidence of a seasonal trend in the bacterial community (ρ = 0.09, P = 0.0028). At the phylum level, all biofilm samples were dominated by Proteobacteria (Figure 3.12). Diatoms (Bacillariophyta) were most abundant in the Barham River, consistent with general abundance patterns of visible taxa under the microscope.

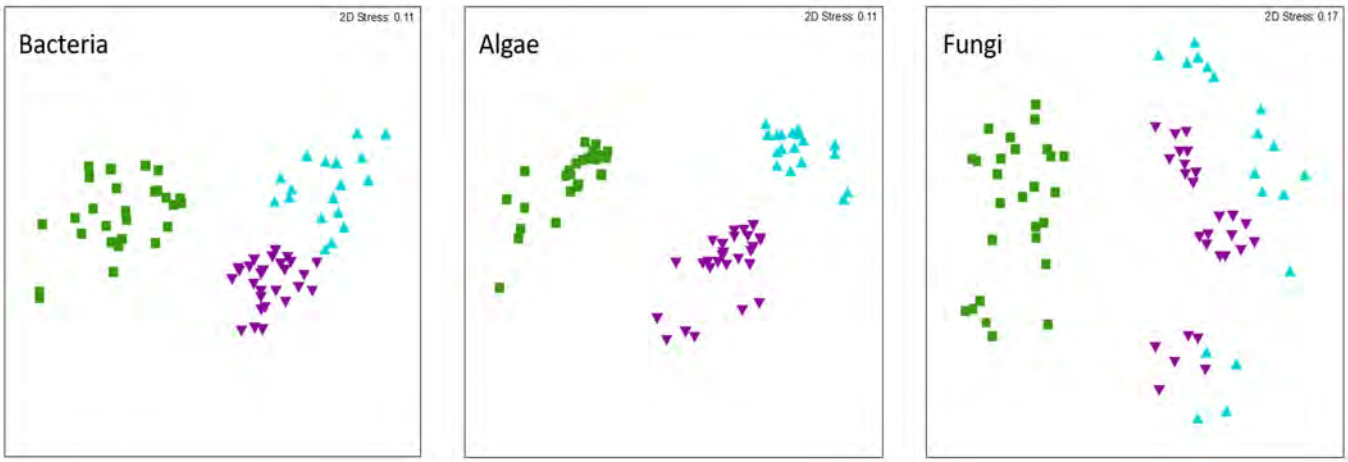

Figure 3.11. Non-metric multidimensional scaling (nMDS) plots of OTU-level bacterial, algal and fungal communities. OTU: operational taxonomic unit. Reaches are represented by colours and symbols (Barham: green squares, Painkalac Downstream: purple inverted triangles, and Painkalac Upstream: turquoise triangles).

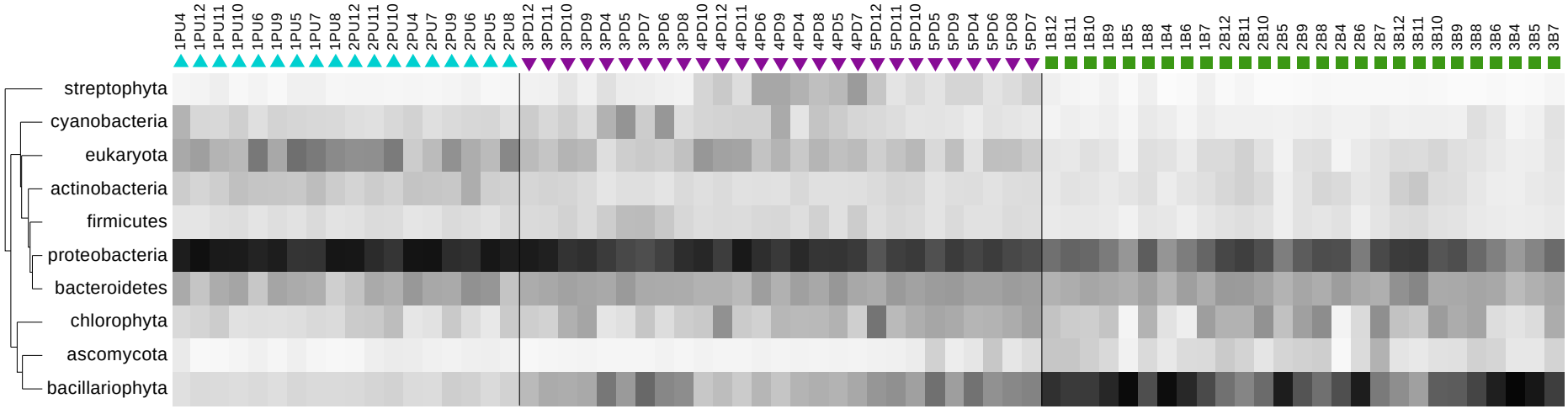

Figure 3.12. Heatmap of relative abundance for the 10 most important phyla for distinguishing reaches based on 16S data. Reaches are represented by colours and symbols (Painkalac Upstream: turquoise triangles, Painkalac Downstream: purple inverted triangles, and Barham: green squares). Samples are numbered by site, reach and set.

Algae

There were significant differences in algal assemblage structure (Figure 3.13A). PERMANOVA results showed that the composition of the algal assemblage varied within (pseudo-$F_{5,71}$ = 4.46, P<0.001) and among river reaches (pseudo-$F_{2,71}$ = 9.32, P<0.01). There were no significant differences in the homogeneity of dispersion among sites (PERMDISP P = 0.9759) or reaches (PERMDISP P = 0.2566). Based on the RELATE test, there was strong evidence of a seasonal trend in the algal community (ρ = 0.71, P = 0.0001). Florideophyceae was the most abundant class across the three reaches. Painkalac Upstream was distinguished by a higher abundance of Euglenida, while biofilm samples from the Barham River contained a consistently high abundance of Chlorodendrophyceae.

Fungi

There were also significant differences in the structure of the fungal assemblage, despite less distinct clusters on the nMDS plot (Figure 3.13A). The PERMANOVA results showed that the composition of the fungal community varied within (pseudo-$F_{5,71}$ = 2.12, P<0.001) and among river reaches (pseudo-$F_{2,71}$ = 8.85, P<0.01). There were no significant differences in the homogeneity of dispersion among sites (PERMDISP P = 0.3385) or reaches (PERMDISP P = 0.0948). Based on the RELATE test, there was evidence of a seasonal trend in the fungal community (ρ = 0.40, P = 0.0001). A higher abundance of Saccharomycetes characterised the Painkalac Upstream reach while Lecanoromycetes were most abundant in the Painkalac Downstream reach.

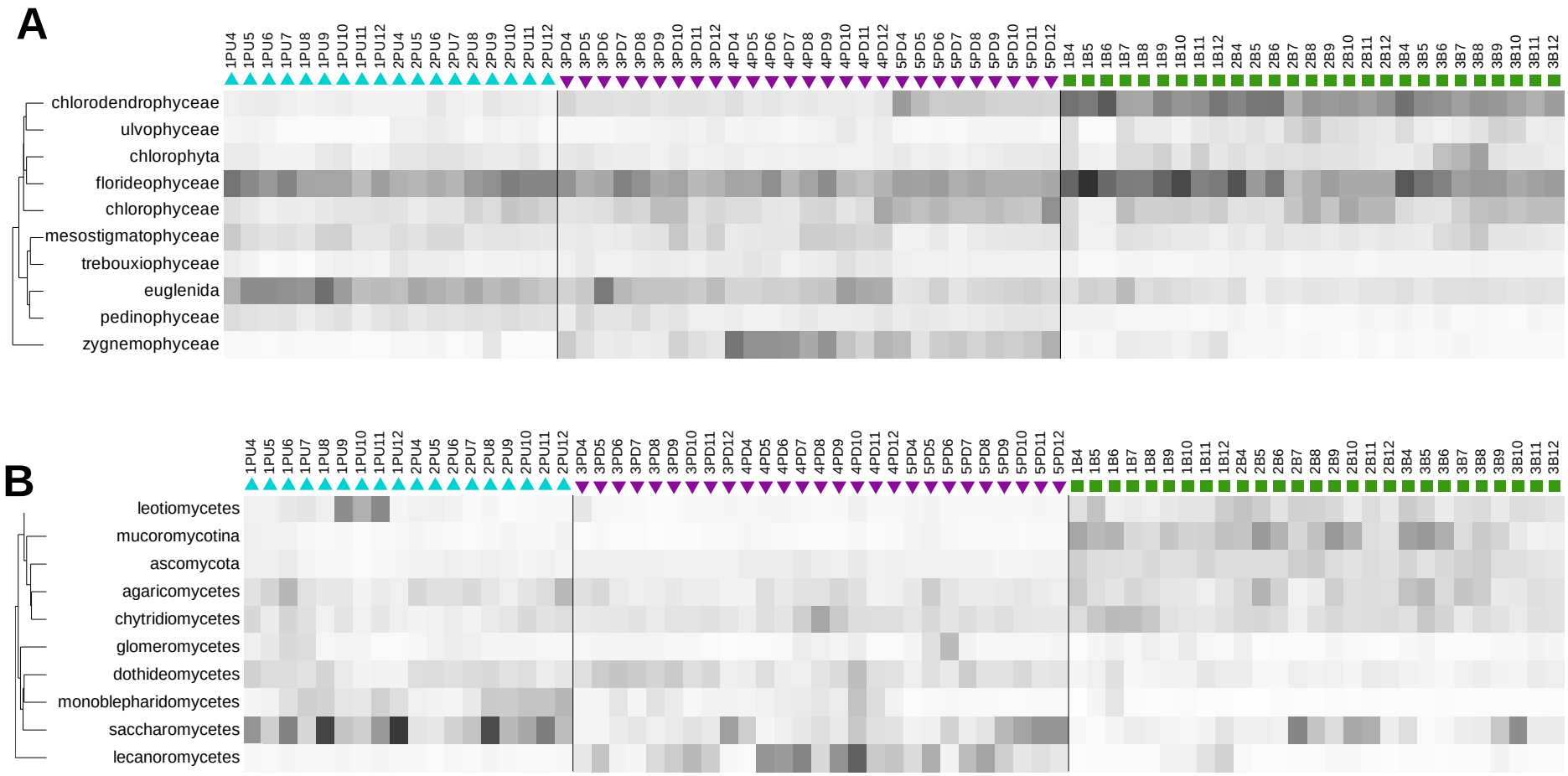

Figure 3.13. Heatmap of relative abundance for the 10 most important classes of A) 23S (algae) and B) ITS (fungi) abundance data. Reaches are represented by colours and symbols (Painkalac Upstream: turquoise triangles, Painkalac Downstream: purple inverted triangles, and Barham: green squares). Samples are numbered by site, reach and set.

3.4.4. Relationship between environmental variables and biota

A series of RELATE tests were performed to compare the matrices of biological abundance, environmental conditions (PCHEM subset) and PLFA composition. There was a significant correlation between each of the biological assemblages and environmental variables (Figure 3.14). Relationships between environmental variables and the biological abundance matrix were the same for the bacterial and algal assemblages ($\rho = 0.81$) and stronger than for the fungal assemblage ($\rho = 0.70$). Based on the BIOENV routine, conductivity was the most important variable in explaining variability within all three biological communities and was most strongly correlated with the bacterial community ($\rho = 0.87$). Each of the biological abundance matrices also showed a significant ($P<0.001$) relationship with PLFA composition and there was a significant relationship between environmental conditions and PLFA composition ($\rho = 0.33$).

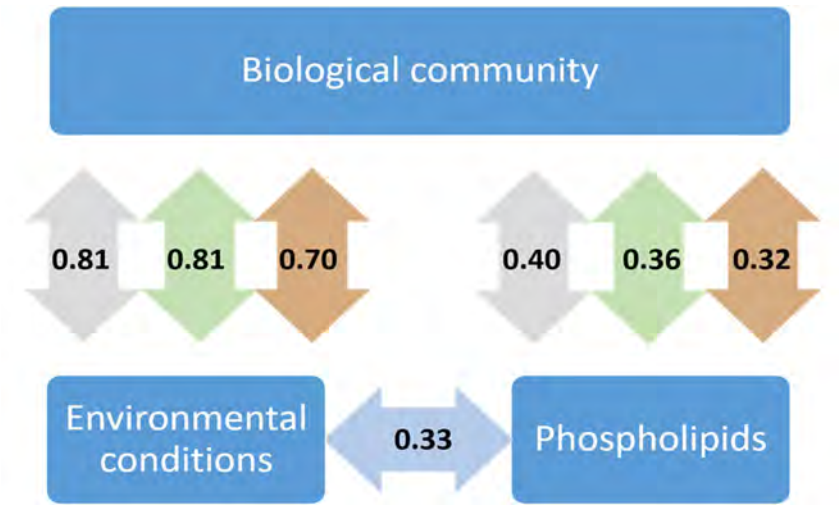

Figure 3.14. Spearman rank correlations between biological resemblance matrices, environmental conditions and PLFA composition. PLFA: phospholipid fatty acid. Environmental conditions comprise the PCHEM subset, and 51 PLFAs were included. Colours indicate biodiversity group (bacteria: grey, algae: green and fungi: brown). All values are significant ($P<0.001$).

To further explore the relationships between biotic and abiotic variables, differences in each biological community were fitted to individual environmental predictor variables in a distance-based linear model using the best selection criterion, with goodness-of-fit examined using AIC. The most parsimonious distance-based model used 12 environmental variables and explained 68.6% of variation in bacterial community structure. The first two dbRDA axes explained 65.9% of fitted variation and 45.2% of total variation (Figure 3.15). High pH, dissolved oxygen and higher phosphorus levels distinguished the Barham River from the two Painkalac reaches. Higher Kjeldahl nitrogen concentration in Painkalac Creek also helped separate these reaches from the Barham River.

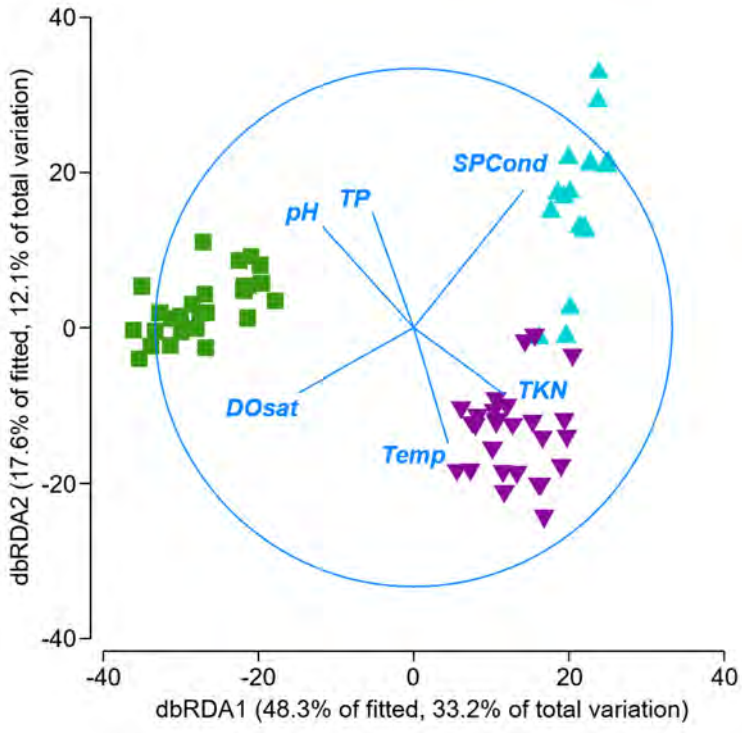

Figure 3.15. dbRDA ordination of bacterial community fitted to 13 environmental variables. dbRDA: Distance-based redundancy analysis. Vector lengths reflect the contribution of each variable, with variables with >40% multiple partial correlation included. Reaches are represented by colours and symbols (Barham: green squares, Painkalac Downstream: purple inverted triangles, and Painkalac Upstream: turquoise triangles). DOsat: dissolved oxygen saturation, TP: total phosphorous, SPCond: conductivity as specific conductance, TKN: total Kjeldahl nitrogen and Temp: temperature.

Based on the importance of Kjeldahl nitrogen as a predictor variable for bacterial community structure according to the dbRDA (Figure 3.15), I plotted the nMDS of the bacterial community but replaced the symbols with bubbles representing Kjeldahl nitrogen concentration by sample (Figure 3.16). This plot further emphasises the relationship between Kjeldahl nitrogen levels and bacterial community structure.

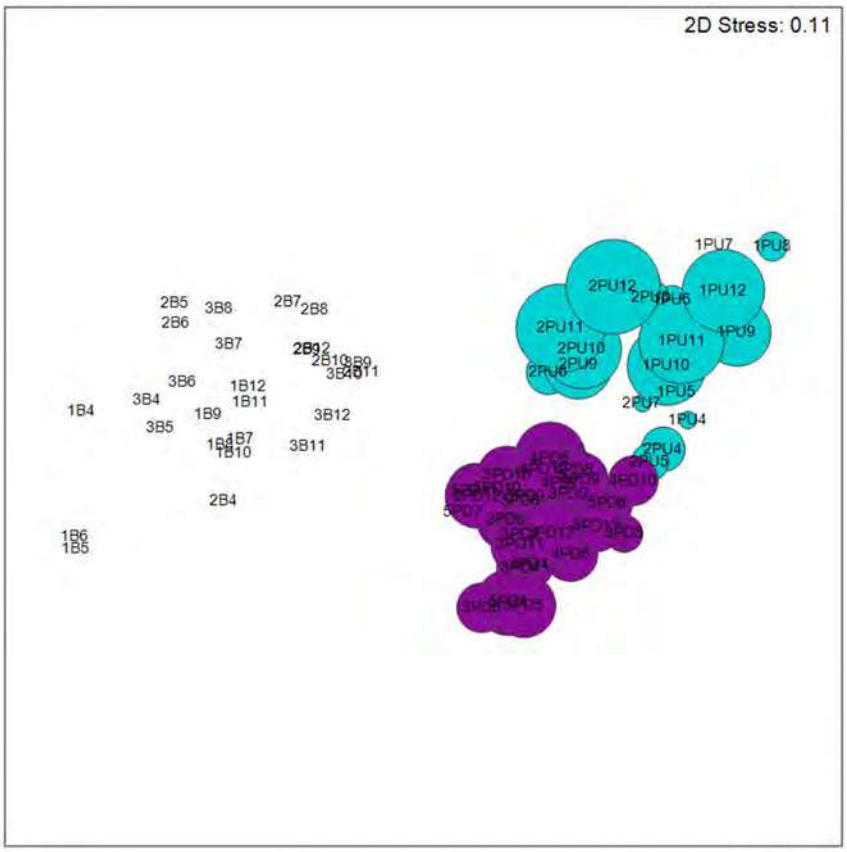

Figure 3.16. nMDS plot of bacterial community structure. nMDS: non-metric multi-dimensional scaling. Bubbles represent Kjeldahl nitrogen concentration by sample. Colours indicate reach (Barham: green, Painkalac Downstream: purple, and Painkalac Upstream: turquoise). Samples are coded by site, reach and set.

For the algal community, the most parsimonious distance-based model used 12 environmental variables to explain 73.1% of variation in community structure. The first two dbRDA axes explained 65.1% of fitted variation and 48.1% of total variation (Figure 3.17). High pH and water velocity distinguished the Barham River from the two Painkalac reaches. The second dbRDA coordinate axis explained 18.4% of fitted variation and 13.6% of total variation and showed that algal compositional differences between the Painkalac reaches were correlated with lower conductivity and higher temperature in Painkalac Downstream. Higher total phosphorous (TP) also differentiated the Barham River samples.

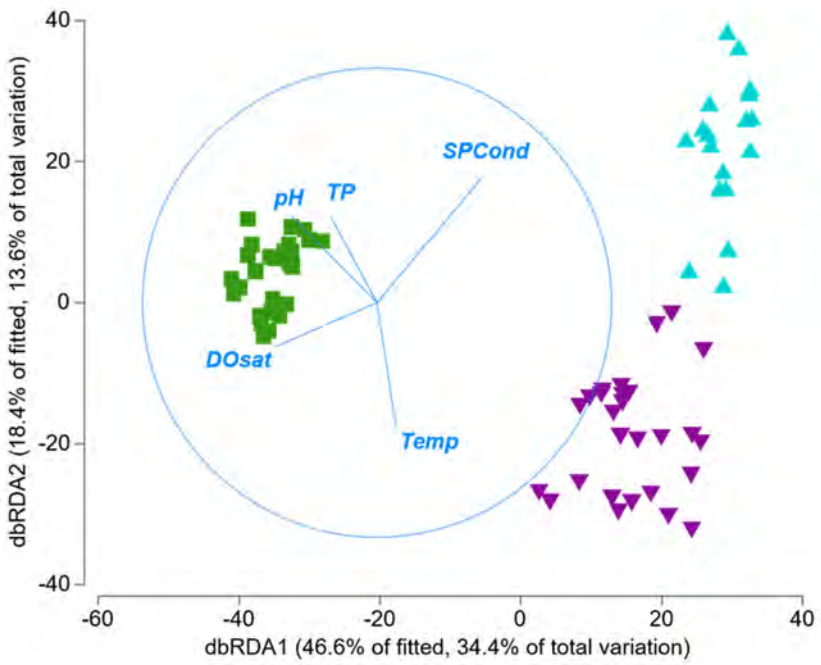

Figure 3.17. dbRDA ordination of algal community fitted to 13 environmental variables. dbRDA: Distance-based redundancy analysis. Vector lengths reflect the contribution of each variable, with variables with >40% multiple partial correlation included. Reaches are represented by colours and symbols (Barham: green squares, Painkalac Downstream: purple inverted triangles, and Painkalac Upstream: turquoise triangles). DOsat: dissolved oxygen saturation, TP: total phosphorous, SPCond: conductivity as specific conductance and Temp: temperature.

For fungi, the most parsimonious distance-based model used 12 environmental variables to explain 61.4% of variation in community structure. The first two dbRDA axes explained 60.5% of fitted variation and 37.2% of total variation (Figure 3.18). Higher pH and flow and lower conductivity distinguished the Barham River fungal community from the two Painkalac communities. The second dbRDA coordinate axis explained 21.4% of fitted variation and 13.1% of total variation and indicated that fungal compositional differences between the Painkalac reaches were correlated with higher nitrite and lower phosphorous in the Painkalac Downstream reach.

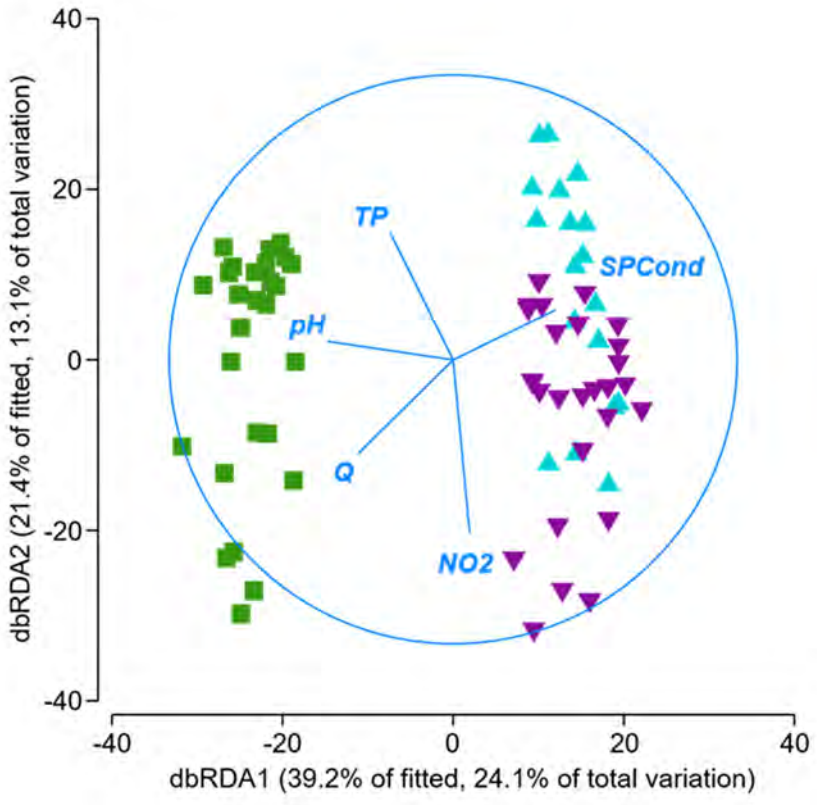

Figure 3.18. dbRDA ordination of fungal community fitted to 13 environmental variables. dbRDA: Distance-based redundancy analysis. Vector lengths reflect the contribution of each variable, with variables with >40% multiple partial correlation included. Reaches are represented by colours and symbols (Barham: green squares, Painkalac Downstream: purple inverted triangles, and Painkalac Upstream: turquoise triangles). TP: total phosphorous, SPCond: conductivity as specific conductance, NO2: nitrite and Q: mean discharge.

Based on the importance of nitrite as a predictor of fungal community structure according to the dbRDA (Figure 3.18), I plotted the nMDS plot of the fungal community but replaced the symbols with bubbles representing the concentration of nitrite by sample (Figure 3.19). The clusters towards the bottom of the nMDS plot are separated largely by higher nitrite levels.

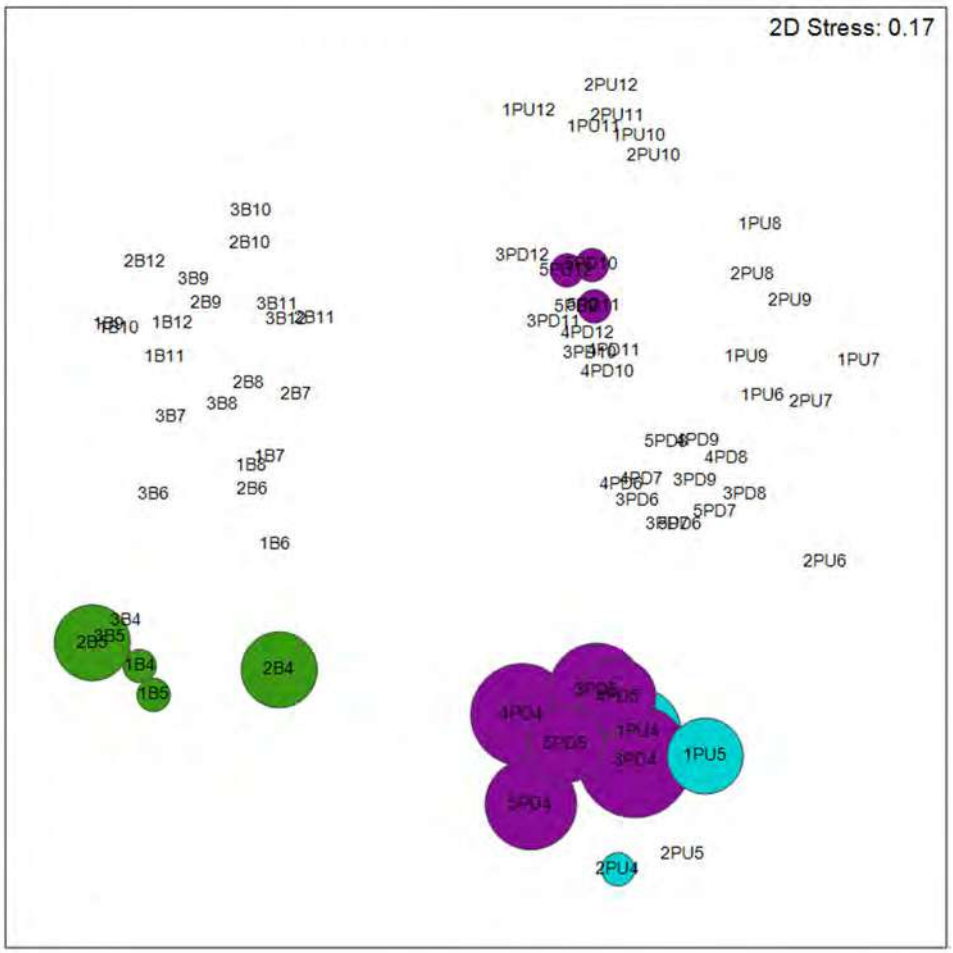

Figure 3.19. nMDS of fungal community structure. nMDS: non-metric multi-dimensional scaling. Bubbles represent nitrite concentration and colours indicate reach (Barham: green, Painkalac Downstream: purple, and Painkalac Upstream: turquoise). Samples are coded by site, reach and set.

To summarise the relationship between environmental conditions and the biological communities, the DistLM procedure was run again using the 'forward' selection procedure and the R^2 selection criterion. Bacterial and algal communities showed similar environmental relationships with the exception of ammonia (NH_4), which did not have a significant relationship with algal community structure (P = 0.08) (Table 3.7). Compared to bacteria and algae, fungi were more weakly correlated with water quality variables, including dissolved oxygen, pH, turbidity, nitrate and Kjeldahl nitrogen.

Table 3.7. Proportion of variation in biological community structure explained by individual environmental variables (R^2) for bacteria, algae and fungi ($P<0.05$).

Variable	Label	Bacteria	Algae	Fungi
Temperature (°C)	Temp	0.07	0.08	0.08
Dissolved oxygen (% sat)	DOsat	0.31	0.32	0.21
Conductivity, specific conductance (µS/cm at 25°C)	SPCond	0.31	0.32	0.20
pH	pH	0.30	0.31	0.22
Turbidity (NTU)	Turbidity	0.18	0.18	0.13
Ammonia (mg/L)	NH_4	0.03	n.s.	0.04
Nitrate (mg/L)	NO_3	0.26	0.24	0.17
Nitrite (mg/L)	NO_2	0.05	0.08	0.09
Total nitrogen as N (mg/L)	TCN	0.07	0.09	0.06
Total Kjeldahl N (mg/L)	TKN	0.26	0.28	0.18
Total P (mg/L)	TP	0.12	0.14	0.12
Mean velocity (m/s)	V	0.20	0.18	0.13
Mean discharge (ML/day)	Q	0.23	0.22	0.17

3.5. Discussion

Biofilm community structure was assessed using multi-metabarcoding (16S, 23S and ITS) to characterise the community structure of bacteria, algae and fungi, respectively. Each barcode assay/amplicon showed strong discrimination at the reach level and all biological communities were significantly and strongly correlated with environmental conditions. All biological communities were also significantly but less strongly correlated with PLFA composition, and stream biofilms showed some variation in lipid quality at the reach level. The two rivers in this study possessed a unique microbiome regardless of which microbiota were assessed.

3.5.1. Biota-environment relationships

Environmental conditions explained a large proportion of the variation in each biofilm assemblage. Both catchments investigated are relatively undisturbed, with low density development above the sampling locations, hence biological communities will reflect water quality and nutrient levels without the confounding influence of other pollutants such as heavy metals or urban runoff. Bacterial, algal and fungal community structure were significantly related to phosphorous levels and sensitive to nitrogen compounds. Indeed, eutrophication is a common and important cause of stream health impairment (Potapova & Charles, 2007). Bacterial community structure was significantly related to total Kjeldahl nitrogen concentrations, while nitrite appeared important in structuring fungal communities.

By integrating and relating environmental conditions to community composition, the stream microbiome could eventually serve as a stream health report card. However, before the stream microbiome can provide a snapshot of stream health, healthy and unhealthy microbiomes must be characterised and differentiated. In a human context, a decline in microbiome diversity (Berg *et al.*, 2020) or departure from an otherwise balanced ecology (Lloyd-Price, Abu-Ali & Huttenhower, 2016) is termed 'dysbiosis' and is associated with various diseases. Although doctors have sought to define a 'healthy microbiome' for humans for decades, diversity across individuals and populations has obscured a broad description of the universal features of a healthy microbiome (Lloyd-Price *et al.*, 2016). The stream microbiome presents the same challenges in defining health across space and time and attributing ecological dysbiosis to specific environmental perturbations.

3.5.2. Barcoding biofilm

Modern sequencing technology enables the characterisation of the spatial and temporal distribution of species from all domains of life across all habitats (Creer *et al.*, 2016) and next-generation sequencing methods have revealed the full breadth and complexity of the stream biofilm community (Battin *et al.*, 2016). However, no single DNA region can characterise the entire tree of life (Bradley *et al.*, 2016). At a minimum, a prokaryote marker and eukaryote marker are required, but metabarcoding with only 16S and 18S can underestimate the diversity of entire families of microorganisms (Marcelino & Verbruggen, 2016). In this study, I applied multi-metabarcoding using the 16S, 23S and ITS amplicons. Each of the three amplicons described significant variation among river reaches and sites and demonstrated a seasonal signal in abundance.

The performance of each amplicon in describing community structure can be assessed in terms of ecological discrimination and the level of taxonomic resolution. A benefit of molecular techniques is their ability to consider diverse benthic taxa without the need for multiple taxon specialists (Tapolczai *et al.*, 2019), but identification rate strongly depends on reference data (Zimmermann, Jahn & Gemeinholzer, 2011). The 16S amplicon is well-represented in public databases and global efforts are underway to improve our understanding of prokaryotic genomes (Zhang *et al.*, 2020). As shown in 0, diatom monitoring may be possible with the 16S amplicon, and the 16S marker offers the advantage of considering both cyanobacteria and photosynthetic eukaryotes using a single amplicon (Eiler *et al.*, 2013; Lehmann *et al.*, 2015; Bennke *et al.*, 2018). Molecular diatom data are not yet part of routine biomonitoring programs, but morphological diatom-based indices are widely used across the European Union and the USA (Charles *et al.*, 2021). Molecular data not only accurately reflect environmental conditions, they

supply more detail in less time than conventional morphological techniques (Hajibabaei *et al.*, 2011; Ji *et al.*, 2013; Dafforn *et al.*, 2014).

Fungal communities have been suggested as indicators of anthropogenic impacts (Bai *et al.*, 2018), but myco-monitoring is still in its infancy. Molecular analyses are revealing a large diversity of so-called 'dark matter fungi' that are environmentally ubiquitous and abundant but are missing from taxonomies of the fungal kingdom and have never been cultured (Grossart *et al.*, 2016). Only 3,000–4,000 species of aquatic fungi have been described, but given estimates of global fungal diversity at several million species, aquatic fungal diversity is greatly underestimated (Grossart & Rojas-Jimenez, 2016).

The number of reference sequences is growing and taxonomy is improving, but there are still fundamental questions about the differential amplification of primer sets and regions (Li *et al.*, 2020). The ITS amplicon is the fungal barcoding standard (Op De Beeck *et al.*, 2014) and more than a billion ITS reads are publicly available, but the region appears to represent ascomycetes and basidiomycetes better than other taxa (Nilsson *et al.*, 2019). Many aquatic fungi studies have focused on the 18S region, but a lack of fungal reference data has prevented phylum-level taxonomic assignment (Nilsson *et al.*, 2019).

The use of the 23S amplicon in barcoding studies is waning and in this study, the region showed poor sequence similarity and poor taxonomic resolution. Perhaps most importantly, the 23S primer set did not amplify any diatom sequences from biofilm samples. I was able to glean some information about the Bacillariophyta community from the 16S reads, but there is uncertainty in the performance of 16S as a marker gene for diatoms. The 18S amplicon is the preferred marker for resolving the taxonomy and phylogeny of protists (Bennke *et al.*, 2018) and would have been a better choice to provide more detail across additional taxa. Not only would 18S characterise microalgae,

but other biofilm meiofauna could be considered, such as ciliates, protozoans and amoebae (Weitere *et al.*, 2018).

The analysis of biological communities at the OTU level is generally losing favour. Amplicon sequence variants (ASV), based on single-nucleotide differences within the sequenced region, provide finer resolution and a consistent and unique barcode by taxon (Berg *et al.*, 2020). The ASV approach also avoids the clustering step that may group multiple organisms under a single representative sequence (Tapolczai *et al.*, 2019). ASVs can serve as indelible fingerprints when taxonomic reshuffling challenges the identity of existing morphospecies (Zimmermann *et al.*, 2014), and they can be traced across multiple studies to explore diversity at unprecedented scales (Thompson *et al.*, 2017).

A taxonomy-free approach that relates molecular sequences directly to ecological conditions (Pawlowski *et al.*, 2016; Apothéloz-Perret-Gentil *et al.*, 2017; Tapolczai *et al.*, 2019) is critical to developing novel microbial bioindicators. Although this approach has been criticised for ignoring the existing knowledge base that links ecological status to Linnaean binomials (Charles *et al.*, 2021), with the exception of diatoms, most microbiota do not have well-established environmental associations (Pawlowski *et al.*, 2016). A compilation of taxa and functional groups associated with different environmental stressors is an important next step in utilising microbiota as bioindicators (Pawlowski *et al.*, 2018; Simonin *et al.*, 2019; Sagova-Mareckova *et al.*, 2021).

I suggest that three 'data clouds' exist for identifying and classifying microbiota: morphological, molecular (Zimmermann *et al.*, 2014) and environmental. Under the 'data cloud' model, data can accumulate simultaneously to establish biotic and abiotic relationships over time. Improved information about a morphological species, a barcode or a set of environmental variables expands a given 'data cloud' and barcodes serve as stable identification benchmarks to link records among 'clouds' and through time

(Zimmermann *et al.*, 2014). As relationships develop between various taxa and stressors, patterns of dysbiosis within the stream microbiome should emerge that can then be tested across large spatial scales.

The revolution in big, open and global data provides an unprecedented opportunity to link and scale project-level monitoring (Dafforn *et al.*, 2016; Keck *et al.*, 2017; Beck *et al.*, 2020). Large collaborations can leverage organisational monitoring investments and capitalise on remote-sensing products. The Earth Microbiome Project (https://earthmicrobiome.org/) is an example of a global collaborative research network that compiles microbial sequences and metadata, including temperature and pH. An example of a river monitoring collaboration is The National Stream Internet Project (https://www.fs.fed.us/rm/boise/AWAE/projects/NationalStreamInternet.html) in the USA where diverse biotic and abiotic monitoring data are compiled within a comprehensive network to amplify monitoring actions and support decision making at multiple scales. Similar collaborative networks and data-sharing frameworks will be required to capture and store the quality and volume of metadata required to make molecular microbial bioindicators most useful in freshwater ecosystem biomonitoring and management.

3.5.3. Phospholipid composition

The characterisation of biofilm phospholipid content was included in this study as a measure of the ecological significance of changes in biological community structure. I observed distinct PLFA patterns at the levels of site and reach but in terms of overall quality, as measured by total EFA, there were no differences among reaches. There were some differences in EPA + DPA levels, which highly correlated with diatom abundance as diatoms are the primary supplier of EPA in healthy freshwater ecosystems (Ruess &

Müller-Navarra, 2019). There is increasing recognition that 'hidden' microbial members of the food web are supplying PUFA and obscuring trophic connections and what constitutes an 'essential' fatty acid is still an active research area with many uncertainties in aquatic food webs (Ruess & Müller-Navarra, 2019).

Biofilm has been treated as a uniform source of primary production for higher order consumers, but multiple trophic levels within the biofilm have rarely been considered (Weitere *et al.*, 2018). In the microbial soup that is biofilm, it is impossible to separate producers from consumers, and grazers may preferentially select certain organisms. Copepods have been shown to selectively graze large rod-shaped bacteria, and heterotrophic flagellates have exhibited specialised species-specific feeding strategies depending on the degree of attachment of bacterial cells (Erken *et al.*, 2012). I routinely observed macrograzers on the biofilm blocks, most commonly grass shrimp (*Paratya australiensis*) (Crustacea) and chironomids (Diptera) but also larval Odonata. These grazers may not only be skewing PLFA composition, they may also be measured alongside primary production. When I harvested the experimental blocks, the larger macroinvertebrates would swim away but the chironomids remained embedded in the biofilm and were therefore sampled and analysed in terms of PLFA content. New insights into specific biofilm feeding strategies have revealed challenges in characterising the trophic relationships within stream food webs using PLFA (Whorley *et al.*, 2019). The complexity of benthic food webs also limits the characterisation of relationships between biotic abundance and PLFA patterns because markers overlap multiple taxa, and some PLFAs may be elevated within a given group but present in lower concentrations in other groups (Kelly & Scheibling, 2012). These confounding factors help to explain why the PLFA compositional data from this study were related to but not predictive of biological community structure.

Almost fifty years ago, Sargent (1976) asserted that fatty acid analyses are, "a rather blunt tool in defining food chain inter-relationships," but they have nevertheless been widely used for tracing aquatic food webs (Iverson, 2009), perhaps for lack of a better option. Recent research has concluded that PLFA characterisation must be paired with other, more precise techniques, to adequately describe community composition (Orwin *et al.*, 2018; Whorley *et al.*, 2019). Although neither accurate nor precise, fatty acid-based methods may still have utility for rapidly and inexpensively describing broad microbial groups (Mrozik *et al.*, 2014).

3.6. Conclusion

All three metabarcoding regions (16S, 23S and ITS) demonstrated utility in describing biofilm community structure and all three biological community datasets were significantly correlated with physicochemical variables and PLFA composition. While PLFA should, in theory, help to confirm biological findings, they are generally coarser in scale and may be confounded by overlapping PLFA markers occurring across unrelated taxa. Due to advances in sequencing technology and data networks, the stream microbiome, as characterised by the biofilm community, can be an important indicator of stream health.

Environmental Flow Effectiveness Testing

4.1. Chapter overview

An experiment was conducted in two coastal streams in Victoria, Australia, to evaluate the impact of environmental flow releases on stream health. Starting in 2018, Painkalac Dam began operating according to an environmental flow prescription calling for brief, four-fold increases in flow during summer. These three-day pulses were designed to mimic the natural flow regime of the creek and improve stream health.

Such brief increases in flow would not be expected to produce changes in aquatic macroinvertebrate assemblages traditionally used as bioindicators. Instead, I examined the more responsive but less studied stream biofilm community that colonises submerged surfaces and supports the base of the stream food web. The nutritional quality of the biofilm as a food resource for higher trophic levels was evaluated by characterising phospholipid fatty acid (PLFA) content. The structure of bacterial, algal and fungal assemblages within the biofilm was examined using multiple DNA barcoding regions (16S, 23S and ITS).

By comparing the regulated stream reach receiving scheduled environmental flow releases and two unregulated reaches with natural streamflow pulses, I tested whether environmental flows shifted the community structure or nutritional quality of biofilm communities. This study is the first to use DNA metabarcoding and PLFA to measure ecological responses to environmental flows.

4.2. Introduction

Streamflow is considered the 'master variable' governing ecological patterns and as such, lotic ecosystems are largely a product of their natural flow regime (Poff *et al.*, 1997). Yet, flow regimes are rarely natural because most lotic systems have some degree of human alteration and three-fourths of the world's large rivers are dammed (Grill *et al.*, 2019).

Environmental flows are intended to restore some semblance of natural flow pattern in regulated rivers under heavy human control (Olden & Naiman, 2010) . Environmental flows are thought to sustain river health and support ongoing human use, but the accounting of environmental benefits lags behind the accounting of economic impacts (Postel & Richter, 2003).

As a field, environmental flow science has been criticised for focusing mainly on method development with little attention given to the monitoring, evaluation and revision of strategies (Souchon *et al.*, 2008; Davies *et al.*, 2014). A subset of the hundreds of environmental flow design methods are holistic, in that they consider the entire ecosystem at the broadest scale possible (Tharme, 2003). Holistic methods rely on a long-term hydrologic time series to develop a set of flow metrics that quantify individual components of the natural flow regime (Poff *et al.*, 1997; Poff, Tharme & Arthington, 2017). Significant advances have been made in characterising stream hydrology and natural flow regimes, but the flow-ecology relationships that underpin environmental flows remain poorly understood, particularly at lower trophic levels (Poff & Zimmerman, 2010; Davies *et al.*, 2014; Warfe *et al.*, 2014).

Gillespie *et al.* (2015) identified 76 peer-reviewed studies published between 1981 and 2012 that reported primary data, assessed the impact of dam outflow modification, and monitored abiotic and biotic downstream effects. They noted that fish,

water quality and macroinvertebrates were all included in about one third of the studies, but primary production was only considered in 15% of studies (Gillespie *et al.*, 2015). Poff and Zimmerman (2010) identified 55 papers published over a 40-year period that quantitatively analysed relationships between flow alteration and ecological responses. The majority of studies focused solely on flow magnitude and few considered other components of the natural flow regime, such as flow duration and rate of change (Poff & Zimmerman, 2010; Gillespie *et al.*, 2015).

Olden and Naiman (2010) highlighted the coupled nature of a river's hydrologic regime with its thermal regime, including the magnitude, frequency, duration, timing and variability of water temperature at a range of spatial and temporal scales. Water temperature has not been widely considered in the modelling and monitoring of environmental flows despite its role as a fundamental ecological variable that affects growth, metabolism, mortality and signal behaviour such as migration and spawning (Olden & Naiman, 2010). Similarly, water quality is related to hydrologic regime but is often overlooked in setting environmental flow prescriptions.

There is therefore a collective call for improved ecological monitoring to better understand environmental flow outcomes and improve decision making (Poff & Zimmerman, 2010; Shafroth *et al.*, 2010; Gillespie *et al.*, 2015; King *et al.*, 2015). It has been suggested that environmental flow projects should function as restoration ecology experiments (Bunn & Arthington, 2002; Arthington & Pusey, 2003) to inform management and clarify cause-effect relationships between flow and ecological variables (Poff & Zimmerman, 2010; Shafroth *et al.*, 2010). In addition, ecological monitoring of flow alterations could be used within an adaptive management framework to evaluate and adjust future actions (Poff *et al.*, 1997; Shafroth *et al.*, 2010; King *et al.*, 2015).

The assessment of environmental flows using non-taxonomic measures began over twenty years ago (Watts & Ryder, 2002) and there has been ongoing focus on changes in biofilm nutritional quality associated with changing flow regimes (Chester & Norris, 2006). It has been postulated that, by resetting the successional clock of the biofilm community, the natural disturbance regime in unregulated rivers supports a more nutritious biofilm supply for consumers (Sheldon & Walker, 1997). Early-stage biofilms dominated by single-celled bacteria and algae have a higher nutritional quality, with lower carbon-to-nutrient ratios than more mature biofilms with a higher proportion of matrix material relative to the living cells (Weitere *et al.*, 2018). At low velocities, flow pulses may stimulate algal growth by supplying nutrients, but above a threshold biofilms are removed by scouring (Ryder *et al.*, 2006; Larned, 2010). Scouring disproportionately removes filamentous algal species but also results in a net decrease in taxonomic richness of the algal community (Ryder *et al.*, 2006). There is evidence that river regulation tends to maintain late-successional biofilm communities dominated by filamentous algae, with food quality inferior to earlier successional communities (Sheldon & Walker, 1997; Burns & Walker, 2000; Chester & Norris, 2006).

The declining ecological condition below Painkalac Dam during the Millennium Drought led to the development of an environmental flow prescription for Painkalac Creek. The prescription was developed in response to community concerns about the impact of the dam on stream and estuary conditions. In 2007, the Corangamite Catchment Authority contracted an environmental flow study of the freshwater reach of Painkalac Creek between the reservoir and the upper limits of the estuary. The environmental flow recommendations for Painkalac Creek were developed largely based on hydraulic modelling of a 230-metre reference reach (Doeg, Vietz & Boon, 2008). A series of cross-sectional transects were established to determine the position of in-channel and near-

channel features, and a Hydrologic Engineering Center River Analysis System (HEC-RAS) model was used to estimate the flows required to achieve inundation in specific habitats and to provide minimum velocity requirements.

The FLOWS method (NRE *et al.*, 2002) relies on modular hydrologically-defined building blocks of flow components associated with specific ecological functions, and FLOWS was used to identify a series of flow-dependent objectives (Doeg *et al.*, 2008). In accordance with FLOWS (NRE *et al.*, 2002; Merz, 2013), flow magnitude and duration targets were set for each of six natural flow regime components: cease-to-flow, low flow, freshes, high flows, bankfull flows and overbank flows. This chapter focuses on assessing the low-flow freshes (LFF) scheduled for delivery four times each summer (Figure 4.1).

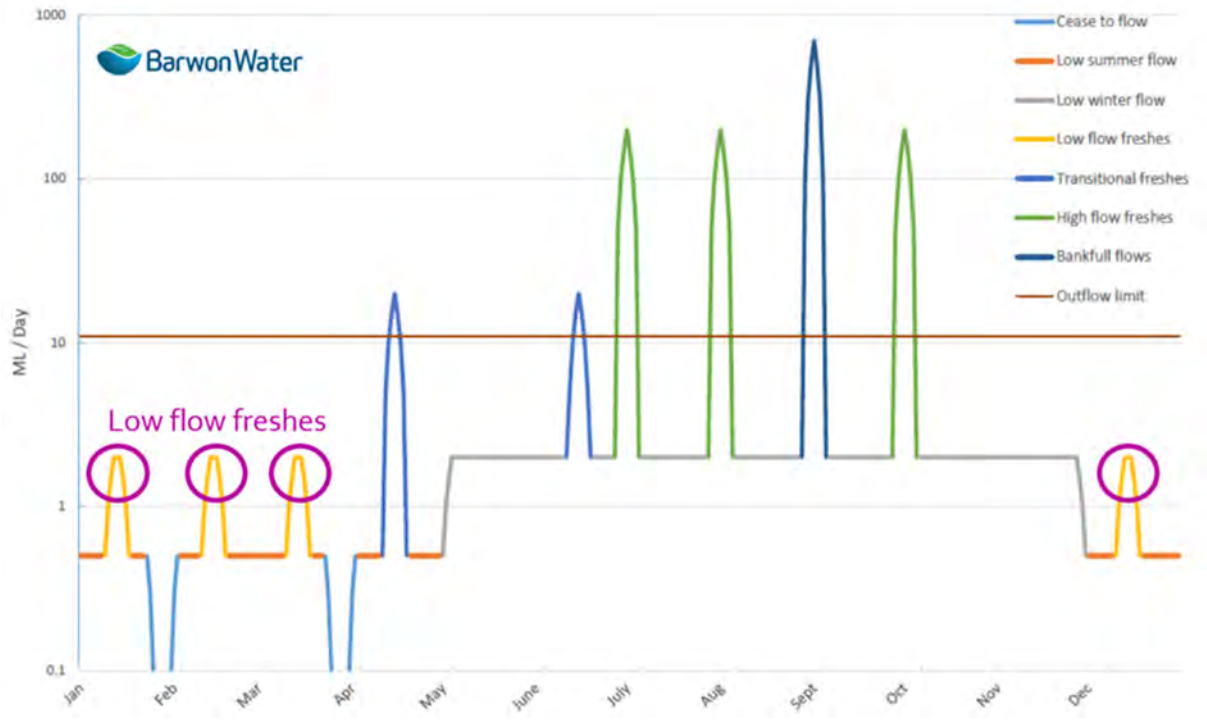

Figure 4.1. Conceptual representation of Painkalac Creek environmental flow recommendations (log scale). Modified from (Barwon Water, 2016).

This study aimed to assess the impacts of environmental flow pulses on stream biofilm community structure and nutritional quality using a manipulative field experiment. I hypothesised that flow events would shift biofilm community structure and nutritional content. I predicted that: 1) algal taxonomic diversity would decrease with pulse flows, 2) bacterial and fungal diversity would increase with pulse flows and 3) pulses would be associated with more nutritious biofilms. I tested these hypotheses by comparing the biofilm response below Painkalac Dam to the biofilm response in two unregulated reaches, one in Painkalac Creek above the reservoir and the other in the nearby Barham River. I examined the structure of bacterial, algal and fungal assemblages using multiple DNA barcoding regions (16S, 23S and ITS), and I evaluated the nutritional quality of the biofilm by characterising phospholipid fatty acid (PLFA) content. This study represents the first attempt to use molecular techniques and phospholipid composition to evaluate the performance of environmental flows. Such data can help establish fundamental flow-ecology relationships at the base of the stream food web.

4.3. Methods

A field experiment was conducted in Victoria, Australia from October 2018 to March 2019 to measure the biological response to the environmental flow releases from Painkalac Reservoir. The experiment was designed, using a before-after-control-impact design (BACI) (Underwood, 1992) to compare the impacted, regulated Painkalac Downstream (PD) reach to the control reaches, Painkalac Upstream (PU) and the Barham River (B) (Figure 3.2).

4.3.1. Streamflow

The experiment was designed around the scheduled LFF in the regulated Painkalac Downstream reach (Table 4.1). Natural flow pulses in the two unregulated reaches occurred in response to precipitation events early in the summer. Discharge data for each reach were obtained through the Water Measurement Information System of Victoria (WMIS) (DELWP, 2016a) for the Barham River (stationID:235233), Painkalac Upstream (stationID:235257) and Painkalac Downstream (stationID:235232). Hydrology and precipitation statistics were compiled and visualised using R 3.5.0 (R Core Team, 2019) and the Hydrostats package (Bond, 2015b). Precipitation data (BOM, 2020a) from Aireys Inlet (stationID:090180) were added to the Painkalac Creek hydrographs and Apollo Bay data (stationID:090001) were added to the Barham River hydrograph following the method from Chuliang Xiao (https://rpubs.com/cxiao/hydrograph-ggplot2-plot).

.

Table 4.1. Scheduled low-flow freshes increasing flow to ~2 ML/day.

Event	Day	Date
1	Tuesday	4/12/2018
	Wednesday	5/12/2018
	Thursday	6/12/2018
2	Tuesday	22/01/2019
	Wednesday	23/01/2019
	Thursday	24/01/2019
3	Wednesday	27/02/2019
	Thursday	28/02/2019
	Friday	29/02/2019
4	Wednesday	20/03/2019
	Thursday	21/03/2019
	Friday	22/03/2019

4.3.2. Testing the effects of flow pulses

The effects of flow pulses on abiotic and biotic variables were tested by a four-factor permutational multivariate analysis of variance (PERMANOVA) using Primer v7 with PERMANOVA+ (Anderson, 2001). The reach, or 'RiverPosition', was treated as a fixed factor with 'Site' nested within 'RiverPosition'. The nested, fixed 'FlowCat' factor was developed based on the cumulative volume of water for each set based on the WMIS gauge corresponding with 'RiverPosition'. The 'Pulse' flow category was assigned as >0.40 (max volume) while 'Base' flow was <0.40 (max volume). The random 'Set' factor was nested within 'FlowCat'.

The two Painkalac positions were contrasted with the Barham position factor and the positions within Painkalac Creek were contrasted with each other. Each analysis term was tested with 9,999 permutations and significance was based on type-III sum of squares. The level of significance was set to $\alpha = 0.05$ for all tests, but values close to the threshold ($0.05<P<0.1$) were also considered. Significant terms were investigated with pairwise comparisons using the same PERMANOVA routine.

The same criteria for assigning the flow category term were applied across the three reaches. The experiment was scheduled around the LFF in the Painkalac Downstream reach so that the deployment of a set of biofilm blocks would correspond to the timing of the flow pulses and each set could be assigned a flow category of 'base' or 'pulse'. I calculated the total volume of flow (ML) during deployment for each set and determined the maximum flow volume by reach during the experimental period. By dividing the flow volume for the LFF sets by the maximum volume in the Painkalac Downstream reach, I determined that a threshold proportion of 0.40 separated the 'Pulse' sets from the 'Base' sets. I then applied this same technique to objectively and

consistently apply the category to the biofilm sets from the two unregulated reaches. The lack of significance of the 'FlowCat' term across all PERMANOVAs conducted provided some evidence that the categorical assignment (Pulse/Base) did not affect the PERMANOVA outcome. However, sensitivity analysis was performed to evaluate the appropriateness of the threshold and the resulting category. When the threshold value for categorical assignment was 0.3, the term was significant in the PERMANOVA analysis (P=0.0208) but the sets retained the same category, the PERMANOVA results were similar and the significance levels of the pairwise comparisons were identical. When a threshold of 0.5 was applied, the sets that experienced the LFF were not categorised as 'pulse' sets so the category became meaningless. Finally, as another test of sensitivity, set 4 was eliminated from the biological abundance matrices before performing the PERMANOVA analysis so that only the LFF would be considered and not the early season higher flow (2 ML). When only sets 5-12 were analysed, the results were the same, with no significant changes in the Painkalac Downstream reach across all amplicons. Based on the results of these analyses, I determined that 0.40 was the most appropriate threshold to assign the flow category.

The primer 'distance among centroids' tool was used to examine the relative sizes and direction of effects. After calculating the distance among centroids using the same resemblance measure selected for the PERMANOVA routine, a principal coordinates analysis (PCO) was constructed to visualise the dispersion (Anderson *et al.*, 2008). Each centroid represents the centre of the multivariate data cloud and the PCO provides a visual representation of the original dissimilarity.

Physicochemical conditions

Details of the measurement of abiotic variables are provided in section

3.3.2. Physicochemical conditions. The subset of variables analysed to test the effects of environmental flow pulses (Table 4.2) differed from that used in Chapter 3 (Table 3.2). To analyse differences in measured abiotic conditions, the PERMANOVA routine was applied to a resemblance matrix of normalised Euclidean distance of environmental variables (Temp, DOsat, SPCond, pH, turbidity, NH_4, DOC, NO_3, NO_2, TCN, TKN, TP and V), herein referred to as 'PCHEMV'. Mean TON was not considered in the analysis because it was strongly correlated (0.99) with nitrate levels. The measured velocity around the experimental frame was included but the calculated average discharge variable (Q) was not considered to prevent redundancy between the assigned flow category and the variable. The distance among centroids was calculated for the same Euclidean resemblance matrix, and a multi-dimensional scaling (MDS) plot was constructed from the resulting distance matrix to visualise the dispersion of environmental variables by flow category.

To test whether the environmental flow releases from Painkalac Reservoir affected the stream temperature differently from rain-fed pulses in the two unregulated segments, I examined the relationship between stream temperature and discharge (Q) for each segment using regression analysis in R v.3.6.0 (R Core Team, 2019) and plotted temperature on the hydrograph (Ladson, 2016).

Table 4.2. Environmental, nutrient and biomass variables with measurement location and method. All variables were used to evaluate relationships between abiotic, biotic and phospholipid fatty acid (PLFA) metrics.

Variable	Shortname	Measured in	Method
Temperature (°C)	Temp	Field	YSI multimeter
Dissolved oxygen (% sat and mg/L)	DO	Field	YSI multimeter
Conductivity, specific conductance (µS/cm at 25°C)	SPCond	Field	YSI multimeter
pH	pH	Field	YSI multimeter
Turbidity (NTU)	turbidity	Field	Hach meter
Mean velocity (m/s)	V	Field	Valdeport meter
Ammonia (mg/L)	NH_4	Lab	ALS
Dissolved organic carbon	DOC	Lab	ALS
Nitrate (mg/L)	NO_3	Lab	ALS
Nitrite (mg/L)	NO_2	Lab	ALS
Total nitrogen as N (calculated)	TCN	Lab	ALS
Total Kjeldahl N (mg/L)	TKN	Lab	ALS
Total P (mg/L)	TP	Lab	ALS

Biological community structure

A full description of the DNA extraction and bioinformatics pipeline is provided in section 3.3.3. Biofilm field experiment. Biological communities from the three amplicons (16S, 23S and ITS) were analysed at the operational taxonomic unit (OTU) level and class level using only the target taxa. To ensure that the 16S OTU-level analysis only considered bacteria, I removed all OTUs identified as chloroplast reads in the targeted bioinformatics process (described in 0). For the 23S assay, I selected the OTUs assigned to the Viridiplantae (including green algae) and Eukaryota (including red algae) clades. For the ITS assay, only the OTUs assigned as Fungi were selected.

To conservatively construct each OTU table, sequences with <80% homology were ignored, and extremely rare OTUs were filtered to include only those with ≥0.1%

abundance in a sample. Read counts were normalised to proportions (McKnight *et al.*, 2019) by applying a 'standardise by total' approach (Clarke & Gorley, 2006) and a Bray-Curtis (B-C) (Bray & Curtis, 1957) similarity matrix was constructed for each amplicon. Relative abundance was visualised using a shade plot (Clarke *et al.*, 2014), and homogeneity of dispersion between groups was tested using PERMDISP (Anderson *et al.*, 2008). Appropriate transformations were performed to reduce the impact of a few dominant taxa in the B-C similarity analysis when assumptions of homogeneity were violated. To evaluate meaningful changes in community structure and to address the inconsistent taxonomic resolution, I conservatively conducted the SIMPER analysis on class-level abundance data of the target taxa for each amplicon. Diversity, represented by OTU richness, was analysed using a two-way ANOVA of reach and flow category with a Tukey-test for pairwise multiple comparisons.

Phospholipid analysis

Phospholipid fatty acid composition (51 individual PLFA, Table 3.5) was evaluated by applying the four-factor PERMANOVA routine (described in section 4.5.3 Flow-ecology relationships) to the Euclidean distance matrix of fourth root-transformed individual PLFA. Lipid quality was assessed by considering the concentrations of individual essential fatty acids (EFA) including eicosapentaenoic acid (EPA), docosahexaenoic acid (DHA), arachidonic acid (ARA), linolenic acid (LIN) and α-linolenic acid (ALA). The assessment of lipid classes, including saturated fatty acids (SFA), monounsaturated fatty acids (MUFA), polyunsaturated fatty acids (PUFA) and the sum of EPA+DHA, was conducted using a two-way ANOVA of reach and flow category with a Tukey-test for pairwise multiple comparisons.

4.4. Results

4.4.1. Streamflow

Natural flows in the Barham River had already dropped to summer low-flow conditions by November 2018 (Figure 4.2C). A storm arrived on the 13 December 2018 and over the next four days, 31.6 mm of rain fell at Apollo Bay (BOM, 2020a). The river rose quickly, reaching a peak flow of 835 ML/d on 15 December. The peak flow of 0.32 ML/d in the upstream reach during the experimental period occurred on 22 December after 11.6 mm of rain fell at Aireys Inlet (Figure 4.2A).

There were no flow pulses associated with the December storms in the regulated Painkalac Downstream reach (Figure 4.2, 4.3). The first LFF, scheduled for early December 2018 (Table 4.1) could not be delivered because the flows had not been adjusted from the 'low winter flow' level of 2 ML/day. On 10 December 2018, the flow was adjusted to the 'low summer flow' condition, which calls for releases of 0.5 ML/day. The first environmental flow release during the biofilm experiment began on 22 January 2019 and Barwon Water delivered three LFF during the experimental period in coordination with the research experiment and consultation with the Corangamite Catchment Management Authority. On 19 February, there was a brief, unexplained increase in discharge that was not the product of a planned release.

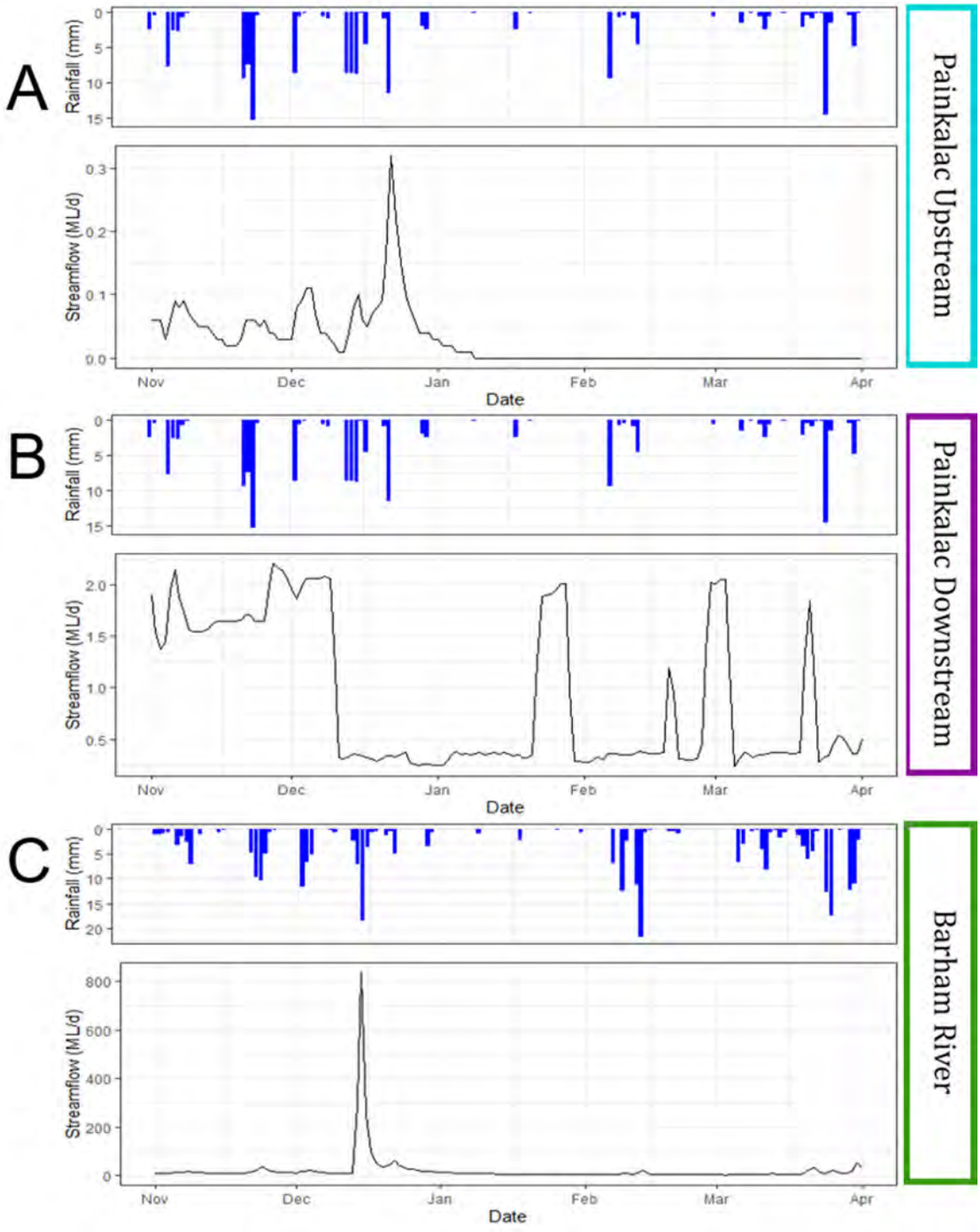

Figure 4.2. Rainfall (mm) and streamflow (ML/d) for each river reach (Nov 2018–Mar 2019). Rainfall (BOM, 2020a) is shown in the upper panels by blue bars and streamflow (DELWP, 2016a) is shown in the lower panels.

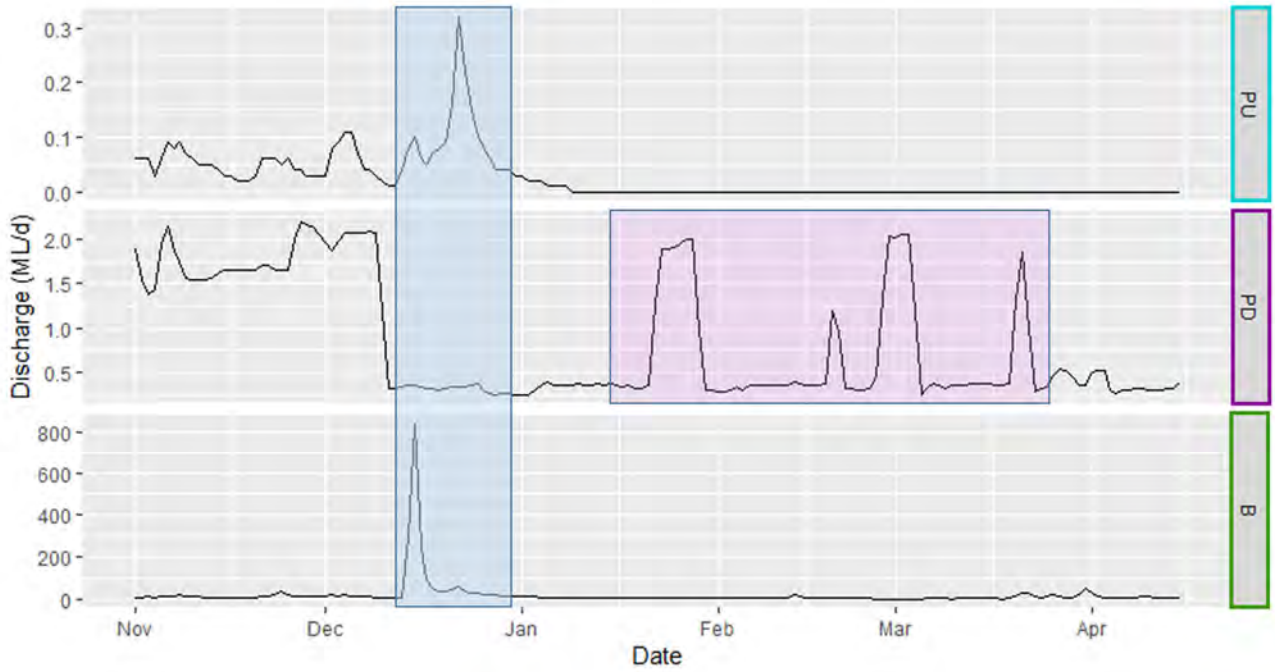

Figure 4.3. Stream hydrographs of three reaches during the experimental period. PU: Painkalac Upstream, PD: Painkalac Downstream and B: Barham from 1/11/2018 to 15/4/2019. Each reach has a unique vertical axis for discharge (ML/d). Natural flow pulses produced by rainfall are highlighted in blue. Environmental flow pulses are highlighted in purple.

During the experimental period, the environmental flow freshes were distinct from the natural flow pulses in their timing and the unique shape of the hydrograph (Figure 4.2, 4.3). Across three years of environmental releases, the mean rate of the rise for the environmental flows was 0.19 ML/day versus a rise of 0.03 ML/day in the upstream reach. The environmental flows ended even faster than they started with a mean rate of the fall of 0.58 ML/day versus a rate of 0.02 ML/day for the natural summer flow pulses during the same time period in the upstream reach.

Table 4.3. Average rate of rise and fall for flow pulses (0.6 quantile) during three summer seasons (15/12 - 15/3) in the Painkalac Upstream (PU) and Painkalac Downstream (PD) reaches.

Reach	Summer	Avg. Rise	Avg. Fall
PU	2017/2018	0.02	0.02
	2018/2019	0.05	0.03
	2019/2020	0.02	0.02
PD	2017/2018	0.17	0.23
	2018/2019	0.17	0.22
	2019/2020	0.24	0.53

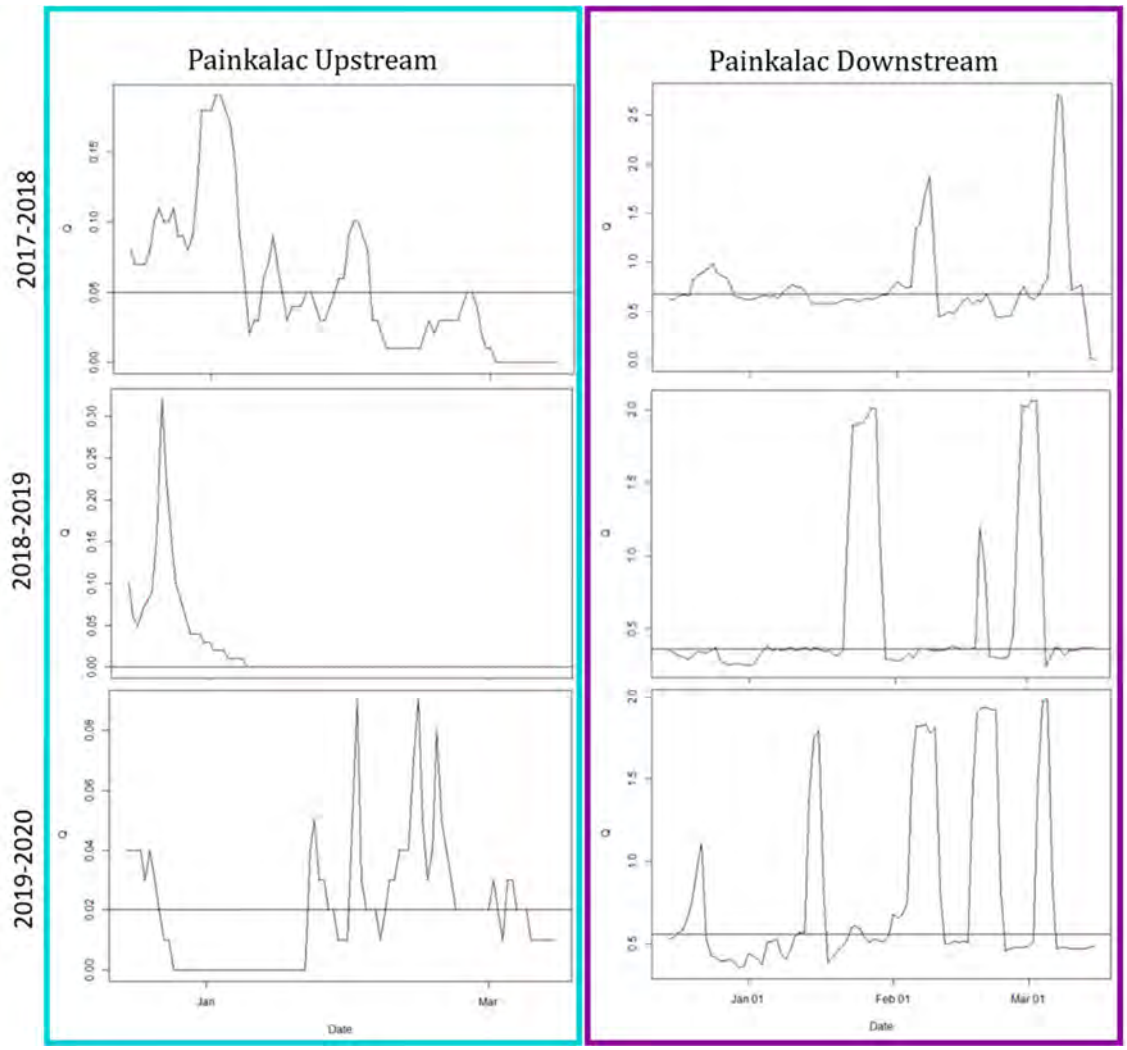

Figure 4.4. Summer hydrographs (15 December to 15 March) for three seasons (2017-2020) in the Painkalac Upstream and Painkalac Downstream reaches. The vertical axis for discharge (Q)(ML/day) varies by reach and year. Bar indicates 0.6 quartile cut-off used to calculate rise and fall rates.

4.4.2. Physicochemical conditions

The abiotic conditions associated with all 94 biofilm samples were analysed together using a mixed effects model (Figure 4.5). According to the PERMANOVA analysis, the two Painkalac reaches were not significantly different (pseudo-$F_{1,93}$ = 3.17, P = 0.1271) but they were distinct from the Barham River (pseudo-$F_{1,93}$ = 15.45, P = 0.0025). This difference between the two rivers was the largest component of variation. There was significant variability among sites and through time (Sets) (Table 4.4). There was no significant effect of the flow category alone but there were significant interactions between the flow category (FlowCat) and both reach (RiverP) and site. There was also a significant interaction between reach (RiverP) and time (Set).

Based on the significant RiverP × FlowCat term, I conducted a PERMANOVA pairwise test of river position by flow (FlowCat) for pairs of the flow category on the transformed, normalised Euclidean resemblance matrix (Table 4.5). Only the Barham River showed a significant difference in measured physicochemical conditions between the Base and Pulse conditions at $\alpha = 0.05$. However, given the variability and small number of Pulse samples from the reach, it may be appropriate to consider the results of the statistical tests using a less conservative *a priori* level of $\alpha = 0.10$. Under this less conservative approach, there were significant environmental changes in the upstream reach of Painkalac Creek associated with pulse flows.

In the Barham River, linear regression demonstrated a significant but weak negative relationship between water temperature and discharge ($R^2 = 0.10$, $F_{1,8736} = 958.4$, $P<0.001$) (Figure 4.6). Upstream of the reservoir in Painkalac Creek, the relationship between water temperature and discharge was also significant and weakly negative ($R^2 = 0.04$, $F_{1,8736} = 958.4$, $P<0.001$). For Painkalac Downstream, regression

analysis showed that water temperature increased slightly but significantly with discharge ($R^2 = 0.35$, $F_{1,8726} = 4736$, $P<0.001$).

Table 4.4. PERMANOVA results from the Euclidean distance matrix of abiotic variables and streamflow variables. Showing reach (RiverP), flow category (FlowCat), sites, sample timing (Set) and interactions between the terms of the model. df: degrees of freedom, SS: sum of squares, MS: mean squares, pseudo-F: ratio of between-cluster variance to within-cluster variance, Perms: number of permutations. Bold indicates P≤0.05.

Factor	df	SS	MS	Pseudo-F	Perms	P(perm)
RiverP	2	290.81	145.4	10.83	9943	**0.0004**
FlowCat	1	15.77	15.771	1.69	9950	0.177
Site(RiverP)	5	74.29	14.858	16.34	9907	**0.0001**
Set(FlowCat)	19	271.01	14.264	15.69	9842	**0.0001**
RiverPxFlowCat	2	68.923	34.462	6.00	9934	**0.0001**
RiverPxSet(FlowCat)	10	37.673	3.7673	4.14	9867	**0.0001**
Site(RiverP)xFlowCat	5	15.35	3.07	3.38	9870	**0.0001**

Table 4.5. PERMANOVA pairwise test results. Tests based on river position by flow for pairs of the flow category level on the transformed, normalised Euclidean resemblance matrix. P(MC): Monte Carlo P-value, t: test statistic, Perms: number of permutations, Den d.f. = denominator degrees of freedom. Bold indicates P(MC)≤0.05 and italics indicate P(MC)<0.1.

Reach	t	Perms	Den d.f.	P(MC)
B	1.88	59	11.99	**0.0474**
PU	1.99	6	3.04	*0.0913*
PD	0.83	59	11.53	0.6176

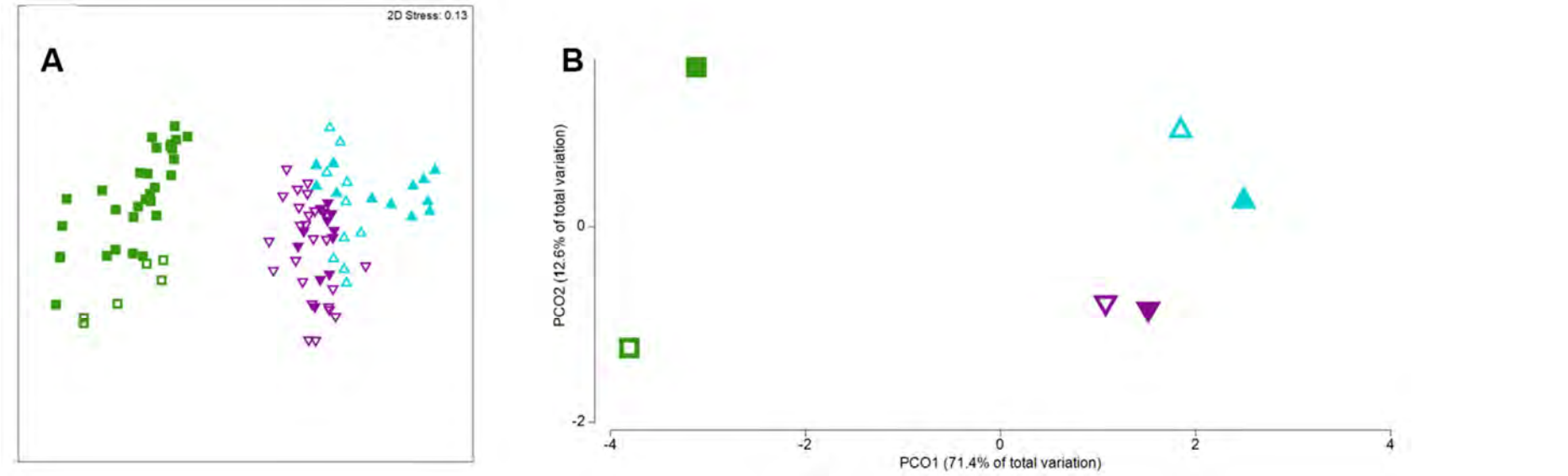

Figure 4.5. A) nMDS of physicochemical variables (PCHEMV). B) PCO of distances among centroids on the basis of the Euclidean distance measure of PCHEMV. Reaches are represented by colours and symbols (Barham: green squares, Painkalac Downstream: purple inverted triangles, and Painkalac Upstream: turquoise triangles). Solid symbols represent base condition and hollow symbols denote pulse condition.

In the Painkalac Upstream and Barham River reaches, flow pulses showed a cooling effect while in the Painkalac Downstream reach, environmental flow releases were associated with elevated water temperature (Figure 4.7). On 22 January 2019, when the first LFF was initiated, maximum temperature recorded on the logger at the Painkalac Downstream site was 38.3°C and on 27 February, at the start of the second planned LFF, maximum logged air temperature was 37.5°C. The unscheduled release that occurred from 9 AM on 19 February and lasted until 10 AM on 20 February did not produce the same warming effect as the longer environmental flow pulses.

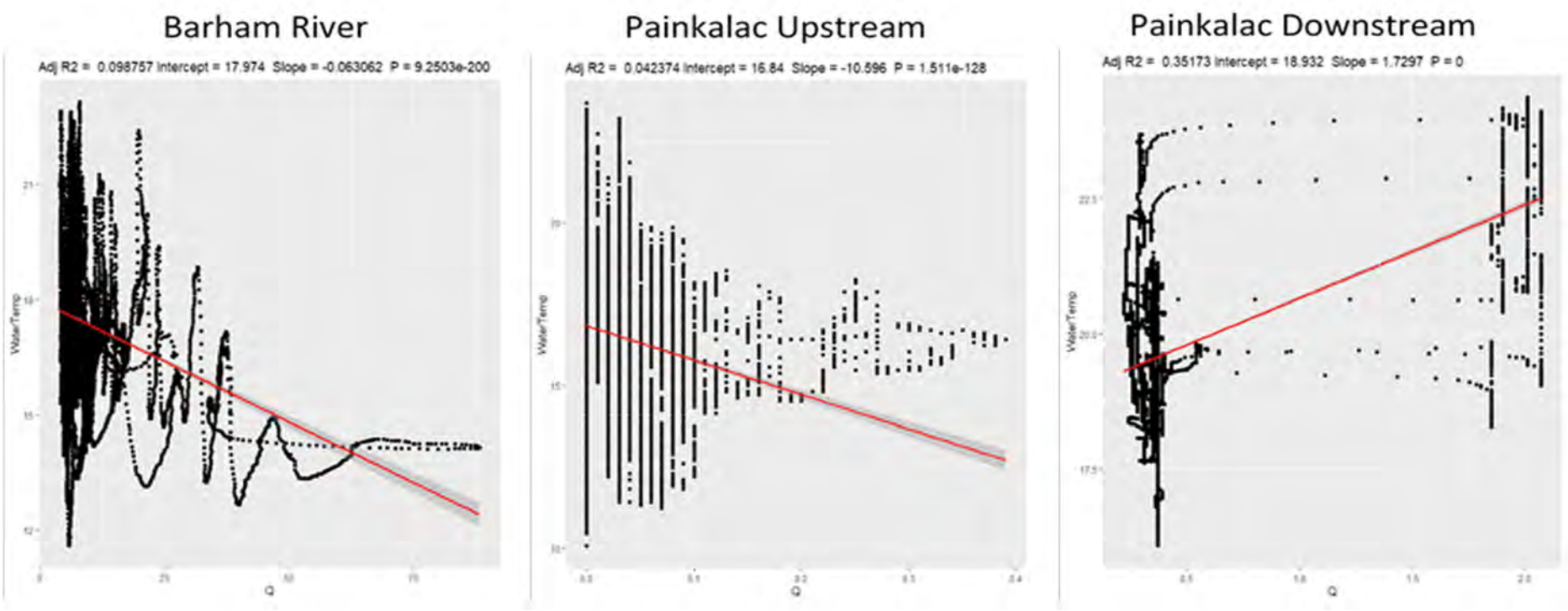

Figure 4.6. Regression analysis of water temperature (°C) and discharge (Q) by river reach during the experimental period.

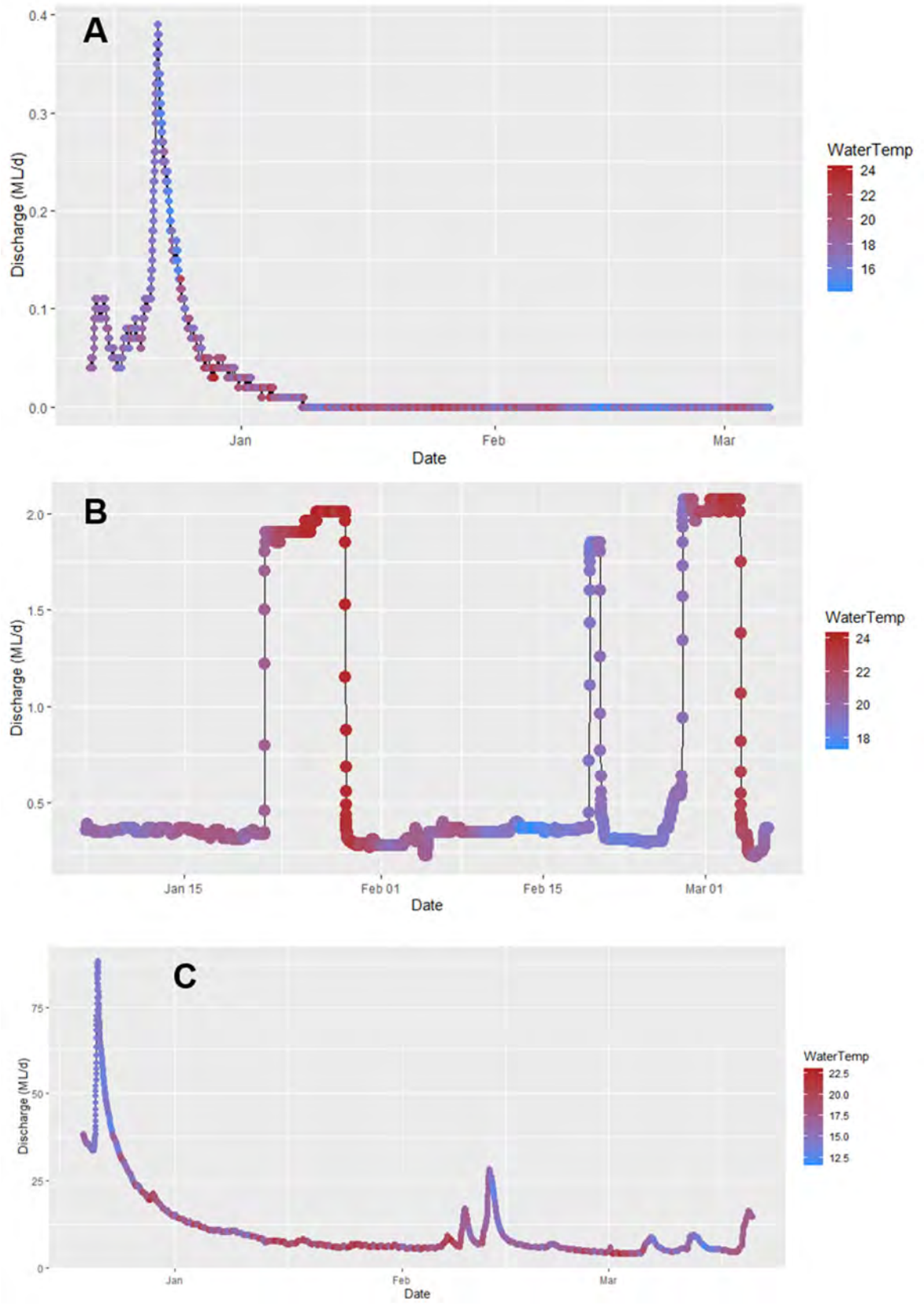

Figure 4.7. Logged water temperature (°C, 15-min interval) overlaid on A) Painkalac Upstream, B) Painkalac Downstream and C) Barham River hydrographs (ML/d). Note varying y-axis scale.

4.4.3. Biodiversity

Based on the PERMANOVA analysis of each OTU-level matrix, all three markers (16S, 23S and ITS) discriminated among river reaches ($P<0.01$) and showed distinct community structure as a result of the interaction between reach and flow condition (RiverP × FlowCat) ($P<0.01$). The PERMANOVA results are presented separately for each biological community but a summary of the PERMANOVA outcomes across the three amplicons is presented in Table 4.6 and details for all biological analyses are presented together in Appendix B.

Table 4.6. PERMANOVA results from flow variables and transformed abundance matrices for bacteria, algae and fungi. Abundance matrices were based on operational taxonomic units (OTUs). Bold indicates $P \leq 0.05$.

Factor	Bacteria	Algae	Fungi
RiverP	**0.0028**	**0.0023**	**0.0039**
FlowCat	0.0762	0.0552	0.3164
Site(RiverP)	**0.0001**	**0.0001**	**0.0001**
Set(FlowCat)	**0.0001**	**0.0001**	**0.0001**
RiverP × FlowCat	**0.0015**	**0.0001**	**0.0002**
RiverP × Set(FlowCat)	**0.0018**	0.3515	**0.0001**
Site(RiverP) × FlowCat	**0.0249**	**0.0019**	**0.0221**

Bacteria

The 1258 OTUs (16S assay) assigned to Bacteria from 72 biofilm samples were analysed using a mixed effects model (Figure 4.8). Based on the PERMANOVA analysis, the largest component of variation was the difference between reaches. The two Painkalac reaches were not significantly different (pseudo-$F_{1,71}$ = 3.57, P = 0.1795), but they were distinct from the Barham River (pseudo-$F_{1,71}$ = 7.84, P = 0.0083). There was no significant effect of flow category alone but there was a significant interaction between low category (FlowCat) and reach (RiverP) (Table 4.7). This led to a pairwise test showing significant community differences among the Base and Pulse conditions, for the Barham River only at $\alpha = 0.05$ (t = 1.79, P(MC) = 0.0134) (Table 4.8).

Although the difference in bacterial community was not significant for the Painkalac Upstream reach at $\alpha = 0.05$, given the variability and small number of Pulse samples from the reach, it may be appropriate to consider the results of the statistical tests using a less conservative *a priori* level of $\alpha = 0.10$. Under this less conservative approach, there were significant changes in bacterial community structure in Painkalac Upstream associated with the pulse flows (Figure 4.8). A seriation test was performed based on the significant Set variability, which showed a slight temporal trend in bacterial community structure ($\rho = 0.09$, p = 0.0028).

Table 4.7. PERMANOVA results from the log-transformed bacterial abundance matrix. The abundance matrix was based on operational taxonomic units (OTUs). df: degrees of freedom, SS: sum of squares, MS: mean squares, pseudo-F: ratio of between cluster variance to within-cluster variance, Perms: number of permutations. Bold indicates P ≤ 0.05.

Factor	df	SS	MS	Pseudo-F	Perms	P(perm)
RiverP	2	25211	12606	6.6675	9939	**0.0028**
FlowCat	1	1602.4	1602.4	1.9083	9926	0.0762
Site(RiverP)	5	10840	2167.9	5.1271	9851	**0.0001**
Set(FlowCat)	13	2301	946.22	2.2378	9750	**0.0001**
RiverPxFlowCat	2	3241.6	1620.8	1.8669	9851	**0.0015**
RiverPxSet(FlowCat)	8	5113.2	639.15	1.5116	9793	**0.0018**
Site(RiverP)xFlowCat	5	2974.2	594.84	1.4068	9821	**0.0249**

Table 4.8. PERMANOVA pairwise test results of river position by flow for pairs of the flow category level on the transformed B-C bacteria resemblance matrix. P(MC): Monte Carlo P-value, t: test statistic, Perms: number of permutations, Den d.f.: denominator degrees of freedom. Bold indicates P(MC)≤0.05 and italics indicate P(MC)<0.1.

Reach	t	Perms	Den d.f.	P(MC)
B	1.79	59	7.93	**0.0134**
PU	1.66	6	2.99	*0.0852*
PD	0.75	59	8.01	0.9447

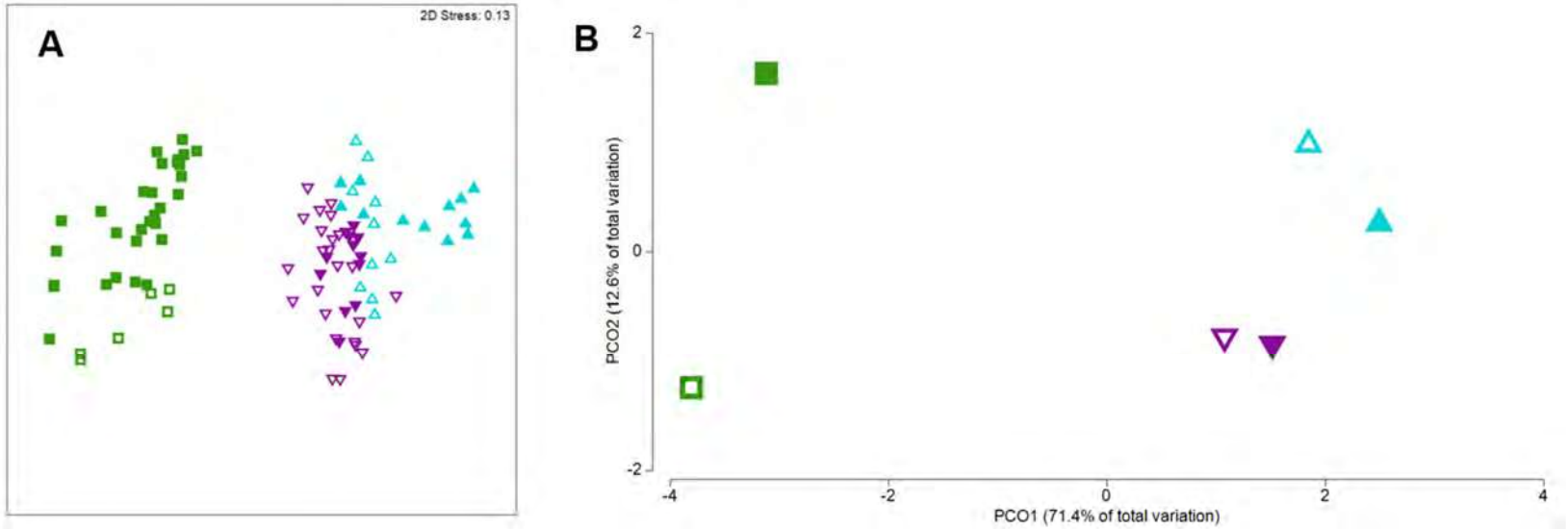

Figure 4.8. A) nMDS of log-transformed bacterial abundance. B) PCO of distances among centroids on the basis of the B-C measure of log-transformed bacterial abundance. Abundance was based on operational taxonomic units (OTUs). Reaches are represented by colours and symbols (Barham: green squares, Painkalac Downstream: purple inverted triangles, and Painkalac Upstream: turquoise triangles). Solid symbols represent Base conditions and hollow symbols denote Pulse conditions.

A SIMPER test considering all classes from the chloroplast-corrected 16S reads revealed that the flow pulses were associated with an increase in Alphaproteobacteria and a decrease in the abundance of Cytophagia and Betaproteobacteria (Table 4.9). There were no significant differences in bacterial OTU richness among reaches and flow (Figure 4.9).

Table 4.9. SIMPER results comparing the dissimilarity of class-level Bacteria abundance data between Base and Pulse categories based on 16S reads. Average abundance (Av. Abund.) is reported for Base and Pulse categories. Average of Bray-Curtis dissimilarities between pairs (Av. Diss.) and the ratio of the average contribution divided by the standard deviation of all pairs of samples (Diss/SD) are reported. Only classes with Diss/SD≥1.0 are included. Contribution to total dissimilarity is given as Contrib. % and the percentages are summed as Cumulative %.

Class	Pulse Av. Abund.	Base Av. Abund.	Av. Diss.	Diss/SD	Contrib. %	Cumulative %
Cytophagia	2.41	2.46	1.43	1.36	9.60	9.60
Betaproteobacteria	5.14	5.35	0.75	1.26	5.06	14.66
Alphaproteobacteria	5.48	5.29	0.73	1.34	4.92	19.58

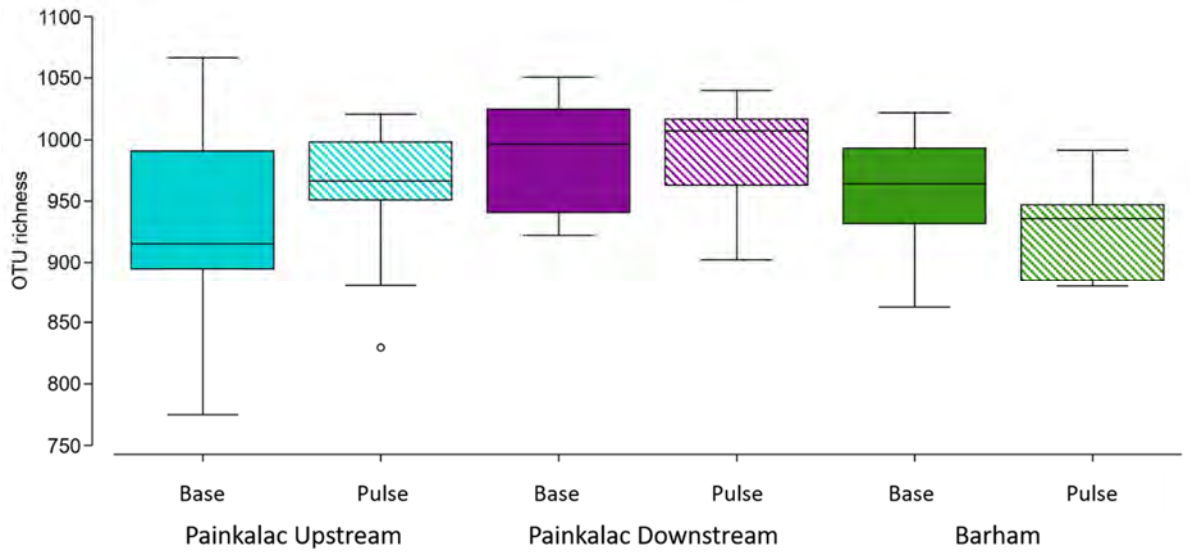

Figure 4.9. Boxplots comparing bacterial richness for Base and Pulse conditions in each reach. Richness was based on operational taxonomic units (OTUs). Colours indicate reach (Barham: green, Painkalac Downstream: purple, and Painkalac Upstream: turquoise). Hatching denotes Pulse condition.

Algae

The 1,287 algae OTUs (23S assay) from 72 biofilm samples were analysed using a mixed effects model (Figure 4.10). The PERMANOVA results showed significant variability among Sites and through time (Sets) (Table 4.10). The largest component of variation was the difference between the three reaches. The two Painkalac reaches were not significantly different (pseudo-$F_{1,71}$ = 4.51, P = 0.166) but they were distinct from the Barham River (pseudo-$F_{1,71}$ = 8.03, P = 0.0158). There was no significant effect of flow category alone and no significant interaction between flow category (FlowCat) and Sets. There was a significant interaction between flow category (FlowCat) and reach (RiverP), which led to a pairwise test showing significant community differences among the Base and Pulse conditions in the Barham River (t = 3.08, P(MC) = 0.0015). There were no significant community structure changes between the Base and Pulse conditions in Painkalac Upstream (t = 1.41, P(MC) = 0.1979) or Painkalac Downstream (t = 0.69, P(MC) = 0.9921) reaches (Table 4.11, Figure 4.10). Based on the significant variability in Sets, I performed a seriation test, which indicated a significant seasonal trend in community structure (ρ = 0.71, P = 0.0001).

Table 4.10. PERMANOVA results from the square root-transformed algal abundance matrix. The abundance matrix was based on operational taxonomic units (OTUs). df: degrees of freedom, SS: sum of squares, MS: mean squares, pseudo-F: ratio of between-cluster variance to within-cluster variance, Perms: number of permutations. Bold indicates P≤0.05.

Factor	df	SS	MS	Pseudo-F	Perms	P(perm)
RiverP	2	44204	22102	8.4353	9952	0.0023
FlowCat	1	2981	2981	2.3236	9950	0.0552
Site(RiverP)	5	18216	3643.3	7.527	9851	0.0001
Set(FlowCat)	13	20391	1568.5	3.2405	9799	0.0001
RiverPxFlowCat	2	7573	3786.5	4.2204	9858	0.0001
RiverPxSet(FlowCat)	8	4039.2	504.9	1.0431	9768	0.3515
Site(RiverP)xFlowCat	5	3814.5	762.9	1.5761	9817	0.0019

Table 4.11. PERMANOVA pairwise test results of river position by flow for pairs of the flow category level on the transformed B-C algae resemblance matrix. P(MC): Monte Carlo P-value, t: test statistic, Perms: number of permutations, Den d.f.: denominator degrees of freedom. Bold indicates P(MC)≤0.05.

Reach	t	Perms	Den d.f.	P(MC)
B	3.08	59	6.68	**0.0015**
PU	1.41	6	2.06	0.1979
PD	0.69	59	8.88	0.9921

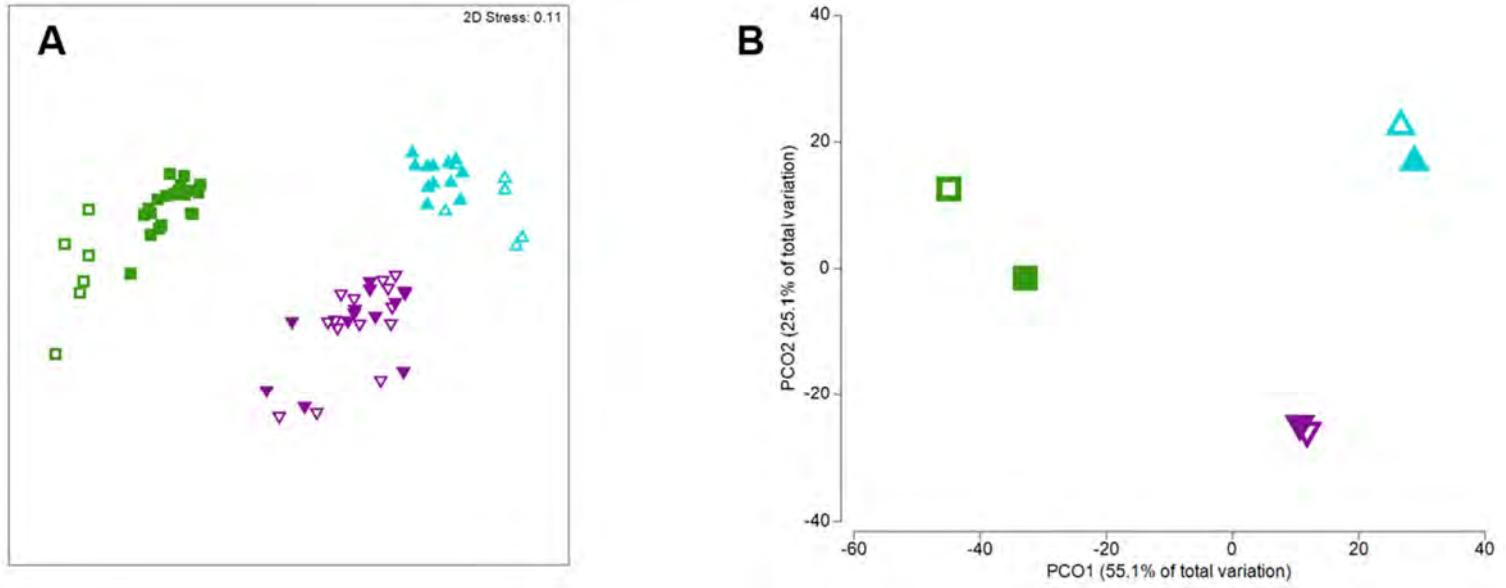

Figure 4.10. A) nMDS of transformed algal abundance. B) PCO of distances among centroids on the basis of the B-C measure of square root-transformed algal abundance. Abundance was based on operational taxonomic units (OTUs). Reaches are represented by colours and symbols (Barham: green squares, Painkalac Downstream: purple inverted triangles, and Painkalac Upstream: turquoise triangles). Solid symbols represent Base conditions and hollow symbols denote Pulse conditions.

The SIMPER results showed eight algal classes (Diss/SD ratios>1) that contributed 76.2% of the dissimilarity between the Base and Pulse conditions (Table 4.12). The classes that showed reduced abundance associated with Pulse flows were all green algae (Chlorodendrophyceae, Chlorophyceae and Ulvophyceae). There was a significant reduction in algal OTU richness associated with the flow pulse in the Barham River (P = 0.001) but no significant changes in Painkalac Creek (Figure 4.11).

Table 4.12. SIMPER results comparing class from 23S reads for Pulse and Base conditions. Average abundance (Av. Abund.) is reported for Base and Pulse categories. Average of Bray-Curtis dissimilarities between pairs (Av. Diss.) and the ratio of the average contribution divided by the standard deviation of all pairs of samples (Diss/SD) are reported. Only classes with Diss/SD≥1.0 are included. Contribution to total dissimilarity is given as Contrib. % and the percentages are summed as Cumulative %.

Class	Pulse Av. Abund.	Base Av. Abund.	Av. Diss.	Diss/SD	Contrib. %	Cumulative %
Chlorodendrophyceae	3.00	3.67	4.66	1.30	16.36	16.36
Euglenida	3.59	3.32	4.06	1.29	14.26	30.62
Zygnemophyceae	2.36	1.41	3.88	1.04	13.62	44.24
Chlorophyceae	2.57	2.98	2.79	1.35	9.79	54.03
Florideophyceae	6.28	6.21	2.11	1.36	7.42	61.44
Mesostigmatophyceae	1.84	1.77	1.55	1.34	5.45	66.89
Pedinophyceae	1.39	1.14	1.47	1.40	5.17	72.06
Ulvophyceae	0.90	1.10	1.19	1.08	4.18	76.24

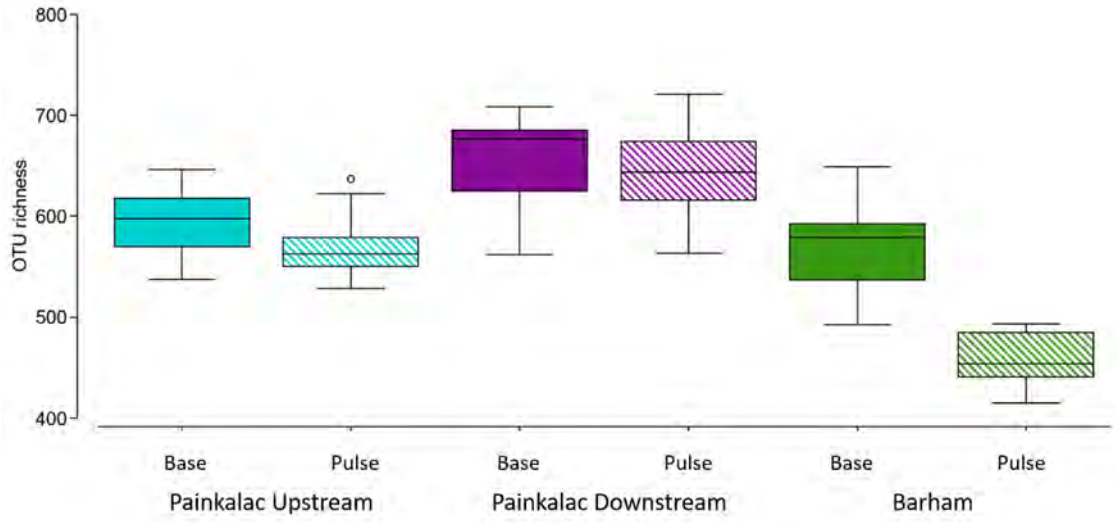

Figure 4.11. Boxplots comparing algal richness for Base and Pulse conditions in each reach. Richness was based on operational taxonomic units (OTUs). Colours indicate reach (Barham: green, Painkalac Downstream: purple, and Painkalac Upstream: turquoise). Hatching denotes Pulse condition.

Fungi

The 896 OTUs (ITS assay) assigned to Fungi from 72 biofilm samples were analysed using a mixed effects model (Figure 4.12). The mixed effects model based on the PERMANOVA analysis of ITS OTU-level results demonstrated that the largest component of variation was the difference between reaches (Table 4.13). The two Painkalac reaches were not significantly different (pseudo-$F_{1,71}$ = 2.81, P = 0.1789) but they were distinct from the Barham River (pseudo-$F_{1,71}$ = 6.22, P = 0.0112). There was significant variability among Sites and through time (Sets).

The RELATE test of seriation showed a seasonal pattern in the fungal community (ρ = 0.40, p = 0.0001). The assigned flow category was not a significant influence but there were significant interactions between all examined variables. The significant interaction between flow category (FlowCat) and reach (RiverP) led to a pairwise test, which showed significant community differences among the Base and Pulse conditions in

the Barham River (t = 1.95, P(MC) = 0.0076) (Table 4.14). There were no significant community structure changes between the Base and Pulse conditions in the Painkalac Upstream (t = 1.76, P(MC) = 0.0631) or Painkalac Downstream (t = 0.70, P(MC) = 0.9955) reaches (Figure 4.12). Although the difference in the fungal community was not significant for the Painkalac Upstream reach at $\alpha = 0.05$, given the variability and small number of Pulse samples from the reach, it may be appropriate to consider the results of the statistical tests using a less conservative *a priori* level of $\alpha = 0.10$. Under this less conservative approach, there were significant changes in the fungal community in the upstream reach of Painkalac Creek associated with the pulse flows (Table 4.14).

The SIMPER results showed 10 fungal classes (Diss/SD ratios>1) contributing 70.8% of the dissimilarity between the Base and Pulse conditions (Table 4.15). The fungal richness in the Barham River biofilm samples was also significantly lower than in both Painkalac Creek reaches ($P<0.0001$) and there was a significant increase in fungal OTU richness ($P = 0.004$) associated with pulse flows in the Painkalac Upstream reach (Figure 4.13).

Table 4.13. PERMANOVA results from the fourth root-transformed fungal abundance matrix. The abundance matrix was based on operational taxonomic units (OTUs). df: degrees of freedom, SS: sum of squares, MS: mean squares, pseudo-F: ratio of between-cluster variance to within-cluster variance, Perms: number of permutations. Bold indicates P ≤ 0.05.

Factor	df	SS	MS	Pseudo-F	Perms	P(perm)
RiverP	2	18460	9229.8	5.3305	9957	**0.0039**
FlowCat	1	1466	1466	1.2275	9930	0.3164
Site(RiverP)	5	8499.9	1700	3.5126	9803	**0.0001**
Set(FlowCat)	13	21165	1628.1	3.3641	9822	**0.0001**
RiverPxFlowCat	2	3551.3	1775.7	1.8152	9799	**0.0002**
RiverPxSet(FlowCat)	8	6136.2	767.02	1.5849	9697	**0.0001**
Site(RiverP)xFlowCat	5	2998.5	599.71	1.2392	9735	**0.0221**

Table 4.14. PERMANOVA pairwise test results of river position by flow for pairs of the flow category level on the transformed fungal B-C resemblance matrix. P(MC): Monte Carlo P-value, t: test statistic, Perms: number of permutations, Den d.f.: denominator degrees of freedom. Bold indicates P(MC)≤0.05 and italics indicate P(MC)<0.1.

Reach	t	Perms	Den d.f.	P(MC)
B	1.95	59	8.64	**0.0076**
PU	1.76	6	3.81	*0.0631*
PD	0.70	59	8.99	0.9955

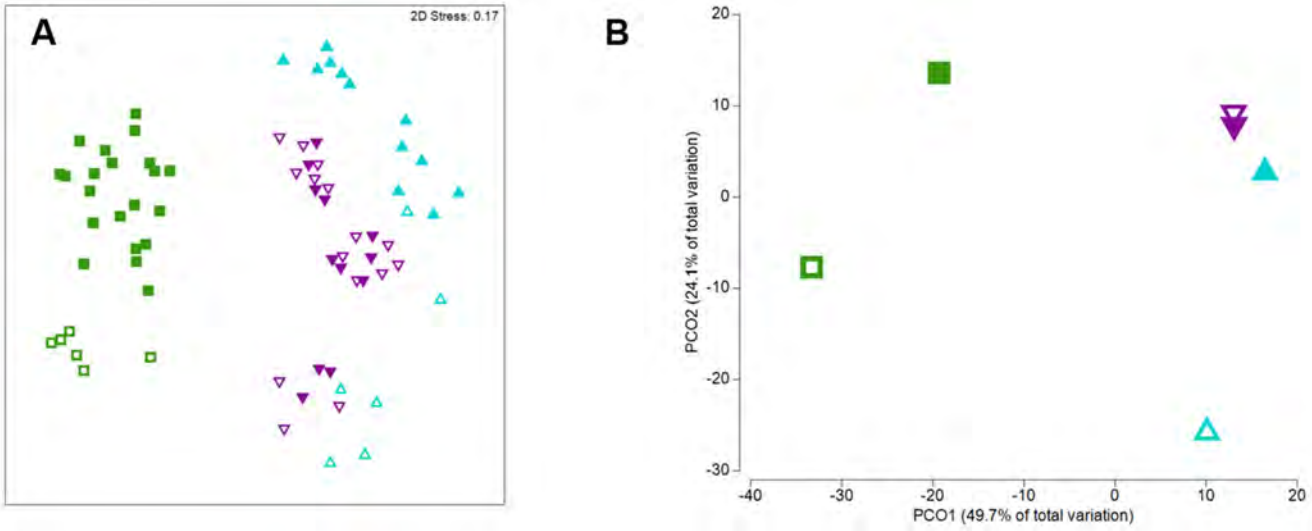

Figure 4.12. A) nMDS of transformed fungal abundance. B) PCO of distances among centroids on the basis of the B-C measure of transformed fungal abundance. A) nMDS of transformed fungal abundance. B) PCO of distances among centroids on the basis of the B-C measure of transformed fungal abundance. Abundance was based on operational taxonomic units (OTUs). Reaches are represented by colours and symbols (Barham: green squares, Painkalac Downstream: purple inverted triangles, and Painkalac Upstream: turquoise triangles). Solid symbols represent Base conditions and hollow symbols denote Pulse conditions.

Table 4.15. SIMPER results of Fungi class-level data for Pulse and Base conditions. Average abundance (Av. Abund.) is reported for Base and Pulse categories. Average of Bray-Curtis dissimilarities between pairs (Av. Diss.) and the ratio of the average contribution divided by the standard deviation of all pairs of samples (Diss/SD) are reported. Only classes with Diss/SD≥1.0 are included. Contribution to total dissimilarity is given as Contrib. % and the percentages are summed as Cumulative %.

Class	Pulse Av. Abund.	Base Av. Abund.	Av. Diss.	Diss/SD	Contrib. %	Cumulative %
Saccharomycetes	3.71	4.07	4.92	1.21	12.53	12.53
Lecanoromycetes	2.73	2.11	4.30	1.02	10.93	23.46
Mucoromycotina	2.06	2.50	3.75	1.03	9.55	33.00
Dothideomycetes	2.92	2.16	2.72	1.30	6.93	39.93
Leotiomycetes	1.77	2.23	2.62	1.01	6.67	46.61
Agaricomycetes	2.99	2.72	2.25	1.32	5.72	52.32
Chytridiomycetes	3.06	2.80	2.00	1.06	5.10	57.42
Ascomycota	1.92	2.21	2.00	1.43	5.10	62.52
Monoblepharidomycetes	1.25	1.46	2.00	1.12	5.08	67.59
Sordariomycetes	1.61	1.16	1.28	1.24	3.25	70.84

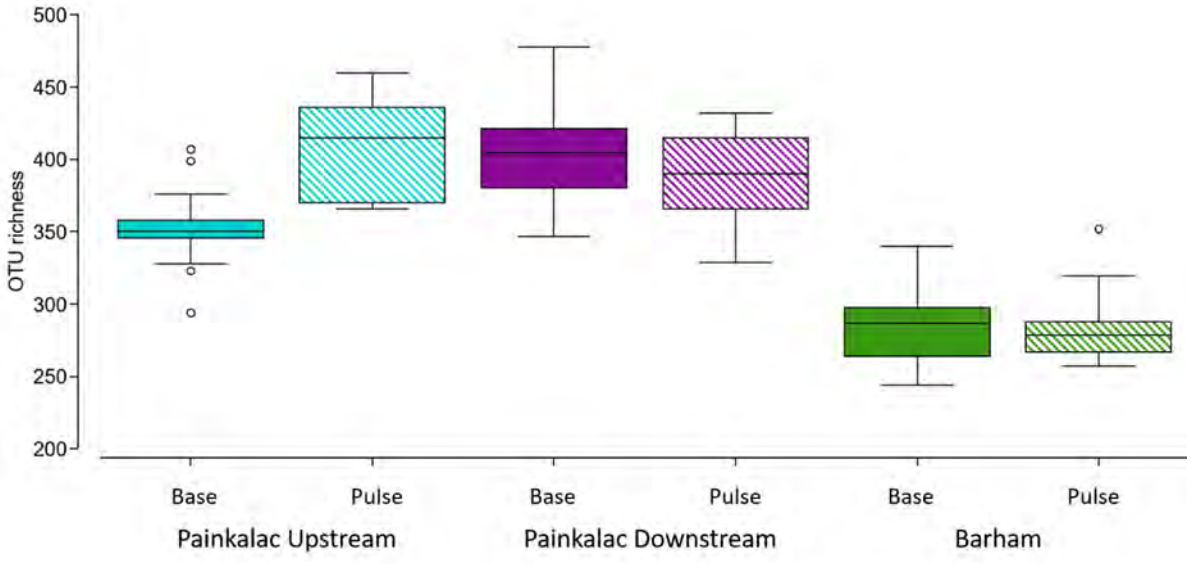

Figure 4.13. Boxplots comparing fungal richness for Base and Pulse conditions in each reach. Boxplots comparing fungal richness for Base and Pulse conditions in each reach. Richness was based on operational taxonomic units (OTUs). Colours indicate reach (Barham: green, Painkalac Downstream: purple, and Painkalac Upstream: turquoise). Hatching denotes Pulse condition.

4.4.4. Phospholipid fatty acids

The phospholipid profile (51 PLFA) of 94 biofilm samples was examined using a mixed model (Figure 4.14). Based on the PERMANOVA results, the greatest component of variation in PLFA composition occurred at the site scale (the residual) followed by the reach (Table 4.16). There was significant variability among Sites and through time (Sets). Based on the significant variability in Sets, a RELATE test was performed, which showed a significant temporal trend ($\rho = 0.28$, $P = 0.0001$). The significant interaction between the flow category (FlowCat) and the reach (RiverP) led to a pairwise test showing there were no significant differences in PLFA profile between the Base and Pulse conditions within individual reach (Table 4.17). Based on the univariate analysis of the major fatty acid classes (SFA, MUFA, PUFA and EPA+DHA), there were no significant differences in biofilm nutritional quality between the base and pulse categories in any reach ($P>0.05$).

Table 4.16 PERMANOVA results from transformed Euclidean PLFA resemblance matrix. The abundance matrix was based on operational taxonomic units (OTUs). df: degrees of freedom, SS: sum of squares, MS: mean squares, pseudo-F: ratio of between-cluster variance to within-cluster variance, Perms: number of permutations. Bold indicates P ≤ 0.05.

Factor	df	SS	MS	Pseudo-F	Perms	P(perm)
RiverP	2	76.782	38.391	3.2176	9950	**0.0097**
FlowCat	1	5.07	5.07	0.67765	9932	0.7153
Site(RiverP)	5	58.027	11.605	1.9744	9875	**0.0022**
Set(FlowCat)	19	170.9	8.9945	1.5302	9777	**0.0005**
RiverPxFlowCat	2	20.567	10.283	1.444	9860	**0.0495**
RiverPxSet(FlowCat)	10	55.103	5.5103	0.93746	9812	0.6319
Site(RiverP)xFlowCat	5	32.524	6.5049	1.1067	9865	0.2798

Table 4.17. PERMANOVA pairwise test results of river position by flow for pairs of the flow category level on the transformed Euclidean PLFA resemblance matrix . P(MC)= Monte Carlo P-value, t = test statistic, Perms = number of permutations, Den d.f. = denominator degrees of freedom.

Reach	t	Perms	Den d.f.	P(MC)
B	1.15	59	7.31	0.2268
PU	1.03	6	3.85	0.4468
PD	0.92	59	8.16	0.6866

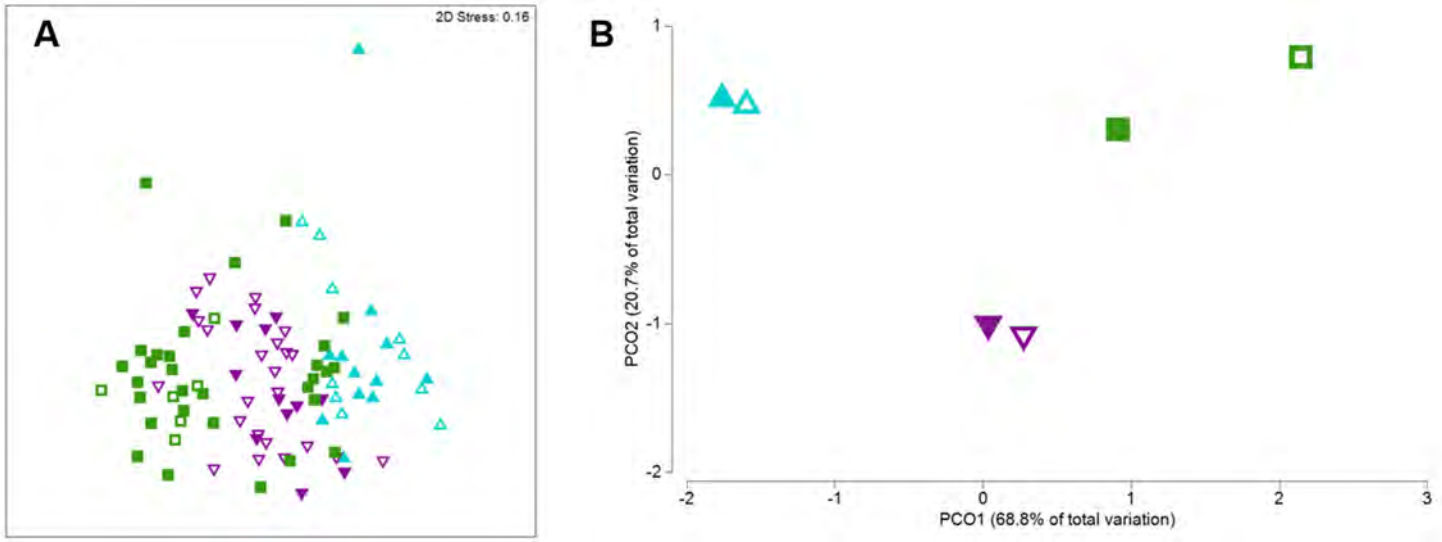

Figure 4.14. A) nMDS of PLFA composition by reach and flow category. B) PCO of distances among centroids on the basis of the Euclidean measure of PLFA composition. Reaches are represented by colour (B= green, PD= purple, PU= turquoise) and symbols reflect Flow condition; solid symbols represent Base condition and hollow symbols denote Pulse condition. Reaches are represented by colour and symbols (B=green squares, PD=purple inverted triangles, PU=turquoise triangles)

4.5. Discussion

In this study, new molecular and established biochemical tools were used to compare biofilm flow response in the regulated stream reach below Painkalac Reservoir to unregulated sites above the reservoir and in the Barham River. Natural flow pulses in the unregulated reaches cooled the water and produced distinct abiotic patterns, while environmental flow pulses warmed the water but otherwise failed to shift abiotic conditions.

All three biofilm community components (bacteria, algae and fungi) showed a significant response to pulse flows in the Barham River. The bacteria and fungi assays also demonstrated some community-level changes in biofilm composition associated with the natural flow pulses in the Painkalac Upstream reach. These data establish ecological responses to flow events and clarify important flow-ecology relationships in natural and regulated scenarios. Together, my results suggest that changes in biofilm nutrition and community structure are largely proportional to flow magnitude and that environmental flows may be insufficient to shift the biofilm resource base. The results underscore the importance of considering flow and thermal regimes in tandem. These data can inform future monitoring of environmental flow outcomes and may help to refine environmental flow targets.

4.5.1. Environmental flow effects

Natural LFF cooled unregulated reaches but environmental flow LFF delivered pulses of warm water downstream. On hot days, when the creek would benefit most from a fresh supply of water, the water released from the reservoir surface was warmer than the stream. Water temperature is a fundamental ecological variable that is often overlooked

in the design and implementation of environmental flows (Olden & Naiman, 2010). Temperature is an important behavioural cue for aquatic biota and thermal pollution caused by dam-induced changes to a river's thermal regime can produce both direct and indirect ecological impacts (Olden & Naiman, 2010). Despite its ecological importance however, the temperature regime is rarely considered in flow alteration studies (Poff & Zimmerman, 2010) and most of the research has focused on the ecological impacts of cold, oxygen-deficient hypolimnetic releases from large reservoirs (Lessard & Hayes, 2003). Just as hypolimnetic releases can cause selective disappearance of susceptible fish and invertebrate species (Bunn & Arthington, 2002), warm, epilimnetic surface releases have been shown to shift the composition of downstream macroinvertebrate and cold-water fish communities (Lessard & Hayes, 2003; Hayes, Dodd, & Lessard, 2006). The epilimnetic, warm water releases from Painkalac Reservoir may therefore be producing changes in downstream community structure that could dampen some of the flow benefits.

The unscheduled flow release on 19 February 2019 did not produce the same warming effect as the other environmental flow pulses. This may have been the result of the short duration of the release, the lower maximum air temperature of 29.9°C on that day (versus 37.5°C) or a difference in delivery method (e.g. pipes and valves). Thermal impacts could potentially be mitigated by modifying the temperature of the water released from the dam in terms of outlet position or through mixing water from several depths (Olden & Naiman, 2010). Another approach would be to consider a thermal maximum where environmental flows are postponed if ambient air temperature exceeds a certain threshold.

Across the full suite of physicochemical variables, there was no significant difference in abiotic conditions measured during environmental flow releases. In

contrast, unregulated stream reaches demonstrated a significantly different set of abiotic conditions during elevated flows. The Barham River showed significant differences in measured physicochemical conditions between the Base and Pulse conditions and the Painkalac Upstream reach showed less dramatic environmental changes. Differential responses would be expected because the Barham River catchment is about 25% larger and discharge is about five-fold higher than in Painkalac Creek, but nevertheless, the lack of measurable abiotic changes associated with environmental flows is noteworthy.

4.5.2. Environmental flow hydrology

The environmental flow regime in Painkalac Creek differs from a natural flow regime not only in the timing and magnitude of flows but also in the shape of the hydrograph (Figure 4.7). The same precipitation events that resulted in natural flow pulses upstream of the reservoir would most likely have resulted in flow pulses in lower reaches of the creek had they not been captured by the reservoir. Conversely, some of the environmental flow pulses occurred during what was otherwise an extended low flow period in the upstream reach. The plumbed delivery of the environmental flows also results in an unnatural hydrograph. John Fleck coined the term 'institutional hydrograph' to describe the unnatural timing and altered flow regime of managed flows (Fleck, 2015) but I would like to propose that the term better describes the square flow peaks that result from opening a valve rather than rainfall being transmitted through a catchment. Although not widely studied, altered rates of change have been associated with changes in invertebrate and waterbird abundance as well as reduced recruitment and survival of riparian vegetation (Poff & Zimmerman, 2010).

The environmental flow prescription for Painkalac Creek was developed based largely on the geomorphology of a stream reach less 300 metres in length and according

to photos and personal accounts, the geomorphology of Painkalac Creek has changed dramatically since the cross-sections were measured and environmental flow targets were set in 2007 (Doeg *et al.*, 2008). The channel flows through soft, unconsolidated sediments and the streambed elevation is only maintained where large woody debris occurs or where hardscape has been added, such as around the Old Coach Road bridge. The channel geomorphology was not surveyed in this study but based on the Doeg *et al.* (2008) photos, and local accounts, today's streambed sits a metre or more below the 2007 channel. Several years ago, a pipe that was installed below and perpendicular to the streambed became suspended above the water level as the bed incised (Graeme McKenzie, personal communication, 19 May 2020). The pipe impeded and collected debris during flood flows and eventually severed under the load but its location serves as benchmark for historic channel elevation. Upstream dams have been shown to produce channel narrowing and a reduced migration rate in other complex, braided channels flowing through soft sediments (Friedman *et al.*, 1998). The current channel incision in Painkalac Creek contrasts with past channel migrations as reflected by the map from the environmental flow assessment (Figure 4.15) (Doeg *et al.*, 2008) which shows that the main channel of the creek recently occupied an adjacent anabranch.

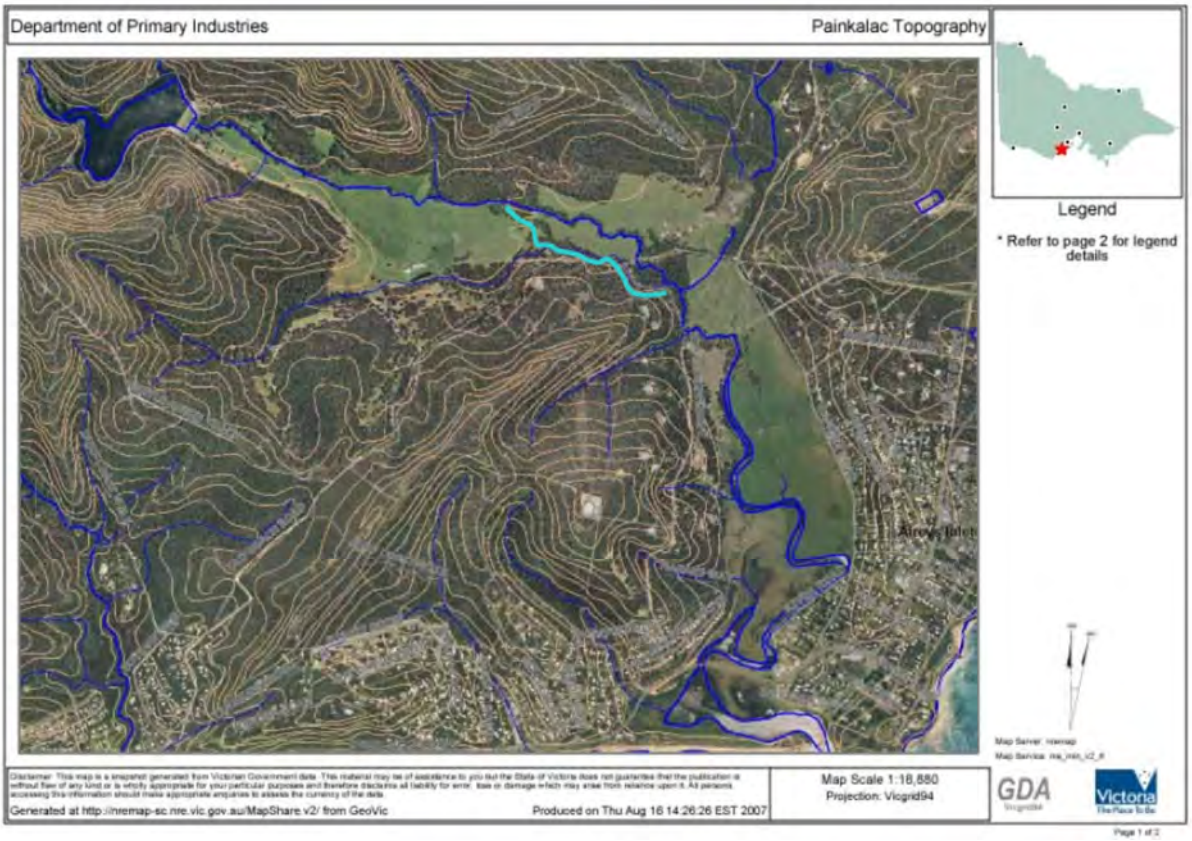

Figure 4.15. Map of Painkalac Creek showing channel migration. (Doeg *et al.*, 2008)

High flows in Painkalac Creek seem to be carving out the channel instead of fanning out across the broad valley. This flow pattern deprives the valley wetlands of fresh water and limits the capacity for the system to store and later release flood flows. Depending on the groundwater level in the alluvial aquifer, the descending channel can also serve to drain the surrounding groundwater system. The sweeping changes in catchment hydrology and geomorphology associated with Painkalac Dam may not be undone by the environmental flow prescription.

4.5.3. Flow-ecology relationships

The molecular characterisation of stream biofilm shows promise for testing flow-ecology relationships across multiple taxa. Distinct communities of bacteria, algae and fungi were associated with increased flow in the unregulated stream reaches but not in the regulated reach. The nature of the shifts in specific taxa within the microbiota deserves more attention, particularly as more becomes known about the role of bacteria and fungi in the stream food web.

Benthic production, as measured by algal abundance, has been suggested as a means to monitor flow regime modification and define alteration thresholds (Warfe *et al.*, 2014). Consistent with my hypothesis that pulse flows would result in decreased algal taxonomic richness due to scouring (Ryder *et al.*, 2006), I observed a significant decrease in algal richness associated with the flow pulse in the Barham River. However, no significant changes in algal richness were observed in either Painkalac Creek reach. I expected flow pulses to result in increased bacterial diversity, but there were no significant differences in bacterial richness across the three reaches and flow categories. It is possible that richness was dampened by ignoring rare OTUs with <0.1% abundance in a sample, but increased microbial richness does not always translate to improved stream health. Increases in bacteria OTU richness have been documented in response to stressors including pharmacological compounds (Chonova *et al.*, 2016) and eutrophication, but decreased bacterial richness can also serve as measure for organic pollution (Sagova-Mareckova *et al.*, 2021). With the high number of bacterial OTUs, richness is less informative than the multivariate patterns of bacterial community structure.

The fungal communities in this study showed strong differentiation by reach and sensitivity to flow. Aquatic fungi are still poorly understood but molecular data suggest more diversity and ecological significance than was previously recognised. (Grossart *et al.*, 2016). There is evidence that PUFAs produced by fungi provide high-quality food to zooplankton (Kagami, Miki & Takimoto, 2014), and fungi are likely an important but overlooked lotic food resource. Aquatic fungi are heterotrophs that depend on external organic matter, either living or dead, and they play a critical role in processing allochthonous and autochthonous carbon in stream ecosystems (Wurzbacher, Kerr & Grossart, 2011).

The increase in fungal OTU richness associated with pulse flows in the Painkalac Upstream reach is most likely explained by the reconnection of isolated pools following rainfall during the second half of the summer. The reconnection was observed in the field but is not evident in the stream hydrograph (Figure 4.7) because the flow remained below a detectable level of discharge. Flow intermittency appears to be typical of the Painkalac Upstream reach with rock pools that dry and disconnect throughout the summer in the absence of precipitation.

Molecular aquatic biomonitoring could be an important tool in evaluating the performance of future environmental flows. Molecular techniques can accurately and non-invasively monitor the abundance of vertebrate and invertebrate aquatic organisms, and environmental DNA (eDNA) collected from filtered water samples is being used to detect rare fish (Burgoa Cardás *et al.*, 2020), iconic species such as the platypus (Lugg *et al.*, 2018) and invasive organisms (Klymus, Marshall & Stepien, 2017) in freshwater ecosystems. Because imperilled fish species are often the target of environmental flow designs, there will likely be expanded use of eDNA to monitor fish presence and spawning success (Tillotson *et al.*, 2018) associated with environmental flow deliveries. The

process of collecting and extracting eDNA is almost identical regardless of the taxa targeted. Depending on the primary organism of interest, a second set of PCR primers could be used to characterise microbiota from the same set of eDNA samples. In the same way that microbes can be used to assess wastewater management objectives (Chonova *et al.*, 2016; Stoeck *et al.*, 2018), microbial community monitoring could be used to assess environmental flow performance.

4.5.4. Flow and biofilm nutritional quality

My experiment did not confirm the theory that the natural disturbance regime in unregulated rivers supports a more nutritious biofilm supply for consumers (Sheldon & Walker, 1997) because PLFA profiling was generally unable to discriminate nutritional differences in the biofilm. There were some differences in composition between reaches but no significant differences in PLFA composition or changes in major lipid classes associated with flow pulses. Flow regimes have not been assessed with PLFA but there is weak evidence for relationships between land use and PLFA composition (Larson *et al.*, 2013). Lipid quality has been described using EFA, but increased EFA content has been associated with reduced water quality and eutrophication (Boechat *et al.*, 2011). In light of the emerging understanding of the role of the microbial loop for nutrient cycling in lotic ecosystems and the complexity of the biofilm food web (Weitere *et al.*, 2018), the nutritional quality of biofilm is defined by much more than its algal composition.

Metabarcoding and PLFA profiling have been described as complementary approaches (Mrozik *et al.*, 2014; Orwin *et al.*, 2018), but the low correlations between PLFA composition and biological community structure in this experiment do not support PLFA as a proxy for biofilm community structure. More work is needed to compare PLFA profiling against community metabarcoding results, but research is constrained by the

need for several barcoding regions to describe different biological domains. When multiple amplicons are investigated, as in this study, it is challenging to connect PLFA composition to multiple biological abundance datasets. To compare PLFA patterns more broadly, a more general barcoding region that reflects community structure across more diverse taxa (such as 18S) could be useful.

4.6. Conclusion

Across all biological, biochemical and physical data analysed, the only significant change produced by environmental flow pulses was an altered thermal regime. Instead of freshening Painkalac Creek, summer low flow freshes released pulses of warm water from the reservoir. Natural flow pulses in the unregulated reaches shifted abiotic conditions and biological communities, but there were no significant changes in biofilm nutritional content associated with increased flow. As databases improve and the understanding of aquatic microbiota grows, DNA metabarcoding of biofilm communities should provide an efficient and economical tool to assess the performance of water management activities (Gionchetta *et al.*, 2020; Minerovic *et al.*, 2020).

Streamflow has been called a 'master variable' that determines the distribution and abundance of biological communities and regulates ecological integrity (Poff *et al.*, 1997). Observed changes in community composition confirm that flow structures biological communities, but my findings also suggest that environmental flows may not be producing the anticipated changes in biological communities. In order to have the desired effects on biota, flow and thermal regimes must be managed simultaneously (Olden & Naiman, 2010) and environmental flow releases from reservoirs may have to go beyond occasional releases to more closely mimic unregulated river systems (Gillespie, Kay & Brown, 2020).

Dumpster Diving for Diatoms with 16S

5.1. Chapter Overview

When the 23S amplicon failed to recover any diatom sequences from the biofilm samples produced by my field experiment, the decision was made to look for diatom chloroplast reads within the existing 16S reads. Since many bacterial 16S rDNA primers also have high affinity for eukaryotic plastid DNA, non-target sequences from chloroplasts and mitochondria are often co-amplified but are typically discarded. This chapter summarises a novel method of recovering and characterising diatom reads that, to the author's knowledge, has never been conducted in a freshwater system or applied in a biomonitoring context. This manuscript has been accepted by the open-access journal Peer-J. Due to the general nature of the methods paper, river reaches are instead referred to a 'segments' in this chapter.

Dumpster diving for diatom plastid 16S rRNA genes

Krista L. Bonfantine[1*], Stacey M. Trevathan-Tackett[1], Ty G. Matthews[1], Ana Neckovic[2], Han Ming Gan[1,3]

[1] Centre for Integrative Ecology, School of Life and Environmental Sciences, Deakin University, Geelong, VIC, Australia

[2] School of Life and Environmental Sciences, Geelong, VIC, Australia

[3] GeneSEQ Sdn Bhd, Rawang, Selangor, Malaysia

*Corresponding Author: Krista Bonfantine[1]

75 Pigdons Road, Waurn Ponds, VIC, 3216, Australia

Email address: krista.bonfantine@deakin.edu.au

5.2. Abstract

High throughput sequencing is improving the efficiency of monitoring diatoms, which inhabit and support aquatic ecosystems across the globe. In this study, we explored the potential of a standard V4 515F-806RB primer pair in recovering diatom plastid 16S rRNA sequences. We used PhytoREF to classify the 16S reads from our freshwater biofilm field sampling from three stream segments across two streams in south-eastern Australia and retrieved diatom community data from other, publicly deposited, Australian 16S amplicon datasets. When these diatom OTUs were traced using the default RDPII and NCBI databases, 68% were characterized as uncultured cyanobacteria.

We analysed the 16S rRNA sequences from 72 stream biofilm samples, separated the chloroplast operational taxonomic units (OTUs), and classified them using the PhytoREF database. After filtering the reads attributed to Bacillariophyta (relative abundance >1%), 71 diatom OTUs comprising more than 90% of the diatom reads in each stream biofilm sample were identified. Beta-diversity analyses demonstrated significantly different diatom assemblages and discrimination among river segments.

To further test the approach, the diatom OTUs from our biofilm sampling were used as reference sequences to identify diatom reads from other Australian 16S rRNA datasets in the NCBI-SRA database. Across the three selected public datasets, 67 of our 71 diatom OTUs were detected in other Australian ecosystems. Our results show that diatom plastid 16S rRNA genes are readily amplified with existing 515F-806RB primer sets. Therefore, the volume of existing 16S rRNA amplicon datasets initially generated for microbial community profiling can also be used to detect, characterize, and map diatom distribution to inform phylogeny and ecological health assessments, and can be extended into a range of ecological and industrial applications. To our knowledge, this study

represents the first attempt to classify freshwater samples using this approach and the first application of PhytoREF in Australia.

5.3. Introduction

Diatoms are microscopic, unicellular powerhouses, supplying more than 40% of marine primary productivity worldwide and cycling oxygen, carbon, and silica through the world's aquatic ecosystems (Mann, 1999). Sensitivity to environmental conditions, rapid growth rates, and durable silica frustules make diatoms robust indicators of current (Stevenson *et al.*, 2010; Keck *et al.*, 2016) and historic (Gasse *et al.*, 1997) aquatic conditions. The taxonomic composition of diatom communities has been used to monitor changes in temperature (Descy & Mouvet, 1984), salinity (Gell, 1997), nutrient enrichment (Hall & Smol, 1992), pH (ter Braak & van Dame, 1989), and to assess pesticide (Larras *et al.*, 2012) and pharmaceutical (Chonova *et al.*, 2019) impacts on aquatic ecosystems. Accurate morphological identification presents a challenge for using diatom community patterns to assess ecological structure, function, and impacts. Significant expertise is required, and distinguishing morphological traits are often so subtle that trained taxonomists can reach different conclusions (Mann *et al.*, 2010). Besides the subtlety, diatom morphology is also dynamic as they are 'shape shifters' whose size and morphological features vary with life stage and environmental conditions (Falasco & Badino, 2011; Medlin, 2018). Classification is then further complicated by the use of taxonomic references from well-studied regions, such as Europe and North America, to describe diatoms in areas with less diatom taxonomic research, such as Australia (Chessman *et al.*, 2007; Hallegraeff *et al.*, 2010).

Across the European Union, countries assess water quality using diatom-based indices, in accordance with the EU Water Framework Directive (2000). The algorithms that translate diatom counts to stream health scores require accurate diatom identification and quantification, as well as sufficient data to establish taxon-level ecological associations (Visco *et al.*, 2015; Apothéloz-Perret-Gentil *et al.*, 2017; Vasselon *et al.*, 2017). However, misidentification is common, and limited underlying environmental data can produce different ecological values for the same species (Tapolczai *et al.*, 2019). When the indices are applied outside of the region of the contributing data, they often perform poorly (Newall, Bate & Metzeling, 2006; Tan *et al.*, 2017). Diatoms have rarely been used for bioassessment in Australia, but there is interest in developing regional indices (Chessman *et al.*, 2007; Oeding & Taffs, 2017).

Given the array of important roles that diatoms play in aquatic ecosystems, the development of more efficient methods to identify and enumerate diatom communities could advance and expand stream health assessment (Visco *et al.*, 2015; Pawlowski *et al.*, 2016) and consequently, improve management and policy decision-making. Molecular techniques based on high-throughput sequencing (HTS) have provided new insights into diatom biology and ecology (Mann *et al.*, 2010; Zimmermann *et al.*, 2011), and ecologists are optimistic about the potential of diatom metabarcoding as a bioassessment tool. When tested, metabarcoding efforts have produced stream health scores similar to traditional approaches, but to-date, molecular diatom data are not part of routine biomonitoring programs (Kermarrec *et al.*, 2013; Visco *et al.*, 2015; Vasselon *et al.*, 2017), perhaps because HTS techniques are generating as many questions as answers. Molecular data are challenging established phylogenetic relationships and uncovering cryptic diversity from samples examined under the microscope (Bennke *et al.*, 2018; Medlin, 2018). Molecular data are also redrawing diatom distribution maps (Piredda *et al.*, 2018).

For example, *Skeletonema costatum* was once considered common and cosmopolitan, but molecular analysis exposed eight distinct species from previously identified *S. costatum*, some with specific, limited regional distributions (Sarno *et al.*, 2005). However, the molecular signature of diatoms may not always reflect a biological species (Medlin, Williams & Sims, 1993) and it is not known if a single barcoding region effectively represents diversity across Bacillariophyta. Of the many gene regions that have been investigated for barcoding diatoms, the 18S nuclear rRNA (Zimmermann *et al.*, 2011; Visco *et al.*, 2015) and *rbcL* chloroplast markers (Evans, Wortley & Mann, 2007; Evans *et al.*, 2008; Mann *et al.*, 2010; Kermarrec *et al.*, 2013) have been widely adopted (Rimet *et al.*, 2016, 2019) despite some limitations. For example, the highly conserved 18S nuclear rRNA gene region has failed to distinguish species within certain genera, such as *Skeletonema* and *Pseudo-nitzschia*, and some species may include several OTUs when using a 97% similarity cut-off (Piredda *et al.*, 2018). Despite the uncertainty generated by reshuffling diatom phylogeny, over time, barcodes should help to resolve taxonomy in diatoms and other microalgae (Oliveira *et al.*, 2018). A hidden resource for unravelling diatom mysteries may sit in the massive number of 16S rRNA sequences archived in public repositories. Since many bacterial 16S rRNA primers also have high affinity for eukaryotic plastid DNA, non-target sequences from chloroplasts and mitochondria are often co-amplified (Gan *et al.*, 2019). These reads that are neglected in prokaryotic-based microbiome studies could provide a resource for identifying eukaryotic microalgae. The reads may also supply a more accurate measure of abundance than nuclear 18S rRNA, due to orders of magnitude less variability in gene copy numbers (Decelle *et al.*, 2015; Needham & Fuhrman, 2016; Bennke *et al.*, 2018). Rather than ignored, some plastid reads have also been misassigned as cyanobacteria in some databases due to the challenge in distinguishing chloroplast DNA from that of cyanobacterial ancestors (Bennke *et al.*,

2018). If correctly attributed, the 16S rRNA marker offers the advantage of considering both cyanobacteria and photosynthetic eukaryotes using a single amplicon (Eiler et al., 2013; Lehmann et al., 2015; Bennke et al., 2018).

The potential for 16S rRNA sequences to describe the abundance and distribution of eukaryotic photoautotrophs can be explored now that a reference database exists for plastidal sequences. Decelle et al. (2015) produced the PhytoREF database by assembling all publicly available plastidal 16S rRNA sequences and amplicons resulting from Sanger sequencing of cultured microalgae (6,490 sequences). PhytoREF includes all major lineages of photosynthetic eukaryotes including three classes of diatoms: Coscinodiscophyceae, Fragilariophyceae and Bacillariophyceae and *in silico* analysis of the V5/V6 primer set has shown good database coverage (92%) of Bacillariophyta (Milici *et al.*, 2016). PhytoRef focuses mainly on marine microalgae and so thus far, it has been used for classifying marine phytoplankton (Milici *et al.*, 2016; Needham & Fuhrman, 2016; Bennke *et al.*, 2018).

Taking advantage of these advances in reference databases, in this study, we present an approach for uncovering diatom assemblage data from 16S rRNA sequences. To our knowledge, the filtered and classification of diatom reads from a universal 16S primer has not been tested for freshwater communities, and PhytoREF has not been trialled in Australia. We developed this approach after failing to detect diatoms in the 23S reads (Sherwood & Presting, 2007) from our stream biofilm samples. We decided to probe the 16S rRNA sequences from the same biofilm samples to see if we could retrieve diatom community structure data from the chloroplast reads. We queried the chloroplast reads against the PhytoREF database to identify sequences belonging to diatoms and evaluated diatom community structure across different river segments. Then, in order to test the broader applicability of the method, we compared the diatom sequences from

this study to three publicly available 16S rRNA sequencing datasets from Australia and demonstrated the capacity to mine digital diatom sequences. With further validation, this method could be applied to examine diatom phylogeny and improve biomonitoring at multiple spatial scales.

5.4. Materials and Methods

5.4.1. Field sampling

We collected biofilm samples from three stream segments in Victoria, Australia. One segment of the Barham River (B) was sampled along with two reaches in Painkalac Creek, one upstream (PU) and one downstream of the reservoir (PD) (Figure 5.1A). Access was provided by the Victoria Department of Environment, Land, Water and Planning under permit # 10008062. We deployed wood blocks, composed of native mountain ash (*Eucalyptus regnans*), as a natural and consistent substrate for biofilm colonization (Ryder *et al.*, 2006) on floating frames in eight locations (Figure 5.1A,C). Two sets of three (60 cm^2) blocks were anchored to each frame with overlapping but non-concurrent time periods (Figure 5.1C). Between December 2018 and March 2019, nine sets of blocks were deployed at each of the eight sites to produce 72 biofilm samples. Only two sites were placed at PU because of limited summer water depth and access. Following each three-week growth period, which captures early and late biofilm successional patterns (Ryder *et al.*, 2006), substrate blocks were removed and replaced and biofilms were scraped from the upper surface of the three blocks into a single composite sample (Figure 5.1D,E). On two occasions, the sides of the blocks were collected and samples were examined and photographed using a compound light microscope for visual, qualitative documentation. A 0.33 mL subsample of the biofilm slurry was transferred to a 1 mL ZR

BashingBead™Lysis tube (0.1 and 0.5 mm silica beads) with 0.66 mL of DNA/RNA Shield (Zymo Research, Irvine, CA), and vigorously mixed. A 0.5 mL subsample was transferred to a 47 mm Whatman GF/F glass fibre filter for subsequent lab analysis of chlorophyll concentration following standard protocol (American Public Health Association (APHA), 1995). All samples were stored at 4°C until processing. Chlorophyll a concentrations per sample were calculated using the total sample volume in the Falcon© tube and then converted to mass per unit area based on the combined surface area (180 cm^2) of the three blocks (Biggs *et al.*, 2000).

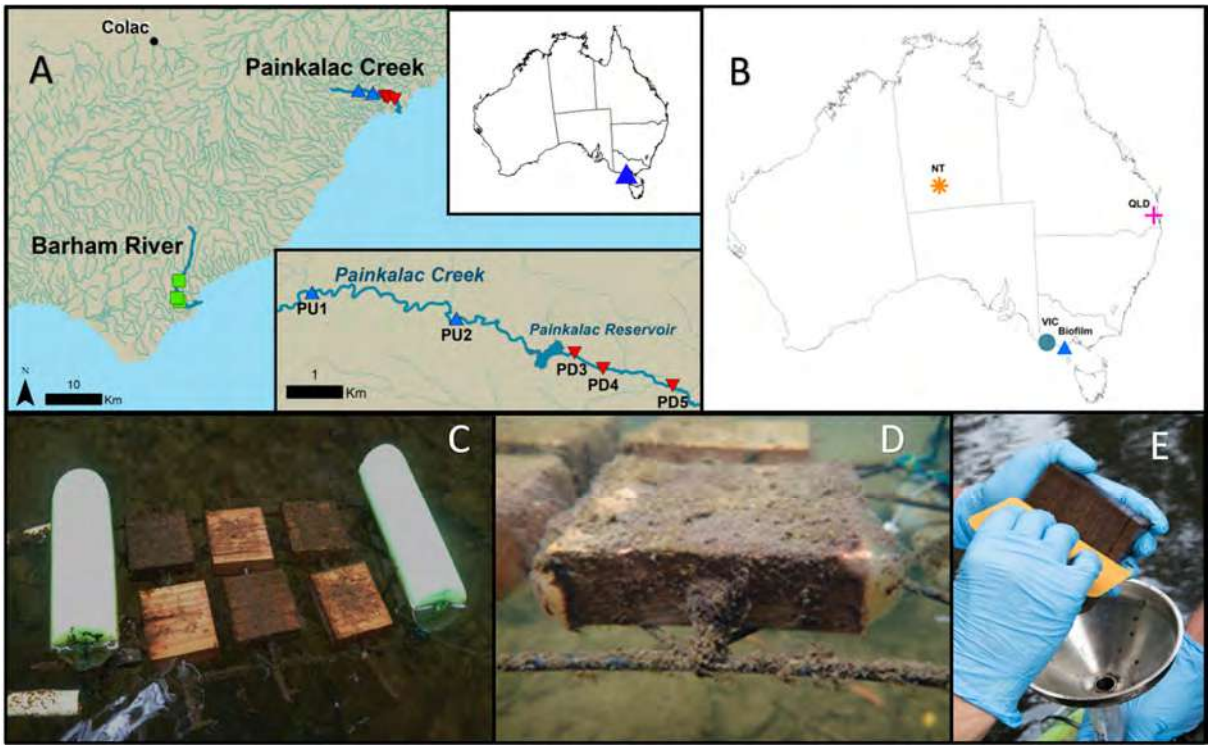

Figure 5.1 Stream biofilm sampling details and database sequence source locations. (A) The biofilm field sampling was conducted in Victoria, Australia. Two Painkalac Creek sites were upstream of Painkalac Reservoir (blue symbols) and three were downstream (red symbols). Three sampling sites were located on the Barham River (green symbols) (map source: Regional Surface Hydrology Lines. Geoscience Australia (Crossman & Li, 2015)) (B) Locations of samples from the stream biofilm sampling (Biofilm) and the publicly available 16S rRNA datasets (Kaestli et al., 2019 (NT); O'Dea et al., 2019 (QLD); Trevathan-Tackett et al., 2020 (VIC)). (C) Experimental floating frame with two sets of wood block substrate deployed two weeks apart. (D) Close-up view of a wood block coated in biofilm 21 days after deployment. (E) Scraping biofilm into stainless steel funnel inserted in Falcon© tube.

5.4.2. Amplicon sequencing and bioinformatics

DNA from the preserved biofilm samples was extracted using a bead beating-based Zymobiomics Miniprep Kit (ZymoResearch) following the manufacturer's instructions. Bead-beating was performed on a Vortex Genie2 at maximum vortex speed for 20 minutes. To improve DNA recovery, elution of DNA from the spin column used pre-heated TE buffer (56°C) with an extended incubation time of 5 minutes. DNA concentration was quantified with a Qubit 4 Fluorometer (Thermo Fisher Scientific).

The purified DNA was sent to MR DNA (Shallowater, Texas, USA) for amplicon sequencing on the Illumina platform. Briefly, the V4 variable region of the 16S rRNA gene was amplified using the 515 (GTGYCAGCMGCCGCGGTAA) (Parada *et al.*, 2016)/806RB (GGACTACNVGGGTWTCTAAT) (Apprill *et al.*, 2015) primer set with an in-line barcode on the forward primer. A single-step polymerase chain reaction (PCR) was performed using the HotStarTaq Plus Master Mix Kit (Qiagen, USA) under the following conditions: 94°C for 3 minutes, followed by 30-35 cycles of 94°C for 30 seconds, 53°C for 40 seconds and 72°C for 1 minute, after which a final elongation step at 72°C for 5 minutes was performed. Successful amplification and the relative intensity of bands were verified in 2% agarose gel. Multiple barcoded samples were pooled together in equal proportions based on molecular weight and DNA concentrations and then purified using calibrated Ampure XP beads (Beckman Coulter). The pooled and purified PCR product were sequenced on the Illumina MiSeq System (Illumina, San Diego, CA) using the run configuration of 2 × 300 bp.

Raw paired-end reads were processed using the MR DNA analysis pipeline. Briefly, paired-end reads were merged, depleted of barcodes followed by the removal of sequences shorter than 150 bp or with ambiguous bases. The sequence data from this study were deposited under BioProject PRJNA588337 in the Sequence Read Archive (SRA) of the National Center for Biotechnology Information (NCBI). Mothur was used for denoising, operational taxonomic unit (OTU) clustering at 97% similarity and chimera removal (Schloss *et al.*, 2009).

The sequencing laboratory classified the 16S OTUs using BLASTn against a curated database derived from RDPII and NCBI (www.ncbi.nlm.nih.gov, http://rdp.cme.msu.edu) and we compared the results to those resulting from our tailored bioinformatics process. A subsequent classification step broadly separated the

OTUs into four major groups (bacteria, archaea, mitochondria, chloroplast) using the QIIME2 q2-sample-classifier plugin (Bokulich *et al.*, 2018) and its supplied Greengenes database (McDonald *et al.*, 2012). The chloroplast-derived OTUs were further classified using the naive Bayes classifier in QIIME2, which has been trained using the PhytoREF database (Decelle *et al.*, 2015). We herein refer to the nomenclature as assigned by PhytoREF which reflects shifting protist phylogeny and nomenclature (Adl *et al.*, 2012, 2019; Guillou *et al.*, 2012).

To determine whether chloroplast sequences accounted for the majority of 16S rRNA sequences (Eiler *et al.*, 2013) and whether the proportion varied by location, we calculated the relative proportion of each of the four major groups (bacteria, archaea, mitochondria, chloroplast) across the total 16S sequence reads for each field site. We then compared the proportion of plastidal sequences (chloroplast + mitochondria) to prokaryotic sequences (bacteria + archaea). PhytoREF places diatoms within phylum Ochrophyta under the super-group Stramenopila (Decelle *et al.*, 2015) and classifies Bacillariophyta as a class. We examined the proportion of Ocrophyta within the total chloroplast reads and the proportion of Bacillariophyta within the Ocrophyta reads. To compare the taxonomy assigned by PhytoREF (Decelle *et al.*, 2015) to those returned by the NCBI non-redundant nucleotide database, we performed a similarity search (mega-blast) of the diatom OTUs identified with and without the 'exclude environmental sample' option selected.

5.4.3. Method validation

To test the amplification of diatom chloroplast sequences by the bacterial primers, three *in silico* validation tests were performed. In the first test, the FastPCR *in silico* tool (Kalendar *et al.*, 2017) was used to analyse the 515F/806RB primer set against the

PhytoREF reference sequences (4641 sequences). For the second test, the FastPCR *in silico* tool (Kalendar *et al.*, 2017) was used to analyse the primer set against 1747 publicly available, eukaryotic sequences from the NCBI nucleotide database obtained using the criteria 'Bacillariophyta AND 16S'. For the third test, the primer alignment was investigated more closely by comparing a few randomly selected members of the phylum Ochrophtya to related phyla and to an *E.coli* sequence generated by the same primer set using ClustalX (Thompson, Gibson & Higgins, 2003).

To evaluate the performance of the PhytoREF database in classifying diatom chloroplast sequences deposited in the NCBI public database, a subset of 1666 Bacillariophyta sequences (complete and nearly complete genomes were excluded) were analysed in R 4.0.4 (R Core Team, 2021 using the DADA2 1.18.0 (Callahan et al., 2016) and Bioconductor 3.12 (Huber et al., 2015) packages. Taxonomy was assigned to the PhytoREF database (Decelle, 2015) through the *assignTaxonomy* function in the DADA2 package, using the Naive Bayesian Classifier method (Wang et al. 2007) with a 50% minimum bootstrap confidence threshold.

5.4.4. Beta-diversity analysis of field biofilm samples

The read counts for each Bacillariophyta (diatom) OTU were used to construct a raw OTU table. Data were normalized to relative abundance (McKnight *et al.*, 2019) and percent composition by OTU was calculated by applying a 'standardize by total' approach (Clarke & Gorley, 2015) based on the total Bacillariophyta read count for each sample. All multivariate analyses were performed using Primer v7 with PERMANOVA+ (Clarke & Gorley, 2015). The relative abundance values were square-root transformed to reduce the impact of a few dominant taxa in the Bray-Curtis similarity analysis (Bray & Curtis,

1957). The Bray-Curtis similarity matrix was conservatively constructed using diatom OTUs that had at least 1% abundance in a sample. An analysis using relative abundance is appropriate here based on consistent field and laboratory methods and orders of magnitude less variability in 16S gene copy numbers (Needham & Fuhrman, 2016; Bennke *et al.*, 2018) than other molecular markers.

Differences between diatom communities among the river segments were examined using two-factor permutational multivariate analysis of variance (PERMANOVA) (Anderson, 2001) with 9999 unique permutations. The random 'site' factor was nested within the fixed 'segment' factor. Homogeneity of dispersion between groups was tested using PERMDISP. A non-metric multidimensional scaling (nMDS) (Kruskal, 1964) plot was constructed to visualize the differences between communities, and pairwise SIMPER analysis (Clarke, 1993) was performed to identify the OTUs driving the significant differences among the sites. The five OTUs with the highest contribution to the dissimilarity plus a dissimilarity/SD ratio of greater than 1 (Clarke & Gorley, 2015) were selected to demonstrate differences between river segments, which were visualized using a heat map created in the 'pheatmap' package (Kolde, 2017) in R (v3.6.0; R Project for Statistical Computing, Vienna, Austria).

5.4.5. Detection of selected diatom OTUs in other Australian 16S rRNA datasets

To test the capability of our approach for detecting diatoms in other microbiome datasets, we searched the NCBI-SRA database for publicly available 16S rRNA sequencing data from freshwater Australian studies. We were interested in the potential for the method to illustrate regional diatom distribution in Australia, so we selected three datasets that used a similar set of primers: two datasets from freshwater samples of a similar

ecosystem to this study but from distant locations, and one dataset, from a brackish estuarine site of close proximity to this study (Figure 5.1B, Table 5.1).

The diatom OTUs in our study were used as reference sequences to perform high-throughput sequence similarity searches using VSEARCH v.2.14.1 (Rognes *et al.*, 2016) with minimum nucleotide identity cut-off of 97% (--usearch_global --id 0.97). This reference sequence based method streamlined the bioinformatics process and focused on the spatial distribution of the diatoms detected in our biofilm samples.

To compare the database diatom communities with each other and with our field data, all data were presence/absence transformed and a Jaccard similarity matrix was constructed (Legendre & Legendre, 1998) using Primer v7 with PERMANOVA+ (Clarke & Gorley, 2015). To visualize the community patterns across locations, the Bray-Curtis matrix was used to construct a shade plot. The distance among centroids was also calculated, and the resulting distance matrix was used to construct a non-metric multidimensional scaling (Kruskal, 1964) ordination.

Table 5.1 Existing Australian 16S datasets used to compare the diatom reads in this study. Publicly available 16S rRNA gene datasets in NCBI-SRA database (Kaestli et al., 2019; O'Dea et al., 2019; Trevathan-Tackett SM et al., 2020).

State	Sample type	Salinity description	Water regime	Sampling date	n	Reference	BioProject ID
NT	biofilm water	freshwater	perennial ephemeral	June 2016	78	Kaestli et al., 2019	PRJEB29669
QLD	water	freshwater	perennial	Mar/Apr 2018	13	O'Dea et al., 2019	PRJNA484387
VIC	seagrass leaf	brackish	estuary flooded	July 2016	5	Trevathan-Tackett et al., 2020	PRJEB36104

5.5. Results

5.5.1 Taxonomic assignment of field biofilm diatom OTUs

After quality filtering, a total of 4.9 million reads were obtained from the 72 stream biofilm samples with an average of 68,273 (±5849) retained reads (Supplemental Table 5.3). The smallest number of raw reads per sample was 34,222, with 30,175 passing the bioinformatics pipeline. Between 3.9 and 34.0% of the reads from each sampling location were classified as chloroplast sequences (mean = 16.5%; median = 15.0%; Supplemental Figure 5.4A, Supplemental Table 5.2). Chloroplasts made up a higher proportion of the reads from the Barham River sites than from the Painkalac Creek sites. In 10 of the 72 samples, all from the Barham River, eukaryotic sequences (chloroplast + mitochondria) exceeded that of identified prokaryotic sequences (bacteria + archaea). Typical of samples rich in eukaryotic DNA (Parada *et al.*, 2016), the samples with a high proportion of chloroplast sequences also yielded 18S sequences, which were ignored as 'unclassified' in the Greengenes classification step.

Based on PhytoREF classification, 87.2% of the 1,464 chloroplast reads were assigned to Ochrophyta (Supplemental Supplemental Figure 5.4A) of which, 63.1% were

attributed to Bacillariophyta (Supplemental Figure 5.4C). Across the 72 biofilm samples, diatom (Bacillariophyta) sequences represented 36.4% of the total chloroplast reads, while green algae accounted for 10.4% (Streptophyta = 6.4%, Chlorophyta = 4%). The relative abundance of diatoms was proportionally calculated based on the 533 OTUs assigned as Bacillariophyta by PhytoREF (Decelle *et al.*, 2015). After conservatively filtering for OTUs with at least 1% relative abundance in a sample, 71 OTUs were retained, herein referred to as 'diatom OTUs'. These 71 diatom OTUs collectively and consistently made up more than 90% of the diatom reads in each stream biofilm sample. The percent identity of the 71 diatom OTUs assigned to the PhytoREF reference sequences ranged from 71.4% to 99.9% with a mean value of 87.6% (Table S3). Six of these OTUs were assigned to order (Surirellales, Naviculales or Chaetocentales) by PhytoREF, and three of these six OTUs could be classified down to genus (*Psammodictyon, Navicula* or *Chaetoceros*) (Supplemental Table 5.2).

The taxonomic assignments for the 71 diatom OTUs were inconsistent using the two 16S amplicon databases. The bioinformatics pipeline based on the curated RDPII and NCBI databases assigned 48 of the 71 diatom OTUs (68%) as cyanobacteria. When we searched the stream biofilm sequences against the NCBI non-redundant nucleotide database, using the default BlastN search setting and database parameter, the majority of the top hits were returned as 'uncultured bacterium'. When environmental samples were excluded from the search query, most of the OTUs were classified as chloroplast sequences, and discordance between NCBI and PhytoREF occurred mostly at the lower taxonomic rank. One major exception was for OTU6 that was classified by PhytoREF as *Chaetoceros,* a diatom genus, while the top NCBI hit was *Gomphoneis minuta* (99% sequence identity), a euglenid from a different phylum.

Visual patterns of diatom abundance, observed under the microscope, were consistent with the molecular patterns of total diatom abundance. Diatoms were most abundant in the Barham River (mean read abundance=19.64), followed by the Painkalac downstream segment (mean read abundance = 7.75), and scant diatom representation in the upstream Painkalac segment (mean read abundance = 1.17). Of the three genera assigned by PhytoREF, only *Navicula* was visually observed in the samples. Four diatom genera that were not identified by their molecular signature (*Nitzschia, Gomphonema, Cymbella,* and *Melosira)* were observed within a single sample from the Barham River (Figure 5.2C,D).

The general pattern of diatom read abundance is also consistent with the chlorophyll concentrations measured within each segment. Barham River biofilm samples had a mean chlorophyll concentration of 18.35 mg/m^2 versus 7.60 mg/m^2 for Painkalac downstream and 0.91 mg/m^2 for Painkalac upstream samples.

5.5.2. Method validation

According to the FastPCR *in silico* test with one mismatch allowed on the 3'-end, the primer set would amplify 90.8% of the PhytoREF sequences and 57.5% of the publicly available eukaryotic sequences labelled as 'Bacillariophyta' in the NCBI database. The Clustal nucleotide alignment confirmed the differences between the eukaryotic chloroplast sequences and prokaryote sequences (Supplemental Figure 5.4D). The Ochrophyta, and other eukaryote reads, showed high sequence conservation with no 3' mismatches in the last 5 bases of both forward and reverse 16S v4-515F and V4-806RB primers. Two mismatches to the *E.coli* 16S rRNA (GT vs TA) were observed across all aligned non-*E.coli* 16S RNA sequences 15 bases upstream of the V4-806 primer-binding site (Supplemental Figure 5.4D).

In terms of database coverage, of the 1666 sequences classified as Bacillariophyta in NCBI, 660 were attributed to Bacillariophyta by PhytoREF. The sequences were distributed across 21 orders but only 33.7% of sequences were assigned at the family level and 22.4% were assigned a genus (Supplemental Figure 5.5).

5.5.3. Distinct diatom assemblage in field biofilm samples

There were significant differences in diatom assemblage structure among the three river segments, indicated by the distinct clusters on the multidimensional scaling plot (Figure 5.2A). The PERMANOVA results show that the composition of the diatom assemblage varied within (pseudo-$F_{5,71}$=4.68; P<0.001) and between the river segments (pseudo-$F_{2,71}$=8.81; P=0.003). There were no significant differences in the homogeneity of dispersion among sites (PERMDISP P=0.74) or segments (PERMDISP P=0.82). In the SIMPER analysis, there was redundancy in the 15 OTUs that contributed most strongly to the separation between river segments, which resulted in 11 non-redundant distinguishing OTUs (Figure 5.2B, Supplemental Table 5.2). OTUs 4668, 8, and 104 were more abundant in the Barham River, while OTUs 4485, 30 and 21053 were characteristic of the Painkalac downstream sites. The Painkalac upstream samples shared OTUs with the other two reaches, but the patterns of abundance were different. For example, OTU 1 was more consistently abundant (min=3.2%, max=18.6%) upstream than in the other two reaches (PD: min 0.7%, max 14.9%; B: min=0.3%, max=43.6%).

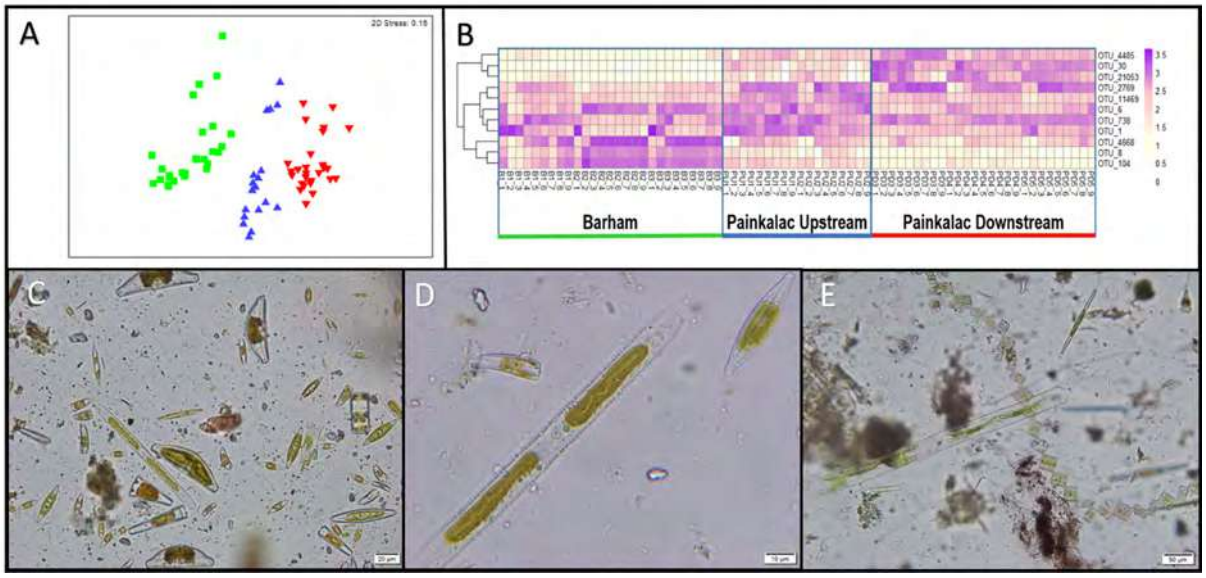

Figure 5.2. Diatom communities in stream biofilm samples. (A) nMDS ordination of Bray-Curtis distances of square-root transformed relative diatom abundance from 72 biofilm samples across 8 sampling sites within three river segments (colors; B=green, PU=blue, PD=red). (B) Heatmap showing relative abundance for 11 non-redundant OTUs identified by pairwise SIMPER analysis for 72 biofilm samples. (C) Sample B1_9 observed under microscope at 400X magnification. (D) A close-up of three diatoms from sample B1_9 at 1000X magnification. (E) Diatoms from sample PD5_6 observed at 200X magnification.

5.5.4. Occurrence of selected diatom OTUs in other Australian 16S rRNA datasets

Of the 71 diatom OTUs identified in this study, 67 were also detected in at least one of the other three Australian environmental 16S rRNA test datasets selected from NCBI-SRA (Table 5.1, Figure 5.3A). Ten OTUs were observed across all four datasets, spanning freshwater and brackish habitats from far inland to estuarine ecosystems. Our stream biofilm samples shared the highest number of diatom OTUs (61) with the water and biofilm samples from the Northern Territory (NT) (Kaestli *et al.*, 2019) (Figure 5.3A). We detected diatoms in all of the NT samples, with diatom reads contributing a minimum of 0.2% of the total reads in a water sample and a maximum of 22.6% in a biofilm sample. The Victorian estuary site (VIC) was much closer geographically to our stream biofilm field locations, but only 27 of the diatoms were shared between the two sites (Figure 5.3A,B). The lowest number of diatoms (24) and lowest similarity was shared with the freshwater samples from Queensland (O'Dea *et al.*, 2019).

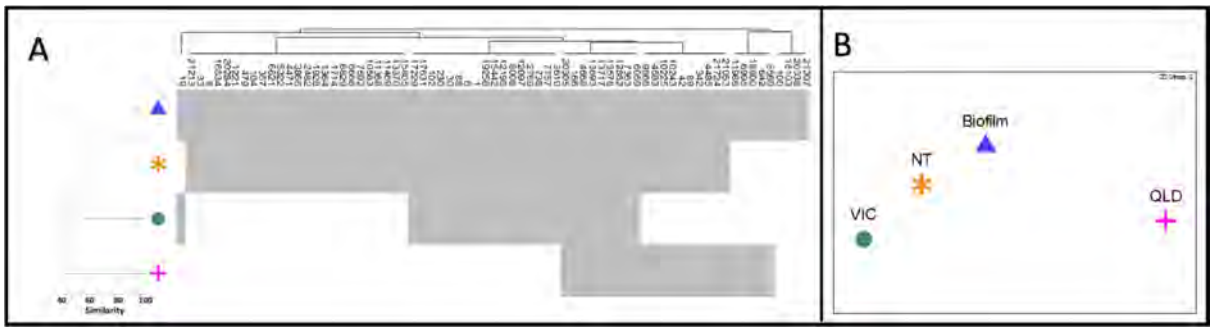

Figure 5.3. Diatom communities in stream biofilm and public database. (A) Shade plot depicting presence/absence of 71 diatom OTUs within each dataset. (B) nMDS based on presence/absence Jaccard similarity matrix including field data from this study (BIOFILM) and publicly available datasets (Kaestli et al., 2019 (NT); O'Dea et al., 2019 (QLD); Trevathan-Tackett SM et al., 2020 (VIC)).

5.6 Discussion

In this study, we show for the first time that the interrogation of 16S rRNA amplicon reads assigned to 'chloroplast' can provide insights into aquatic Australian diatom community composition and distribution. Additionally, this study showed that the PhytoREF database, typically used for describing marine phototroph lineages (Milici *et al.*, 2016; Bennke *et al.*, 2018), can provide some limited information for freshwater samples. The chloroplast reads that were filtered from the stream biofilm 16S amplicon data, and classified as diatom OTUs, showed distinct assemblage patterns at the river segment level. Further, OTUs shared between our field samples and public database samples described diatom occurrence across habitats at a continental scale.

We have shown that useful diatom community data can be constructed from mined 16S sequences but our experiment was not designed with this research in mind. Rather, we developed this approach in an attempt to characterise a community that was absent from our molecular data. Our biofilm field experiment employed a multi-metabarcoding approach, which included the 23S amplicon to detect photosynthetic eukaryotes (Sherwood & Presting, 2007), but no diatoms were detected. Using the

method we present here, we uncovered the presence of a hidden resource within our 16S sequences but the quality of that resource remains uncertain based on limited reference database quality and knowledge gaps around non-target primer performance.

In examining the prokaryotic community structure based upon our 16S data, more sequences were discarded than used in 10 of our 72 samples. This highlights that non-target reads are not only a waste of sequencing power, but also suggests a missed opportunity for characterizing photosynthetic eukaryotes. We also identified misclassifications of diatoms as cyanobacteria, which could falsely inflate estimates of cyanobacterial abundance using the amplicon approach (Bennke *et al.*, 2018) and thereby affect ecological inferences. Misclassifications are particularly relevant if cyanobacteria are to be used as bioindicators, as suggested by Mateo et al. (2015).

5.6.1. Method validation

Research on the performance of prokaryotic primers in amplifying eukaryotic plastids has focused on reducing non-target amplification so little is known about primer bias and taxonomic coverage in non-target taxa. While our study does not comprehensively investigate these issues, our *in silico* results provide some relevant details. The primer set 515F/806RB amplified 90.8% of the PhytoREF sequences and about half (57.5%) of the publicly available 'Bacillariophyta' sequences deposited in NCBI. The NCBI sequences were mostly partial (95%), many lacked the target region, and some may be incorrectly annotated in the database. It is difficult to assess primer bias across taxa when 61% of the NCBI sequences (1017) are from 'uncultured diatoms' and only 39.6% of the sequences were attributed to Bacillariophyta when analysed against PhytoREF. The plastid sequences in NCBI have largely been discarded as nuisance reads so the nature and quality of these 'trashed' sequences requires more investigation.

Based on our alignment, there were no 3' mismatches in the last five bases of either primer (Supplemental Figure 5.4D) which are generally thought to prevent amplification (Sipos *et al.*, 2007; Hanshew *et al.*, 2013). Because chloroplasts are amplified so readily by the universal bacterial primers (515F/806RB), the mismatch between positions 783-799 (based on *E.coli* numbering), just upstream of our 806RB primer, has been targeted by bacterial primers designed to reduce chloroplast contamination of 16S data (Hanshew *et al.*, 2013). Within this region, 15 bases upstream of the V4-806 primer-binding site, we observed two mismatches to the *E.coli* 16S rRNA (GT vs TA) across all the eukaryotic sequences we evaluated. This mismatch could be targeted in designing a diatom-specific 16S primer pair.

Further research is required to validate the performance of 16S primers across diatom taxa. A pairwise test of the V4 regions from 16S and 18S assays on a mock community of prokaryotes and photosynthetic eukaryotes would provide fundamental data on primer bias and efficiency. Needham and Fuhrman (2016) found highly concordant patterns of phytoplankton dynamics when comparing 16S and 18S abundance estimates but their direct comparison is unusual. Most investigations have considered the prokaryotic community using 16S and the eukaryotic community using 18S (e.g. Brinkmann *et al.*, 2015; Laroche *et al.*, 2018; de Sousa *et al.*, 2019). Additional details about the diatom assemblage could be gathered by analysing the discarded 16S plastid sequences from these studies alongside the 18S results. Eiler (2013) suggested 16S as an ideal first step analysis that could be coupled to a second method such as 18S with higher taxonomic resolution and deeper sampling of protist diversity. In cases where 18S may have provided ambiguous results at lower taxonomic levels, 16S reads could supply additional resolution and the diversity. To our knowledge, this has not been

tested but the large volume of publicly available 16S microbiome research means that supplemental data may be available locally or regionally.

The use of PhytoREF to assign taxa to the eukaryotic fraction of 16S reads is becoming a common practice (e.g. Zamora-Terol, Novotny & Winder, 2020; Alcamán-Arias *et al.*, 2021) but the taxonomic resolution for PhytoREF is limited, even for marine taxa. In their marine bacterioplankton analysis, Milici (2016) found 59-69% assignment at the order level and only 16-24% at the genus level. Our efforts to classify the 16S Bacillariophyta reads in NCBI against PhytoREF was less specific, with only 33.8% of the sequences assigned an order.

According to the PhytoREF taxonomic assignment of our biofilm chloroplast sequences, the highest proportion (36.4%) were attributed to diatoms. Of the 71 diatom OTUs with at least 1% abundance in a sample, three were identified to genus. These identifications are suspect, however, as only *Navicula* was observed under the microscope and the other two genera are predominantly marine. The *Chaetoceros* genus contains some freshwater species but *Psammodictyon* is considered a marine genus and is therefore unlikely to be encountered (Round, Crawford & Mann, 1990). There were 65 diatoms that could not be classified at the order level which may reflect the limited representation of freshwater microalgae in the PhytoREF library, the limited protist databases (Pawlowski *et al.*, 2016), and the lack of molecular data for Australian diatoms. In light of the ongoing accumulation of sequences and refinements to diatom phylogeny and taxonomy, an updated version of PhytoREF, including freshwater algae, would be a valuable resource.

5.6.2. Applications of the method

Currently, 16S sequences from freshwater diatoms can be utilised using a taxonomy-free approach (Pawlowski *et al.*, 2016; Apothéloz-Perret-Gentil *et al.*, 2017) that does not rely upon on identification. Under this approach, diatom community data mined from existing 16S reads can be related directly to ecological conditions to help fill knowledge gaps around diatom phylogeny and ecology and to develop novel stream health indices. We suggest that three 'data clouds' exist for identifying and classifying diatoms: morphological, molecular, and environmental. Improved information about a morphological species, an OTU (DNA barcode), or a set of environmental variables expands a given 'data cloud' and barcodes serve as stable identification benchmarks to link records between 'clouds' and through time (Zimmermann *et al.*, 2014). DNA barcodes also serve as indelible fingerprints when taxonomic reshuffling challenges the identity of existing morphospecies (Zimmermann *et al.*, 2014). Under the 'data cloud' model, data can accumulate simultaneously to establish biotic and abiotic relationships over time. The ten diatom OTUs that we documented in all four locations from inland, freshwater sites to estuarine seagrass communities (Figure 5.3A) are an example of how barcodes can link distant and diverse sites. The value of this information increases, if or when, existing morphological records and site-level environmental conditions are compared across locations.

In this study, the 67 diatom OTUs that were shared between our field samples and public database samples describe the occurrence of similar diatom taxa across diverse habitats at a continental scale (Figure 5.1B, 5.3A, 5.3B). The limited overlap of 27 OTUs with the nearby estuary site in Victoria (VIC) could reflect environmental differences or there may be selective pressures that restrict the diatom assemblage on seagrass leaves.

There is potential to consider this and other ecological questions by assembling diatom community patterns from microbial data that were generated for another purpose. For example, the samples that O'Dea et al. (2019) sequenced to track the microbial signatures of wastewater shared 34% of the diatom OTUs from coastal streams in Victoria (BIOFILM). Our analysis shows high overlap (86%) with the samples that Kaestli et al. (2019) used to compare microbial communities in perennial and ephemeral water bodies in the Australian arid zone (NT), suggesting similar diatom communities among the distant sites. It should be noted that this similarity could be, in part, a product of the larger sample number (n=78) relative to that of the VIC site (n=5). Kaestli et al. (2019) describe a consistently large proportion of cyanobacteria across their samples but our consistent detection of diatom OTUs suggests that the proportion could be skewed due the misattribution of chloroplast sequences in standard 16S rRNA databases.

In this study, we tested whether 16S amplicon reads from stream biofilm samples could describe local diatom assemblage patterns, and then verified the approach on a larger but limited biogeographic scale. However, scaling up this approach to broader diatom biogeographic ranges could be considered by directly mapping public 16S libraries against PhytoREF, as shown in different systems. For example, del Campo et al. (2017) screened 16S sequences to study the global distribution of the green algae, *Ostreobium*, and documented consistent co-occurrence with hard coral. A similar approach could evaluate the degree of community similarity and test assumptions of cosmopolitan diatom distribution and ecological preferences (Gell, 2019).

Accurate, efficient, and cost-effective characterization of diatoms could be widely beneficial across an array of ecological and management applications. For example, several toxic diatom species are monitored in coastal Australian regions due to their role in harmful algal blooms (HAB) (Ajani *et al.*, 2020). HAB surveillance monitoring would

benefit from the use of a single amplicon, such as our approach here, that could characterize both diatom and cyanobacteria populations. As established bioindicators, diatom community structure could also augment the assessment of wastewater treatment methods that have so far, relied upon microbial communities (Chonova *et al.*, 2016; Stoeck *et al.*, 2018). Diatom community patterns have even been used to trace the past locations of sea turtles (Rivera *et al.*, 2018) and human bodies (Scott *et al.*, 2014) and digging diatom data out of 16S microbiome studies presents a promising opportunity to advance biosurveillance, forensic, biodiversity, and bioassessment efforts.

5.7. Conclusions

We show that in-depth diatom community data can be uncovered from existing but underutilized 16S rRNA plastidal sequences from microbial community profiling. Even in a poorly studied region, diatom OTUs filtered from 16S chloroplast reads can describe community composition and improved characterization of the chloroplast reads may, in some cases, lead to different conclusions about community dominance and water quality. Digging into existing 16S datasets may inform phylogeny in regions where diatoms have been extensively studied, or may provide a first pass for detecting diatoms and considering broad spatial relationships in regions of limited research. This study provides proof of concept for the mining of digital diatom sequences, a method, which could be applied to local, regional, and global research questions.

We suggest that the universality of the 515/806 primer and the variability of the 16S region warrant further investigation as a tool to characterise photosynthetic eukaryotes. With additional primer performance validation and improved reference databases, the massive volume of publicly available environmental microbiome data

could potentially provide a treasure trove for studying diatoms and other microalgae with minimal field or laboratory costs.

5.8. Supplemental information

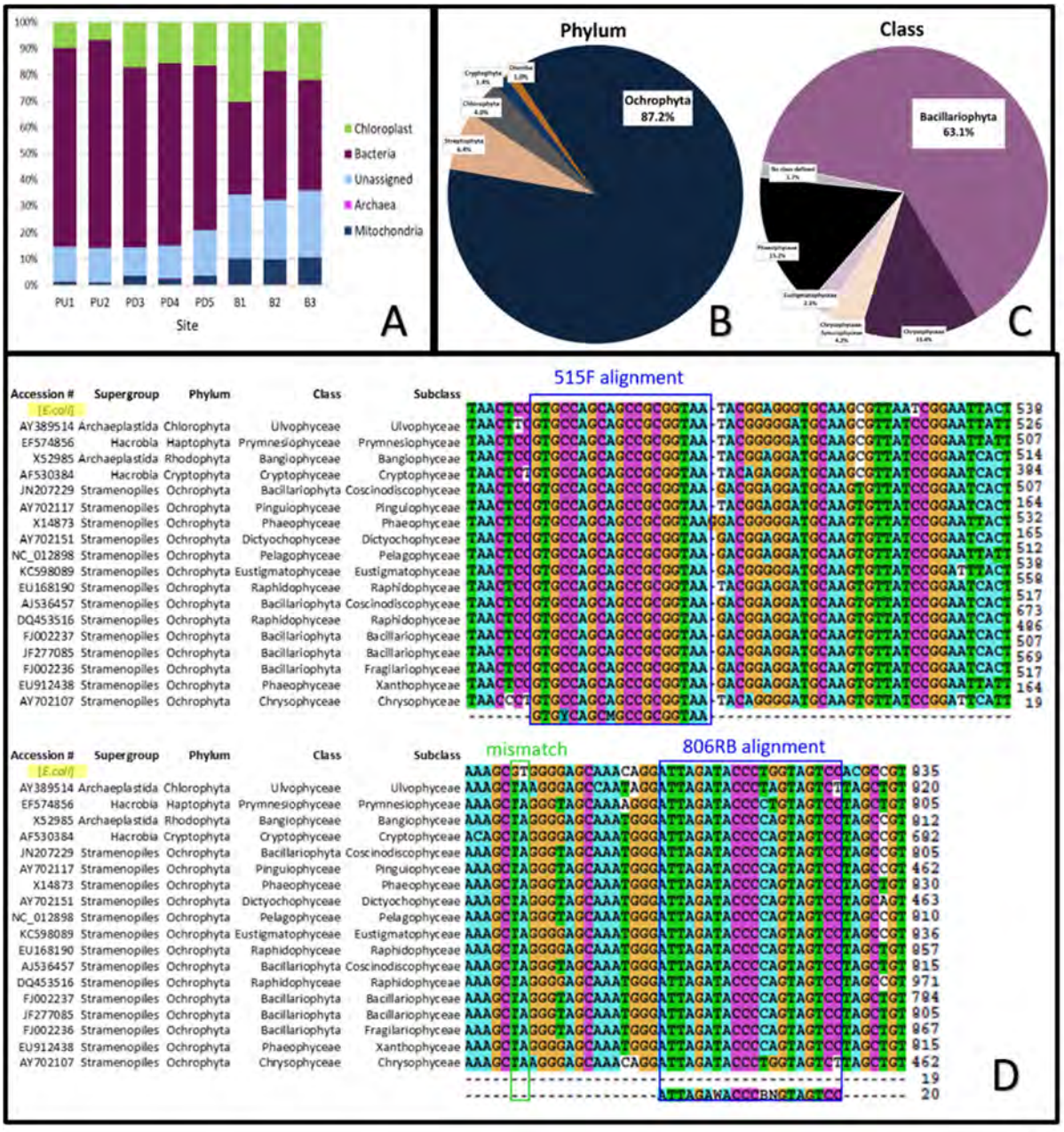

Supplemental Figure 5.4. Chloroplast reads and 16S rRNA. (A) Contribution of each major group to the 16S reads for each site (9 samples per site). (B) Chloroplast reads by phylum (>1%). (C) Ochrophyta reads by class (>1%, diatoms as Bacillariophyta). (D) Alignment of the PCR primers to selected 16S rRNA plastid sequences used MAFFT (default setting).

Supplemental Figure 5.5. NCBI sequences and PhytoREF. Proportion of the publicly available, partial 'Bacillariophyta' 16S sequences (1666 total) in NCBI that were classified at each taxonomic level against the PhytoREF database.

Supplemental Table 5.2. Taxonomy for 11 OTUs as assigned by NCBI (restricted), NCBI default and PhytoREF databases.

OTU	NCBI restricted			NCBI default			PhytoRef
	Accession #	Taxonomy	% Id	Accession #	Taxonomy	% Id	Taxonomy
1	KY498709.1	Angulodiscorbis quadrangularis isolate AQ159-89	99%	MH934704.1	Uncultured bacterium clone Sum14ACA187	99%	Kingdom.Eukaryota;Supergroup.Stramenopiles; Phylum.Ochrophyta; Class.Bacillariophyta; Subclass.Bacillariophyta_X; Order.Naviculales; Suborder.Naviculales_X
	KY498706.1	Glabratella patelliformis isolate GP446-17	99%	KT977116.1	Uncultured prokaryote clone	99%	
	KP792485.1	Planoglabratella opercularis isolate GO863-27	99%	KF964592.1	Uncultured bacterium clone Sum14ACA187	99%	
6	KY499654.1	Gomphoneis minuta var. cassieae chloroplast	99%	KM134804.1	Uncultured bacterium clone LNH_9_9_11_Water.252201	99%	Kingdom.Eukaryota; Supergroup.Stramenopiles; Phylum.Ochrophyta; Class.Bacillariophyta; Subclass.Bacillariophyta_X; Order.Chaetocerotales; Suborder.Chaetocerotales_X; Family.Chaetocerotaceae; Genus.Chaetoceros; Species.Chaetoceros
	KC509523.1	Didymosphenia geminata chloroplast	98%	KM133341.1	Uncultured bacterium clone LNH_9_9_11_Water.207325	99%	
	MH011748.1	Chaetoceros sp. isolate GF104-16S_7	97%	KM133339.1	Uncultured bacterium clone LNH_9_9_11_Water.207294	99%	
8	KT952293.1	Pinnularia sp. U-strain	97%	AY212583.1	Uncultured bacterium clone 133ds10	99%	Kingdom.Eukaryota; Supergroup.Stramenopiles; Phylum.Ochrophyta; Class.Bacillariophyta; Subclass.Bacillariophyta_X
	FJ002185.1	Pennate diatom sp. CCAP 1008/1 16S	97%	MG715848.1	Uncultured bacterium clone 293	98%	
	HM449710.1	Navicula minima 12S ribosomal RNA	97%	JF929325.1	Uncultured cyanobacterium clone CMMG12	98%	
30	LN735382.3	Fragilaria sp. RCC2508 chloroplast	99%	KC246081.1	Uncultured cyanobacterium clone XSLA025	99%	Kingdom.Eukaryota; Supergroup.Stramenopiles; Phylum.Ochrophyta; Class.Bacillariophyta
	LN735323.3	Synedropsis sp. RCC2043 chloroplast	99%	JQ654955.1	Uncultured bacterium clone lagoon_D14	99%	
	FJ002235.1	Synedra hyperborea isolate C44 16S	99%	EU290435.1	Uncultured bacterium clone Tc48Tet1mesTet2ect	99%	
104	KT952293.1	Pinnularia sp. U-strain	97%	AY212583.1	Uncultured bacterium clone 133ds10	99%	Kingdom.Eukaryota; Supergroup.Stramenopiles; Phylum.Ochrophyta; Class.Bacillariophyta; Subclass.Bacillariophyta_X
	FJ002185.1	Pennate diatom sp. CCAP 1008/1	97%	MN156759.1	Uncultured bacterium clone A204	97%	
	HM449710.1	Navicula minima 12S ribosomal RNA	97%	JF280491.1	Uncultured bacterium clone GBX-B-COQ1-157	97%	
738	LN735309.2	Psammodictyon sp. RCC1970 chloroplast	99%	KP076635.1	Uncultured bacterium clone M8UC_PoM_110m_20	99%	Kingdom.Eukaryota; Supergroup.Stramenopiles; Phylum.Ochrophyta; Class.Bacillariophyta; Subclass.Bacillariophyta_X; Order.Surirellales; Suborder.Surirellales_X; Family.Surirellaceae; Genus.Psammodictyon; Species.Psammodictyon
	KY498708.1	Glabratella patelliformis isolate GP446-20	99%	JN986365.1	Uncultured bacterium clone U1370-196	99%	
	KY498705.1	Glabratella patelliformis isolate GP446-16	99%	JF272054.1	Uncultured bacterium clone 8M73	99%	

2769	KY498709.1	Angulodiscorbis quadrangularis isolate AQ159-89	100%	KY498709.1	Angulodiscorbis quadrangularis isolate AQ159-89	100%	Kingdom.Eukaryota; Supergroup.Stramenopiles; Phylum.Ochrophyta; Class.Bacillariophyta; Subclass.Bacillariophyta_X; Order.Naviculales; Suborder.Naviculales_X; Family.Naviculaceae; Genus.Navicula; Species.Navicula
	KY498706.1	Glabratella patelliformis isolate GP446-17	100%	KY498706.1	Glabratella patelliformis isolate GP446-17	100%	
	KP792485.1	Planoglabratella opercularis isolate GO863-27	100%	MF361026.1	Uncultured bacterium clone C11	100%	
4485	AF277540.1	Diatom sp. ARCTIC.149	98%	MF451026.1	Uncultured bacterium clone OTU1470	99%	Kingdom.Eukaryota; Supergroup.Stramenopiles; Phylum.Ochrophyta; Class.Bacillariophyta; Subclass.Bacillariophyta_X
	AF277476.1	Diatom sp. SIC.42333	98%	MH819045.1	Uncultured diatom clone H1910-16S_42	99%	
	MK045450.1	Halamphora americana chloroplast	98%	MH819039.1	Uncultured diatom clone H1910-16S_35	99%	
4668	LN735393.3	Bacillaria paxillifer chloroplast	98%	FJ355395.1	Uncultured organism clone 051011_S3_142	99%	Kingdom.Eukaryota; Supergroup.Stramenopiles; Phylum.Ochrophyta; Class.Bacillariophyta; Subclass.Bacillariophyta_X
	FJ002242.1	Leyanella arenaria isolate C70	98%	MH818908.1	Uncultured diatom clone H1724-16S_07	98%	
	FJ002223.1	Cylindrotheca closterium isolate C16	98%	KJ811885.1	Uncultured bacterium clone 0727N7_3_2_F09838	98%	
11469	FJ002185.1	Pennate diatom sp. CCAP 1008/1	98%	MN156759.1	Uncultured bacterium clone A204	98%	Kingdom.Eukaryota; Supergroup.Stramenopiles; Phylum.Ochrophyta; Class.Bacillariophyta; Subclass.Bacillariophyta_X
	MK045450.1	Halamphora americana chloroplast	98%	MF558965.1	Uncultured bacterium clone 3383	98%	
	NC_037997.1	1 Plagiogrammopsis vanheurckii chloroplast	98%	KT013522.1	Uncultured prokaryote clone OTU_214	98%	
21053	JQ088178.1	Synedra acus chloroplast	99%	LC065762.1	Uncultured bacterium gene	99%	Kingdom.Eukaryota; Supergroup.Stramenopiles; Phylum.Ochrophyta; Class.Bacillariophyta
	KP792487.1	Bacillariophyta sp. 867-32	98%	LC065737.1	Uncultured bacterium gene	99%	
	KP792478.1	Planoglabratella opercularis isolate GO_m25-21	98%	LC065719.1	Uncultured bacterium gene	99%	

Supplemental Table 5.3. 16S run details.

Run	Sample	# Raw Sequences	# Sequences Passed Bioinformatic Pipeline	# Bacterial Sequences	# Chloroplast Sequences
SRR10445439	PU1.1	78165	67948	51857	7969
SRR10445438	PU1.2	91289	74172	48160	8748
SRR10445327	PU1.3	42913	38539	27139	3576
SRR10445300	PU1.4	91263	80839	55393	10003
SRR10445289	PU1.5	72377	65614	49447	7221
SRR10445278	PU1.6	47003	42401	33267	3512
SRR10445267	PU1.7	101797	89104	75321	6719
SRR10445256	PU1.8	72778	65419	52433	4936
SRR10445245	PU1.9	53200	48655	38977	3801
SRR10445283	B1.1	119847	115693	27983	38307
SRR10445282	B1.2	127315	122360	30098	41624
SRR10445281	B1.3	70876	66565	25999	21364
SRR10445280	B1.4	83957	75345	31300	19875
SRR10445279	B1.5	66328	59751	29722	14772
SRR10445277	B1.6	91488	82731	28450	25221
SRR10445276	B1.7	93714	84260	37484	24192
SRR10445275	B1.8	54899	50597	21857	14114
SRR10445274	B1.9	80124	73719	26569	21582
SRR10445234	PU2.1	79822	69022	61733	3805
SRR10445437	PU2.2	88927	76929	67725	4994
SRR10445426	PU2.3	38383	34123	28194	2420
SRR10445415	PU2.4	68804	61556	54525	2423
SRR10445404	PU2.5	54760	49614	36292	4359
SRR10445393	PU2.6	101409	89027	66175	6842
SRR10445382	PU2.7	76671	66916	44075	6313
SRR10445371	PU2.8	59575	52716	38668	3380
SRR10445360	PU2.9	87734	77461	58691	5320
SRR10445273	B2.1	85632	74360	45159	22613
SRR10445272	B2.2	140376	135323	39286	31235
SRR10445271	B2.3	84910	79845	25989	19284
SRR10445270	B2.4	87462	80308	42808	9275
SRR10445269	B2.5	43006	39740	21649	6339
SRR10445268	B2.6	80378	73944	35514	12202
SRR10445266	B2.7	104446	94045	52996	13639
SRR10445265	B2.8	47441	42881	29130	5072
SRR10445264	B2.9	93118	83607	52204	11756
SRR10445349	PD3.1	83657	77145	50451	17390
SRR10445338	PD3.2	86025	77829	49790	17358
SRR10445326	PD3.3	70548	63421	41422	14315
SRR10445315	PD3.4	72556	65427	38002	13341
SRR10445308	PD3.5	55848	50356	36195	6409

SRR10445307	PD3.6	38933	35068	24556	3777
SRR10445306	PD3.7	78893	68971	48865	9081
SRR10445305	PD3.8	50987	45309	35741	5040
SRR10445304	PD3.9	64573	57215	45033	6432
SRR10445263	B3.1	149850	143532	30018	41579
SRR10445262	B3.2	116983	112290	33424	31191
SRR10445261	B3.3	77835	72960	24014	21179
SRR10445260	B3.4	93984	87248	36254	17773
SRR10445259	B3.5	48034	44540	19247	7853
SRR10445258	B3.6	72003	64964	36083	10654
SRR10445257	B3.7	84612	76552	39651	12857
SRR10445255	B3.8	50314	44313	36226	3438
SRR10445254	B3.9	63530	56346	42711	6446
SRR10445303	PD4.1	91903	81188	59205	10994
SRR10445302	PD4.2	89333	79620	54015	12438
SRR10445301	PD4.3	86462	75228	54183	11341
SRR10445299	PD4.4	70948	64267	42334	13503
SRR10445298	PD4.5	51315	45519	31361	6807
SRR10445297	PD4.6	54692	47664	29873	10899
SRR10445296	PD4.7	80915	72313	52252	9152
SRR10445295	PD4.8	52653	47845	36488	5816
SRR10445294	PD4.9	75777	67837	41810	10646
SRR10445293	PD5.1	92877	80721	50936	16247
SRR10445292	PD5.2	89505	80119	45125	15453
SRR10445291	PD5.3	50824	44806	28685	6008
SRR10445290	PD5.4	63143	54853	33028	8921
SRR10445288	PD5.5	58374	51416	33046	7726
SRR10445287	PD5.6	34222	30175	20933	3839
SRR10445286	PD5.7	62221	54392	37302	7395
SRR10445285	PD5.8	57934	49948	34432	7651
SRR10445284	PD5.9	66640	59165	31900	10539

Supplemental Table 5.4. PhytoREF taxonomy and percent homology.

OTU	PhytoREF Taxonomy	Percent homology
1	Kingdom.Eukaryota;Supergroup.Stramenopiles;Phylum.Ochrophyta;Class.Bacillariophyta;Subclass.Bacillariophyta_X;Order.Naviculales;Suborder.Naviculales_X	0.71
6	Kingdom.Eukaryota;Supergroup.Stramenopiles;Phylum.Ochrophyta;Class.Bacillariophyta;Subclass.Bacillariophyta_X;Order.Chaetocerotales;Suborder.Chaetocerotales_X;Family.Chaetocerotaceae;Genus.Chaetoceros;Species.Chaetoceros	0.89
8	Kingdom.Eukaryota;Supergroup.Stramenopiles;Phylum.Ochrophyta;Class.Bacillariophyta;Subclass.Bacillariophyta_X	0.85
19	Kingdom.Eukaryota;Supergroup.Stramenopiles;Phylum.Ochrophyta;Class.Bacillariophyta;Subclass.Bacillariophyta_X	0.83
30	Kingdom.Eukaryota;Supergroup.Stramenopiles;Phylum.Ochrophyta;Class.Bacillariophyta	1.00
33	Kingdom.Eukaryota;Supergroup.Stramenopiles;Phylum.Ochrophyta;Class.Bacillariophyta;Subclass.Bacillariophyta_X	0.78
42	Kingdom.Eukaryota;Supergroup.Stramenopiles;Phylum.Ochrophyta;Class.Bacillariophyta;Subclass.Bacillariophyta_X;Order.Naviculales;Suborder.Naviculales_X	0.72
88	Kingdom.Eukaryota;Supergroup.Stramenopiles;Phylum.Ochrophyta;Class.Bacillariophyta;Subclass.Bacillariophyta_X;Order.Bacillariophyta_XX;Suborder.Bacillariophyta_XXX	0.98
89	Kingdom.Eukaryota;Supergroup.Stramenopiles;Phylum.Ochrophyta;Class.Bacillariophyta;Subclass.Bacillariophyta_X	0.90
100	Kingdom.Eukaryota;Supergroup.Stramenopiles;Phylum.Ochrophyta;Class.Bacillariophyta;Subclass.Bacillariophyta_X	0.82
102	Kingdom.Eukaryota;Supergroup.Stramenopiles;Phylum.Ochrophyta;Class.Bacillariophyta	1.00
104	Kingdom.Eukaryota;Supergroup.Stramenopiles;Phylum.Ochrophyta;Class.Bacillariophyta;Subclass.Bacillariophyta_X	0.88
166	Kingdom.Eukaryota;Supergroup.Stramenopiles;Phylum.Ochrophyta;Class.Bacillariophyta	1.00
230	Kingdom.Eukaryota;Supergroup.Stramenopiles;Phylum.Ochrophyta;Class.Bacillariophyta;Subclass.Bacillariophyta_X;Order.Bacillariophyta_XX;Suborder.Bacillariophyta_XXX	0.97
342	Kingdom.Eukaryota;Supergroup.Stramenopiles;Phylum.Ochrophyta;Class.Bacillariophyta;Subclass.Bacillariophyta_X	0.79
357	Kingdom.Eukaryota;Supergroup.Stramenopiles;Phylum.Ochrophyta;Class.Bacillariophyta	1.00
479	Kingdom.Eukaryota;Supergroup.Stramenopiles;Phylum.Ochrophyta;Class.Bacillariophyta;Subclass.Bacillariophyta_X	0.73
642	Kingdom.Eukaryota;Supergroup.Stramenopiles;Phylum.Ochrophyta;Class.Bacillariophyta;Subclass.Bacillariophyta_X	0.84
738	Kingdom.Eukaryota;Supergroup.Stramenopiles;Phylum.Ochrophyta;Class.Bacillariophyta;Subclass.Bacillariophyta_X;Order.Surirellales;Suborder.Surirellales_X;Family.Surirellaceae;Genus.Psammodictyon;Species.Psammodictyon	0.89
1221	Kingdom.Eukaryota;Supergroup.Stramenopiles;Phylum.Ochrophyta;Class.Bacillariophyta;Subclass.Bacillariophyta_X	0.82
1364	Kingdom.Eukaryota;Supergroup.Stramenopiles;Phylum.Ochrophyta;Class.Bacillariophyta;Subclass.Bacillariophyta_X	0.88
1714	Kingdom.Eukaryota;Supergroup.Stramenopiles;Phylum.Ochrophyta;Class.Bacillariophyta;Subclass.Bacillariophyta_X	0.80
1928	Kingdom.Eukaryota;Supergroup.Stramenopiles;Phylum.Ochrophyta;Class.Bacillariophyta;Subclass.Bacillariophyta_X	0.77
2482	Kingdom.Eukaryota;Supergroup.Stramenopiles;Phylum.Ochrophyta;Class.Bacillariophyta;Subclass.Bacillariophyta_X	0.83
2769	Kingdom.Eukaryota;Supergroup.Stramenopiles;Phylum.Ochrophyta;Class.Bacillariophyta;Subclass.Bacillariophyta_X;Order.Naviculales;Suborder.Naviculales_X;Family.Naviculaceae;Genus.Navicula;Species.Navicula	0.88
3610	Kingdom.Eukaryota;Supergroup.Stramenopiles;Phylum.Ochrophyta;Class.Bacillariophyta	1.00
3866	Kingdom.Eukaryota;Supergroup.Stramenopiles;Phylum.Ochrophyta;Class.Bacillariophyta	1.00
4471	Kingdom.Eukaryota;Supergroup.Stramenopiles;Phylum.Ochrophyta;Class.Bacillariophyta	1.00
4485	Kingdom.Eukaryota;Supergroup.Stramenopiles;Phylum.Ochrophyta;Class.Bacillariophyta;Subclass.Bacillariophyta_X	0.93
4583	Kingdom.Eukaryota;Supergroup.Stramenopiles;Phylum.Ochrophyta;Class.Bacillariophyta;Subclass.Bacillariophyta_X	0.80
4668	Kingdom.Eukaryota;Supergroup.Stramenopiles;Phylum.Ochrophyta;Class.Bacillariophyta;Subclass.Bacillariophyta_X	0.72
5322	Kingdom.Eukaryota;Supergroup.Stramenopiles;Phylum.Ochrophyta;Class.Bacillariophyta;Subclass.Bacillariophyta_X	0.85
5560	Kingdom.Eukaryota;Supergroup.Stramenopiles;Phylum.Ochrophyta;Class.Bacillariophyta	0.82
6059	Kingdom.Eukaryota;Supergroup.Stramenopiles;Phylum.Ochrophyta;Class.Bacillariophyta;Subclass.Bacillariophyta_X	0.93
6621	Kingdom.Eukaryota;Supergroup.Stramenopiles;Phylum.Ochrophyta;Class.Bacillariophyta;Subclass.Bacillariophyta_X	0.78
6666	Kingdom.Eukaryota;Supergroup.Stramenopiles;Phylum.Ochrophyta;Class.Bacillariophyta	1.00

6829	Kingdom.Eukaryota;Supergroup.Stramenopiles;Phylum.Ochrophyta;Class.Bacillariophyta;Subclass.Bacillariophyta_X	0.85
6995	Kingdom.Eukaryota;Supergroup.Stramenopiles;Phylum.Ochrophyta;Class.Bacillariophyta;Subclass.Bacillariophyta_X	0.73
7363	Kingdom.Eukaryota;Supergroup.Stramenopiles;Phylum.Ochrophyta;Class.Bacillariophyta	1.00
7592	Kingdom.Eukaryota;Supergroup.Stramenopiles;Phylum.Ochrophyta;Class.Bacillariophyta	1.00
7757	Kingdom.Eukaryota;Supergroup.Stramenopiles;Phylum.Ochrophyta;Class.Bacillariophyta	0.95
8008	Kingdom.Eukaryota;Supergroup.Stramenopiles;Phylum.Ochrophyta;Class.Bacillariophyta	1.00
9868	Kingdom.Eukaryota;Supergroup.Stramenopiles;Phylum.Ochrophyta;Class.Bacillariophyta;Subclass.Bacillariophyta_X	0.78
10225	Kingdom.Eukaryota;Supergroup.Stramenopiles;Phylum.Ochrophyta;Class.Bacillariophyta;Subclass.Bacillariophyta_X	0.88
10243	Kingdom.Eukaryota;Supergroup.Stramenopiles;Phylum.Ochrophyta;Class.Bacillariophyta	1.00
10583	Kingdom.Eukaryota;Supergroup.Stramenopiles;Phylum.Ochrophyta;Class.Bacillariophyta;Subclass.Bacillariophyta_X;Order.Surirellales;Suborder.Surirellales_X;Family.Surirellaceae;Genus.Psammodictyon;Species.Psammodictyon	0.75
11368	Kingdom.Eukaryota;Supergroup.Stramenopiles;Phylum.Ochrophyta;Class.Bacillariophyta;Subclass.Bacillariophyta_X	0.89
11469	Kingdom.Eukaryota;Supergroup.Stramenopiles;Phylum.Ochrophyta;Class.Bacillariophyta;Subclass.Bacillariophyta_X	0.84
11986	Kingdom.Eukaryota;Supergroup.Stramenopiles;Phylum.Ochrophyta;Class.Bacillariophyta;Subclass.Bacillariophyta_X	0.74
12097	Kingdom.Eukaryota;Supergroup.Stramenopiles;Phylum.Ochrophyta;Class.Bacillariophyta;Subclass.Bacillariophyta_X	0.85
12198	Kingdom.Eukaryota;Supergroup.Stramenopiles;Phylum.Ochrophyta;Class.Bacillariophyta	1.00
12882	Kingdom.Eukaryota;Supergroup.Stramenopiles;Phylum.Ochrophyta;Class.Bacillariophyta	1.00
13370	Kingdom.Eukaryota;Supergroup.Stramenopiles;Phylum.Ochrophyta;Class.Bacillariophyta;Subclass.Bacillariophyta_X	0.79
13578	Kingdom.Eukaryota;Supergroup.Stramenopiles;Phylum.Ochrophyta;Class.Bacillariophyta;Subclass.Bacillariophyta_X	0.86
13693	Kingdom.Eukaryota;Supergroup.Stramenopiles;Phylum.Ochrophyta;Class.Bacillariophyta;Subclass.Bacillariophyta_X	0.81
13717	Kingdom.Eukaryota;Supergroup.Stramenopiles;Phylum.Ochrophyta;Class.Bacillariophyta	1.00
15103	Kingdom.Eukaryota;Supergroup.Stramenopiles;Phylum.Ochrophyta;Class.Bacillariophyta	0.92
15442	Kingdom.Eukaryota;Supergroup.Stramenopiles;Phylum.Ochrophyta;Class.Bacillariophyta;Subclass.Bacillariophyta_X	0.92
15805	Kingdom.Eukaryota;Supergroup.Stramenopiles;Phylum.Ochrophyta;Class.Bacillariophyta;Subclass.Bacillariophyta_X	0.83
16834	Kingdom.Eukaryota;Supergroup.Stramenopiles;Phylum.Ochrophyta;Class.Bacillariophyta	0.79
17229	Kingdom.Eukaryota;Supergroup.Stramenopiles;Phylum.Ochrophyta;Class.Bacillariophyta;Subclass.Bacillariophyta_X	0.76
17631	Kingdom.Eukaryota;Supergroup.Stramenopiles;Phylum.Ochrophyta;Class.Bacillariophyta;Subclass.Bacillariophyta_X	0.77
18800	Kingdom.Eukaryota;Supergroup.Stramenopiles;Phylum.Ochrophyta;Class.Bacillariophyta;Subclass.Bacillariophyta_X	0.74
19256	Kingdom.Eukaryota;Supergroup.Stramenopiles;Phylum.Ochrophyta;Class.Bacillariophyta	1.00
20284	Kingdom.Eukaryota;Supergroup.Stramenopiles;Phylum.Ochrophyta;Class.Bacillariophyta;Subclass.Bacillariophyta_X	0.84
20305	Kingdom.Eukaryota;Supergroup.Stramenopiles;Phylum.Ochrophyta;Class.Bacillariophyta	1.00
20338	Kingdom.Eukaryota;Supergroup.Stramenopiles;Phylum.Ochrophyta;Class.Bacillariophyta;Subclass.Bacillariophyta_X	0.83
21053	Kingdom.Eukaryota;Supergroup.Stramenopiles;Phylum.Ochrophyta;Class.Bacillariophyta	1.00
21207	Kingdom.Eukaryota;Supergroup.Stramenopiles;Phylum.Ochrophyta;Class.Bacillariophyta;Subclass.Bacillariophyta_X	0.94
21213	Kingdom.Eukaryota;Supergroup.Stramenopiles;Phylum.Ochrophyta;Class.Bacillariophyta	0.80
21724	Kingdom.Eukaryota;Supergroup.Stramenopiles;Phylum.Ochrophyta;Class.Bacillariophyta;Subclass.Bacillariophyta_X	0.88

Concluding Remarks

In expressing regret over his role in a large dam project, former US senator Barry Goldwater concluded, "When you dam a river you always lose something."(Postel & Richter, 2003). In the case of Painkalac Creek, the losses include hydrologic functionality, habitat connectivity and ecological integrity. Prior to the dam construction, the downstream reach of Painkalac Creek reportedly supported platypus, freshwater mussels and blackfish (Graeme McKenzie, personal communication 16 January 2018) but it is now deeply incised, sometimes anoxic and the only freshwater fish that are frequently encountered are common galaxiids. Upon inspection of the logged dissolved oxygen data from this study, a stream ecologist described the condition of Painkalac Creek as the worst continuous record he has ever seen.

The altered and disconnected hydrology is reflected in the distinct stream microbiome below Painkalac Dam. There is currently no rubric for scoring stream health based on the microbiome but metabarcoding offers exciting opportunities to characterise the stream biofilm community and connect biological community data with environmental conditions. The 16S amplicon, in particular, is a promising tool for considering important groups within a single assay. There are also exciting opportunities to investigate aquatic fungi as bioindicators in freshwater ecosystems.

Aside from the warming effect, the biotic and abiotic parameters measured in this study did not shift in response to the environmental flows but there may have been unmeasured benefits. One of the goals of the environmental flow prescription was the reconnection of isolated pools in the downstream reach but because the reach has not

become disconnected since the withdrawals ceased, the flow pulses did not provide this intended benefit. The flow pulses may have supported the dispersal of fish or macroinvertebrates throughout the downstream reach but that would be impossible to know without a targeted monitoring campaign. Beyond the stream channel, there may have been benefits to riparian vegetation or recharge to groundwater, but the short duration and amplitude of the environmental flows make broad-scale changes unlikely.

A radical but fundamental question is whether Painkalac Dam is necessary? Painkalac Reservoir fills to capacity in a single storm event in most years so the sense of security that downstream residents have with regards to the control of the creek that is afforded by the reservoir is more perceived than actual. Quite the opposite may actually be true as climate change increases the probability of extreme events and the subsequent potential for dam failure. A fire in the catchment could increase peak flows and deliver a large volume of woody debris to the reservoir so the presence of the dam could be characterised as an increasing liability as the climate warms, the forest dries, and the dam ages. The reservoir cost-benefit accounting should also consider that almost 60% of the 160 ML/year that was previously consumed continues to be lost to evaporation each year as a result of the impoundment.

The removal of the dam that currently sits at the head of Painkalac Valley could reconnect native fish populations and restore a vital source of freshwater to sustain local wetlands. These wetlands could in-turn help to protect the residents of Aireys Inlet from natural boom and bust cycles by absorbing high flows and releasing them back to the stream during dry periods. These and other potential benefits of dam removal should be given critical consideration.

Successful stream restoration improves ecological condition and satisfies stakeholders (Palmer *et al.*, 2005) so the future management of Painkalac Creek needs to

include the community values that were not assessed as part of the environmental flow design process. Engagement with the Traditional Owners and completion of an Aboriginal Waterways survey would be good next steps in managing Painkalac Creek more holistically. Collectively, the local residents hold a vast natural history knowledge bank that has so far been underutilised in guiding water resource decision-making. Future management should be informed by this diverse knowledge and guided by the social, ecological, and spiritual values associated with Painkalac Creek.

References

Ackman R.G. (2002). The gas chromatograph in practical analyses of common and uncommon fatty acids for the 21st century. *Analytica Chimica Acta* **465**, 175–192. https://doi.org/10/c8dk2q

Adl S.M., Bass D., Lane C.E., Lukeš J., Schoch C.L., Smirnov A., *et al.* (2019). Revisions to the Classification, Nomenclature, and Diversity of Eukaryotes. *Journal of Eukaryotic Microbiology* **66**, 4–119. https://doi.org/10/gfx825

Adl S.M., Simpson A.G.B., Lane C.E., Lukeš J., Bass D., Bowser S.S., *et al.* (2012). The Revised Classification of Eukaryotes. *Journal of Eukaryotic Microbiology* **59**, 429–514. https://doi.org/10/f4djnc

Ajani P.A., Larsson M.E., Woodcock S., Rubio A., Farrell H., Brett S., *et al.* (2020). Fifteen years of Pseudo-nitzschia in an Australian estuary, including the first potentially toxic P. delicatissima bloom in the southern hemisphere. *Estuarine, Coastal and Shelf Science* **236**, 106651. https://doi.org/10/ggtjjz

Akinwole P.O., Lefevre E., Powell M.J. & Findlay R.H. (2014). Unique Odd-Chain Polyenoic Phospholipid Fatty Acids Present in Chytrid Fungi. *Lipids* **49**, 933–942. https://doi.org/10/f6f4nw

Alcamán-Arias M.E., Fuentes-Alburquenque S., Vergara-Barros P., Cifuentes-Anticevic J., Verdugo J., Polz M., *et al.* (2021). Coastal Bacterial Community Response to Glacier Melting in the Western Antarctic Peninsula. *Microorganisms* **9**, 88. https://doi.org/10/ghzvzf

Allen G.R., Midgley S.H. & Allen M. (2002). *Field guide to the freshwater fishes of Australia.* Western Australian Museum.

Allen R.G., Dhungel R., Dhungana B., Huntington J., Kilic A. & Morton C. (2021). Conditioning point and gridded weather data under aridity conditions for calculation of reference evapotranspiration. *Agricultural Water Management* **245**, 106531. https://doi.org/10/gj993g

American Public Health Association (APHA) (1995). *Standard Methods for the Examination of Water and Waste Water*, 19th edn. American Public Health Association, Washington, DC, USA.

Anderson M., Gorley R.N. & Clarke R.K. (2008). *Permanova+ for primer: Guide to software and statistical methods*. Primer-E Limited.

Anderson M.J. (2001). A new method for non-parametric multivariate analysis of variance. *Austral Ecology* **26**, 32–46. https://doi.org/10.1046/j.1442-9993.2001.01070.x

Apothéloz-Perret-Gentil L., Cordonier A., Straub F., Iseli J., Esling P. & Pawlowski J. (2017). Taxonomy-free molecular diatom index for high-throughput eDNA biomonitoring. *Molecular Ecology Resources* **17**, 1231–1242. https://doi.org/10/f935fp

Apprill A., McNally S., Parsons R. & Weber L. (2015). Minor revision to V4 region SSU rRNA 806R gene primer greatly increases detection of SAR11 bacterioplankton. *Aquatic Microbial Ecology* **75**, 129–137. https://doi.org/10/gc96tb

Arthington A.H. & Pusey B.J. (2003). Flow restoration and protection in Australian rivers. *River Research and Applications* **19**, 377–395. https://doi.org/10.1002/rra.745

Arts M.T., Ackman R.G. & Holub B.J. (2001). “Essential fatty acids” in aquatic ecosystems: a crucial link between diet and human health and evolution. *Canadian Journal of Fisheries and Aquatic Sciences* **58**, 122–137. https://doi.org/10.1139/cjfas-58-1-122

Bai Y., Wang Q., Liao K., Jian Z., Zhao C. & Qu J. (2018). Fungal Community as a Bioindicator to Reflect Anthropogenic Activities in a River Ecosystem. *Frontiers in Microbiology* **9**. https://doi.org/10/ggzxk2

Baird D.J. & Hajibabaei M. (2012). *Biomonitoring 2.0: a new paradigm in ecosystem assessment made possible by next-generation DNA sequencing*.

Bärlocher F., Stewart M. & Ryder D.S. (2011). Analyzing aquatic fungal communities in Australia: impacts of sample incubation and geographic distance of streams. *Czech Mycology* **63**, 113–132. https://doi.org/10/gg36x5

Barwon Water (2016). *Watering proposal for Painkalac Creek*. Barwon Water.

Battin T.J., Besemer K., Bengtsson M.M., Romani A.M. & Packmann A.I. (2016). The ecology and biogeochemistry of stream biofilms. *Nature Reviews Microbiology* **14**, 251–263. https://doi.org/10/f3s4rk

Beck M.W., O’Hara C., Lowndes J.S.S., Mazor R.D., Theroux S., Gillett D.J., *et al.* (2020). The importance of open science for biological assessment of aquatic environments. *PeerJ* **8**, e9539. https://doi.org/10/gjtbj9

Bellinger E.G. & Sigee D.C. (2015). *Freshwater Algae : Identification, Enumeration and Use As Bioindicators*. John Wiley & Sons, Incorporated, Hoboken, United Kingdom.

Bennke C.M., Pollehne F., Müller A., Hansen R., Kreikemeyer B. & Labrenz M. (2018). The distribution of phytoplankton in the Baltic Sea assessed by a prokaryotic 16S rRNA gene primer system. *Journal of Plankton Research* **40**, 244–254. https://doi.org/10.1093/plankt/fby008

Berg G., Rybakova D., Fischer D., Cernava T., Vergès M.-C.C., Charles T., *et al.* (2020). Microbiome definition re-visited: old concepts and new challenges. *Microbiome* **8**. https://doi.org/10/gg3r87

Biggs B.J., Kilroy C., New Zealand, & Ministry for the Environment (2000). *Stream periphyton monitoring manual*. NIWA, Christchurch, N.Z.

Billing P. (1983). *Otways Fire No 22 - 1982/83. Aspects of Fire Behaviour*. Fire Research Branch.

Boechat I.G., Krueger A., Giani A., Figueredo C.C. & Guecker B. (2011). Agricultural land-use affects the nutritional quality of stream microbial communities. *Fems Microbiology Ecology* **77**, 568–576. https://doi.org/10.1111/j.1574-6941.2011.01137.x

Bokulich N.A., Dillon M.R., Bolyen E., Kaehler B.D., Huttley G.A. & Caporaso J.G. (2018). q2-sample-classifier: machine-learning tools for microbiome classification and regression. *Journal of open research software* **3**. https://doi.org/10/gghgbc

BOM (2020a). Australian Bureau of Meterology Climate Data. *Rainfall - total*

BOM (2020b). Australian Bureau of Meterology Climate Data. *Temperature - maximum*

Bonada N., Prat N., Resh V.H. & Statzner B. (2006). Developments in aquatic insect biomonitoring: a comparative analysis of recent approaches. *Annu Rev Entomol* **51**. https://doi.org/10.1146/annurev.ento.51.110104.151124

Bond N. (2015a). Hydrologic time-series summary tool

Bond N. (2015b). hydrostats: Hydrologic indices for daily time series data. *R package version 0.2* **4**, 16

Bond N.R. & Kennard M.J. (2017). Prediction of hydrologic characteristics for ungauged catchments to support hydroecological modeling. *Water Resources Research* **53**, 8781–8794. https://doi.org/10/gcp44d

Boulton A.J. & Boon P.I. (1991). A review of methodology used to measure leaf litter decomposition in lotic environments: Time to turn over an old leaf? *Marine and Freshwater Research* **42**, 1–43. https://doi.org/10/dc8b8f

ter Braak C.J.F. & van Dame H. (1989). Inferring pH from diatoms: a comparison of old and new calibration methods. *Hydrobiologia* **178**, 209–223. https://doi.org/10/bvmb32

Bradley I.M., Pinto A.J. & Guest J.S. (2016). Design and Evaluation of Illumina MiSeq-Compatible, 18S rRNA Gene-Specific Primers for Improved Characterization of Mixed Phototrophic Communities. *Applied and Environmental Microbiology* **82**, 5878–5891. https://doi.org/10/f85b3m

Bray J.R. & Curtis J.T. (1957). An Ordination of the Upland Forest Communities of Southern Wisconsin. *Ecological Monographs* **27**, 326–349. https://doi.org/10/dcm5hn

Brinkmann N., Hodač L., Mohr K.I., Hodačová A., Jahn R., Ramm J., *et al.* (2015). Cyanobacteria and Diatoms in Biofilms of Two Karstic Streams in Germany and Changes of Their Communities Along Calcite Saturation Gradients. *Geomicrobiology Journal* **32**, 255–274. https://doi.org/10/gf3372

Brisbane Declaration (2007). In: *Environmental Flows are Essential for Freshwater Ecosystem Health and Human Well-Being.* Brisbane, Australia.

Brooks K.N., Ffolliott P.F. & Magner J.A. (2012). *Hydrology and the Management of Watersheds*. John Wiley & Sons.

Brunner P., Simmons C.T. & Cook P.G. (2009). Spatial and temporal aspects of the transition from connection to disconnection between rivers, lakes and groundwater. *Journal of Hydrology* **376**, 159–169. https://doi.org/10/frbb67

Bunn S.E., Abal E.G., Smith M.J., Choy S.C., Fellows C.S., Harch B.D., *et al.* (2010). Integration of science and monitoring of river ecosystem health to guide investments in catchment protection and rehabilitation. *Freshwater Biology* **55**, 223–240. https://doi.org/10/bg7q3f

Bunn S.E. & Arthington A.H. (2002). Basic Principles and Ecological Consequences of Altered Flow Regimes for Aquatic Biodiversity. *Environmental Management* **30**, 492–507. https://doi.org/10.1007/s00267-002-2737-0

Burger J. (2006). Bioindicators: A Review of Their Use in the Environmental Literature 1970–2005. *Environmental Bioindicators* **1**, 136–144. https://doi.org/10/d57z3x

Burgoa Cardás J., Deconinck D., Márquez I., Peón Torre P., Garcia-Vazquez E. & Machado-Schiaffino G. (2020). New eDNA based tool applied to the specific detection and monitoring of the endangered European eel. *Biological Conservation* **250**, 108750. https://doi.org/10.1016/j.biocon.2020.108750

Burns A. & Ryder D.S. (2001). Potential for biofilms as biological indicators in Australian riverine systems. *Ecological Management and Restoration* **2**, 53–64. https://doi.org/10.1046/j.1442-8903.2001.00069.x

Burns A. & Walker K.F. (2000). Effects of water level regulation on algal biofilms in the River Murray, South Australia. *Regulated Rivers: Research & Management* **16**, 433–444. https://doi.org/10.1002/1099-1646(200009/10)16:5<433::AID-RRR595>3.0.CO;2-V

Cai W. & Jones R. (2005). Response of potential evaporation to climate variability and change: what GCMs simulate. In: *Pan Evaporation: An Example of the Detection*

and Attribution of Trends in Climate Variables, Proceedings of a workshop, Australian Academy of Science. pp. 71–78. Gifford RM, Australia.

Charles D., Kelly M., Stevenson R., Poikane S., Theroux S., Zgrundo A., *et al.* (2021). Benthic algae assessments in the EU and the US: Striving for consistency in the face of great ecological diversity. *Ecological Indicators* **121**. https://doi.org/10/gjtbhr

Charles S.P., Bari M.A., Kitsios A. & Bates B.C. (2007). Effect of GCM bias on downscaled precipitation and runoff projections for the Serpentine catchment, Western Australia. *International Journal of Climatology* **27**, 1673–1690. https://doi.org/10/b4x4s7

Chessman B.C., Bate N., Gell P.A. & Newall P. (2007). A diatom species index for bioassessment of Australian rivers. *Marine and Freshwater Research* **58**, 542. https://doi.org/10/d6snqm

Chester H. & Norris R. (2006). Dams and flow in the Cotter River, Australia: Effects on instream trophic structure and benthic metabolism. *Hydrobiologia* **572**, 275–286. https://doi.org/10.1007/s10750-006-0219-8

Chiew F., Potter N., Vaze J., Petheram C., Zhang L., Teng J., *et al.* (2014). Observed hydrologic non-stationarity in far south-eastern Australia: Implications for modelling and prediction. *Stochastic Environmental Research and Risk Assessment* **28**. https://doi.org/10/f5kk7j

Chiew F., Wang Q.J., McConachy F., James R., Wright W. & deHoedt G. (2002). Evapotranspiration maps for Australia. In: *Water Challenge: Balancing the Risks: Hydrology and Water Resources Symposium 2002*. p. 167. Institution of Engineers, Australia.

Chiew F.H.S., Teng J., Vaze J., Post D.A., Perraud J.M., Kirono D.G.C., *et al.* (2009). Estimating climate change impact on runoff across southeast Australia: Method, results, and implications of the modeling method. *Water Resources Research* **45**. https://doi.org/10/dgdztz

Chiew F.H.S., Young W.J., Cai W. & Teng J. (2011). Current drought and future hydroclimate projections in southeast Australia and implications for water resources management. *Stochastic Environmental Research and Risk Assessment* **25**, 601–612. https://doi.org/10/brdbb2

Chonova T., Keck F., Labanowski J., Montuelle B., Rimet F. & Bouchez A. (2016). Separate treatment of hospital and urban wastewaters: A real scale comparison of effluents and their effect on microbial communities. *Science of The Total Environment* **542**, 965–975. https://doi.org/10/gf6rgh

Chonova T., Kurmayer R., Rimet F., Labanowski J., Vasselon V., Keck F., *et al.* (2019). Benthic Diatom Communities in an Alpine River Impacted by Waste Water Treatment Effluents as Revealed Using DNA Metabarcoding. *Frontiers in Microbiology* **10**. https://doi.org/10.3389/fmicb.2019.00653

Clarke K. & Warwick R. (2001). Change in Marine Communities: An Approach to Statistical Analysis and Interpretation. Primer-E Ltd: Plymouth, UK.

Clarke K.R. (1993). Non-parametric multivariate analyses of changes in community structure. *Australian journal of ecology* **18**, 117–143. https://doi.org/10/d7x85z

Clarke K.R. & Gorley R.N. (2006). PRIMER v6: user manual/tutorial, Primer E: Plymouth. *Plymouth Marine Laboratory, Plymouth, UK*

Clarke K.R. & Gorley R.N. (2015). PRIMER v7: User Manual. *Tutorial. PRIMER. Plymouth: Scientific Research Publish*

Clarke K.R., Tweedley J.R. & Valesini F.J. (2014). Simple shade plots aid better long-term choices of data pre-treatment in multivariate assemblage studies. *Journal of the Marine Biological Association of the United Kingdom* **94**, 1–16

Conlan J.A., Jones P.L., Turchini G.M., Hall M.R. & Francis D.S. (2014). Changes in the nutritional composition of captive early-mid stage Panulirus ornatus phyllosoma over ecdysis and larval development. *Aquaculture* **434**, 159–170. https://doi.org/10.1016/j.aquaculture.2014.07.030

Coron L., Andréassian V., Perrin C., Lerat J., Vaze J., Bourqui M., *et al.* (2012). Crash testing hydrological models in contrasted climate conditions: An experiment on 216 Australian catchments. *Water Resources Research* **48**. https://doi.org/10/ghvjzj

Costerton J. (1999). Introduction to biofilm. *International Journal of Antimicrobial Agents* **11**, 217–221. https://doi.org/10/c3nm7q

Couturier L.I.E., Michel L.N., Amaro T., Budge S.M., da Costa E., De Troch M., *et al.* (2020). State of art and best practices for fatty acid analysis in aquatic sciences. *ICES Journal of Marine Science* **77**, 2375–2395. https://doi.org/10/gjrqcz

Creer S., Deiner K., Frey S., Porazinska D., Taberlet P., Thomas W.K., *et al.* (2016). The ecologist's field guide to sequence-based identification of biodiversity. *Methods in Ecology and Evolution* **7**, 1008–1018. https://doi.org/10.1111/2041-210X.12574

Crosbie R.S., Jolly I.D., Leaney F.W. & Petheram C. (2010). Can the dataset of field based recharge estimates in Australia be used to predict recharge in data-poor areas? *Hydrology and Earth System Sciences* **14**, 2023–2038. https://doi.org/10/dcgfpx

Dafforn K.A., Baird D.J., Chariton A.A., Sun M.Y., Brown M.V., Simpson S.L., *et al.* (2014). Faster, Higher and Stronger? The Pros and Cons of Molecular Faunal Data for Assessing Ecosystem Condition. In: *Advances in Ecological Research*. pp. 1–40. Elsevier.

Dafforn K.A., Johnston E.L., Ferguson A., Humphrey C.L., Monk W., Nichols S.J., *et al.* (2016). Big data opportunities and challenges for assessing multiple stressors across scales in aquatic ecosystems. *Marine and Freshwater Research* **67**, 393. https://doi.org/10.1071/MF15108

Dalsgaard J., St John M., Kattner G., Muller-Navarra D. & Hagen W. (2003). Fatty acid trophic markers in the pelagic marine environment. In: *Advances in Marine Biology, Vol 46*. (Eds A.J. Southwards, P.A. Tyler, C.M. Young & L.A. Fuiman), pp. 225–340.

Dalu T., Galloway A.W.E., Richoux N.B. & Froneman P.W. (2016). Effects of substrate on essential fatty acids produced by phytobenthos in an austral temperate river system. *Freshwater Science* **35**, 1189–1201. https://doi.org/10.1086/688698

Davies P.M., Naiman R.J., Warfe D.M., Pettit N.E., Arthington A.H. & Bunn S.E. (2014). Flow-ecology relationships: Closing the loop on effective environmental flows. *Marine and Freshwater Research* **65**, 133–141. https://doi.org/10.1071/MF13110

Decelle J., Romac S., Stern R.F., Bendif E.M., Zingone A., Audic S., *et al.* (2015). PhytoREF: a reference database of the plastidial 16S rRNA gene of photosynthetic eukaryotes with curated taxonomy. *Molecular Ecology Resources* **15**, 1435–1445. https://doi.org/10.1111/1755-0998.12401

DELWP (2019). Department of Environment, Land, Water and Planning, Victoria. Groundwater resource reports. *Water and catchments*

DELWP (2016a). Department of Environment, Land, Water and Planning, Victoria. Water Measurement Information System

DELWP (2016b). Department of Environment, Land, Water and Planning, Victoria. Water Measurement Information System, State Observation Bore Network

Descy J.P. & Mouvet C. (1984). Impact of the Tihange nuclear power plant on the periphyton and the phytoplankton of the Meuse River (Belgium). *Hydrobiologia* **119**, 119–128. https://doi.org/10/cc2scx

Doeg T., Vietz G. & Boon P. (2008). *Environmental Flow Determination for Painkalac Creek- Final Recommendations*. Corangamite Catchment Mangement Authority.

Doeg T., Vietz G. & Boon P. (2007). *Environmental Flow Determination for Painkalac Creek: Site Paper*. Corangamite Catchment Mangement Authority.

Dooge J.C.I., Bruen M. & Parmentier B. (1999). A simple model for estimating the sensitivity of runoff to long-term changes in precipitation without a change in vegetation. *Advances in Water Resources* **23**, 153–163. https://doi.org/10/bdsr5r

DSE (2008). 1983 Season Wildfire Extent

Eiler A., Drakare S., Bertilsson S., Pernthaler J., Peura S., Rofner C., *et al.* (2013). Unveiling Distribution Patterns of Freshwater Phytoplankton by a Next Generation Sequencing Based Approach. *PLoS ONE* **8**, e53516. https://doi.org/10/f2zqd8

Erken M., Farrenschon N., Speckmann S., Arndt H. & Weitere M. (2012). Quantification of Individual Flagellate - Bacteria Interactions within Semi-natural Biofilms. *Protist* **163**, 632–642. https://doi.org/10/crxt2t

European Commission (2000). *EU Water Framework Directive*. Directive 2000/60/EC of the European Parliament and of the Council of 23rd October 2000. Establishing a framework for community action in the field of water policy.

Evans K.M., Wortley A.H. & Mann D.G. (2007). An Assessment of Potential Diatom "Barcode" Genes (cox1, rbcL, 18S and ITS rDNA) and their Effectiveness in Determining Relationships in Sellaphora (Bacillariophyta). *Protist* **158**, 349–364. https://doi.org/10/d4p9xk

Evans K.M., Wortley A.H., Simpson G.E., Chepurnov V.A. & Mann D.G. (2008). A molecular systematic approach to explore diversity within the Sellaphora pupula species complex (Bacillariophyta). *Journal of Phycology* **44**, 215–231. https://doi.org/10/dfw2m2

Falasco E. & Badino G. (2011). The Role of Environmental Factors in Shaping Diatom Frustule: Morphological Plasticity and Teratological Forms. In: *Diatoms: ecology and life cycle*. pp. 1–36. Nova Science Publishers, Inc., New York, NY.

Fish K.E. & Boxall J.B. (2018). Biofilm Microbiome (Re)Growth Dynamics in Drinking Water Distribution Systems Are Impacted by Chlorine Concentration. *Frontiers in Microbiology* **9**. https://doi.org/10/gfnpcz

Fleck J. (2015). The institutional hydrograph: New Mexico's Rio Grande in December. *jfleck at inkstain*

Forsyth D.A. & Ransome S.W. (1978). *A proposal for proclamation prepared for consideration by the Land Conservation Council*. Soil Conservation Authority, Kew, Victoria.

Friedman, Osterkamp W.R., Scott M.L. & Auble G.T. (1998). Downstream effects of dams on channel geometry and bottomland vegetation: Regional patterns in the great plains. *Wetlands* **18**, 619–633. https://doi.org/10/ct8k78

Frost A.J., Ramchurn A. & Oke A. (2017). Daily gridded evapotranspiration estimates for Australia. In: *22nd International Congress on Modelling and Simulation. MODSIM, Hobart, Tasmania, Australia*.

Gallant J., Wilson N., Dowling T., Read A. & Inskeep C. (2011). SRTM-derived 1 Second Digital Elevation Models Version 1.0. Record 1.

Galloway A.W.E. & Winder M. (2015). Partitioning the Relative Importance of Phylogeny and Environmental Conditions on Phytoplankton Fatty Acids. *Plos One* **10**, e0130053. https://doi.org/10.1371/journal.pone.0130053

Gan H.M., Szegedi E., Fersi R., Chebil S., Kovács L., Kawaguchi A., *et al.* (2019). Insight Into the Microbial Co-occurrence and Diversity of 73 Grapevine (Vitis vinifera) Crown Galls Collected Across the Northern Hemisphere. *Frontiers in Microbiology* **10**. https://doi.org/10/ggtcvv

Gardes M. & Bruns T.D. (1993). ITS primers with enhanced specificity for basidiomycetes - application to the identification of mycorrhizae and rusts. *Molecular Ecology* **2**, 113–118. https://doi.org/10/ffw4pk

Gasse F., Barker P., Gell P.A., Fritz S.C. & Chalie F. (1997). Diatom-inferred salinity in palaeolakes: An indirect tracer of climate change. *Quaternary Science Reviews* **16**, 547–563. https://doi.org/10/bt9bcx

Gell P.A. (1997). The Development of a Diatom Database for Inferring Lake Salinity, Western Victoria, Australia: Towards a Quantitative Approach for Reconstructing Past Climates. *Australian Journal of Botany* **45**, 389–423. https://doi.org/10/dwcbg3

Gell P.A. (2019). Watching the tide roll away – contested interpretations of the nature of the Lower Lakes of the Murray Darling Basin. *Pacific Conservation Biology*. https://doi.org/10/gf6knf

Gillespie B.R., Desmet S., Kay P., Tillotson M.R. & Brown L.E. (2015). A critical analysis of regulated river ecosystem responses to managed environmental flows from reservoirs. *Freshwater Biology* **60**, 410–425. https://doi.org/10.1111/fwb.12506

Gillespie B.R., Kay P. & Brown L.E. (2020). Limited impacts of experimental flow releases on water quality and macroinvertebrate community composition in an upland regulated river. *Ecohydrology* **13**, e2174. https://doi.org/10/gjz6bq

Gionchetta G., Oliva F., Romaní A.M. & Bañeras L. (2020). Hydrological variations shape diversity and functional responses of streambed microbes. *Science of The Total Environment* **714**, 136838. https://doi.org/10/gjsjng

Grill G., Lehner B., Thieme M., Geenen B., Tickner D., Antonelli F., *et al.* (2019). Mapping the world's free-flowing rivers. *Nature* **569**, 215–221. https://doi.org/10/c5k8

Grossart H.-P. & Rojas-Jimenez K. (2016). Aquatic fungi: targeting the forgotten in microbial ecology. *Current Opinion in Microbiology* **31**, 140–145. https://doi.org/10/ggbwrp

Grossart H.-P., Wurzbacher C., James T.Y. & Kagami M. (2016). Discovery of dark matter fungi in aquatic ecosystems demands a reappraisal of the phylogeny and ecology of zoosporic fungi. *Fungal Ecology* **19**, 28–38. https://doi.org/10/ghwtsn

Guerschman J.P., Van Dijk A.I.J.M., Mattersdorf G., Beringer J., Hutley L.B., Leuning R., *et al.* (2009). Scaling of potential evapotranspiration with MODIS data reproduces flux observations and catchment water balance observations across Australia. *Journal of Hydrology* **369**, 107–119. https://doi.org/10/bv9hzz

Guillou L., Bachar D., Audic S., Bass D., Berney C., Bittner L., *et al.* (2012). The Protist Ribosomal Reference database (PR2): a catalog of unicellular eukaryote Small

Sub-Unit rRNA sequences with curated taxonomy. *Nucleic Acids Research* **41**, D597–D604. https://doi.org/10/gf6h5p

Gulis V. & Suberkropp K. (2003). Leaf litter decomposition and microbial activity in nutrient-enriched and unaltered reaches of a headwater stream. *Freshwater Biology* **48**, 123–134. https://doi.org/10.1046/j.1365-2427.2003.00985.x

Guo F., Kainz M.J., Sheldon F. & Bunn S.E. (2015). Spatial variation in periphyton fatty acid composition in subtropical streams. *Freshwater Biology* **60**, 1411–1422. https://doi.org/10.1111/fwb.12578

Hajibabaei M., Baird D.J., Fahner N.A., Beiko R. & Golding G.B. (2016). A new way to contemplate Darwin's tangled bank: how DNA barcodes are reconnecting biodiversity science and biomonitoring. *Phil. Trans. R. Soc. B* **371**, 20150330. https://doi.org/10.1098/rstb.2015.0330

Hajibabaei M., Shokralla S., Zhou X., Singer G.A. & Baird D.J. (2011). Environmental barcoding: a next-generation sequencing approach for biomonitoring applications using river benthos. *PLoS One* **6**. https://doi.org/10.1371/journal.pone.0017497

Hall R.I. & Smol J.P. (1992). A weighted—averaging regression and calibration model for inferring total phosphorus concentration from diatoms in British Columbia (Canada) lakes. *Freshwater Biology* **27**, 417–434. https://doi.org/10/b4d7md

Hallegraeff G.M., Bolch C.J.S., Hill D.R.A., Jameson I., LeRoi J.M., McMinn A., *et al.* (2010). *Algae of Australia: phytoplankton of temperate coastal waters.*

Hanshew A.S., Mason C.J., Raffa K.F. & Currie C.R. (2013). Minimization of chloroplast contamination in 16S rRNA gene pyrosequencing of insect herbivore bacterial communities. *Journal of Microbiological Methods* **95**, 149–155. https://doi.org/10/f5jg6r

Hawkins E. (2019). ShowYourStripes. *ShowYourStripes*

Hayes D.B., Dodd, H. & Lessard J. (2006). Effects of Small Dams on Cold Water Stream Fish Communities. In: *American Fisheries Society Symposium*. p. 16. American Fisheries Society.

Hieber M. & Gessner M.O. (2002). Contribution of Stream Detrivores, Fungi, and Bacteria to Leaf Breakdown Based on Biomass Estimates. *Ecology* **83**, 1026–1038. https://doi.org/10.1890/0012-9658(2002)083[1026:COSDFA]2.0.CO;2

Hill B.H., Herlihy A.T., Kaufmann P.R., Stevenson R.J., McCormick F.H. & Johnson C.B. (2000). Use of periphyton assemblage data as an index of biotic integrity. *Journal of the North American Benthological Society* **19**, 50–67. https://doi.org/10.2307/1468281

Hill W.R., Rinchard J. & Czesny S. (2011). Light, nutrients and the fatty acid composition of stream periphyton. *Freshwater Biology* **56**, 1825–1836. https://doi.org/10.1111/j.1365-2427.2011.02622.x

Hornberger G.M., Wiberg P.L., Raffensperger J.P. & D'Odorico P. (2014). *Elements of Physical Hydrology*. JHU Press.

Horne A.C., Nathan R., Poff N.L., Bond N.R., Webb J.A., Wang J., *et al.* (2019). Modeling Flow-Ecology Responses in the Anthropocene: Challenges for Sustainable Riverine Management. *BioScience* **69**, 789–799. https://doi.org/10/gj824r

Huxman T.E., Wilcox B.P., Breshears D.D., Scott R.L., Snyder K.A., Small E.E., *et al.* (2005). Ecohydrological implications of woody plant encroachment. *Ecology* **86**, 308–319. https://doi.org/10/fd49qf

Iverson S.J. (2009). Tracing Aquatic Food Webs Using Fatty Acids: From Qualitative Indicators to Quantitative Determination. In: *In Lipids in Aquatic Ecosystems; Arts*. pp. 281–309. Springer.

Jarchow C.J., Nagler P.L., Glenn E.P., Ramirez-Hernandez J. & Eliana Rodriguez-Burgueno J. (2017). Evapotranspiration by remote sensing: An analysis of the Colorado River Delta before and after the Minute 319 pulse flow to Mexico. *Ecological Engineering* **106**, 725–732. https://doi.org/10.1016/j.ecoleng.2016.10.056

Jeffrey S.J., Carter J.O., Moodie K.B. & Beswick A.R. (2001). Using spatial interpolation to construct a comprehensive archive of Australian climate data. *Environmental Modelling & Software* **16**, 309–330. https://doi.org/10/d9fd53

Ji Y., Ashton L., Pedley S.M., Edwards D.P., Tang Y., Nakamura A., *et al.* (2013). Reliable, verifiable and efficient monitoring of biodiversity via metabarcoding. *Ecology Letters* **16**, 1245–1257. https://doi.org/10.1111/ele.12162

Kaestli M., Munksgaard N., Gibb K. & Davis J. (2019). Microbial diversity and distribution differ between water column and biofilm assemblages in arid-land waterbodies. *Freshwater Science*, 000–000. https://doi.org/10/ggbwh3

Kagami M., Miki T. & Takimoto G. (2014). Mycoloop: chytrids in aquatic food webs. *Frontiers in Microbiology* **5**. https://doi.org/10/ggsnw8

Kalendar R., Muterko A., Shamekova M. & Zhambakin K. (2017). In Silico PCR Tools for a Fast Primer, Probe, and Advanced Searching. *Methods in molecular biology (Clifton, N.J.)* **1620**, 1–31. https://doi.org/10/gh2pwf

Keck F., Rimet F., Franc A. & Bouchez A. (2016). Phylogenetic signal in diatom ecology: perspectives for aquatic ecosystems biomonitoring. *Ecological Applications* **26**, 861–872. https://doi.org/10.1890/14-1966

Keck F., Vasselon V., Tapolczai K., Rimet F. & Bouchez A. (2017). Freshwater biomonitoring in the Information Age. *Frontiers in Ecology and the Environment* **15**, 266–274. https://doi.org/10/gbjr9j

Kelly J.R. & Scheibling R.E. (2012). Fatty acids as dietary tracers in benthic food webs. *Marine Ecology Progress Series* **446**, 1–22. https://doi.org/10/fx2567

Kermarrec L., Franc A., Rimet F., Chaumeil P., Humbert J.F. & Bouchez A. (2013). Next-generation sequencing to inventory taxonomic diversity in eukaryotic communities: a test for freshwater diatoms. *Molecular Ecology Resources* **13**, 607–619. https://doi.org/10.1111/1755-0998.12105

Khan S. (2008). Managing climate risks in Australia: options for water policy and irrigation management. *Australian Journal of Experimental Agriculture* **48**, 265–273. https://doi.org/10.1071/EA06090

King A.J., Gawne B., Beesley L., Koehn J.D., Nielsen D.L. & Price A. (2015). Improving Ecological Response Monitoring of Environmental Flows. *Environmental Management* **55**, 991–1005. https://doi.org/10.1007/s00267-015-0456-6

Klymus K.E., Marshall N.T. & Stepien C.A. (2017). Environmental DNA (eDNA) metabarcoding assays to detect invasive invertebrate species in the Great Lakes. *PLOS ONE* **12**, e0177643. https://doi.org/10/f987qc

Koehn J. & O'Connor W. (1990). Distribution of freshwater fish in the Otway region, south-western Victoria. *Proceedings of the Royal Society of Victoria* **102**, 29–39

Kolde R. (2017). Pheatmap: pretty heatmaps. 2015. *R package version* **1**

Kruskal J.B. (1964). Nonmetric multidimensional scaling: A numerical method. *Psychometrika* **29**, 115–129. https://doi.org/10/c276kc

Ladson A. (2011). *Hydrology–An Australian Introduction*. Oxford University Press, Australia and New Zealand.

Ladson T. (2016). Plotting water quality samples on a hydrograph. *tonyladson*

Lane D.J., Pace B., Olsen G.J., Stahl D.A., Sogin M.L. & Pace N.R. (1985). Rapid determination of 16S ribosomal RNA sequences for phylogenetic analyses. *Proceedings of the National Academy of Sciences* **82**, 6955–6959. https://doi.org/10.1073/pnas.82.20.6955

Lang I., Hodac L., Friedl T. & Feussner I. (2011). Fatty acid profiles and their distribution patterns in microalgae: a comprehensive analysis of more than 2000 strains from the SAG culture collection. *BMC Plant Biology* **11**, 124. https://doi.org/10.1186/1471-2229-11-124

Larned S.T. (2010). A prospectus for periphyton: recent and future ecological research. *Journal of the North American Benthological Society* **29**, 182–206. https://doi.org/10/gjnqnw

Laroche O., Wood S.A., Tremblay L.A., Ellis J.I., Lear G. & Pochon X. (2018). A cross-taxa study using environmental DNA/RNA metabarcoding to measure biological impacts of offshore oil and gas drilling and production operations. *Marine Pollution Bulletin* **127**, 97–107. https://doi.org/10.1016/j.marpolbul.2017.11.042

Larras F., Bouchez A., Rimet F. & Montuelle B. (2012). Using Bioassays and Species Sensitivity Distributions to Assess Herbicide Toxicity towards Benthic Diatoms. *PLoS ONE* **7**, e44458. https://doi.org/10/ggrqz4

Larson J.H., Richardson W.B., Knights B.C., Bartsch L.A., Bartsch M.R., Nelson J.C., *et al.* (2013). Fatty Acid Composition at the Base of Aquatic Food Webs Is Influenced by Habitat Type and Watershed Land Use. *PLoS ONE* **8**. https://doi.org/10.1371/journal.pone.0070666

Legendre P. & Legendre L. (1998). *Numerical ecology*, 2nd English Edition. Elsevier, Amsterdam.

Lehmann K., Singer A., Bowes M.J., Ings N.L., Field D. & Bell T. (2015). 16S rRNA assessment of the influence of shading on early-successional biofilms in experimental streams. *FEMS Microbiology Ecology* **91**. https://doi.org/10.1093/femsec/fiv129

Lehner B. & Grill G. (2013). Global river hydrography and network routing: baseline data and new approaches to study the world's large river systems. *Hydrological Processes* **27**, 2171–2186

Lehner F., Wahl E.R., Wood A.W., Blatchford D.B. & Llewellyn D. (2017). Assessing recent declines in Upper Rio Grande runoff efficiency from a paleoclimate perspective. *Geophysical Research Letters* **44**, 4124–4133. https://doi.org/10/gbhq6v

Lessard J.L. & Hayes (2003). Effects of elevated water temperature on fish and macroinvertebrate communities below small dams. *River Research and Applications* **19**, 721–732. https://doi.org/10.1002/rra.713

Li S., Deng Y., Wang Z., Zhang Z., Kong X., Zhou W., *et al.* (2020). Exploring the accuracy of amplicon-based internal transcribed spacer markers for a fungal community. *Molecular Ecology Resources* **20**, 170–184. https://doi.org/10/gjtfzc

Ling F., Whitaker R., LeChevallier M.W. & Liu W.-T. (2018). Drinking water microbiome assembly induced by water stagnation. *The ISME Journal* **12**, 1520–1531. https://doi.org/10/gdb9mv

Lloyd-Price J., Abu-Ali G. & Huttenhower C. (2016). The healthy human microbiome. *Genome Medicine* **8**, 51. https://doi.org/10/gfszs8

Lock M.A., Wallace R.R., Costerton J.W., Ventullo R.M. & Charlton S.E. (1984). River Epilithon: Toward a Structural-Functional Model. *Oikos* **42**, 10–22. https://doi.org/10/fp4srb

Lovern J.A. (1934). Fat metabolism in fishes. *Biochemical Journal* **28**, 1961–1963

Lowe R.L. & LaLiberte G.D. (2017). Benthic stream algae: distribution and structure. In: *Methods in Stream Ecology, Volume 1*. pp. 193–221. Elsevier.

Lowe R.L. & Pan Y. (1996). Use of benthic algae in water quality monitoring. In: *Algal Ecology: Freshwater Benthic Ecosystems*. pp. 705–739. Academic Press, San Diego, CA.

Lücking R. & Hawksworth D.L. (2018). Formal description of sequence-based voucherless Fungi: promises and pitfalls, and how to resolve them. *IMA Fungus* **9**, 143–166. https://doi.org/10.5598/imafungus.2018.09.01.09

Ludwig J.A., Wilcox B.P., Breshears D.D., Tongway D.J. & Imeson A.C. (2005). VEGETATION PATCHES AND RUNOFF–EROSION AS INTERACTING ECOHYDROLOGICAL PROCESSES IN SEMIARID LANDSCAPES. *Ecology* **86**, 288–297. https://doi.org/10/bqmbhx

Lugg W.H., Griffiths J., Rooyen A.R. van, Weeks A.R. & Tingley R. (2018). Optimal survey designs for environmental DNA sampling. *Methods in Ecology and Evolution* **9**, 1049–1059. https://doi.org/10/gc5vhx

Magellan K., Pinchuck S. & Swartz E.R. (2014). Short and long-term strategies to facilitate aerial exposure in a galaxiid: aerial survival strategies in a galaxiid. *Journal of Fish Biology* **84**, 748–758. https://doi.org/10.1111/jfb.12320

Mann D.G. (1999). The species concept in diatoms. *Phycologia* **38**, 437–495. https://doi.org/10/cmp7bg

Mann D.G., Sato S., Trobajo R., Vanormelingen P. & Souffreau C. (2010). DNA barcoding for species identification and discovery in diatoms.

Marcelino V.R. & Verbruggen H. (2016). Multi-marker metabarcoding of coral skeletons reveals a rich microbiome and diverse evolutionary origins of endolithic algae. *Scientific Reports* **6**. https://doi.org/10.1038/srep31508

Marchesi J.R. & Ravel J. (2015). The vocabulary of microbiome research: a proposal. *Microbiome* **3**, 31, s40168-015-0094–5. https://doi.org/10/gft447

Mateo P., Leganés F., Perona E., Loza V. & Fernández-Piñas F. (2015). Cyanobacteria as bioindicators and bioreporters of environmental analysis in aquatic ecosystems. *Biodiversity and Conservation* **24**, 909–948. https://doi.org/10/f68kgm

McArdle B.H. & Anderson M.J. (2001). Fitting multivariate models to community data: A comment on distance-based redundancy analysis. *Ecology* **82**, 290–297. https://doi.org/10.1890/0012-9658(2001)082[0290:FMMTCD]2.0.CO;2

McDonald D., Price M.N., Goodrich J., Nawrocki E.P., DeSantis T.Z., Probst A., *et al.* (2012). An improved Greengenes taxonomy with explicit ranks for ecological and evolutionary analyses of bacteria and archaea. *The ISME Journal* **6**, 610–618. https://doi.org/10/ddv8fz

McGeoch M.A. & Chown S.L. (1998). Scaling up the value of bioindicators. *Trends in Ecology & Evolution* **13**, 46–47. https://doi.org/10/dqmf37

McKnight D.T., Huerlimann R., Bower D.S., Schwarzkopf L., Alford R.A. & Zenger K.R. (2019). Methods for normalizing microbiome data: An ecological perspective. *Methods in Ecology and Evolution* **10**, 389–400. https://doi.org/10/gfknh5

McMahon T.A., Peel M.C., Lowe L., Srikanthan R. & McVicar T.R. (2013). Estimating actual, potential, reference crop and pan evaporation using standard

meteorological data: a pragmatic synthesis. *Hydrology and Earth System Sciences* **17**, 1331–1363. https://doi.org/10/gb9nd9

Medlin L.K. (2018). Mini review: Diatom species as seen through a molecular window. *Brazilian Journal of Botany* **41**, 457–469. https://doi.org/10.1007/s40415-018-0444-1

Medlin L.K., Williams D.M. & Sims P.A. (1993). The evolution of the diatoms (Bacillariophyta). I. Origin of the group and assessment of the monophyly of its major divisions. *European Journal of Phycology* **28**, 261–275. https://doi.org/10/bnsbk4

Merz S.K. (2013). *Flows: a method for determining environmental water requirements in Victoria / report prepared by Sinclair Knight Merz, Peter Cottingham and Associates, DoDo Environmental and Griffith University for the Department of Environment and Primary Industries*. Department of Environment and Primary Industries, Melbourne.

Miles N.G., Walsh C.T., Butler G., Ueda H. & West R.J. (2014). Australian diadromous fishes – challenges and solutions for understanding migrations in the 21st century. *Marine and Freshwater Research* **65**, 12. https://doi.org/10/gkgmw8

Milici M., Deng Z.-L., Tomasch J., Decelle J., Wos-Oxley M.L., Wang H., *et al.* (2016). Co-occurrence Analysis of Microbial Taxa in the Atlantic Ocean Reveals High Connectivity in the Free-Living Bacterioplankton. *Frontiers in Microbiology* **7**. https://doi.org/10/ggqqb2

Milly P.C.D., Betancourt J., Falkenmark M., Hirsch R.M., Kundzewicz Z.W., Lettenmaier D.P., *et al.* (2008). Stationarity Is Dead: Whither Water Management? *Science* **319**, 573–574. https://doi.org/10/bsrkbm

Minerovic A.D., Potapova M.G., Sales C.M., Price J.R. & Enache M.D. (2020). 18S-V9 DNA metabarcoding detects the effect of water-quality impairment on stream biofilm eukaryotic assemblages. *Ecological Indicators* **113**, 106225. https://doi.org/10/gkcwkh

Mondon J., Sherwood J. & Chandler F. (2003). *Western Victorian Estuaries Classification Project*. Report for Western Coastal Board, Warrnambol, Victoria, Australia.

Morton F.I. (1983). Operational estimates of areal evapotranspiration and their significance to the science and practice of hydrology. *Journal of Hydrology* **66**, 1–76. https://doi.org/10/b3c599

Morton F.I. (1986). Practical Estimates of Lake Evaporation. *Journal of Applied Meteorology and Climatology* **25**, 371–387. https://doi.org/10/ckn5qz

Mrozik A., Nowak A. & Piotrowska-Seget Z. (2014). Microbial diversity in waters, sediments and microbial mats evaluated using fatty acid-based methods. *International Journal of Environmental Science and Technology* **11**, 1487–1496. https://doi.org/10/gjrpv3

Nagler P.L., Doody T.M., Glenn E.P., Jarchow C.J., Barreto-Muñoz A. & Didan K. (2016). Wide-area estimates of evapotranspiration by red gum (Eucalyptus camaldulensis) and associated vegetation in the Murray-Darling River Basin, Australia. *Hydrological Processes* **30**, 1376–1387. https://doi.org/10.1002/hyp.10734

Napolitano G., Hill W., Guckert J., Stewart A., Nold S. & White D. (1994). Changes in periphyton fatty-acid composition in chlorine-polluted streams. *Journal of the North American Benthological Society* **13**, 237–249. https://doi.org/10.2307/1467242

Needham D.M. & Fuhrman J.A. (2016). Pronounced daily succession of phytoplankton, archaea and bacteria following a spring bloom. *Nature Microbiology* **1**. https://doi.org/10/gfb6jm

Newall P., Bate N. & Metzeling L. (2006). A comparison of diatom and macroinvertebrate classification of sites in the Kiewa River system, Australia. *Hydrobiologia* **572**, 131–149. https://doi.org/10/c7gnk4

Niewójt L. (2010). Gadubanud society in the Otway Ranges,Victoria: an environmental history. *Aboriginal History Journal* **33**. https://doi.org/10/gj7m9v

Nilsson R.H., Anslan S., Bahram M., Wurzbacher C., Baldrian P. & Tedersoo L. (2019). Mycobiome diversity: high-throughput sequencing and identification of fungi. *Nature Reviews Microbiology* **17**, 95–109. https://doi.org/10.1038/s41579-018-0116-y

Noske P., Lane P. & Sheridan G. (2017). *Improving post-fire hydro-geomorphic risk assessment in the Otway Ranges*. Unpublished technical report for the Victorian Department of Environment, Land, Water and Planning. pp 19.

NRE, Merz S.K., Cooperative Research Centre for Freshwater Ecology, & Freshwater Ecology (NRE) (2002). *FLOWS: a method for determining environmental water requirements in Victoria*. Cooperative Research Centre for Freshwater Ecology.

O'Connor W.G. & Koehn J.D. (1998). Spawning of the broad-finned Galaxias, Galaxias brevipinnis Günther (Pisces: Galaxiidae) in coastal streams of southeastern Australia. *Ecology of Freshwater Fish* **7**, 95–100. https://doi.org/10/bgk332

O'Day K. (2016). rclimate.wordpress.com. *RClimate Script to Assess Local Hot Day Trends*

O'Dea C., Zhang Q., Staley C., Masters N., Kuballa A., Fisher P., *et al.* (2019). Compositional and temporal stability of fecal taxon libraries for use with SourceTracker in sub-tropical catchments. *Water Research* **165**, 114967. https://doi.org/10/ggf3cs

Oeding S. & Taffs K.H. (2017). Developing a regional diatom index for assessment and monitoring of freshwater streams in sub-tropical Australia. *Ecological Indicators* **80**, 135–146. https://doi.org/10.1016/j.ecolind.2017.05.009

Olden J.D. & Naiman R.J. (2010). Incorporating thermal regimes into environmental flows assessments: Modifying dam operations to restore freshwater ecosystem integrity. *Freshwater Biology* **55**, 86–107. https://doi.org/10.1111/j.1365-2427.2009.02179.x

Oliveira M.C., Repetti S.I., Iha C., Jackson C.J., Díaz-Tapia P., Lubiana K.M.F., *et al.* (2018). High-throughput sequencing for algal systematics. *European Journal of Phycology* **53**, 256–272. https://doi.org/10.1080/09670262.2018.1441446

Op De Beeck M., Lievens B., Busschaert P., Declerck S., Vangronsveld J. & Colpaert J.V. (2014). Comparison and Validation of Some ITS Primer Pairs Useful for Fungal Metabarcoding Studies. *PLoS ONE* **9**. https://doi.org/10.1371/journal.pone.0097629

Orwin K.H., Dickie I.A., Holdaway R. & Wood J.R. (2018). A comparison of the ability of PLFA and 16S rRNA gene metabarcoding to resolve soil community change and predict ecosystem functions. *Soil Biology and Biochemistry* **117**, 27–35. https://doi.org/10/gc27n2

Palmer M.A., Bernhardt E.S., Allan J.D., Lake P.S., Alexander G., Brooks S., *et al.* (2005). Standards for ecologically successful river restoration: Ecological success in river restoration. *Journal of Applied Ecology* **42**, 208–217. https://doi.org/10.1111/j.1365-2664.2005.01004.x

Parada A.E., Needham D.M. & Fuhrman J.A. (2016). Every base matters: assessing small subunit rRNA primers for marine microbiomes with mock communities, time series and global field samples. *Environmental Microbiology* **18**, 1403–1414. https://doi.org/10/f8n8hp

Parks Victoria, Victoria, & DSE (2009). *Caring for country - the Otways and you: Great Otway National Park and Otway Forest Park management plan*. Parks Victoria and Dept. of Sustainability and Environment, Melbourne, Vic.

Parrish C.C. (2009). Essential fatty acids in aquatic food webs. In: *Lipids in Aquatic Ecosystems*. (Eds M. Kainz, M.T. Brett & M.T. Arts), pp. 309–326. Springer, New York, NY.

Pawlowski J., Kelly-Quinn M., Altermatt F., Apothéloz-Perret-Gentil L., Beja P., Boggero A., *et al.* (2018). The future of biotic indices in the ecogenomic era: Integrating (e)DNA metabarcoding in biological assessment of aquatic ecosystems. *Science of The Total Environment* **637–638**, 1295–1310. https://doi.org/10.1016/j.scitotenv.2018.05.002

Pawlowski J., Lejzerowicz F., Apotheloz-Perret-Gentil L., Visco J. & Esling P. (2016). Protist metabarcoding and environmental biomonitoring: Time for change. *European Journal of Protistology* **55**, 12–25. https://doi.org/10.1016/j.ejop.2016.02.003

Peel M.C., McMahon T.A. & Finlayson B.L. (2004). Continental differences in the variability of annual runoff-update and reassessment. *Journal of Hydrology* **295**, 185–197. https://doi.org/10/bs8zbc

Petheram C., Zhang L., Walker G. & Grayson R. (2014). *Towards a Framework for Predicting Impacts of Land-use on Recharge: A Review of Recharge Studies in Australia*.

Piredda R., Claverie J.-M., Decelle J., de Vargas C., Dunthorn M., Edvardsen B., *et al.* (2018). Diatom diversity through HTS-metabarcoding in coastal European seas. *Scientific Reports* **8**. https://doi.org/10.1038/s41598-018-36345-9

Poff N.L., Allan J.D., Bain M.B., Karr J.R., Prestegaard K.L., Richter B.D., *et al.* (1997). The Natural Flow Regime. *BioScience* **47**, 769–784. https://doi.org/10.2307/1313099

Poff N.L., Tharme R.E. & Arthington A.H. (2017). Evolution of Environmental Flows Assessment Science, Principles, and Methodologies. In: *Water for the Environment*. pp. 203–236. Elsevier.

Poff N.L. & Zimmerman J.K.H. (2010). Ecological responses to altered flow regimes: a literature review to inform the science and management of environmental flows: Review of altered flow regimes. *Freshwater Biology* **55**, 194–205. https://doi.org/10.1111/j.1365-2427.2009.02272.x

Porter T.M. & Hajibabaei M. (2018). Scaling up: A guide to high-throughput genomic approaches for biodiversity analysis. *Molecular Ecology* **27**, 313–338. https://doi.org/10.1111/mec.14478

Post D.A., Chiew F.H.S., Vaze J., Teng J., Perraud J.M. & Viney N.R. (2010). *Future runoff projections (~ 2030) for south-eastern Australia*. CSIRO Land and Water, Canberra.

Postel S. & Richter B. (2003). *Rivers for life: managing water for people and nature*. Island Press.

Potapova M. & Charles D.F. (2007). Diatom metrics for monitoring eutrophication in rivers of the United States. *Ecological indicators* **7**, 48–70. https://doi.org/10/fm36pd

Priestley C.H.B. & Taylor R.J. (1972). On the Assessment of Surface Heat Flux and Evaporation Using Large-Scale Parameters. *Monthly Weather Review* **100**, 81–92. https://doi.org/10/cr3qwn

R Core Team (2019). *R: A language and environment for statistical computing*. R Foundation for Statistical Computing, Vienna, Austria.

Raadik T.A., Nicol M., Victoria, Department of Environment and Primary Industries, & Arthur Rylah Institute for Environmental Research (2013). *Searching for threatened upland galaxiids (Teleostei, Galaxiidae) in the Thomson and La Trobe river catchments, West Gippsland, Victoria*.

Redfield A.C. (1958). The biological control of chemical factors in the environment. *American Scientist* **46**, 230A–221

Richter B.D. & Thomas G.A. (2007). Restoring environmental flows by modifying dam operations. *Ecology and Society* **12**

Rimet F. & Bouchez A. (2012). Biomonitoring river diatoms: Implications of taxonomic resolution. *Ecological Indicators* **15**, 92–99. https://doi.org/10/b7nb5p

Rimet F., Chaumeil P., Keck F., Kermarrec L., Vasselon V., Kahlert M., *et al.* (2016). R-Syst::diatom: an open-access and curated barcode database for diatoms and freshwater monitoring. *Database: The Journal of Biological Databases and Curation* **2016**. https://doi.org/10.1093/database/baw016

Rimet F., Gusev E., Kahlert M., Kelly M.G., Kulikovskiy M., Maltsev Y., *et al.* (2019). Diat.barcode, an open-access curated barcode library for diatoms. *Scientific Reports* **9**, 1–12. https://doi.org/10/ggttsv

Rivera S.F., Vasselon V., Ballorain K., Carpentier A., Wetzel C.E., Ector L., *et al.* (2018). DNA metabarcoding and microscopic analyses of sea turtles biofilms: Complementary to understand turtle behavior. *PLOS ONE* **13**, e0195770. https://doi.org/10.1371/journal.pone.0195770

Rognes T., Flouri T., Nichols B., Quince C. & Mahé F. (2016). VSEARCH: a versatile open source tool for metagenomics. *PeerJ* **4**. https://doi.org/10/gftph2

Rohde R.A. & Hausfather Z. (2020). The Berkeley Earth land/ocean temperature record. *Earth System Science Data* **12**, 3469–3479

Round F.E., Crawford R.M. & Mann D.G. (1990). *The Diatoms. Morphology and biology of the genera*. Cambridge University Press.

Ruess L. & Müller-Navarra D.C. (2019). Essential Biomolecules in Food Webs. *Frontiers in Ecology and Evolution* **7**. https://doi.org/10/gjskwm

Ryder D.S., Watts R.J., Nye E. & Burns A. (2006). Can flow velocity regulate epixylic biofilm structure in a regulated floodplain river? *Marine and Freshwater Research* **57**, 29–36. https://doi.org/10.1071/MF05099

Saft M., Western A.W., Zhang L., Peel M.C. & Potter N.J. (2015). The influence of multiyear drought on the annual rainfall-runoff relationship: An A ustralian perspective. *Water Resources Research* **51**, 2444–2463. https://doi.org/10/f7c982

Sagova-Mareckova M., Boenigk J., Bouchez A., Cermakova K., Chonova T., Cordier T., *et al.* (2021). Expanding ecological assessment by integrating microorganisms into routine freshwater biomonitoring. *Water Research* **191**, 116767. https://doi.org/10/gjddbw

Sargent J. (1976). The structure, metabolism, and function of lipids in marine organisms. In: *Biochemical and biophysical perspectives in marine biology*. pp. 150–212. Academic Press, London.

Sarno D., Kooistra W.H.C.F., Medlin L.K., Percopo I. & Zingone A. (2005). Diversity in the genus Skeletonema (Bacillariophyceae). II. An assessment of the taxonomy of S. costatum-like species with the description of four new species. *Journal of Phycology* **41**, 151–176. https://doi.org/10/fnsftr

Scanlon B.R., Keese K.E., Flint A.L., Flint L.E., Gaye C.B., Edmunds W.M., *et al.* (2006). Global synthesis of groundwater recharge in semiarid and arid regions. *Hydrological Processes* **20**, 3335–3370. https://doi.org/10/d47ssp

Schloss P.D., Westcott S.L., Ryabin T., Hall J.R., Hartmann M., Hollister E.B., *et al.* (2009). Introducing mothur: Open-Source, Platform-Independent, Community-Supported Software for Describing and Comparing Microbial Communities. *Applied and Environmental Microbiology* **75**, 7537–7541. https://doi.org/10/fqcv8t

Schnurr P.J., Drever M.C., Elner R.W., Harper J. & Arts M.T. (2020). Peak Abundance of Fatty Acids From Intertidal Biofilm in Relation to the Breeding Migration of Shorebirds. *Frontiers in Marine Science* **7**. https://doi.org/10/ggxf6d

Scholz O. & Boon P.I. (1993). Biofilms on submerged River Red Gum (Eucalyptus camaldulensis Dehnh. Myrtaceae) wood in billabongs: an analysis of bacterial assemblages using phospholipid profiles. *Hydrobiologia* **259**, 169–178. https://doi.org/10/d4kz3d

Scott K.R., Morgan R.M., Jones V.J. & Cameron N.G. (2014). The transferability of diatoms to clothing and the methods appropriate for their collection and analysis in forensic geoscience. *Forensic Science International* **241**, 127–137. https://doi.org/10/f6cr5b

Shafroth P.B., Wilcox A.C., Lytle D.A., Hickey J.T., Andersen D.C., Beauchamp V.B., *et al.* (2010). Ecosystem effects of environmental flows: modelling and experimental floods in a dryland river: Environmental flows in a dryland river. *Freshwater Biology* **55**, 68–85. https://doi.org/10.1111/j.1365-2427.2009.02271.x

Sharma K.K., Schuhmann H. & Schenk P.M. (2012). High Lipid Induction in Microalgae for Biodiesel Production. *Energies* **5**, 1532–1553. https://doi.org/10/f99336

Sheldon F. & Walker K.F. (1997). Changes in biofilms induced by flow regulation could explain extinctions of aquatic snails in the lower River Murray, Australia. 12

Sherwood A.R., Chan Y.L. & Presting G.G. (2008). Application of universally amplifying plastid primers to environmental sampling of a stream periphyton community. *Molecular Ecology Resources* **8**, 1011–1014. https://doi.org/10.1111/j.1755-0998.2008.02138.x

Sherwood A.R. & Presting G.G. (2007). Universal primers amplify a 23S rDNA plastid marker in eukaryotic algae and cyanobacteria. *Journal of Phycology* **43**, 605–608. https://doi.org/10.1111/j.1529-8817.2007.00341.x

Sigee D. (2005). *Freshwater microbiology: biodiversity and dynamic interactions of microorganisms in the aquatic environment*. John Wiley & Sons.

Simonin M., Voss K.A., Hassett B.A., Rocca J.D., Wang S.-Y., Bier R.L., *et al.* (2019). In search of microbial indicator taxa: shifts in stream bacterial communities along an urbanization gradient. *Environmental Microbiology* **21**, 3653–3668. https://doi.org/10/ggb5xv

Sipos R., Székely A.J., Palatinszky M., Révész S., Márialigeti K. & Nikolausz M. (2007). Effect of primer mismatch, annealing temperature and PCR cycle number on 16S rRNA gene-targetting bacterial community analysis. *FEMS Microbiology Ecology* **60**, 341–350. https://doi.org/10/d6j33x

Souchon Y., Sabaton C., Deibel R., Reiser D., Kershner J., Gard M., *et al.* (2008). Detecting biological responses to flow management: missed opportunities; future directions. *River Research and Applications* **24**, 506–518. https://doi.org/10.1002/rra.1134

de Sousa A.G.G., Tomasino M.P., Duarte P., Fernández-Méndez M., Assmy P., Ribeiro H., *et al.* (2019). Diversity and Composition of Pelagic Prokaryotic and Protist Communities in a Thin Arctic Sea-Ice Regime. *Microbial Ecology*. https://doi.org/10.1007/s00248-018-01314-2

Stelzer R.S. & Lamberti G.A. (2001). Effects of N: P ratio and total nutrient concentration on stream periphyton community structure, biomass, and elemental composition. *Limnology and Oceanography* **46**, 356–367. https://doi.org/10/ffzkts

Stevenson R.J., Pan Y. & Van Dam H. (2010). Assessing environmental conditions in rivers and streams with diatoms. In: *The Diatoms: Applications for the Environmental and Earth Sciences*, 2nd edn. pp. 57–85. Cambridge University Press, Cambridge, MA.

Stoeck T., Pan H., Dully V., Forster D. & Jung T. (2018). Towards an eDNA metabarcode-based performance indicator for full-scale municipal wastewater treatment plants. *Water Research* **144**, 322–331. https://doi.org/10/gfhv6s

Surf Coast Shire (undated). *Painkalac Estuary Management Plan*. Surf Coast Shire.

Tan X., Zhang Q., Burford M.A., Sheldon F. & Bunn S.E. (2017). Benthic Diatom Based Indices for Water Quality Assessment in Two Subtropical Streams. *Frontiers in Microbiology* **8**. https://doi.org/10/gf6b7w

Tapolczai K., Vasselon V., Bouchez A., Stenger-Kovács C., Padisák J. & Rimet F. (2019). The impact of OTU sequence similarity threshold on diatom-based bioassessment: A case study of the rivers of Mayotte (France, Indian Ocean). *Ecology and Evolution* **9**, 166–179. https://doi.org/10.1002/ece3.4701

Tharme R.E. (2003). A global perspective on environmental flow assessment: emerging trends in the development and application of environmental flow methodologies for rivers. *River Research and Applications* **19**, 397–441. https://doi.org/10.1002/rra.736

Thompson J.D., Gibson T.J. & Higgins D.G. (2003). Multiple sequence alignment using ClustalW and ClustalX. *Current protocols in bioinformatics*, 2.3. 1-2.3. 22

Thompson L.R., Sanders J.G., McDonald D., Amir A., Ladau J., Locey K.J., *et al.* (2017). A communal catalogue reveals Earth's multiscale microbial diversity. *Nature* **551**, 457–463. https://doi.org/10/gchbpz

Thornthwaite C.W. (1948). An Approach toward a Rational Classification of Climate. *Geographical Review* **38**, 55–94. https://doi.org/10/cxvgdp

Tillotson M.D., Kelly R.P., Duda J.J., Hoy M., Kralj J. & Quinn T.P. (2018). Concentrations of environmental DNA (eDNA) reflect spawning salmon abundance at fine spatial and temporal scales. *Biological Conservation* **220**, 1–11. https://doi.org/10/gdf8c3

UM & DSE (2012). *Otway Wildfire Hydrologic Risk - Assessment and Mitigation Tools Project. Final Project Report*. University of Melbourne, Department of Forest and Ecosystem Science & Department of Sustainability and Environment, Victoria.

Underwood A.J. (1992). Beyond BACI: the detection of environmental impacts on populations in the real, but variable, world. *Journal of Experimental Marine Biology and Ecology* **161**, 145–178. https://doi.org/10.1016/0022-0981(92)90094-Q

Van Horn D., Sinsabaugh R., Takacs-Vesbach C., Mitchell K. & Dahm C. (2011). Response of heterotrophic stream biofilm -communities to a gradient of resources. *Aquatic Microbial Ecology* **64**, 149–161. https://doi.org/10.3354/ame01515

Vasselon V., Rimet F., Tapolczai K. & Bouchez A. (2017). Assessing ecological status with diatoms DNA metabarcoding: Scaling-up on a WFD monitoring network (Mayotte island, France). *Ecological Indicators* **82**, 1–12. https://doi.org/10/gf6b7m

Visco J.A., Apothéloz-Perret-Gentil L., Cordonier A., Esling P., Pillet L. & Pawlowski J. (2015). Environmental Monitoring: Inferring the Diatom Index from Next-Generation Sequencing Data. *Environmental Science & Technology* **49**, 7597–7605. https://doi.org/10.1021/es506158m

VVG (2021). Visualising Victorias Groundwater. *Centre for eResearch and Digital Innovation, Federation University Australia, Mt Helen, Ballarat, Victoria*

Warfe D.M., Hardie S.A., Uytendaal A.R., Bobbi C.J. & Barmuta L.A. (2014). The ecology of rivers with contrasting flow regimes: Identifying indicators for setting environmental flows. *Freshwater Biology* **59**, 2064–2080. https://doi.org/10.1111/fwb.12407

Watts R. & Ryder D. (2002). Developing biological indicators for the assessment of environmental flows. *Australasian Journal of Water Resources* **5**, 119–122. https://doi.org/10.1080/13241583.2002.11465198

Webb-Robertson B.-J., Bunn A.L. & Bailey V.L. (2011). Phospholipid fatty acid biomarkers in a freshwater periphyton community exposed to uranium: discovery by non-linear statistical learning. *Journal of Environmental Radioactivity* **102**, 64–71. https://doi.org/10.1016/j.jenvrad.2010.09.005

Weitere M., Erken M., Majdi N., Arndt H., Norf H., Reinshagen M., *et al.* (2018). The food web perspective on aquatic biofilms. *Ecological Monographs* **88**, 543–599

Werner A.D. (2010). A review of seawater intrusion and its management in Australia. *Hydrogeology Journal* **18**, 281–285. https://doi.org/10/dvst92

Wetzel R.G. (1983). Limnology (2nd edn). *Saunders Collage Pub. New York*

Whipps J.M., Lewis K. & Cooke R.C. (1988). Mycoparasitism and plant disease control. *Fungi in biological control systems*, 161–187

White T.J., Bruns T., Lee S. & Taylor J. (1990). Amplification and direct sequencing of fungal ribosomal RNA genes for phylogenetics. *PCR protocols: a guide to methods and applications* **18**, 315–322

Whorley S.B., Smucker N.J., Kuhn A. & Wehr J.D. (2019). Urbanisation alters fatty acids in stream food webs. *Freshwater Biology*, 1–13. https://doi.org/10.1111/fwb.13279

Whorley S.B. & Wehr J.D. (2016). Connecting algal taxonomic information to essential fatty acid content in agricultural streams. *Phycologia* **55**, 531–542. https://doi.org/10/f9g46s

Wickham H., Averick M., Bryan J., Chang W., McGowan L.D., François R., *et al.* (2019). Welcome to the Tidyverse. *Journal of Open Source Software* **4**, 1686. https://doi.org/10/ggddkj

Willers C., Rensburg P.J.J. van & Claassens S. (2015). Phospholipid fatty acid profiling of microbial communities–a review of interpretations and recent applications. *Journal of Applied Microbiology* **119**, 1207–1218. https://doi.org/10/f7vztq

Wolff B.A., Clements W.H. & Hall E.K. (2021). Metals Alter Membership but Not Diversity of a Headwater Stream Microbiome. *Applied and Environmental Microbiology* **87**. https://doi.org/10/gjmhn4

Wurzbacher C., Kerr J. & Grossart H.-P. (2011). Aquatic fungi

Zajaczkowski J. & Jeffrey S. (2020). Potential evaporation and evapotranspiration data provided by SILO. *Department of Environment and Science, Queensland Government*

Zamora-Terol S., Novotny A. & Winder M. (2020). Reconstructing marine plankton food web interactions using DNA metabarcoding. *Molecular Ecology* **29**, 3380–3395. https://doi.org/10/gh3qkn

Zhang L., Dawes W.R. & Walker G.R. (2001). Response of mean annual evapotranspiration to vegetation changes at catchment scale. *Water Resources Research* **37**, 701–708. https://doi.org/10/fcwcr7

Zhang Y., Zheng H., Chiew F.H.S., Arancibia J.P.- & Zhou X. (2016). Evaluating Regional and Global Hydrological Models against Streamflow and Evapotranspiration Measurements. *Journal of Hydrometeorology* **17**, 995–1010. https://doi.org/10/f8cz8b

Zhang Z., Wang J., Wang J., Wang J. & Li Y. (2020). Estimate of the sequenced proportion of the global prokaryotic genome. *Microbiome* **8**, 134. https://doi.org/10/gjtfx6

Zimmermann J., Abarca N., Enk N., Skibbe O., Kusber W.-H. & Jahn R. (2014). Taxonomic Reference Libraries for Environmental Barcoding: A Best Practice Example from Diatom Research. *PLoS ONE* **9**, e108793. https://doi.org/10/gf3xrq

Zimmermann J., Jahn R. & Gemeinholzer B. (2011). Barcoding diatoms: evaluation of the V4 subregion on the 18S rRNA gene, including new primers and protocols. *Organisms Diversity & Evolution* **11**, 173–192. https://doi.org/10/bvgd9c

Appendix A. Fish observations

During the design of the environmental flows for Painkalac Creek, there was uncertainty over the fish species inhabiting Painkalac Creek so the design documents lists species that were potentially present (Doeg *et al.*, 2007). Fish population surveys were not included in this study but fish were incidentally observed by experienced fish biologists during the course of the field research. These observations of fish presence in the three different study reaches are included here to augment the scant record of freshwater fish occurrence in the region. Because fish were not collected in this study, identification was based on a few spot observations. All of the fish that we observed are diadromous species that migrate between freshwater and marine habitats (Table A.1) (Miles *et al.*, 2014). Although some groups, such as galaxiids, can complete their life cycle even when landlocked, river regulation poses a key threat to many diadromous species by blocking migration, changing the natural flow regime and altering critical environmental cues such as temperature (Bunn & Arthington, 2002; Miles *et al.*, 2014). Some migratory fish may be able to move around Painkalac Dam or use the spillway when the reservoir is full, but otherwise, fish attempt to migrate through the plumbing system.

Table A.1. Fish observations by stream reach during 2017-2019. Painkalac Upstream (PU), Painkalac Downstream (PD), Barham River (B).

Common name	Latin name	Native?	PU	PD	B
Short-finned Eel	*Anguilla australis*	Yes	✓		
Common Galaxias	*Galaxias maculatus*	Yes		✓	
Spotted Galaxias	*Galaxias truttaceus*	Yes	✓		
Broad-finned Galaxias	*Galaxias brevipennis*	Yes	✓	✓	
Pouched Lamprey	*Geotria australis*	Yes			✓
Australian Grayling	*Prototroctes maraena*	Yes			✓
Brown Trout	*Salmo trutta*	No			✓

Painkalac Creek

Galaxiids – Family Galaxidae

The galaxiids are the most dominant family occurring in the fresh waters of Southern Australia (Allen, Midgley & Allen, 2002). We frequently encountered the common galaxias or jollytail (*Galaxias maculatus*) throughout the downstream reach of Painkalac Creek. Adults of this common and widespread species typically migrate into estuaries during autumn for spawning (Allen *et al.*, 2002). Larvae are washed to the sea where they spend several months before returning to freshwater habitats the following spring.

We observed two galaxiid species in the Painkalac Upstream reach that we identified as *Galaxias brevipennis* and *G. truttaceus.* Both of these species are amphidromous, with eggs laid in freshwater and larval fish moving to the sea soon after hatching and returning to freshwater habitats as juveniles (Miles *et al.*, 2014).

On 17 January 2018, we observed several fish in a large pool on the left fork of Painkalac Creek (-38.43124, 144.01662). We assumed that the different sizes and body shapes represented two distinct species but were unable to positively identify either species. One type was represented by at least 10 fish that were approximately 20 cm long and were air-breathing at the water surface (Figure A.1). This was the only time these large fish were observed, and their behaviour was not surprising given that the dissolved oxygen concentration in the pool was 1.8 mg/L. We were unable to note any distinguishing characteristics of the second, smaller species.

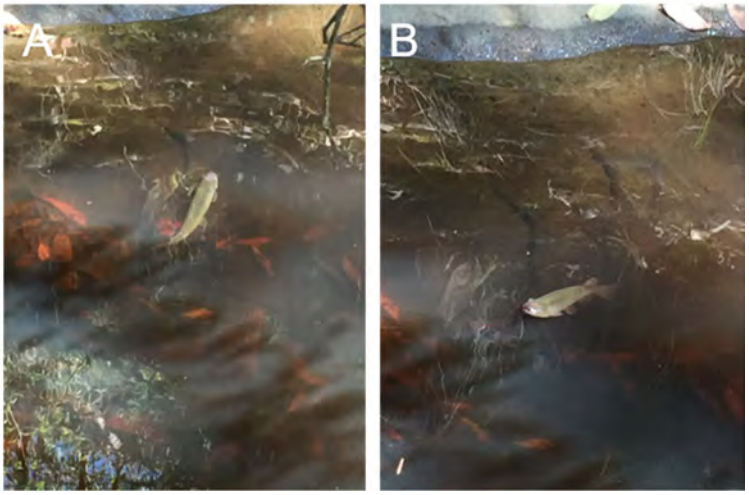

Figure A.1. Large, air-breathing fish in Painkalac Upstream reach.

Approximately one month later (23 February 2018) on the right fork of the creek above Iron Bark Spur Track (-38.43103, 144.01662), we observed *Galaxias brevipennis*. This identification was made based on fin position, mottling pattern and dark patch above the base of the pectoral fin (Allen *et al.*, 2002). The creek had dried to isolated pools and water quality was declining. We watched as an individual fish, approximately 10 cm in length, wriggled its way from the water and remained exposed with only its caudal fin submerged (Figure A.2). Also known as climbing galaxias, juvenile *Galaxias brevipennis* are known to use their large pectoral and pelvic fins to 'climb' damp, vertical surfaces (O'Connor & Koehn, 1998) but the physiology of their survival out of the water is less studied. We continued to watch the exposed fish, and after about 20 minutes, droplets of water formed behind the operculum. When aerial exposure was studied in another Galaxias species, in South Africa, they documented adaptations in skin pores and changes to the gill structures that facilitate long-term survival out of the water (Magellan, Pinchuck & Swartz, 2014). When we returned to the site, no fish were present in the pool but fish were observed in another pool, just downstream. On 22 February 2018, a juvenile *Galaxias brevipennis* (9 cm) was observed near the stream gauge in the Painkalac Downstream reach (-38.44423, 144.07043).

Figure A.2. *Galaxias brevipinnis* A) emerging from rock pool with surrounding habitat visible and B) close-up of the same fish. Blue arrow indicates fish position.

We recorded the presence of the trout minnow or spotted galaxiid (*Galaxias truttaceus)* in the Painkalac Upstream reach based on a single encounter of a dead fish on 23 February 2018, at the Duck Pond Track gauge site (-38.43619, 144.04630). The creek had recently desiccated, and we found the body floating in a tiny rock pool that still had water (**Error! Reference source not found.**A). We identified the specimen as *Galaxias truttaceus* based on the spotting pattern, diagonal stripe below eye, size (15 cm) and slightly posterior position of the anal fin (Allen *et al.*, 2002) (Figure A.3B).

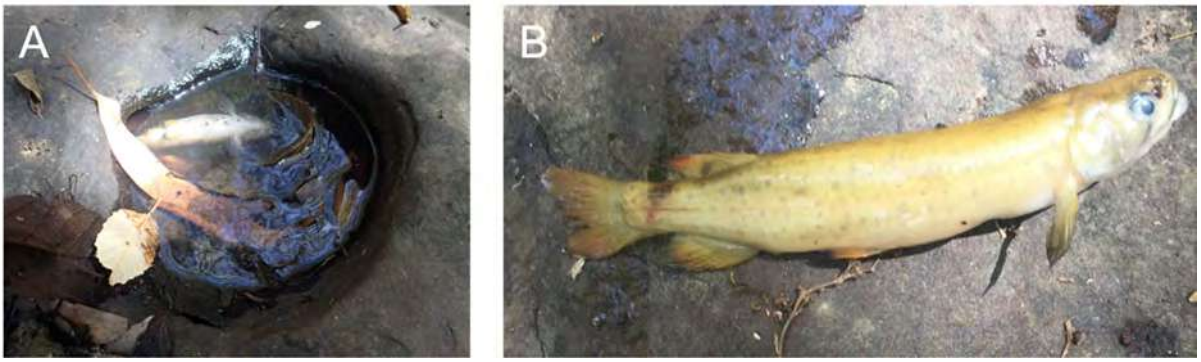

Figure A.3. A) Deceased *Galaxias truttaceus* as found and B) upon examination

The Painkalac Estuary Management Plan (Surf Coast Shire, undated) states that Mountain Galaxias have been recorded in Painkalac Creek. However, Doeg and colleagues (2007) could not find any documented records of the species and Koehn and O'Connor (1990) state that Mountain Galaxias is missing from all of the coastal Otway streams from Anglesea to Apollo Bay. Previously treated as a single species, Mountain Galaxias has been recently identified as a species complex composed of at least 15 species, some of which are new to science (Raadik *et al.*, 2013).

Barham River

At the location of the stream gauge in the Barham River, we commonly encountered brown trout (*Salmo trutta*) and Australian grayling (*Prototroctes maraena*) (-38.75507, 143.62500). Brown trout are a popular, introduced game species that can negatively impact native fish stocks (O'Connor & Koehn, 1998) while Australian grayling is a nationally threatened diadromous fish that is the only surviving member of the Prototroctidae (Miles *et al.*, 2014). The grayling population that we observed was consistently present just above the rock fish ladder that was installed to support fish passage in the Barham River. We also observed a single larval ammocoete that we assumed to be pouched lamprey (Geotria australis) at the lowermost site in the Barham River, site (-38.73488, 143.62469) on 7 November 2018 (Figure A.4).

Figure A.4. Larval lamprey in Barham River.

Appendix B. Environmental flow PERMANOVA summary

PERMANOVA results from A) the log-transformed bacterial abundance matrix, B) the square root-transformed algal abundance matrix, C) the fourth root-transformed fungal abundance matrix and D) the transformed Euclidean PLFA resemblance matrix. Abundance matrices were based on operational taxonomic units (OTUs). PLFA: phospholipid fatty acid, df: degrees of freedom, SS: sum of squares, MS: mean squares, pseudo-F: ratio of between-cluster variance to within-cluster variance, Perms: number of permutations. Bold indicates P≤0.05.

Factor	df	SS	MS	Pseudo-F	Perms	P(perm)
A) Bacteria						
RiverP	2	25211	12606	6.6675	9939	**0.0028**
FlowCat	1	1602.4	1602.4	1.9083	9926	0.0762
Site(RiverP)	5	10840	2167.9	5.1271	9851	**0.0001**
Set(FlowCat)	13	2301	946.22	2.2378	9750	**0.0001**
RiverP × FlowCat	2	3241.6	1620.8	1.8669	9851	**0.0015**
RiverP × Set(FlowCat)	8	5113.2	639.15	1.5116	9793	**0.0018**
Site(RiverP) × FlowCat	5	2974.2	594.84	1.4068	9821	**0.0249**
B) Algae						
RiverP	2	44204	22102	8.4353	9952	**0.0023**
FlowCat	1	2981	2981	2.3236	9950	0.0552
Site(RiverP)	5	18216	3643.3	7.527	9851	**0.0001**
Set(FlowCat)	13	20391	1568.5	3.2405	9799	**0.0001**
RiverP × FlowCat	2	7573	3786.5	4.2204	9858	**0.0001**
RiverP × Set(FlowCat)	8	4039.2	504.9	1.0431	9768	0.3515
Site(RiverP) × FlowCat	5	3814.5	762.9	1.5761	9817	**0.0019**
C) Fungi						
RiverP	2	18460	9229.8	5.3305	9957	**0.0039**
FlowCat	1	1466	1466	1.2275	9930	0.3164
Site(RiverP)	5	8499.9	1700	3.5126	9803	**0.0001**
Set(FlowCat)	13	21165	1628.1	3.3641	9822	**0.0001**
RiverP × FlowCat	2	3551.3	1775.7	1.8152	9799	**0.0002**
RiverP × Set(FlowCat)	8	6136.2	767.02	1.5849	9697	**0.0001**
Site(RiverP) × FlowCat	5	2998.5	599.71	1.2392	9735	**0.0221**
D) PLFA						
RiverP	2	76.782	38.391	3.2176	9950	**0.0097**
FlowCat	1	5.07	5.07	0.67765	9932	0.7153
Site(RiverP)	5	58.027	11.605	1.9744	9875	**0.0022**
Set(FlowCat)	19	170.9	8.9945	1.5302	9777	**0.0005**
RiverP × FlowCat	2	20.567	10.283	1.444	9860	**0.0495**
RiverP × Set(FlowCat)	10	55.103	5.5103	0.93746	9812	0.6319
Site(RiverP) × FlowCat	5	32.524	6.5049	1.1067	9865	0.2798